

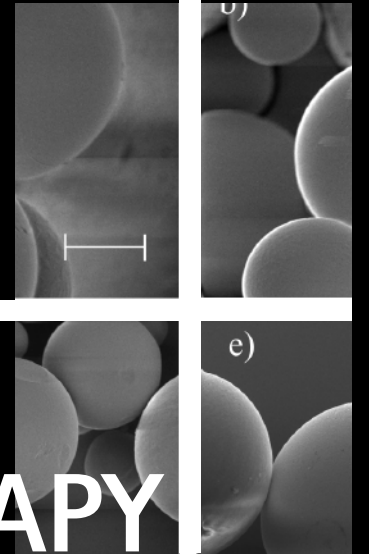
LANTHANIDE BEARING RADIOACTIVE PARTICLES FOR CANCER THERAPY AND MULTIMODALITY IMAGING

Sander Zielhuis



LANTHANIDE BEARING RADIOACTIVE PARTICLES FOR CANCER THERAPY AND MULTIMODALITY IMAGING

Sander Zielhuis



Lanthanide Bearing Radioactive Particles for Cancer Therapy and Multimodality Imaging

S.W. Zielhuis – Utrecht, University Medical Center Utrecht
PhD thesis Utrecht University – with a summary in Dutch

The research described in this thesis was carried out at the department of Nuclear Medicine, University Medical Center Utrecht (Utrecht, The Netherlands), under the auspices of ImagO, the Utrecht Graduate School for Biomedical Imaging Sciences. The project was financially supported by the Dutch Technology Foundation (Stichting Technische Wetenschappen UGT 6069). Financial support for this research and the publication of this thesis was also provided by Stichting de Drie Lichten, Maurits en Anna de Kock Stichting, Nijbakker-Morra Stichting, ImagO, Pharmachemie, Philips Medical, Tyco Healthcare and GE Healthcare.

Copyright © 2006 by S.W. Zielhuis. All rights reserved.

ISBN 90-393-4258-X
(ISBN-13) ISBN 978-90-393-4258-9

Designed by ECHT! Johan Manschot, Utrecht | Printed by Febodruk B.V., Enschede, The Netherlands

LANTHANIDE BEARING RADIOACTIVE PARTICLES FOR CANCER THERAPY AND MULTIMODALITY IMAGING

LANTHANIDE BEVATTENDE RADIOACTIEVE DEELTJES
VOOR KANKERTHERAPIE EN MULTIMODALE BEELDVORMING
(met een samenvatting in het Nederlands)

Proefschrift

ter verkrijging van de graad van doctor aan de Universiteit Utrecht op gezag van
de rector magnificus, prof. dr. W.H. Gispen, ingevolge het besluit van het college
voor promoties in het openbaar te verdedigen op
maandag 22 mei 2006 des middags te 12.45 uur

door

Sander Wilhelm Zielhuis

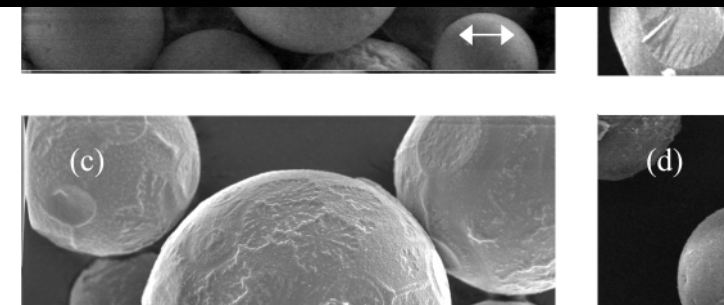
geboren op 26 juni 1976 te Zwolle

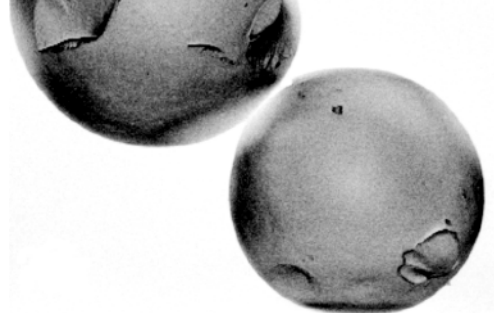
Promotoren: prof.dr. P.P. van Rijk
 prof.dr.ir. W.E. Hennink
 prof.dr.ir. M.A. Viergever

Co-promotoren: dr. A.D. van het Schip
 dr. J.F.W. Nijsen

Chapter 1	Introduction	7
Chapter 2	Lanthanide bearing microparticulate systems for multi modality imaging and targeted therapy of cancer	13
Chapter 3	Surface characteristics of holmium loaded Poly(L-lactic acid) microspheres	43
Chapter 4	Removal of chloroform from biodegradable therapeutic microspheres by radiolysis	61
Chapter 5	Holmium loaded poly(L-lactic acid) microspheres: an in vitro degradation study	81
Chapter 6	Biocompatibility study of holmium loaded poly(L-lactic acid) microspheres in rats	101
Chapter 7	Production of GMP-grade radioactive holmium loaded poly(L-lactic acid) microspheres for clinical application	121
Chapter 8	Holmium loaded alginate microspheres for multimodality imaging and therapeutic applications	137
Chapter 9	Lanthanide loaded liposomes for multimodality imaging and therapy)	153
Chapter 10	Summary and concluding remarks	169

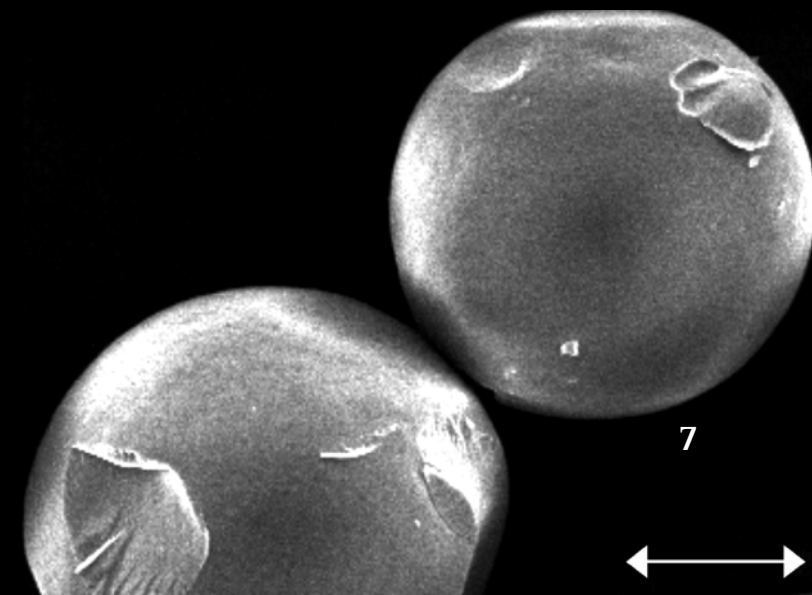
Samenvatting | Dankwoord | Publications | Curriculum Vitae





Chapter 1

Introduction



1. Introduction

Of the one million patients diagnosed with colorectal cancer each year world wide [1], more than half will develop liver metastases in the course of their disease [2]. Untreated hepatic colorectal metastasis has a poor prognosis and is associated with a median survival of 6–12 months [2]. It is estimated that only 20–30 % of patients with colorectal metastases will have isolated liver metastases and are candidates for curative liver resection [3]. The yearly incidence of primary liver cancer is around 600,000, from which 82% are in developing countries. These patients have also a very poor prognosis; the number of deaths is 95 % of the yearly incidence [1].

When patients are not eligible for curative surgery alternative treatments have to be applied. The most active and widely used chemotherapeutic agent for treatment of primary liver cancer is doxorubicine. However, the overall partial response rate is very poor, namely less than 20%, and only a small number of patients can be cured using chemotherapy [4]. The standard chemotherapeutic treatment for hepatic colorectal metastasis is a combination of 5-fluorouracil and leucovorin. Again, the response rate is low (~25%), and a negligible number of patients can be cured using this chemotherapeutic combination [5].

Alternative treatment options that have been developed are ultrasonography guided radio-frequency ablation (RFA) and cryoablation. These are effective methods to induce necroses of liver metastases with a size up to 4 cm in diameter. RFA is currently the most widely used method for ablation of unresectable liver metastases and can be performed percutaneously, during laparoscopy or laparotomy. However, RFA is limited by the number, size and localization of the tumors [6].

Local radionuclide therapy of liver malignancies by use of radioactive microspheres is a promising alternative therapy for patients that can not be treated by surgery or ablation methods [7]. Local radionuclide therapy makes use of the fact that liver malignancies are almost exclusively dependent on arterial blood supply [8]. This is in sharp contrast to normal liver tissue, which receives most of its flow from the portal vein [8]. Based on this difference in blood supply between tumours and normal liver tissue, radioactive microspheres with a diameter between 20 and 50 μm that are injected into the hepatic artery, will selectively lodge in and around the tumours and as a consequence irradiate the surrounding tissue [7].

The department of Nuclear Medicine of the University Medical Center Utrecht started in the mid-nineties the development of holmium-166 loaded polymer-based microspheres [9]. Cancer treatment with holmium-166 has obvious advantages over other radionuclides applied for therapeutic purposes. Holmium-165 is an element from the group of lanthanides with a natural abundance of 100 % and can be neutron-activated to yield holmium-166 (a gamma and beta-emitter) with a favourable half-life (26.8 h) for therapeutic applications [7,9]. The photons (80.6 keV, yield 6.2 %) allow visualisation with a gamma camera whereas the beta-radiation ($E_{\text{max}} = 1.84 \text{ MeV}$) is suitable for the local radiotherapy of tumours.

Poly(L-lactic acid) microspheres loaded with holmium-165-acetylacetonate (HoAcAc) can be produced using a solvent evaporation technique. The microspheres are rendered radioactive with thermal neutrons in a nuclear reactor within a period of hours. Although the molecular weight of the PLLA decreased due to the neutron irradiation, the microspheres retained their integrity [10] and the leaching of holmium-166 in urine and faeces of treated rabbits during 2 days was less than 0.1% [11]. In vivo studies (rat) demonstrated that these microspheres were successfully targeted to liver tumours; the tumour to normal liver tissue ratio was about 6:1 [12].

The element holmium has a very high magnetic susceptibility [13]. This means that the presence of holmium in human tissue affects the MRI signal. The resultant signal change is dependent on the holmium concentration, which allows direct visualization of radioactive and non-radioactive holmium microspheres and exploitation for dosimetric studies [14]. This phenomenon has been successfully applied in tumour bearing rabbits as well as in healthy pigs [15]. Holmium microspheres were administrated via the hepatic artery and visualized with both scintigraphy and MRI.

Before HoAcAc loaded PLLA-MS (Ho-PLLA-MS) can be clinically applied in patients, the pharmaceutical quality of the microspheres must be well defined, and in addition, the entire production procedure should be in compliance with the Good Manufacturing Practice (GMP) regulations promulgated by the European Agency for the Evaluation of Medicinal Products (EMA) [16]. The amount of residual solvents and endotoxins has to be limited and sterility must be guaranteed. Furthermore, also a pharmaceutically acceptable suspending

vehicle for the microspheres has to be identified. Moreover, the administration of Ho-PLLA-MS must not lead to toxic effects. In vitro and in vivo animal studies have to generate insight into their biodegradability and biocompatibility. As mentioned, holmium-166 is a therapeutic radionuclide with a logistically favourable half-life that can be produced easily, and which can be visualised with both gamma cameras and MRI. These unique characteristics open the way for the development of other holmium based particulate systems for imaging and treatment of cancer.

2. Outline of this thesis

Chapter 2 gives an overview of the currently developed lanthanide loaded microparticulate systems and their possible diagnostic and therapeutic oncological applications. In **Chapter 3** the surface characteristics of Ho-PLLA-MS before and after neutron and gamma irradiation were investigated in order to get insight into their suspending behaviour and to identify suitable surfactants for clinical application of these systems. **Chapter 4** describes the removal of residual chloroform from the microspheres since it was observed that relatively large amounts of this solvent remained in the microspheres before neutron irradiation. It is known that chloroform is susceptible for high-energy radiation, and therefore we investigated whether neutron and gamma irradiation could result in the removal of residual chloroform in Ho-PLLA-MS by radiolysis. In **Chapter 5** the in vitro degradability and in **Chapter 6** the in vivo degradability and biocompatibility of Ho-PLLA-MS are investigated. **Chapter 7** describes the aspects of the production of a (relatively) large-scale GMP batch of Ho-PLLA-MS. Regarding its unique physical properties, holmium is also a very interesting element for other diagnostic and therapeutic applications. Therefore, other particulate systems in addition to PLLA-microspheres were developed. In **Chapter 8** the development of lanthanide loaded liposomes and in **Chapter 9** the production of holmium loaded alginate microspheres are described. Both lanthanide loaded liposomes and alginate microspheres can be used for multimodality imaging and radionuclide tumour therapy. **Chapter 10** concisely summarises this thesis and in a general discussion suggestions for further research are given.

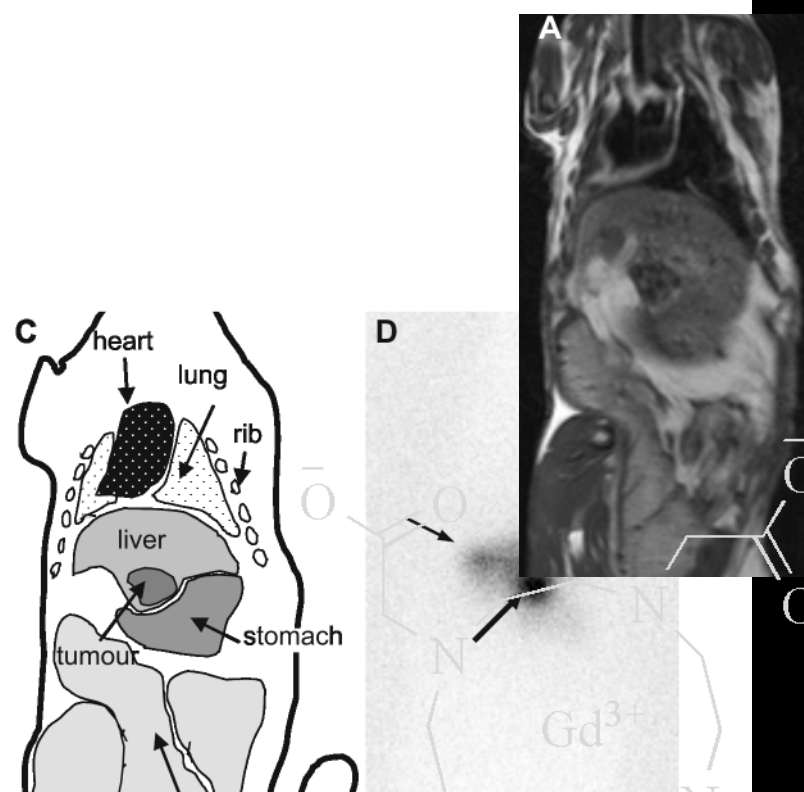
References

- [1] Parkin DM, Bray F, Ferlay J, Pisani P. Global cancer statistics, 2002. *Ca Cancer J Clin* 2005; 55: 74-108.
- [2] Bentrem DJ, Dematteo RP, Blumgart LH. Surgical therapy for metastatic disease to the liver. *Annu Rev Med* 2005; 56: 139-56.
- [3] Bennett JJ, Cao D, Posner MC. Determinants of unresectability and outcome of patients with occult colorectal hepatic metastases. *J Surg Oncol* 2005; 92: 64-9.
- [4] Llovet JM, Sala M, Bruix J. Nonsurgical treatment of hepatocellular carcinoma. *Liver Transplant* 2000; 6: S11-S15.
- [5] Piedbois P, Buyse M, Rustum Y, Machover D, Erlichman C, Carlson RW, Valone F, Labianca R, Doroshow JH, Petrelli N. Modulation of Fluorouracil by Leucovorin in Patients with Advanced Colorectal-Cancer - Evidence in Terms of Response Rate. *J of Clin Oncology* 1992; 10: 896-903.
- [6] Nordlinger B, Rougier P. Nonsurgical methods for liver metastases including cryotherapy, radiofrequency ablation, and infusional treatment: what's new in 2001? *Curr Opin Oncology* 2002; 14: 420-3.
- [7] Nijssen JFW, van het Schip AD, Hennink WE, Rook DW, van Rijk PP, de Klerk JMH. Advances in nuclear oncology: Microspheres for internal radionuclide therapy of liver metastases. *Curr Med Chem* 2002; 9: 73-82.
- [8] Lambert B, Van de Wiele C. Treatment of hepatocellular carcinoma by means of radiopharmaceuticals. *Eur J Nucl Med Mol Imaging* 2005; 32: 980-9.
- [9] Nijssen JFW, Zonnenberg BA, Woittiez JR, Rook DW, Swildens-van Woudenberg IA, van Rijk PP, van het Schip AD. Holmium-166 poly lactic acid microspheres applicable for intra-arterial radionuclide therapy of hepatic malignancies: effects of preparation and neutron activation techniques. *Eur J Nucl Med* 1999; 26: 699-704.
- [10] Nijssen JFW, van het Schip AD, van Steenberg MJ, Zielhuis SW, Kroon-Batenburg LM, van de Weert M, van Rijk PP, Hennink WE. Influence of neutron irradiation on holmium acetylacetonate loaded poly(L-lactic acid) microspheres. *Biomaterials* 2002; 23: 1831-9.
- [11] van Es RJ, Nijssen JFW, van het Schip AD, Dullens HF, Slootweg PJ, Koole R. Intra-arterial embolization of head-and-neck cancer with radioactive holmium-166 poly(L-lactic acid) microspheres: an experimental study in rabbits. *Int J Oral Maxillofac Surg* 2001; 30: 407-13.
- [12] Nijssen JFW, Rook DW, Brandt CWJM, Meijer R, Dullens HFJ, Zonnenberg BA, de Klerk JMH, van Rijk PP, Hennink WE, van het Schip AD. Targeting of liver tumour in rats by selective delivery of holmium-166 loaded microspheres: a biodistribution study. *Eur J Nucl Med* 2001; 28: 743-9.
- [13] Handbook of Chemistry and Physics, 84th edition. CRC Press, Boca Raton (FL) 2003.
- [14] Nijssen JFW, Seppenwoolde JH, Havenith T, Bos C, Bakker CJG, van het Schip AD. Liver Tumors: MR Imaging of Radioactive Holmium Microspheres—Phantom and Rabbit Study. *Radiology* 2004; 231: 491-9.
- [15] Seppenwoolde JH, Nijssen JFW, Bartels LW, Zielhuis SW, van het Schip AD, Bakker CJ. Internal radiation therapy of liver tumors: Qualitative and quantitative magnetic resonance imaging of the biodistribution of holmium-loaded microspheres in animal models. *Magn Reson Med* 2004; 53: 76-84.
- [16] de Vos FJ, de Decker M, Dierckx RA. The good laboratory practice and good clinical practice requirements for the production of radiopharmaceuticals in clinical research. *Nucl Med Commun* 2005; 26: 575-9.

Chapter 2

Lanthanide bearing microparticulate systems for multi-modality imaging and targeted therapy of cancer

SW Zielhuis, JFW Nijssen, JH Seppenwoolde, BA Zonnenberg, CJG Bakker, WE Hennink, PP van Rijk and AD van het Schip



Abstract

The rapid developments of high-resolution imaging techniques are offering unique possibilities for the guidance and follow up of recently developed sophisticated anticancer therapies. Advanced biodegradable drug delivery systems, e.g. based on liposomes and polymeric nanoparticles or microparticles, are very effective tools to carry these anticancer agents to their site of action. Elements from the group of lanthanides have very interesting physical characteristics for imaging applications and are the ideal candidates to be co-loaded either in their non-radioactive or radioactive form into these advanced drug delivery systems because of the following reasons:

Firstly, they can be used both as magnetic resonance imaging (MRI) and computed tomography (CT) contrast agents and for single photon emission computed tomography (SPECT).

Secondly, they can be used for radionuclide therapies which, importantly, can be monitored with SPECT, CT, and MRI

Thirdly, they have a relatively low toxicity, especially when they are complexed to ligands.

This review gives a survey of the currently developed lanthanide-loaded microparticulate systems that are under investigation for cancer imaging and/or cancer therapy.

1. Introduction

The rapid developments of clinical diagnostic imaging technologies, in combination with medical and pharmaceutical progress, have led to major advances in healthcare. Imaging of biologic processes at cellular and molecular levels, termed “molecular imaging”, is one of the most innovative examples [1]. The development of highly sensitive contrast agents and radiopharmaceuticals will make early detection of deviant biologic processes feasible. In contradistinction to “conventional” diagnostic imaging with less specific and less sensitive contrast agents, the new agents set forth to probe abnormalities that are the basis of diseases, rather than imaging the end effects of severe disorders. This will cause a shift in the treatment options and possibilities of patients. It is expected that much emphasis will be placed on diagnosing and treating early symptoms before late symptoms occur, which demands a new category of therapeutic strategies. To cope with these expectations, the development of innovative and nanosized carrier systems for imaging agents is prerequisite.

In recent years, it has been shown that advanced drug delivery systems such as liposomes, polymeric microparticles and nanoparticles are able to substantially alter the tissue distribution and pharmacokinetics of an associated drug. They are, therefore, used to improve the therapeutic index of drugs by increasing their efficacy and/or reducing their toxicity [2,3]. If these delivery systems are carefully designed with respect to the aimed target site and route of administration, they may provide a solution for the delivery problems posed by new classes of macromolecular therapeutics such as peptides, proteins and genes [4,5]. It would be a revolution when these systems could also be loaded with components that can be visualized with dedicated imaging modalities such as magnetic resonance imaging (MRI), nuclear imaging (for example single photon emission computed tomography (SPECT)), and computed tomography (CT) making image-guided drug therapy achievable [6,7]. When these imaging techniques can be combined, real-time information about the tissue distribution of these systems will be generated. Several elements from the lanthanide group have very interesting physical properties (like their density and magnetic susceptibility) and, therefore, lanthanide bearing systems can be deployed for (multi-modality) imaging [8], and radionuclide anticancer therapies [9]. This review gives a survey of currently developed lanthanide-loaded microparticulate systems which are under evaluation for cancer imaging and cancer therapy or a combination of these.

2. Lanthanides in general

2.1 Chemistry

The lanthanide series are the 15 rare earth chemical elements that comprise lanthanum and lutetium. Their atomic numbers are between 57 and 71. Sometimes yttrium (atomic number 39) and scandium (atomic number 21) are also categorized in this group, due to their similarity in chemistry. Lanthanides are elements in which the f orbitals are partly or completely filled, while the outermost p and d orbitals are empty. Since the f orbitals do not have as much effect on the chemical properties as the p , and d , they are chemically very similar. The chemical characteristics of the lanthanides are dominated by their +3 oxidation state. Despite the high charge, the large size of the lanthanide(III) ions results in low charge densities and their bonding is predominantly ionic in character.

2.2 Biodistribution and toxicity

The lanthanides have no known role as tracer elements in living organisms. Compared with heavy metals, their toxicity is relatively low, especially when they are complexed to ligands [8]. Based on an analogy principle, the toxicity of a metal ion is determined by its degree of deviation from the relevant essential element as reference, which is Ca^{2+} in the case of the lanthanides [10,11].

Softness (according to the Hard and Soft Acid/Base theory [12]), covalence and redox tendency are the most decisive among the factors determining how far a metal ion deviates from Ca^{2+} . The lanthanide ions are very close to Ca^{2+} in these properties and their pharmacological effects originate from their deviation in charge, radii and $4f$ orbital involvement. In general, the toxicity of lanthanides decreases with increasing atomic number, probably due to a greater solubility, and ionic stability, and smaller radius (see Table 1) [13].

The distribution and excretion of lanthanides in laboratory animals is well known. When lanthanides are administered intravenously as salts the main part of the dose (around 60-80 %) accumulates in the skeleton and the liver. It has been shown that the higher the atomic number of the lanthanide, the higher the distribution ratio liver vs. bone (see Table 1). The remaining part of the injected dose (up to 40 %) is excreted by faeces and urine and a minor part of the administered dose distributes to other organs [14]. When lanthanides are chelated with organic ligands such as diethylenetriamine pentaacetic acid (DTPA) these

molecular complexes distribute more homogeneously in the body and are essentially excreted by the kidneys in a few hours [15].

The toxicity (TD50 and LD50 values) of the lanthanides was studied decades ago in rodents. Their toxicity was dependent on the route of administration, their chemical form and the used animal model. LD50 values of intravenously or intraperitoneally lanthanide salts varied from about 50-500 mg/kg bodyweight. Intravenous injection of soluble lanthanide salts can result in various pharmacological effects. The most important effects are the blocking of Kupffer cells (probably due to the formation of lanthanide colloids) [16] and cardiovascular effects (due to their Ca^{2+} similarity) [17]. After oral administration there are hardly any toxic effects, due to the fact that there is no (or low) absorption from the gastrointestinal tract [18-20].

Table 1. Ionic Radii and Distribution of Lanthanide Elements in Rats [14].

Element	Atomic number	Ionic radius (pm)	% Injected dose				
			Bone	Liver	Faeces	Urine	Other tissues
Lanthanum (La)	57	106	18	65	3	3	11
Cerium (Ce)	58	103	28	51	9	6	6
Praseodymium (Pr)	59	101	27	48	9	7	9
Neodymium (Nd)	60	100	31	27	10	22	10
Promethium (Pm)	61	98	36	41	6	10	7
Samarium (Sm)	62	96	33	35	13	13	6
Europium (Eu)	63	95	36	25	11	17	11
Gadolinium (Gd)	64	94	41	12	10	27	10
Terbium (Tb)	65	92	60	7	7	16	10
Dysprosium (Dy)	66	91	60	3	6	24	7
Holmium (Ho)	67	89	56	2	13	21	8
Erbium (Er)	68	88	56	1	7	27	9
Thulium (Tm)	69	87	64	2	5	22	7
Ytterbium (Yb)	70	86	58	3	7	19	13
Lutetium (Lu)	71	85	68	3	7	16	6

3. Imaging

3.1 MRI

MRI is an important imaging modality that allows non-invasive diagnosis of tumours because of the inherent contrast between soft tissues. The contrast between the soft tissues results from a different response (relaxation) of the MRI signal that originates from the protons (i.e. the water). It is well known that the presence of paramagnetic ions locally alters the responses of the MRI signal by affecting the relaxation behaviour of tissues. The elements europium, gadolinium, terbium, dysprosium, holmium, erbium and thulium have a very high magnetic susceptibility [21] (given in Table 2), creating local magnetic field inhomogeneities that enhance the relaxation of the MRI signal. Recalling that a different relaxation generally results in contrast, paramagnetic lanthanides are used as MRI contrast agents [8,22]. Chelated gadolinium is used for the detection of tumours and has proven its clinical value [23,24]. However, adequate targeting of the contrast agent is necessary to create an observable MRI signal. Therefore, advanced formulations were developed to deliver the contrast agents in e.g. tumour tissue which in turn results in a locally high concentration and thus in a more sensitive and specific MRI signal.

Table 2. Magnetic Susceptibility (SI Units) of the Lanthanides (as Pure Metals) [21]

Element	Volume Susceptibility (ppm)
La	66
Ce	3,086
Pr	3,024
Nd	3,432
Pm	3,024
Sm	1,288
Eu	14,815
Gd	116,645
Tb	95,475
Dy	68,352
Ho	48,767
Er	30,121
Tm	17,698
Yb	119
Lu	129

3.1.1 Liposomes

Liposomes are nano-sized vesicles (~50-500 nm) with an aqueous space surrounded by a lipid bilayer. They are attractive drug delivery vehicles and can be targeted to various tumour sites [25-28]. Liposomes have also interesting features for diagnostic tools. In order to enhance tumour diagnosis with MRI, amphiphilic gadolinium derivatives were synthesized and incorporated into the liposomal bilayer. Examples of used chelators are DTPA, 1,4,7,10-tetraazacyclododecane-1,4,7,10-tetraacetic acid (DOTA) or 1,4,7,10-tetraazacyclododecane-1,4,7-triacetic acid (DO3A) [29] (see Fig. (1)). It has been shown that surface modification of gadolinium-loaded liposomes with polymers like poly(ethylene glycol) (PEG) improves their MRI properties (called relaxivity), probably due the fact that more water and thus protons are associated with the membrane of liposomes [30]. When an adequate tumour targeting of liposomes is reached, the physiological circumstances in the tumour can be deployed to optimize the MRI procedure. Because of the fact that the interstitial pH in tumours is lower than in healthy tissue [31], pH sensitive liposomes were designed [31-34]. These liposomes locally enhance the relaxation of the MRI signal at a lower pH due to their destabilization at this low interstitial tumour pH whereupon the encapsulated MRI contrast agent is released into the surrounding tissue.

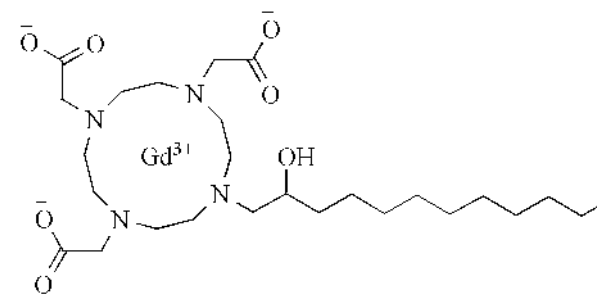


Fig. 1 Gd-(2-hydroxyhexadecyl)-DO3A, as synthesized by Gløgaard et al. [29]

A promising way to actively target liposomes to (tumour) tissues is the coupling of so called homing devices, e.g. (fragments) of antibodies, to the surface of liposomes. Mulder et al. [35] labelled an anti-E-selectin antibody to the distal

end of PEG-chains of gadolinium containing liposomes (see Fig. (2)). These systems were successfully targeted (in vitro) to human umbilical vein endothelial cells and can therefore be a useful diagnostic tool for the imaging of molecular processes on endothelial cells. A very promising way of targeting diagnostics to tumour tissues is the exploitation of over-expressed glucose transporters such as the glucose receptor GLUT-1 [36]. Luciani et al. [37] included N-palmitoyl glucosamine in the membrane of liposomes and loaded them with gadolinium by entrapping gadobenate dimeglumine within the aqueous core of the vesicle. They successfully targeted these systems to an implanted human prostate adenocarcinoma in mice after intravenous injection. The local gadolinium concentrations were sufficiently high to apply adequate MR imaging, which make these systems promising tools for tumour diagnosis [38].

The nanoscale size of liposomes makes them interesting candidates for a sentinel node procedure [39]. This procedure is in general based on the principle that nano-sized particles which are injected around solid tumours (like melanoma, breast tumours etc.) drain to the lymph nodes. The particles are loaded with a radionuclide and with a gamma camera and a hand held monitor the first lymph node which receives lymphatic flow from a tumour site can be detected. This lymph node (called the sentinel node) is subsequently surgically removed and examined by microscopy. When this sentinel node contains tumour cells (is positive) a surgical procedure for the resection of the following lymph nodes (of the lymphatic system) is required [40]. The sentinel node can also be detected using MRI [41-44] with the advantage that MRI gives an anatomical reference and that in some cases MRI is able to discriminate between positive and negative lymph nodes [45,46]. Indeed, liposomes loaded with gadobutrol or gadolinium-DTPA [30,47,48] were recently successfully used for the sentinel node procedure.

One of the most difficult tumours to reach with macromolecular systems are brain tumours and therefore convention enhanced delivery (CED) was developed [49]. CED is a method by which agents are directly infused into the central nervous system (CNS). Mamot et al. [50] showed that CED of gadodiamide-loaded liposomes in the CNS was feasible by monitoring the biodistribution of these liposomes with MRI. In another study of the same group gadolinium-labelled liposomes were infused into tumour (glioma and gliosarcoma) bearing

rats simultaneously with doxorubicin containing liposomes [6]. They concluded that MRI-monitoring of CED, using these gadolinium-loaded liposomes, is an important stipulation for clinical application of CED.

Due to the fact that tumour cells are more sensitive than healthy cells to heating, hyperthermia is applied as tumour therapy [51]. These thermal therapies require guidance and monitoring and therefore heat-sensitive liposomes were developed [52-54]. These liposomes were designed to destabilize above a predetermined critical temperature, called the gel-to-liquid crystalline phase transition temperature. Above this temperature (in case of hyperthermia) the incorporated gadolinium diethylenetriaminepentaacetic acid bis(methylamide) is released into the surrounding tissue fluid which results in a local enhancement of the detected MRI signal.

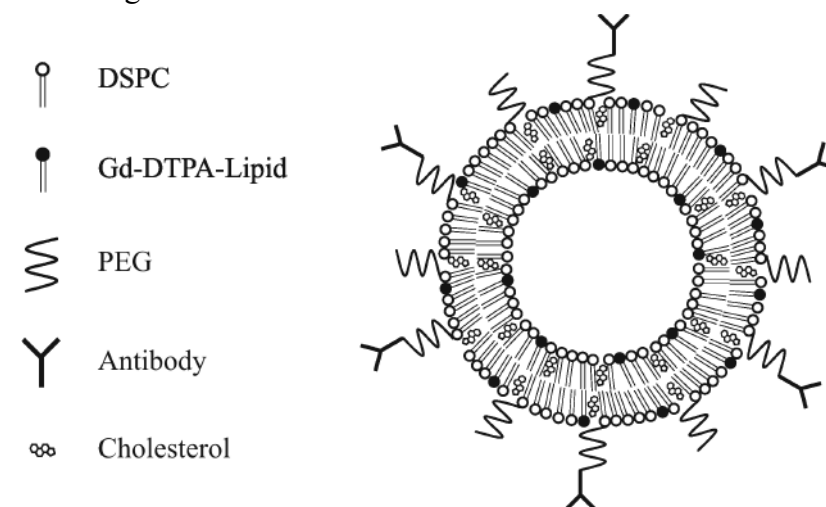


Fig. 2 Schematic representation of a pegylated paramagnetic liposome that is composed of Gd-DTPA-bis(stearylamide), 1,2-distearoyl-*sn*-glycero-3-phosphocholine (DSPC), cholesterol, and 1,2-distearoyl-*sn*-glycero-3-phosphoethanolamine-*N*-[methoxy(poly(ethylene glycol))-2000] and has antibodies coupled to the distal end of the PEG-chains. Adapted from [35].

3.1.2 Other nanosystems

Besides liposomes, also other gadolinium-loaded colloidal carriers have been developed for MRI. Examples are solid lipid nanoparticles [55], artificial virus-like envelopes [56] and even micelles (with a size below 50 nm) [57]. Micelles consist of amphiphilic molecules which organize themselves spontaneously in

an aqueous environment in particles with a hydrophobic core and a hydrophilic shell. To associate gadolinium stably with micelles, amphiphiles consisting of a hydrophilic chelating group and a hydrophobic tail are incorporated into micelles. Gadolinium can then be coupled to the outside of the micelles which give them a very high relaxivity. The used amphiphilic molecules are comparable to those applied for the formation of liposomes (see Fig. (1)) [58,59].

Accardo et al. [60] designed a tumour specific micellar MRI contrast agent. They coupled a cholecystokinin octapeptide (CCK8) using two oxoethylene linkers and a glycine residue to a C18 tail (C18CCK8). Their CCK8 peptide has a very high affinity for cholecystokinin receptors which are overexpressed in many tumour cells. Gadolinium was coupled to another C18 chain by a DTPA-glutamate complex ((C18DTPAGlu)(see Fig. (3)). The micelles were not tested in vivo yet, but in vitro measurements showed a very high relaxivity and thus promising features for these systems.

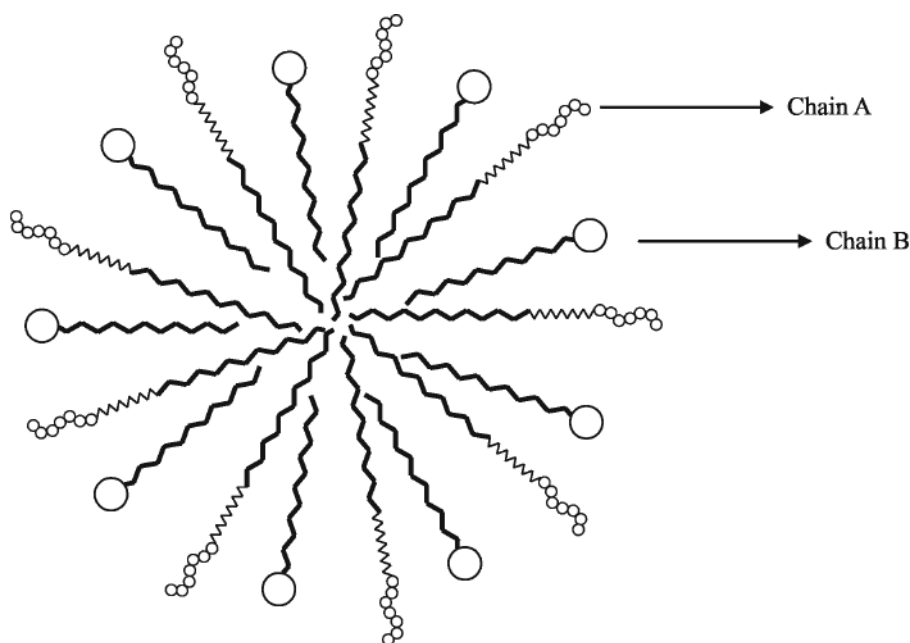


Fig. 3 Schematic representation of a micel according to Accardo et al. [60]. Chain A represents $C_{18}H_{37}CONH(AdOO)_2-G-CCK8$ abbreviated as (C18CCK8). Chain B represents $C_{18}H_{37}CONHLys(DTPAGlu(Gd))CONH_2$ abbreviated as (C18DTPAGlu(Gd)).

3.1.3 Polymer based systems

Polymers play an important role in the design of advanced drug delivery systems and many polymer-based MRI contrast agents have been developed so far. One of the most frequently used polymers is the polysaccharide dextran. The chelators DTPA and DOTA can be linked to the hydroxyl groups [61,62] of dextran or they can be coupled via amide (to aminated dextran) [63] and ester bonds [64]. Such systems are suitable for the detection of the lymphatic drainage in the liver [65]. Other DTPA-modified polymers that have been used for the coupling of gadolinium are poly(L-lysine) [66], inulin [67] and poly(L-glutamic acid) [68]. The latter mentioned polymer was used for 3D MR imaging of nude mice bearing human ovarian carcinoma.

Gadolinium-DTPA has also been coupled to PEG for MRI contrast enhancement and to prolong its circulation time [69,70]. Dafni et al. [71-73] used gadolinium-DTPA-labelled albumin to visualize the lymphatic drain and peritumoural interstitial convection with MRI. The aim of their work was to determine if these processes were affected by vascular endothelial growth factor (VEGF) induced hyperpermeability and their results in a mouse model indeed revealed that there was a direct role for VEGF.

3.2 CT

Due to the fact that lanthanides have a very high density they can be deployed as X-ray Computed Tomography (CT) contrast agents [74]. Krause et al. developed a lanthanide-based liver specific contrast agent for the detection of liver tumours [75-78]. Dysprosium, gadolinium and ytterbium were coupled to ethoxybenzyl diethylenetriamine pentaacetic acid (EOB-DTPA) and after intravenous injection of these contrast agents in rabbits, liver tumours were successfully detected with CT [75]. A comparable animal model was used by Vera et al. [79] who synthesized a water soluble CT contrast agent by labelling dextran with dysprosium-DTPA, and were able to detect implanted VX2-tumours. Microparticles with a size between 1-4 μm consisting of glutaraldehyde crosslinked albumin loaded with gadolinium oxide and gadolinium were prepared by McDonald et al. [80]. The authors concluded that their particles were suitable for multimodality imaging with both CT and MRI, although this was not verified by animal studies.

4. Imaging and Therapy

4.1 Radionuclides

A number of lanthanides are used as medical useful radionuclides [81-91]. A summary of the physical characteristics of these radionuclides is given in Table 3. These isotopes can be produced by neutron irradiation in a nuclear reactor, or with protons using an accelerator, or they can be obtained from a generator. As shown in Table 3, all β -emitters from the group of lanthanides that are suitable for cancer therapy also emit γ -rays. These γ -rays can in most cases (depending on their energy) be used for imaging with a gamma camera to follow the biodistribution and allow dosimetry.

The radionuclides can be directly injected into tumours, e.g. melanoma, as simple salts like holmium-166 nitrate [92] or they can be chelated to agents like DTPA and targeted to bone metastases [85]. Instead of 'normal' chelators, fullerenes were used to create stable water soluble lanthanide systems by incorporating the metal ions into the carbon cage of the fullurene structure [93]. More advanced targeting of radionuclides to bone metastases was achieved by cou-

pling of these nuclides to bone seeking phosphonates [94-98] and polyphosphonates [86]. Samarium-153-lexidronam is an example of a phosphonate [99] and clinical trials have demonstrated that this agent was active in the relief of pain associated with metastatic bone lesions derived from several tumour types [100,101].

Lanthanides like lutetium were also complexed with chelator conjugated monoclonal antibodies that target tumour-associated antigens [90,91,102-104] or to peptides like bombesin [83] and octreotide [84,105]. The latter mentioned peptide was labelled with lutetium-177 and successfully applied in patients with gastroenteropancreatic tumours [106,107].

Holmium-166 and dysprosium-165 are radionuclides that have been incorporated into microparticles or macroaggregates [9,108-132]. Microparticles can be used for treatment of malignancies by direct injection into a tumour [129] or by an embolization procedure [126]. Radioactive lanthanides can be directly labelled to chitosan [129,130], resin [131] or ferric hydroxide macroaggregates [108-111]. Lanthanides have also been incorporated into glass [112-115,132] or polymer [9,117-121,123-128] based systems like microspheres which are neutron activated after preparation of the lanthanide-loaded particles. Our research group has developed polymer-based microspheres for radionuclide therapy of liver malignancies [124]. Holmium-165-acetylacetonate (HoAcAc) was incorporated into microspheres of poly(L-lactic acid) (PLLA). These microspheres were made radioactive with thermal neutrons in a nuclear reactor. Although the molecular weight of the PLLA decreased due to the neutron irradiation, the microspheres retained their integrity [124] and the leaching of holmium-166 in urine and faeces of treated rabbits was less than 0.1% in 2 days [128]. In vivo studies (rat) demonstrated that these microspheres were successfully targeted to liver tumours; the tumour to normal liver tissue ratio was about 6:1. As shown in Table 2, holmium has a very high magnetic susceptibility. This means that the presence of holmium in human tissue affects the MRI signal. The resultant signal change is dependent on the holmium concentration, which allows direct visualization of radioactive and non-radioactive holmium microspheres and exploitation for dosimetric studies [9]. This phenomenon has been successfully applied in tumour bearing rabbits. Holmium microspheres were administrated via the hepatic artery of the rabbit and visualized with both scintigraphy and MRI (see Fig. (4))[9].

Table 3. Lanthanides as Radionuclides

Radionuclide	Half-life (h)	γ (MeV)	β_{\max} (MeV)	α (MeV)	Production*
La-140	40	0.487 0.329	1.31 2.18		N, G
Pm-149	53	0.286	1.07		N
Sm-153	46.8	0.070 0.103	0.80		N
Tb-149	4.2	**	β^-	3.97	P
Tb-152	17.5	0.344	β^+		P
Dy-165	2.4	0.095	1.29		N
Ho-166	26.8	0.081	1.84 1.78		N
Er-169	230.4	0.008	0.34		N
Yb-175	100.8	0.113 0.144 0.286 0.396	0.48		N
Lu-177	160.8	0.208 0.113	0.50		N

*production of radionuclides with neutrons (N), protons (P) or a generator (G)

**The decay of Tb-149 results in the emission of many intense gamma rays with energies between 0.165 and 0.853 MeV.

Whereas β -emitters are used for treatment of lesions with a size of a few millimetres, α -emitters have the potency to be used for treatment of micro-metastases [133]. Due to the short range of α -radiation (< 100 nm), the radionuclide must be targeted into the tumour cells. Importantly, when successful targeting has been achieved with an α -emitter loaded microparticle or nanoparticle, the total radiation dose on healthy tissue will be lower than the dose of a β -emitter [134]. Terbium-149 is a radionuclide that emits α -particles and has been used for cancer therapies [135]. Here, the radionuclide was complexed via a chelator to immunoconjugates [136-138]. Beyer et al. labelled a CD-20 targeting antibody (rituximab) with terbium and proved in a mouse model that single cancer cells could be sterilized [87]. Another interesting terbium-isotope is terbium-152, a positron emitter that has been used for positron emission tomography (PET) [88]. It has a relatively long half life of 17.5 h which allows longer function times and easier logistics than currently used PET-tracers such as fluorine-18. However, it must be realised that the production of these terbium isotopes is very complex and requires advanced facilities.

4.2 Neutron Capture Therapy

Gadolinium-157 (Gd-157) is a stable element with a thermal neutron capture cross-section of 254,000 barn, the highest of all naturally occurring isotopes [139]. Because of this high cross section Gd-157 is very easy to activate with neutrons even in vivo [140]. The Gd-157 neutron capture reaction produces high-energy γ -rays, internal conversion electrons and Auger electrons which are suitable for cancer therapy [139].

There are many pharmaceutical approaches to achieve targeting of gadolinium to tumour cells. Chitosan microparticles and nanoparticles loaded with gadolinium-DTPA were directly injected into solid tumours [141-144]. The nanoparticles were successfully applied in mice bearing subcutaneous melanoma; after 60 min of neutron irradiation tumour growth was significantly suppressed [143]. Comparable results were obtained by Matsumura et al. [145] after intratumoral injection of gadolinium-dimeglumine. It must be realised that intratumoral injection is only applicable for one or a few solitary tumours and that treatment of multiple metastases requires other approaches. Nanoparticles with a size below 100 nm can easily penetrate the tumour tissue through the discontinuous capillary endothelium in the tumour, the so-called EPR effect (enhanced

permeation and retention) [146-148]. Intravenous injection of gadolinium-loaded lipid nanoemulsions into tumour bearing hamsters resulted in relatively high tumour concentrations of gadolinium. Unfortunately, the gadolinium concentrations in liver and spleen were even higher [147], and it can therefore be questioned if these particles are suitable for clinical application. Oyewumi et al. [149-151] suggested that folate-coated nanoparticles could be delivered more specifically to tumour cells. Human cancer cells overexpress folate receptors and binding of folic acid modified nanoparticles to these receptors results in receptor mediated endocytosis. Nanoparticles were made of polyoxyl 20 stearyl ether and PEG-400 monostearate or emulsifying wax, and gadolinium was incorporated as its acetylacetonate or hexanedione complex. Folate was linked to distearoyl ethanolamine and the resulting folate ligand was used for coating of nanoparticles [149,151]. In vivo experiments with these folate coated nanoparticles were done in tumour bearing mice. PEG coated nanoparticles without targeting ligand were used as a control [150]. Both particles had a com

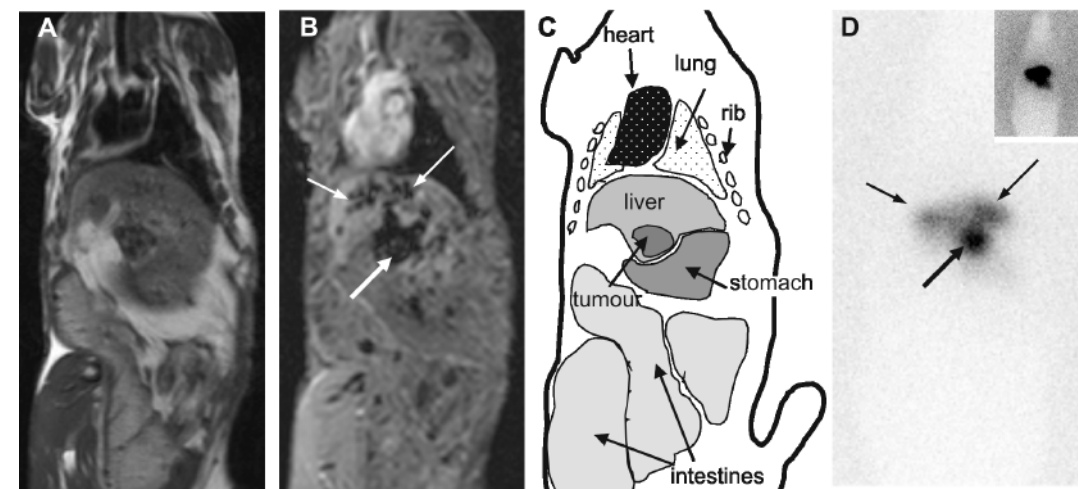


Fig. 4 Coronal MR and scintigraphic images of a tumour-bearing rabbit treated with holmium microspheres **A**: Anatomic T1-weighted spin-echo MR image **B**: Holmium-sensitive T2*-weighted fast field echo MRI image showing the biodistribution of holmium microspheres in relation to the surrounding areas. Increased accumulations of paramagnetic holmium are seen on the T2*-weighted MR image as signal voids (small arrows) due to the paramagnetic nature of the holmium. The larger arrow indicates the substantial accumulation of microspheres in and around the tumour. **C**: Schematic representation shows the organs and tumour in the rabbit. **D**: Whole-body scintigraphic image of the rabbit. Increased accumulation of radioactivity due to holmium microspheres is indicated by small arrows. Larger arrow shows increased radioactivity in and around the tumour. Adapted from [9].

parable biodistribution and tumour accumulation. This was in contrast to in vitro studies where higher concentrations of gadolinium in tumour cells were observed for the folate coated nanoparticles [151]. The authors concluded that accumulation of their nanoparticles in tumours was mainly driven by particle extravasation via the leaky microvasculature. The same group also used thiamine, which transporters are also overexpressed in tumour cells, for coating of their nanoparticles [152], but these nanoparticles were not tested in vivo yet. Kobayashi et al. [153] proposed polyamidoamine dendrimers as suitable carriers for gadolinium neutron capture therapy. These dendrimers are water-soluble highly branched spherical polymers which have at their surface 256 amine groups. To these amine groups, about one molecule of biotin (as a targeting ligand) and 254 molecules of the chelating agent (2-(*p*-isothiocyanatobenzyl)-6-methyl-diethylene triamine penta-acetic acid)) were coupled. After labelling with gadolinium, these dendrimers were injected intraperitoneally in tumour bearing mice, and after 1 day the tumour to non-tumour ratio was up to 638:1. In vitro MRI measurements showed an adequate MRI signal enhancement, and the authors suggested that the biodistribution of their dendrimer could be monitored with MRI.

Table 4. Imaging characteristics of lanthanide radionuclides

Element	radionuclide therapy	gamma camera	MRI*	CT
La-140	β	yes	no	yes
Pm-149	β	yes	no	yes
Sm-153	β	yes	no	yes
Gd-157	neutron capture	no	yes	yes
Tb-149	α	yes (and PET)	yes	yes
Tb-152	no	PET	yes	yes
Dy-165	β	yes	yes	yes
Ho-166	β	yes	yes	yes
Er-169	β	no	yes	yes
Yb-175	β	yes	no	yes
Lu-177	β	yes	no	yes

* especially in case of T2*-weighted MRI

5. Perspective

This review shows that lanthanides are attractive nuclides in cancer diagnosis and therapy. The use of advanced drug delivery technology and the introduction of paramagnetic gadolinium has resulted in nanoparticulate and microparticulate systems with very promising MRI contrast properties for the detection of cancer. Other paramagnetic lanthanides such as erbium, dysprosium, terbium and holmium have also been used for advanced drug delivery based radionuclide therapies, whereas nuclear imaging and/or MRI and/or CT can be used for monitoring the biodistribution of these systems. A summary of the imaging characteristics of radionuclides within the group of lanthanides is given in Table 4. This table shows that dysprosium and holmium are elements that can be visualised with all these imaging modalities. Combined with the ideal half-life of holmium (26.8 h, which allows good logistics) it makes this element the ideal candidate for radionuclide therapies, as shown by our group [9].

Tb-149 is an α -emitter which can be applied for cancer therapy and Tb-152 is a positron emitter which can be used for PET. Since Tb is highly paramagnetic it can also be imaged with MRI allowing multimodality imaging of Tb-based radionuclide therapies. However, it should be realised that the production of terbium isotopes is very complicated and requires advanced technologies.

Gadolinium-loaded microparticulate systems have the possibility to be deployed for cancer treatment using the neutron capture principle. Before subjecting a patient to neutron irradiation, the biodistribution of the administered gadolinium delivery vehicle can be monitored with MRI. However, neutron capture therapies require advanced reactor facilities and thus are very expensive. Therefore, gadolinium neutron capture therapy has not been applied in patients yet.

Lanthanides are elements with very similar chemical properties. Therefore, different lanthanides can be labelled to the same system, combining in this way the best diagnostic or therapeutic properties of these elements. The development of new lanthanide loaded diagnostic and therapeutic agents combined with the improvement of medical imaging techniques (higher resolution CT scanners, MRI scanners and gamma cameras) and the development of multimodality imaging (like PET-CT and SPECT-CT) will lead to the major goal of molecular imaging: combining early stage cancer diagnosis with an optimised patient specific therapy and monitoring.

Acknowledgements

This research was supported by the Technology Foundation STW (UGT.6069), applied science division of NWO and the technology programme of the Ministry of Economic Affairs.

References

- [1] Massoud TF, Gambhir SS. Molecular imaging in living subjects: seeing fundamental biological processes in a new light. *Genes Dev* 2003; 17: 545-80.
- [2] Brigger I, Dubernet C, Couvreur P. Nanoparticles in cancer therapy and diagnosis. *Adv Drug Deliv Rev* 2002; 54: 631-51.
- [3] Brannon-Peppas L, Blanchette JO. Nanoparticle and targeted systems for cancer therapy. *Adv Drug Deliv Rev* 2004; 56: 1649-59.
- [4] Crommelin DJ, Storm G, Jiskoot W, Stenekes R, Mastrobattista E, Hennink WE. Nanotechnological approaches for the delivery of macromolecules. *J Control Release* 2003; 87: 81-8.
- [5] Mastrobattista E, Kapel RH, Eggenhuisen MH, Roholl PJ, Crommelin DJA, Hennink WE, Storm G. Lipid-coated polyplexes for targeted gene delivery to ovarian carcinoma cells. *Cancer Gene Ther* 2001; 8: 405-13.
- [6] Saito R, Bringas JR, McKnight TR, Wendland MF, Mamot C, Drummond DC, Kirpotin DB, Park JW, Berger MS, Bankiewicz KS. Distribution of liposomes into brain and rat brain tumor models by convection-enhanced delivery monitored with magnetic resonance imaging. *Cancer Res* 2004; 64: 2572-9.
- [7] Wunderlich G, Gruning T, Paulke BR, Lieske A, Kotzerke J. ^{99m}Tc labelled model drug carriers - labeling, stability and organ distribution in rats. *Nucl Med Biol* 2004; 31: 87-92.
- [8] Thunus L, Lejeune R. Overview of transition metal and lanthanide complexes as diagnostic tools. *Coord Chem Rev* 1999; 184: 125-55.
- [9] Nijssen JFW, Seppenwoolde JH, Havenith T, Bos C, Bakker CJG, van het Schip AD. Liver Tumors: MR Imaging of Radioactive Holmium Microspheres—Phantom and Rabbit Study. *Radiology* 2004;231:491-9.
- [10] Beedle AM, Hamid J, Zamponi GW. Inhibition of transiently expressed low- and high-voltage-activated calcium channels by trivalent metal cations. *J Membrane Biol* 2002; 187: 225-38.
- [11] Cheng Y, Liu MZ, Li RC, Wang C, Bai CL, Wang K. Gadolinium induces domain and pore formation of human erythrocyte membrane: an atomic force microscopic study. *Biochimica et Biophysica Acta-Biomembranes* 1999; 1421: 249-60.
- [12] Pearson RG. The HSAB principle - More quantitative aspects. *Inorganica Chimica Acta* 1995; 240: 93-8.
- [13] Wang K, Li RC, Cheng Y, Zhu B. Lanthanides - the future drugs? *Coordination Chemistry Reviews* 1999; 192: 297-308.
- [14] Taylor DM, Leggett RW. A generic biokinetic model for predicting the behaviour of the lanthanide elements in the human body. *Radiation Protection Dosimetry* 2003; 105: 193-8.
- [15] Bartolini ME, Pekar J, Chettle DR, McNeill F, Scott A, Sykes J, Prato FS, Moran GR. An investigation of the toxicity of gadolinium based MRI contrast agents using neutron activation analysis. *Magnetic Resonance Imaging* 2003; 21: 541-4.
- [16] Hardonk MJ, Dijkhuis FWJ, Hulstaert CE, Koudstaal J. Heterogeneity of Rat-Liver and Spleen Macrophages in Gadolinium Chloride-Induced Elimination and Repopulation. *Journal of Leukocyte Biology* 1992; 52: 296-302.
- [17] Pereira DTB, Nozaki PN, Menani JV, Colombari E, De Luca LA, Schoorlemmer GHM. Effect of the gadolinium ion on body fluid regulation. *Pharmacology Biochemistry and Behavior* 2003; 76: 275-83.
- [18] Arvela P. Toxicity of rare-earths. *Progress in Pharmacology* 2, 73-113. 1979.
- [19] Graca JG, Davison FC, Feavel JB. Comparative Toxicity of stable Rare Earth Compounds. *Arch.Environ.Health.* 5, 437-444. 1962.
- [20] Haley TJ, Koste L, Komesu N, Efros MUHC. Pharmacology and Toxicology of Dysprosium, Holmium, and Erbium Chlorides. *Tox.App.Pharm.* 8, 37-43. 1966.
- [21] Handbook of Chemistry and Physics, 84th edition. CRC Press, Boca Raton (FL) 2003.
- [22] Fossheim S, Johansson C, Fahlvik AK, Grace D, Klaveness J. Lanthanide-based susceptibility contrast agents: assessment of the magnetic properties. *Magn Reson Med* 1996; 35: 201-6.
- [23] Knopp MV, Runge VM, Essig M, Hartman M, Jansen O, Kirchin MA, Moeller A, Seeberg AH, Lodemann KP. Primary and secondary brain tumors at MR imaging: Bicentric intraindividual crossover comparison of gadobenate dimeglumine and gadopentetate dimeglumine. *Radiology* 2004; 230: 55-64.
- [24] Engelbrecht MR, Huisman HJ, Laheij RJF, Jager GJ, van Leenders GJLH, Hulsbergen-Van De Kaa CA, de la Rosette JJMC, Blickman JG, Barentsz JO. Discrimination of prostate cancer from normal peripheral zone and central gland tissue by using dynamic contrast-enhanced MR imaging. *Radiology* 2003; 229: 248-54.
- [25] Eliaz RE, Nir S, Marty C, Szoka FC. Determination and modeling of kinetics of cancer cell killing by doxorubicin and doxorubicin encapsulated in targeted liposomes. *Cancer Research* 2004; 64: 711-8.
- [26] van Broekhoven CL, Parish CR, Demangel C, Britton WJ, Altin JG. Targeting dendritic cells with antigen-containing liposomes: A highly effective procedure for induction of antitumor immunity and for tumor immunotherapy. *Cancer Research* 2004; 64: 4357-65.
- [27] Gabizon A, Horowitz AT, Goren D, Tzemach D, Shmeeda H, Zalipsky S. In vivo fate of folate-targeted polyethylene-glycol liposomes in tumor-bearing mice. *Clinical Cancer Research* 2003; 9: 6551-9.
- [28] Peer D, Margalit R. Loading mitomycin C inside long circulating hyaluronan targeted nano-liposomes increases its antitumor activity in three mice tumor models. *International Journal of Cancer* 2004; 108: 780-9.
- [29] Glogard C, Stensrud G, Hovland R, Fossheim SL, Klaveness J. Liposomes as carriers of amphiphilic gadolinium chelates: the effect of membrane composition on incorporation efficacy and in vitro relaxivity. *International Journal of Pharmaceutics* 2002; 233: 131-40.

- [30] Trubetskoy VS, Cannillo JA, Milshtein A, Wolf GL, Torchilin VP. Controlled Delivery of Gd-Containing Liposomes to Lymph-Nodes - Surface Modification May Enhance Mri Contrast Properties. *Magnetic Resonance Imaging* 1995; 13: 31-7.
- [31] Lokling KE, Skurtveit R, Dyrstad K, Klaveness J, Fossheim SL. Tuning the MR properties of blood-stable pH-responsive paramagnetic liposomes. *International Journal of Pharmaceutics* 2004; 274: 75-83.
- [32] Lokling KE, Fossheim SL, Skurtveit R, Bjornerud A, Klaveness J. pH-sensitive paramagnetic liposomes as MRI contrast agents: in vitro feasibility studies. *Magnetic Resonance Imaging* 2001; 19: 731-8.
- [33] Lokling KE, Skurtveit R, Bjornerud A, Fossheim SL. Novel pH-sensitive paramagnetic liposomes with improved MR properties. *Magnetic Resonance in Medicine* 2004; 51: 688-96.
- [34] Lokling KE, Skurtveit R, Fossheim SL, Smistad G, Henriksen I, Klaveness J. pH-Sensitive paramagnetic liposomes for MRI: assessment of stability in blood. *Magnetic Resonance Imaging* 2003; 21: 531-40.
- [35] Mulder WJ, Strijkers GJ, Griffioen AW, van Bloois L, Molema G, Storm G, Koning GA, Nicolay K. A liposomal system for contrast-enhanced magnetic resonance imaging of molecular targets. *Bioconjug Chem* 2004; 15: 799-806.
- [36] Yen TC, See LC, Lai CH, Yah-Huei CW, Ng KK, Ma SY, Lin WJ, Chen JT, Chen WJ, Lai CR, Hsueh S. 18F-FDG uptake in squamous cell carcinoma of the cervix is correlated with glucose transporter 1 expression. *J Nucl Med* 2004; 45: 22-9.
- [37] Luciani A, Olivier JC, Clement O, Siauve N, Brillet PY, Bessoud B, Gazeau F, Uchegbu IF, Kahn E, Frija G, Cuenod CA. Glucose-receptor MR imaging of tumors: study in mice with PEGylated paramagnetic liposomes. *Radiology* 2004; 231: 135-42.
- [38] Reimer P. Tumor-targeted MR contrast agents: hype or future hope? *Radiology* 2004; 231: 1-2.
- [39] Plut EM, Hinkle GH, Guo W, Lee RJ. Kit formulation for the preparation of radioactive blue liposomes for sentinel node lymphoscintigraphy. *J Pharm Sci* 2002; 91: 1717-32.
- [40] Gaston MS, Dixon JM. A survey of surgical management of the axilla in UK breast cancer patients. *Eur J Cancer* 2004; 40: 1738-42.
- [41] Suga K, Yuan Y, Ogasawara N, Okada M, Matsunaga N. Localization of breast sentinel lymph nodes by MR lymphography with a conventional gadolinium contrast agent. Preliminary observations in dogs and humans. *Acta Radiol* 2003; 44: 35-42.
- [42] Kobayashi H, Kawamoto S, Sakai Y, Choyke PL, Star RA, Brechbiel MW, Sato N, Tagaya Y, Morris JC, Waldmann TA. Lymphatic drainage imaging of breast cancer in mice by micro-magnetic resonance lymphangiography using a nano-size paramagnetic contrast agent. *J Natl Cancer Inst* 2004; 96: 703-8.
- [43] Kobayashi H, Kawamoto S, Star RA, Waldmann TA, Tagaya Y, Brechbiel MW. Micro-magnetic resonance lymphangiography in mice using a novel dendrimer-based magnetic resonance imaging contrast agent. *Cancer Res* 2003; 63: 271-6.

- [44] Kobayashi H, Kawamoto S, Choyke PL, Sato N, Knopp MV, Star RA, Waldmann TA, Tagaya Y, Brechbiel MW. Comparison of dendrimer-based macromolecular contrast agents for dynamic micro-magnetic resonance lymphangiography. *Magn Reson Med* 2003; 50: 758-66.
- [45] Harisinghani MG, Barentsz J, Hahn PF, Deserno WM, Tabatabaei S, van de Kaa CH, de la RJ, Weissleder R. Noninvasive detection of clinically occult lymph-node metastases in prostate cancer. *N Engl J Med* 2003; 348: 2491-9.
- [46] Harisinghani MG, Barentsz JO, Hahn PF, Deserno W, de la RJ, Saini S, Marten K, Weissleder R. MR lymphangiography for detection of minimal nodal disease in patients with prostate cancer. *Acad Radiol* 2002; 9 Suppl 2: S312-S313.
- [47] Misselwitz B, Sachse A. Interstitial MR lymphography using Gd-carrying liposomes. *Acta Radiol Suppl* 1997; 412: 51-5.
- [48] Fujimoto Y, Okuhata Y, Tyngi S, Namba Y, Oku N. Magnetic resonance lymphography of profundus lymph nodes with liposomal gadolinium-diethylenetriamine pentaacetic acid. *Biol Pharm Bull* 2000; 23: 97-100.
- [49] Yang W, Barth RF, Adams DM, Ciesielski MJ, Fenstermaker RA, Shukla S, Tjarks W, Caligiuri MA. Convection-enhanced delivery of boronated epidermal growth factor for molecular targeting of EGF receptor-positive gliomas. *Cancer Res* 2002; 62: 6552-8.
- [50] Mamot C, Nguyen JB, Pourdehnad M, Hadaczek P, Saito R, Bringas JR, Drummond DC, Hong K, Kirpotin DB, McKnight T, Berger MS, Park JW, Bankiewicz KS. Extensive distribution of liposomes in rodent brains and brain tumors following convection-enhanced delivery. *J Neurooncol* 2004; 68: 1-9.
- [51] Wust P, Hildebrandt B, Sreenivasa G, Rau B, Gellermann J, Riess H, Felix R, Schlag PM. Hyperthermia in combined treatment of cancer. *Lancet Oncol* 2002; 3: 487-97.
- [52] McDannold N, Fossheim SL, Rasmussen H, Martin H, Vykhodtseva N, Hynynen K. Heat-activated liposomal MR contrast agent: initial in vivo results in rabbit liver and kidney. *Radiology* 2004; 230: 743-52.
- [53] Fossheim SL, Fahlvik AK, Klaveness J, Muller RN. Paramagnetic liposomes as MRI contrast agents: influence of liposomal physicochemical properties on the in vitro relaxivity. *Magn Reson Imaging* 1999; 17: 83-9.
- [54] Fossheim SL, Il'yasov KA, Hennig J, Bjornerud A. Thermosensitive paramagnetic liposomes for temperature control during MR imaging-guided hyperthermia: in vitro feasibility studies. *Acad Radiol* 2000; 7: 1107-15.
- [55] Morel S, Terreno E, Ugazio E, Aime S, Gasco MR. NMR relaxometric investigations of solid lipid nanoparticles (SLN) containing gadolinium(III) complexes. *Eur J Pharm Biopharm* 1998; 45: 157-63.
- [56] Heverhagen JT, Graser A, Fahr A, Muller R, Alfke H. Encapsulation of gadobutrol in AVE-based liposomal carriers for MR detectability. *Magn Reson Imaging* 2004; 22: 483-7.
- [57] Glogard C, Stensrud G, Klaveness J. Novel high relaxivity colloidal particles based on the specific phase organisation of amphiphilic gadolinium chelates with cholesterol. *Int J Pharm* 2003; 253: 39-48.
- [58] Trubetskoy VS, Frank-Kamenetsky MD, Whiteman KR, Wolf GL, Torchilin VP. Stable polymeric

- micelles: lymphangiographic contrast media for gamma scintigraphy and magnetic resonance imaging. *Acad Radiol* 1996; 3: 232-8.
- [59] Hovland R, Glogard C, Aasen AJ, Klaveness J. Preparation and in vitro evaluation of a novel amphiphilic GdPCTA-[12] derivative; a micellar MRI contrast agent. *Org Biomol Chem* 2003; 1: 644-7.
- [60] Accardo A, Tesaro D, Roscigno P, Gianolio E, Paduano L, D'Errico G, Pedone C, Morelli G. Physicochemical properties of mixed micellar aggregates containing CCK peptides and Gd complexes designed as tumor specific contrast agents in MRI. *J Am Chem Soc* 2004; 126: 3097-107.
- [61] Hosseinkhani H, Aoyama T, Ogawa O, Tabata Y. Tumor targeting of gene expression through metal-coordinated conjugation with dextran. *J Control Release* 2003; 88: 297-312.
- [62] Tabata Y, Noda Y, Matsui Y, Ikada Y. Targeting of tumor necrosis factor to tumor by use of dextran and metal coordination. *J Control Release* 1999; 59: 187-96.
- [63] Rebizak R, Schaefer M, Dellacherie E. Macromolecular contrast agents for magnetic resonance imaging. Influence of polymer content in ligand on the paramagnetic properties. *Eur J Pharm Sci* 1999; 7: 243-8.
- [64] Rongved P, Fritzell TH, Strande P, Klaveness J. Polysaccharides as carriers for magnetic resonance imaging contrast agents: Synthesis and stability of a new amino acid linker derivative. *Carbohydrate Research* 1996; 287: 77-89.
- [65] Siauve N, Clement O, Cuenod CA, Benderbous S, Frija G. Capillary leakage of a macromolecular MRI agent, carboxymethyl-dextran-Gd-DTPA, in the liver: Pharmacokinetics and imaging implications. *Magnetic Resonance Imaging* 1996; 14: 381-90.
- [66] Weissig V, V, Babich J, Torchilin V, V. Long-circulating gadolinium-loaded liposomes: potential use for magnetic resonance imaging of the blood pool. *Colloids Surf B Biointerfaces* 2000; 18: 293-9.
- [67] Lebduskova P, Kotek J, Hermann P, Vander EL, Muller RN, Lukes I, Peters JA. A gadolinium(III) complex of a carboxylic-phosphorus acid derivative of diethylenetriamine covalently bound to inulin, a potential macromolecular MRI contrast agent. *Bioconjug Chem* 2004; 15: 881-9.
- [68] Lu ZR, Wang X, Parker DL, Goodrich KC, Buswell HR. Poly(L-glutamic acid) Gd(III)-DOTA conjugate with a degradable spacer for magnetic resonance imaging. *Bioconjug Chem* 2003; 14: 715-9.
- [69] Unger EC, Shen D, Wu G, Stewart L, Matsunaga TO, Trouard TP. Gadolinium-containing copolymeric chelates—a new potential MR contrast agent. *MAGMA* 1999; 8: 154-62.
- [70] Li KC, Pelc LR, Napel SA, Goris ML, Lin DT, Song CK, Leung AN, Rubin GD, Hollett MD, Harris DP. MRI of pulmonary embolism using Gd-DTPA-polyethylene glycol polymer enhanced 3D fast gradient echo technique in a canine model. *Magn Reson Imaging* 1997; 15: 543-50.
- [71] Dafni H, Israely T, Bhujwalla ZM, Benjamin LE, Neeman M. Overexpression of vascular endothelial growth factor 165 drives peritumor interstitial convection and induces lymphatic drain: magnetic resonance imaging, confocal microscopy, and histological tracking of triple-labeled albumin. *Cancer Res* 2002; 62: 6731-9.
- [72] Dafni H, Landsman L, Schechter B, Kohen F, Neeman M. MRI and fluorescence microscopy of the acute

- vascular response to VEGF165: vasodilation, hyper-permeability and lymphatic uptake, followed by rapid inactivation of the growth factor. *NMR Biomed* 2002; 15: 120-31.
- [73] Dafni H, Gilead A, Nevo N, Eilam R, Harmelin A, Neeman M. Modulation of the pharmacokinetics of macromolecular contrast material by avidin chase: MRI, optical, and inductively coupled plasma mass spectrometry tracking of triply labeled albumin. *Magn Reson Med* 2003; 50: 904-14.
- [74] Cardinal HN, Holdsworth DW, Drangova M, Hobbs BB, Fenster A. Experimental and theoretical x-ray imaging performance comparison of iodine and lanthanide contrast agents. *Med Phys* 1993; 20: 15-31.
- [75] Krause W, Handreke K, Schuhmann-Giampieri G, Rupp K. Efficacy of the iodine-free computed tomography liver contrast agent, Dy-EOB-DTPA, in comparison with a conventional iodinated agent in normal and in tumor-bearing rabbits. *Invest Radiol* 2002; 37: 241-7.
- [76] Krause W, Mahler M, Hanke B, Milius W, Kaufmann J, Rogalla P, Hamm B. Dy-EOB-DTPA: tolerance and pharmacokinetics in healthy volunteers and preliminary liver imaging in patients. *Invest Radiol* 2001; 36: 431-44.
- [77] Krause W, Schuhmann-Giampieri G, Bauer M, Press WR, Muschick P. Ytterbium- and dysprosium-EOB-DTPA. A new prototype of liver-specific contrast agents for computed tomography. *Invest Radiol* 1996; 31: 502-11.
- [78] Schmitz SA, Wagner S, Schuhmann-Giampieri G, Krause W, Wolf KJ. A prototype liver-specific contrast medium for CT: preclinical evaluation of gadoxetic acid disodium, or Gd-EOB-DTPA. *Radiology* 1997; 202: 407-12.
- [79] Vera DR, Mattrey RF. A molecular CT blood pool contrast agent. *Acad Radiol* 2002; 9: 784-92.
- [80] McDonald MA, Watkin KL. Small particulate gadolinium oxide and gadolinium oxide albumin microspheres as multimodal contrast and therapeutic agents. *Investigative Radiology* 2003; 38: 305-10.
- [81] Nijssen JFW, van het Schip AD, Hennink WE, Rook DW, van Rijk PP, De Klerk JMH. Advances in nuclear oncology: Microspheres for internal radionuclide therapy of liver metastases. *Curr Med Chem* 2002; 9: 73-82.
- [82] Neves M, Kling A, Lambrecht RM. Radionuclide production for therapeutic radiopharmaceuticals. *Appl Radiat Isot* 2002; 57: 657-64.
- [83] Hu F, Cutler CS, Hoffman T, Sieckman G, Volkert WA, Jurisson SS. Pm-149 DOTA bombesin analogs for potential radiotherapy. in vivo comparison with Sm-153 and Lu-177 labeled DO3A-amide-betaAla-BBN(7-14)NH(2). *Nucl Med Biol* 2002; 29: 423-30.
- [84] Li WP, Smith CJ, Cutler CS, Hoffman TJ, Ketring AR, Jurisson SS. Aminocarboxylate complexes and octreotide complexes with no carrier added 177Lu, 166Ho and 149Pm. *Nucl Med Biol* 2003; 30: 241-51.
- [85] Li WP, Ma DS, Higginbotham C, Hoffman T, Ketring AR, Cutler CS, Jurisson SS. Development of an in vitro model for assessing the in vivo stability of lanthanide chelates. *Nucl Med Biol* 2001; 28: 145-54.
- [86] Mathew B, Chakraborty S, Das T, Sarma HD, Banerjee S, Samuel G, Venkatesh M, Pillai MR. 175Yb labeled polyaminophosphonates as potential agents for bone pain palliation. *Appl Radiat Isot* 2004; 60: 635-42.
- [87] Beyer GJ, Miederer M, Vranjes-Duric S, Comor JJ, Kunzi G, Hartley O, Senekowitsch-Schmidtke R, Soloviev D, Buchegger F. Targeted alpha therapy in vivo: direct evidence for single cancer cell kill using

- 149Tb-rituximab. *Eur J Nucl Med Mol Imaging* 2004; 31: 547-54.
- [88] Allen BJ, Goozee G, Sarkar S, Beyer G, Morel C, Byrne AP. Production of terbium-152 by heavy ion reactions and proton induced spallation. *Appl Radiat Isot* 2001; 54: 53-8.
- [89] Chakraborty S, Unni PR, Venkatesh M, Pillai MRA. Feasibility study for production of Yb-175: a promising therapeutic radionuclide. *Appl Radiat Isot* 2002; 57: 295-301.
- [90] Stimmel JB, Kull FC, Jr. Samarium-153 and lutetium-177 chelation properties of selected macrocyclic and acyclic ligands. *Nucl Med Biol* 1998; 25: 117-25.
- [91] Dadachova E, Mirzadeh S, et al. Radiolabeling Antibodies with Holmium-166. *Appl Radiat Isot* 48, 477-481. 1997.
- [92] Lee JD, Yang WI, Lee MG, Ryu YH, Park JH, Shin KH, Kim GE, Suh CO, Seong JS, Han BH, Choi CW, Kim EH, Kim KH, Park KB. Effective local control of malignant melanoma by intratumoural injection of a beta-emitting radionuclide. *Eur J Nucl Med Mol Imaging* 2002; 29: 221-30.
- [93] Cagle DW, Kennel SJ, Mirzadeh S, Alford JM, Wilson LJ. In vivo studies of fullerene-based materials using endohedral metallofullerene radiotracers. *Proc Natl Acad Sci USA* 1999; 96: 5182-7.
- [94] Giralt S, Bensinger W, Goodman M, Podoloff D, Eary J, Wendt R, Alexanian R, Weber D, Maloney D, Holmberg L, Rajandran J, Breitz H, Ghalie R, Champlin R. 166Ho-DOTMP plus melphalan followed by peripheral blood stem cell transplantation in patients with multiple myeloma: results of two phase 1/2 trials. *Blood* 2003; 102: 2684-91.
- [95] Rajendran JG, Eary JF, Bensinger W, Durack LD, Vernon C, Fritzberg A. High-dose 166Ho-DOTMP in myeloablative treatment of multiple myeloma: pharmacokinetics, biodistribution, and absorbed dose estimation. *J Nucl Med* 2002; 43: 1383-90.
- [96] Bayouth JE, Macey DJ, Kasi LP, Garlich JR, McMillan K, Dimopoulos MA, Champlin RE. Pharmacokinetics, dosimetry and toxicity of holmium-166-DOTMP for bone marrow ablation in multiple myeloma. *J Nucl Med* 1995; 36: 730-7.
- [97] Bartlett ML, Webb M, Durrant S, Morton AJ, Allison R, Macfarlane DJ. Dosimetry and toxicity of Quadramet for bone marrow ablation in multiple myeloma and other haematological malignancies. *Eur J Nucl Med Mol Imaging* 2002; 29: 1470-7.
- [98] Brenner W, Kampen WU, Brummer C, Von Forstner C, Zuhayra M, Czech N, Muhle C, Henze E. Bone uptake studies in rabbits before and after high-dose treatment with 153Sm-EDTMP or 186Re-HEDP. *J Nucl Med* 2003; 44: 247-51.
- [99] Sartor O, Reid RH, Hoskin PJ, Quick DP, Ell PJ, Coleman RE, Kotler JA, Freeman LM, Olivier P. Samarium-153-Lexidronam complex for treatment of painful bone metastases in hormone-refractory prostate cancer. *Urology* 2004; 63: 940-5.
- [100] Resche I, Chatal JF, Pecking A, Ell P, Duchesne G, Rubens R, Fogelman I, Houston S, Fauser A, Fischer

- M, Wilkins D. A dose-controlled study of 153Sm-ethylenediaminetetramethylenephosphonate (EDTMP) in the treatment of patients with painful bone metastases. *Eur J Cancer* 1997; 33: 1583-91.
- [101] Serafini AN, Houston SJ, Resche I, Quick DP, Grund FM, Ell PJ, Bertrand A, Ahmann FR, Orihuela E, Reid RH, Lerski RA, Collier BD, McKillop JH, Purnell GL, Pecking AP, Thomas FD, Harrison KA. Palliation of pain associated with metastatic bone cancer using samarium-153 lexidronam: a double-blind placebo-controlled clinical trial. *J Clin Oncol* 1998; 16: 1574-81.
- [102] Koppe MJ, Bleichrodt RP, Soede AC, Verhofstad AA, Goldenberg DM, Oyen WJ, Boerman OC. Biodistribution and therapeutic efficacy of (125/131)I-, (186)Re-, (88/90)Y-, or (177)Lu-labeled monoclonal antibody MN-14 to carcinoembryonic antigen in mice with small peritoneal metastases of colorectal origin. *J Nucl Med* 2004; 45: 1224-32.
- [103] Fani M, Vranjes S, Archimandritis SC, Potamianos S, Xanthopoulos S, Bouziotis P, Varvarigou AD. Labeling of monoclonal antibodies with 153Sm for potential use in radioimmunotherapy. *Appl Radiat Isot* 2002; 57: 665-74.
- [104] Fani M, Xanthopoulos S, Archimandritis SC, Stratis N, Bouziotis P, Loudos G, Varvarigou AD. Biodistribution and scintigraphic studies of 153Sm-labeled anti-CEA monoclonal antibody for radioimmunoscintigraphy and radioimmunotherapy. *Anticancer Res* 2003; 23: 2195-9.
- [105] Breeman WA, De Jong M, Visser TJ, Erion JL, Krenning EP. Optimising conditions for radiolabelling of DOTA-peptides with 90Y, 111In and 177Lu at high specific activities. *Eur J Nucl Med Mol Imaging* 2003; 30: 917-20.
- [106] Kwekkeboom DJ, Bakker WH, Kam BL, Teunissen JJ, Kooij PP, de Herder WW, Feelders RA, van Eijck CH, De Jong M, Srinivasan A, Erion JL, Krenning EP. Treatment of patients with gastro-entero-pancreatic (GEP) tumours with the novel radiolabelled somatostatin analogue [177Lu-DOTA(0),Tyr3]octreotate. *Eur J Nucl Med Mol Imaging* 2003; 30: 417-22.
- [107] Teunissen JJ, Kwekkeboom DJ, Krenning EP. Quality of life in patients with gastroenteropancreatic tumors treated with [177Lu-DOTA0,Tyr3]octreotate. *J Clin Oncol* 2004; 22: 2724-9.
- [108] Makela OT, Lammi MJ, Uusitalo H, Hyttinen MM, Vuorio E, Helminen HJ, Tulamo RM. Analysis of lapine cartilage matrix after radiosynovectomy with holmium-166 ferric hydroxide macroaggregate. *Ann Rheum Dis* 2003; 62: 43-9.
- [109] Makela O, Penttila P, Kolehmainen E, Sukura A, Sankari S, Tulamo RM. Experimental radiation synovectomy in rabbit knee with holmium-166 ferric hydroxide macroaggregate. *Nucl Med Biol* 2002; 29: 593-8.
- [110] Makela O, Sukura A, Penttila P, Hiltunen J, Tulamo RM. Radiation synovectomy with holmium-166 ferric hydroxide macroaggregate in equine metacarpophalangeal and metatarsophalangeal joints. *Vet Surg* 2003; 32: 402-9.
- [111] Ofluoglu S, Schwameis E, Zehetgruber H, Havlik E, Wanivenhaus A, Schwegger I, Weiss K, Sinzinger

- H, Pirich C. Radiation synovectomy with (166)Ho-ferric hydroxide: a first experience. *J Nucl Med* 2002; 43: 1489-94.
- [112] Conzone SD, Brown RF, Day DE, Ehrhardt GJ. In vitro and in vivo dissolution behavior of a dysprosium lithium borate glass designed for the radiation synovectomy treatment of rheumatoid arthritis. *J Biomed Mater Res* 2002; 60: 260-8.
- [113] Conzone SD, Hall MM, Day DE, Brown RF. Biodegradable radiation delivery system utilizing glass microspheres and ethylenediaminetetraacetate chelation therapy. *J Biomed Mater Res* 2004; 70A: 256-64.
- [114] Adnani N. Dosimetry of in-situ activated dysprosium microspheres : A Monte Carlo study. *Medical Physics* 2003; 30: 1512.
- [115] Adnani N. Dosimetry of in situ activated dysprosium microspheres. *Phys Med Biol* 2004; 49: 733-46.
- [116] Shimofure S, Koizumi S, Ichikawa K, Ichikawa H, Dobashi T. Preparation of microcapsules containing rare-earth metal elements. *J Microencapsul* 2001; 18: 13-7.
- [117] Mumper RJ. Polymeric Microspheres for Radionuclide Synovectomy Containing Neutron-Activated Holmium-166. *J.Nucl.Med.* 33, 398-402. 1992.
- [118] Mumper RJ, Jay M. Biodegradable Radiotherapeutic Polyester Microspheres: Optimization and in-vitro / in-vivo Evaluation. *J.Contr.Rel.* 18, 193-204. 1992.
- [119] Mumper RJ, Jay M. Formation and Stability of Lanthanide Complexes and Their Encapsulation into Polymeric Microspheres. *J.Phys.Chem.* 96, 8626-8631. 1992.
- [120] Mumper RJ, Ryo UY, Jay M. Neutron-activated holmium-166-poly (L-lactic acid) microspheres: a potential agent for the internal radiation therapy of hepatic tumors. *J Nucl Med* 1991; 32: 2139-43.
- [121] Mumper RJ, Jay M. Poly(L-lactic acid) microspheres containing neutron-activatable holmium-165: a study of the physical characteristics of microspheres before and after irradiation in a nuclear reactor. *Pharm Res* 1992; 9: 149-54.
- [122] Jay M, Khare SS, Mumper RJ, Ryo UY. Microencapsulation of activable radiotherapeutic agents. *Prog Clin Biol Res* 1989; 292:293-300.: 293-300.
- [123] Nijsen JFW, van Steenberg MJ, Kooijman H, Talsma H, Kroon-Batenburg LM, van de Weert M, van Rijk PP, De Witte A, van het Schip AD, Hennink WE. Characterization of poly(L-lactic acid) microspheres loaded with holmium acetylacetonate. *Biomaterials* 2001; 22: 3073-81.
- [124] Nijsen JFW, Zonnenberg BA, Woittiez JR, Rook DW, Swildens-van Woudenberg IA, van Rijk PP, van het Schip AD. Holmium-166 poly lactic acid microspheres applicable for intra-arterial radionuclide therapy of hepatic malignancies: effects of preparation and neutron activation techniques. *Eur J Nucl Med* 1999; 26: 699-704.
- [125] Nijsen JFW, van het Schip AD, van Steenberg MJ, Zielhuis SW, Kroon-Batenburg LM, van de Weert M, van Rijk PP, Hennink WE. Influence of neutron irradiation on holmium acetylacetonate loaded poly(L-lactic acid) microspheres. *Biomaterials* 2002; 23: 1831-9.
- [126] Nijsen JFW, Rook DW, Brandt CWJM, Meijer R, Dullens HFJ, Zonnenberg BA, de Klerk JMH, van Rijk

- PP, Hennink WE, van het Schip AD. Targeting of liver tumour in rats by selective delivery of holmium-166 loaded microspheres: a biodistribution study. *Eur J Nucl Med* 2001; 28: 743-9.
- [127] van Es RJ, Nijsen JFW, Dullens HF, Kicken M, van der Bilt A, Hennink WE, Koole R, Slootweg PJ. Tumour embolization of the Vx2 rabbit head and neck cancer model with Dextran hydrogel and Holmium-poly(L-lactic acid) microspheres: a radionuclide and histological pilot study. *J Craniomaxillofac Surg* 2001; 29: 289-97.
- [128] van Es RJ, Nijsen JFW, van het Schip AD, Dullens HF, Slootweg PJ, Koole R. Intra-arterial embolization of head-and-neck cancer with radioactive holmium-166 poly(L-lactic acid) microspheres: an experimental study in rabbits. *Int J Oral Maxillofac Surg* 2001; 30: 407-13.
- [129] Suzuki YS, Momose Y, Higashi N, Shigematsu A, Park KB, Kim YM, Kim JR, Ryu JM. Biodistribution and kinetics of holmium-166-chitosan complex (DW-166HC) in rats and mice. *J Nucl Med* 1998; 39: 2161-6.
- [130] Song J, Suh CH, Park YB, Lee SH, Yoo NC, Lee JD, Kim KH, Lee SK. A phase I/IIa study on intra-articular injection of holmium-166-chitosan complex for the treatment of knee synovitis of rheumatoid arthritis. *Eur J Nucl Med* 2001; 28: 489-97.
- [131] Turner JH, Claringbold PG, Klemp PF, Cameron PJ, Martindale AA, Glancy RJ, Norman PE, Hetherington EL, Najdovski L, Lambrecht RM. 166Ho-microsphere liver radiotherapy: a preclinical SPECT dosimetry study in the pig. *Nucl Med Commun* 1994; 15: 545-53.
- [132] Brown RF, Lindesmith LC, Day DE. 166Holmium-containing glass for internal radiotherapy of tumors. *Int J Rad Appl Instrum B* 1991; 18: 783-90.
- [133] Sofou S, Thomas JL, Lin HY, McDevitt MR, Scheinberg DA, Sgouros G. Engineered Liposomes for potential alpha-particle therapy of metastatic cancer. *Journal of Nuclear Medicine* 2004; 45: 253-60.
- [134] Jurcic JG, Larson SM, Sgouros G, McDevitt MR, Finn RD, Divgi CR, Ballangrud AM, Hamacher KA, Ma DS, Humm JL, Brechbiel MW, Molinet R, Scheinberg DA. Targeted at particle immunotherapy for myeloid leukemia. *Blood* 2002; 100: 1233-9.
- [135] Allen BJ, Blagojevic N. Alpha- and beta-emitting radiolanthanides in targeted cancer therapy: The potential role of terbium-149. *Nuclear Medicine Communications* 1996; 17: 40-7.
- [136] Rizvi SMA, Sarkar S, Goozee G, Allen BJ. Radioimmunoconjugates for targeted alpha therapy of malignant melanoma. *Melanoma Research* 2000; 10: 281-9.
- [137] Rizvi SM, Allen BJ, Tian Z, Goozee G, Sarkar S. In vitro and preclinical studies of targeted alpha therapy (TAT) for colorectal cancer. *Colorectal Dis* 2001; 3: 345-53.
- [138] Miederer M, Seidl C, Beyer GJ, Charlton DE, Vranjes-Duric S, Comor JJ, Huber R, Nikula T, Apostolidis C, Schuhmacher C, Becker KF, Senekowitsch-Schmidtke R. Comparison of the radiotoxicity of two alpha-particle-emitting immunoconjugates, terbium-149 and bismuth-213, directed against a tumor-specific, exon 9 deleted (d9) E-cadherin adhesion protein. *Radiat Res* 2003; 159: 612-20.

- [139] Smith DR, Lorey DR, Chandra S. Subcellular SIMS imaging of gadolinium isotopes in human glioblastoma cells treated with a gadolinium containing MRI agent. *Applied Surface Science* 2004; 231-2: 457-61.
- [140] Shih JL, Brugger RM. Gadolinium as a neutron capture therapy agent. *Med Phys* 1992; 19: 733-44.
- [141] Tokumitsu H, Ichikawa H, Fukumori Y, Block LH. Preparation of gadopentetic acid-loaded chitosan microparticles for gadolinium neutron-capture therapy of cancer by a novel emulsion-droplet coalescence technique. *Chemical & Pharmaceutical Bulletin* 1999; 47: 838-42.
- [142] Tokumitsu H, Ichikawa H, Fukumori Y. Chitosan-gadopentetic acid complex nanoparticles for gadolinium neutron-capture therapy of cancer: Preparation by novel emulsion-droplet coalescence technique and characterization. *Pharmaceutical Research* 1999; 16: 1830-5.
- [143] Tokumitsu H, Hiratsuka J, Sakurai Y, Kobayashi T, Ichikawa H, Fukumori Y. Gadolinium neutron-capture therapy using novel gadopentetic acid-chitosan complex nanoparticles: in vivo growth suppression of experimental melanoma solid tumor. *Cancer Lett* 2000; 150: 177-82.
- [144] Shikata F, Tokumitsu H, Ichikawa H, Fukumori Y. In vitro cellular accumulation of gadolinium incorporated into chitosan nanoparticles designed for neutron-capture therapy of cancer. *Eur J Pharm Biopharm* 2002; 53: 57-63.
- [145] Matsumura A, Zhang T, Yamamoto T, Yoshida F, Sakurai Y, Shimojo N, Nose T. In vivo gadolinium neutron capture therapy using a potentially effective compound (Gd-BOPTA). *Anticancer Res* 2003; 23: 2451-6.
- [146] Oyewumi MO, Mumper RJ. Gadolinium-loaded nanoparticles engineered from microemulsion templates. *Drug Dev Ind Pharm* 2002; 28: 317-28.
- [147] Watanabe T, Ichikawa H, Fukumori Y. Tumor accumulation of gadolinium in lipid-nanoparticles intravenously injected for neutron-capture therapy of cancer. *Eur J Pharm Biopharm* 2002; 54: 119-24.
- [148] Maeda H, Sawa T, Konno T. Mechanism of tumor-targeted delivery of macromolecular drugs, including the EPR effect in solid tumor and clinical overview of the prototype polymeric drug SMANCS. *Journal of Controlled Release* 2001; 74: 47-61.
- [149] Oyewumi MO, Mumper RJ. Engineering tumor-targeted gadolinium hexanedione nanoparticles for potential application in neutron capture therapy. *Bioconjug Chem* 2002; 13: 1328-35.
- [150] Oyewumi MO, Yokel RA, Jay M, Coakley T, Mumper RJ. Comparison of cell uptake, biodistribution and tumor retention of folate-coated and PEG-coated gadolinium nanoparticles in tumor-bearing mice. *J Control Release* 2004; 95: 613-26.
- [151] Oyewumi MO, Mumper RJ. Influence of formulation parameters on gadolinium entrapment and tumor cell uptake using folate-coated nanoparticles. *Int J Pharm* 2003; 251: 85-97.
- [152] Oyewumi MO, Liu S, Moscow JA, Mumper RJ. Specific association of thiamine-coated gadolinium nanoparticles with human breast cancer cells expressing thiamine transporters. *Bioconjug Chem* 2003; 14: 404-11.
- [153] Kobayashi H, Kawamoto S, Saga T, Sato N, Ishimori T, Konishi J, Ono K, Togashi K, Brechbiel MW.

Avidin-dendrimer-(1B4M-Gd)(254): a tumor-targeting therapeutic agent for gadolinium neutron capture therapy of intraperitoneal disseminated tumor which can be monitored by MRI. *Bioconjug Chem* 2001; 12: 587-93.

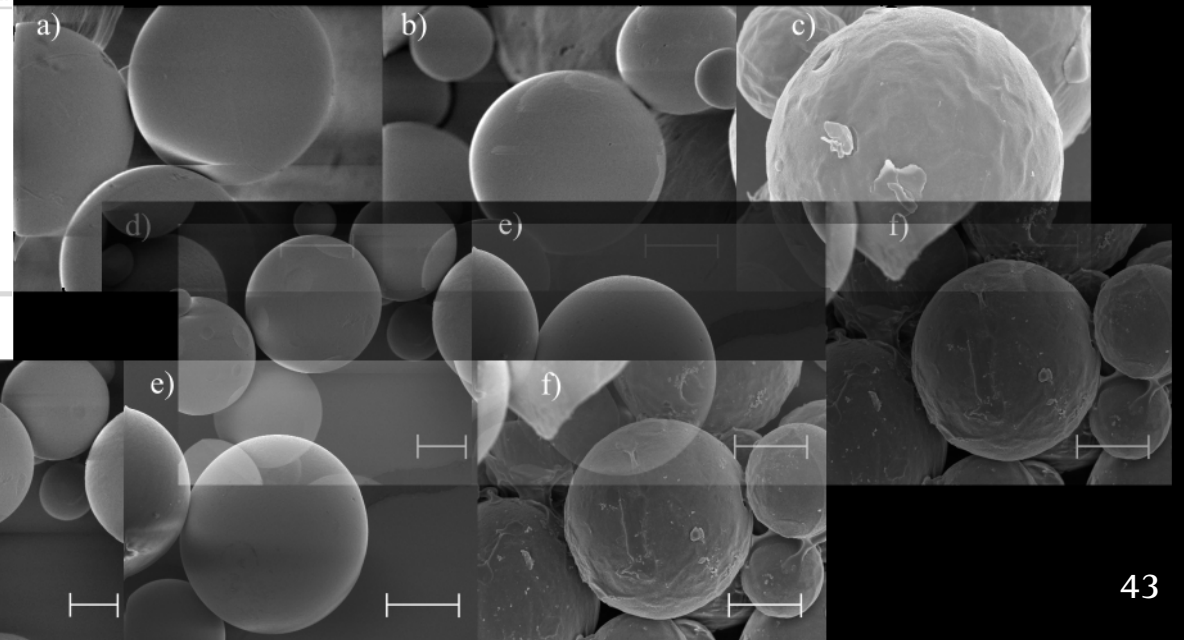
Chapter 3

Surface characteristics of holmium loaded Poly(L-lactic acid) microspheres

SW Zielhuis, JFW Nijsen JF, R Figueiredo, B Feddes, AM Vredenberg, AD van het Schip and WE Hennink

Table 2. Contact angles of films coated with various types of

Film	Contact angle, water ($^{\circ} \pm 2\%$)	Contact angle, 10% ethanol
PLLA	70	
PLLA + PVA	29	
PLLA + Pluronic F68	59	
PLLA + Pluronic F127	55	
Ho-PLLA	85	
Ho-PLLA+ PVA	55	
Ho-PLLA+ Pluronic F68	40	
Ho-PLLA+ Pluronic F127	42	



Abstract

Radioactive holmium-166 loaded poly(L-lactic acid) microspheres (Ho-PLLA-MS) are promising systems for the treatment of liver malignancies. The surface characteristics of Ho-PLLA-MS before and after both neutron and gamma irradiation were investigated in order to get insight into their suspending behaviour and to identify suitable surfactants for clinical application of these systems. X-ray photoelectron spectroscopy (XPS) and scanning electron microscopy (SEM) were used for surface characterization. The residual amounts of poly(vinyl alcohol) (PVA) of the microspheres, which was used as an emulsifier during the solvent evaporation process, were determined using a colorimetric iodine borate method and the wettability of microspheres and PLLA films with and without holmium (Ho) loading was tested using suspending experiments and contact angle measurements.

XPS showed that the surface of Ho-PLLA-MS mainly consisted of PLLA, less than 10% of the surface was covered with PVA after several washing and sieving steps. A colorimetric assay showed that the microspheres contained 0.2-0.3% (w/w) PVA. Combined with XPS data, this assay demonstrates that the PVA is likely dissolved in the core of the microspheres. XPS analysis also showed that after neutron irradiation, some holmium appeared on the surface. Moreover, Ho-loaded PLLA films had a much higher contact angle (85°) than non-loaded films (70°). Therefore, the Ho on the surface of neutron irradiated Ho-PLLA-MS is probably the reason for their poor suspending behaviour in saline. No surface changes were seen with XPS after gamma irradiation.

Based on their surface characteristics, a pharmaceutically acceptable solvent (1% Pluronic F68 or F127 in 10% ethanol) was formulated with which a homogeneous suspension of radioactive Ho-PLLA-MS could be easily obtained, making these systems feasible for further clinical evaluation.

1. Introduction

The use of radionuclide loaded microspheres is a promising treatment of liver malignancies. When microspheres (20–50 µm) are administered into the hepatic artery of patients suffering from liver malignancies, they will lodge in and around the tumour and irradiate the surrounding tissue [1-3]. For this purpose poly(L-lactic acid) microspheres can be loaded with holmium acetylacetonate (HoAcAc). These microspheres (Ho-PLLA-MS) were prepared by a solvent evaporation method as previously described by Nijsen et al. [4]. After preparation the microspheres are activated by neutron irradiation in a nuclear reactor [5]. Before administration into the patient via a catheter [6], the microspheres should be suspended completely, because aggregated microspheres may either lodge in the catheter or can give an undesirable biodistribution. Furthermore, suspension of the microspheres in a suitable solvent prior to administration should be easy and rapid in order to reduce radiation burden to personnel. Ideally, a suspending solvent is added to a vial containing dry radioactive microspheres whereupon a suspension is obtained by gently shaking without opening this vial. However, we experienced that it was difficult to create a homogeneous suspension of Ho-PLLA-MS in saline after neutron activation by simple means. The surface properties of the microspheres determine to a great extent their suspensibility. Therefore, we investigated the surface characteristics of Ho-PLLA-MS before and after neutron irradiation, in order to understand their suspending behaviour and to identify suitable excipients.

Although the microspheres receive a very high radiation dose, neutron irradiation is not an approved sterilization method yet [7]. Consequently, the microspheres require a pharmaceutically accepted sterilization method. Gamma irradiation is the method of choice to sterilize PLLA microspheres [8]. However, it is well known that gamma irradiation also changes the microsphere properties [9] and therefore the effect of gamma irradiation on the surface properties was also studied. Many articles have been published about the surface properties of PLLA-based micro- and nanoparticles. PLLA as such is a rather hydrophobic polymer and consequently microspheres based on this polymer have a poor suspending behaviour [10]. For the solvent evaporation process partly hydrolysed polyvinyl alcohol (PVA) is frequently used as an emulsifier (e.g. [4,11]). It has been reported that the PLLA micro- and nanoparticles are often surrounded by a layer of

the used PVA [11-14]. This surface associated PVA will increase the hydrophilicity of the surface and improve the wettability of microspheres.

In this study we investigated the effect of both neutron and gamma irradiation and of the processing conditions on the surface properties of Ho-PLLA-MS in order to understand and predict their suspending behaviour in solvents that can be used in parenteral formulations [15]. Pluronic F68 and F127 were chosen as surfactant candidates and ethanol was used as a surface tension lowering agent so as to create a clinically applicable formulation for the arterial administration of Ho-PLLA-MS.

X-ray photoelectron spectroscopy (XPS) and scanning electron microscopy (SEM) were used for the characterization of the surface of irradiated and non-irradiated microspheres. Residual amounts of PVA were determined using an iodine borate method and the wettability of microspheres was investigated using suspending behaviour tests and polymer films were tested for their hydrophobicity using contact angle measurements.

2. Materials and Methods

2.1 Materials

All chemicals were commercially available and used as obtained. Acetylacetone, 2,4-pentanedione (AcAc; > 99%), chloroform (CHCl_3 ; HPLC-grade), poly(vinyl alcohol) (PVA; MW 30 000 – 70 000, 88% hydrolyzed), ammonium hydroxide (NH_4OH ; 29.3% in water), Pluronic F 68[®] ($\text{PEO}_{78}\text{PPO}_{30}\text{PEO}_{78}$; MW 7 680 – 9 510) and Pluronic F 127[®] ($\text{PEO}_{100}\text{PPO}_{65}\text{PEO}_{100}$; MW 9 840 – 14 600) were supplied by Sigma Aldrich (Steinheim, Germany). Sodium hydroxide (NaOH ; 99.9%) was purchased from Riedel-de Haën (Seelze, Germany). Holmium (III) chloride hexahydrate ($\text{HoCl}_3 \cdot 6\text{H}_2\text{O}$; 99.9%) was obtained from Phase Separations BV (Waddinxveen, The Netherlands). Poly(L-lactic acid) (PLLA; MW 26 000, intrinsic viscosity 0.09 l/g in chloroform at 25°C) was purchased from Purac Biochem (Gorinchem, The Netherlands). Ethanol ($\text{C}_2\text{H}_5\text{OH}$; Ph Eur 99.9%), xylenol-orange ($\text{C}_{31}\text{H}_{28}\text{N}_2\text{Na}_4\text{O}_{13}\text{S}$; Ph Eur 99.9%), potassium nitrate (KNO_3 ; 99.9%), ethylene dinitrilotetraacetic acid (EDTA, >99.0%), hydrochloric acid (HCl ; 37%), boric acid (H_3BO_3 ; >99.5%), potassium iodine (KI; 99.9%) and iodine (I_2 ; > 99.8%) were purchased from Merck (Darmstadt, Germany).

2.2 Preparation of microspheres and films

HoAcAc and Ho-PLLA-MS were prepared by a solvent evaporation technique as described previously [4]. HoAcAc (10 g) and PLLA (6 g) were dissolved in chloroform (186 g). The resulting homogeneous solution was added to one litre of an aqueous solution of PVA (2%). The mixture was stirred (500 rpm) for 40 hours at room temperature and the formed microspheres were collected by centrifugation. The microspheres were washed three times with water, three times with 0.1 M HCl to remove non-incorporated HoAcAc, and finally three times with water. The obtained microspheres were suspended in water (200 ml) and fractionated according to size using stainless steel sieves of 20 and 50 μm with a sprinkler system (Analysette 3 system, Fritsch GmbH) using 8 l of water. The collected microsphere fractions were dried at 50 °C for 48 h and analysed with a Coulter Counter (Multisizer 3, Beckman Coulter). PLLA-MS without HoAcAc loading were prepared in the same way.

HoAcAc loaded PLLA (Ho-PLLA) films were prepared by dissolving 2.5 g PLLA and 2.5 g HoAcAc in 50 ml chloroform. About 1 ml of the resulting solution was poured onto a glass plate (2.5 by 7 cm) and the solvent was allowed to evaporate for 24 hours at room temperature resulting in thin films (<100 μm). PLLA films were prepared in the same way, leaving out the HoAcAc.

2.3 Neutron and gamma irradiation

Neutron irradiation was performed in the pneumatic rabbit system (PRS) in the reactor facilities in Petten, The Netherlands. The PRS (neutron flux $5 \times 10^{13} \text{ cm}^{-2} \cdot \text{s}^{-1}$, 1h) irradiations were carried out on samples of 500 mg of dry (washed and sieved) microspheres, which were packed in polyethylene vials. Gamma sterilization was performed using a cobalt 60 source (Isotron, Ede, The Netherlands). Samples (1 g of dried, washed and sieved microspheres in polyethylene vials) received a dose of 25.0 kGy. Analyses of neutron activated and gamma-irradiated samples were performed after 1 month storage at room temperature in closed vials excluding moisture.

2.4 Determination of holmium content in microspheres

The holmium content in microspheres was determined by a complexometric titration. Microspheres (100 μg) were destructed using 10 ml of 5 M sodium

hydroxide. The resulting solution was neutralized with 5 M hydrochloric acid. After adding 5 grams of hexamethylenetetramine and 50 mg of a 1:100 mixture of xylenol-orange with potassium nitrate, the pH was adjusted to 5.0 using 1 M hydrochloric acid. The solution was titrated with 0.01 M EDTA until the colour changed from pink to yellow. Analyses were performed in triplicate.

2.5 Determination of PVA

The amount of PVA in the microspheres was determined using the iodine-borate method [13]. The method consists in solubilizing PVA by destructing the microspheres (100 mg) with 2 ml of 1 M NaOH for 20 min at 90°C. The resulting solutions were neutralized with 1 M HCl. Next, 3 ml of a boric acid solution (3.7% w/v) and 0.5 ml of an iodine solution (1.66% KI + 1.27% I₂ in distilled water) were added and the volume was adjusted to 10 ml with distilled water. Samples were measured at 690 nm using a Perkin Elmer spectrophotometer. Analyses were performed in triplicate. Known amounts of PVA added to 100 mg of PLLA were treated in the same way and were used as standards.

2.6 Suspending behaviour of microspheres

Microspheres (100 mg) were weighed in a test tube and 3 ml of a suspending solvent was added. The used suspending solvents were saline, 10% ethanol in saline, 1% Pluronic F68, Pluronic F127 or PVA in saline and 1% Pluronic F68, Pluronic F127 or PVA in 10% ethanol in saline. To study the suspending behaviour, the microspheres plus the different solvents were vortexed for ten seconds and it was assessed visually whether a homogeneous suspension without aggregates was obtained. If this did not occur, the same test tubes with microspheres were ultrasonically processed for one minute. If there was still no homogeneous suspension, microspheres were stirred with a spatula for three minutes.

2.7 Wettability of polymer films

Contact angles of polymer films were measured by pipetting droplets of 1 µl of distilled water or 10% ethanol in distilled water onto the different films. The droplet was observed using a light microscope and the contact angle was determined. Contact angles of films which were previously immersed in a Pluronic F68, Pluronic F127 or PVA solution (all 1% w/w in saline), washed once with

distilled water and dried for 24 hours at room temperature, were also measured. Analyses were performed in triplicate.

2.8 Scanning electron microscopy

The surface morphology of Ho-PLLA-MS was investigated by SEM using a Philips XL30 FEGSEM. A voltage of 5 or 10 kV was applied. Samples of microspheres were mounted on aluminium stubs and sputter-coated with a Pt/Pd layer of about 10 nm.

2.9 X-ray photoelectron spectroscopy

XPS analyses were performed for C1s and Ho4d, using a Vacuum Generators CLAM-2 hemispherical analyser operating at 50 eV pass energy. A Mg K α source (Vacuum Generators twin-anode XR2E2) was used at 120 W. The angle between the surface and the analyser axis was 15°, and the angle between the analyser and the x-ray source axis was 33.5°.

For XPS analysis of (Ho) PLLA-MS, samples (200 mg) taken at different points in the washing and sieving process, were mixed with a small amount of water (200 µl) and the resulting paste was spread on the XPS sample plate and dried in a vacuum chamber.

Samples of PVA, PLLA and HoAcAc were made by powder compression with a pressure of 10⁴ kg/cm² using an infra-red tablet press. Spectra obtained from the PVA and PLLA samples were used to simulate the following two models in order to analyse the surface composition of the microspheres:

Model 1

If it is assumed that the top layer of a microsphere is a mixture of PLLA and PVA, the resulting signal intensity ($I(E)_{tot}$) can be considered as a superposition of the PLLA and PVA signals, according to:

$$I(E)_{tot} = c \cdot I(E)_{PVA} + (1 - c) \cdot I(E)_{PLLA}$$

In this equation, $I(E)_{PVA}$ and $I(E)_{PLLA}$ are the signal intensities of PVA and PLLA respectively, E is the binding energy of the electrons, and c is the relative amount of PVA in the mixture.

Model II

If the surface of PLLA is coated with a layer of PVA, the resulting signal intensity ($I(E)_{tot}$) is given by:

$$I(E)_{tot} = I(E)_{PVA} \cdot \left[1 - \exp\left(\frac{-d}{\lambda(E_{C(1s)}) \cos\theta}\right) \right] + I(E)_{PLLA} \cdot \exp\left(\frac{-d}{\lambda(E_{C(1s)}) \cos\theta}\right)$$

For the analyses we used the C(1s) peak and an angle θ of 15° . $\lambda(E_{C(1s)})$ is the so-called attenuation length (AL) of C(1s) electrons in PVA. The AL of C(1s) electrons was calculated using the modified Bethe equation (TPP-2M) as proposed by Tanuma et al. for the Inelastic

Mean Free Path (IMFP) of elemental, inorganic, and organic solids [16]. We calculated the TPP-2M formula using a software package, available from NIST [17]. The IMFP for a C(1s) electron (binding energy ~ 285 eV, kinetic energy ~ 969 eV) was found to be ~ 3.0 nm. To convert the calculated IMFPs to ALs, we used the formula, proposed by Seah [18]:

The resulting AL was found to be 2.7 nm. The resulting signal intensity ($I(E)_{tot}$) was calculated for a varying coating thickness d . Thus, with XPS analysis either the relative amount of PVA in the top layer (model I), or the maximum PVA coating thickness (model II) is estimated.

3. Results

3.1 Preparation of microspheres

About 5 g of Ho-PLLA-MS with 17.0 ± 0.5 % (w/w) of holmium were prepared. The particles have a rather broad size distribution (10-60 μm). Sieving was very effective to narrow the particle size distribution: more than 96% of the microspheres had a size between 20-50 μm after sieving, yielding an amount of 4 g.

3.2 PVA content

The amount of microsphere-associated PVA in different batches of both Ho-PLLA-MS and PLLA-MS varied from 0.4-0.9% (w/w) before washing and sieving, and 0.2-0.3% (w/w) after washing and sieving.

3.3 Suspending behaviour

The suspending behaviour of irradiated and non-irradiated microspheres is

shown in Table 1. It was observed that non-irradiated Ho-PLLA-MS were more difficult to suspend in saline than PLLA-MS. Neutron irradiated Ho-PLLA-MS showed the worst suspending behaviour. Only a combination of both a surfactant and ethanol resulted in a satisfactory suspending behaviour. There were no differences seen between the three types of surfactants. γ -Irradiation had no effect on the suspending behaviour of both Ho-PLLA-MS and PLLA-MS.

Table 1. Suspending characteristics of different PLLA microspheres after vortexing (V), ultrasonic processing (U) and stirring (S)

formulation	saline			10% ethanol in saline			1% surfactant ^a in saline			1% surfactant ^a in 10% ethanol in saline		
procedure	V	U	S	V	U	S	V	U	S	V	U	S
PLLA-MS	=	+	+	+	+	+	+	+	+	+	+	+
PLLA-MS, gamma	=	+	+	+	+	+	+	+	+	+	+	+
PLLA-MS, neutron	=	+	+	+	+	+	+	+	+	+	+	+
Ho-PLLA-MS	-	\pm	+	\pm	+	+	\pm	+	+	+	+	+
Ho-PLLA-MS gamma	-	\pm	+	\pm	+	+	\pm	+	+	+	+	+
Ho-PLLA-MS neutron	-	-	\pm	-	\pm	+	-	\pm	+	\pm	+	+

^aPluronic F68, Pluronic F127 and PVA gave similar results

- poor wetting of microspheres

\pm wetting of microspheres, but still aggregates present,

+ homogeneous suspension

3.4 Contact angles

The water and 10% ethanol in water contact angles of the various films are given in Table 2. PLLA films had a water contact angle of 70° which is in agreement with literature data [19]. A PLLA/HoAcAc film had a higher water contact angle (85°). The water contact angles of the PLLA and the Ho-PLLA films coated with surfactants were lower than those of the non-coated films demonstrating that these surface active compounds lower the interfacial tension between the solid and liquid phase. The Pluronic F68 or Pluronic F127 coated Ho-PLLA films showed a better wettability than the PVA coated films. The opposite effect was observed for the PLLA films. All contact angles of water with 10% ethanol were lower than those of pure water.

3.5 SEM

SEM analysis demonstrates that the surface of both PLLA-MS and Ho-PLLA-MS was slightly affected after neutron irradiation (Fig. 1). Small fragments were released from the surface and in general the surfaces showed more roughness. However, the microspheres retained their spherical character. After γ - irradiation no changes were observed (Fig. 1).

3.6 XPS

The XPS-spectra of PLLA, PVA and HoAcAc samples and the simulated models are given in Fig. 2. Fig. 3a shows the XPS C1s spectra of PLLA-MS after several washing steps. This figure shows that the spectra of the microspheres after the first 1-3 washing steps (with water) resemble the PVA spectrum (Fig. 2a). This demonstrates that the microspheres had a PVA layer on their surface, which is in agreement with literature [20,21]. Because the spectra of the PLLA-MS do not show the presence of PLLA on their surface, the PVA layer is at least several nanometres. However, the XPS spectrum of extensively washed and sieved PLLA-MS shows more resemblance to that of PLLA indicating the presence of PLLA on their surface. When this spectrum was fitted using the models given in section 2.10, it is calculated that the amount of PVA that covers the surface is about 20% of the total surface (model 1) or the PVA layer is limited to a few nanometres (model 2).

C1s spectra of Ho-PLLA-MS after several washing steps (Fig. 3b) demonstrate that almost all PVA was washed away after 9 washing steps. After sieving, the

XPS-spectrum of microspheres did not change substantially anymore. When the peak intensities of the washed and sieved Ho-PLLA-MS were fitted using the proposed models, the total amount of PVA that covers the surface was less than 10 % of the total surface (model 1) or the PVA layer was thinner than one nanometre (model 2). Fig. 3c demonstrates that no holmium could be detected on the surface of washed and sieved Ho-PLLA-MS. After 3 washing steps with water large amounts of holmium were seen, which was probably caused by the presence of non-incorporated HoAcAc on the surface of the microspheres. This was removed upon washing with three washing steps of 0.1 M HCl.

The C1s spectra of PLLA-MS before and after neutron irradiation were identical (Fig. 4a). The XPS C1s signals for neutron irradiated and non-irradiated Ho-PLLA-MS show that the surface composition of neutron irradiated Ho-PLLA-MS had been changed (Fig. 4a). In line herewith, Fig. 4b shows that holmium was detected on the surface of neutron irradiated Ho-PLLA-MS.

Since the C1s and Ho4d spectra of both Ho-PLLA-MS and PLLA-MS before and after gamma irradiation were comparable, gamma irradiation had no effect on the surface composition (data not shown).

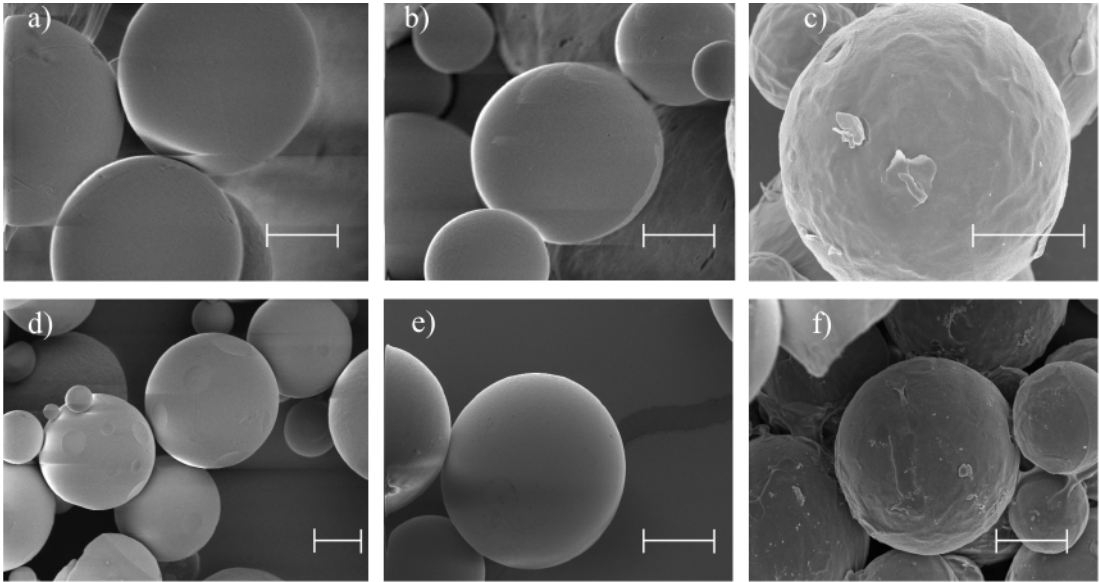


Fig. 1 SEM pictures of Ho-PLLA-MS a) non-irradiated, b) gamma-irradiated, c) neutron-irradiated and PLLA-MS d) non-irradiated, e) gamma-irradiated, f) neutron-irradiated. Bars represent 20 μm .

Table 2. Contact angles of films coated with various types of surfactants

Film	Contact angle, water ($^{\circ} \pm 2\%$)	Contact angle, 10% ethanol ($^{\circ} \pm 2\%$)
PLLA	70	54
PLLA + PVA	29	24
PLLA + Pluronic F68	59	54
PLLA + Pluronic F127	55	49
Ho-PLLA	85	63
Ho-PLLA+ PVA	55	51
Ho-PLLA+ Pluronic F68	40	33
Ho-PLLA+ Pluronic F127	42	37

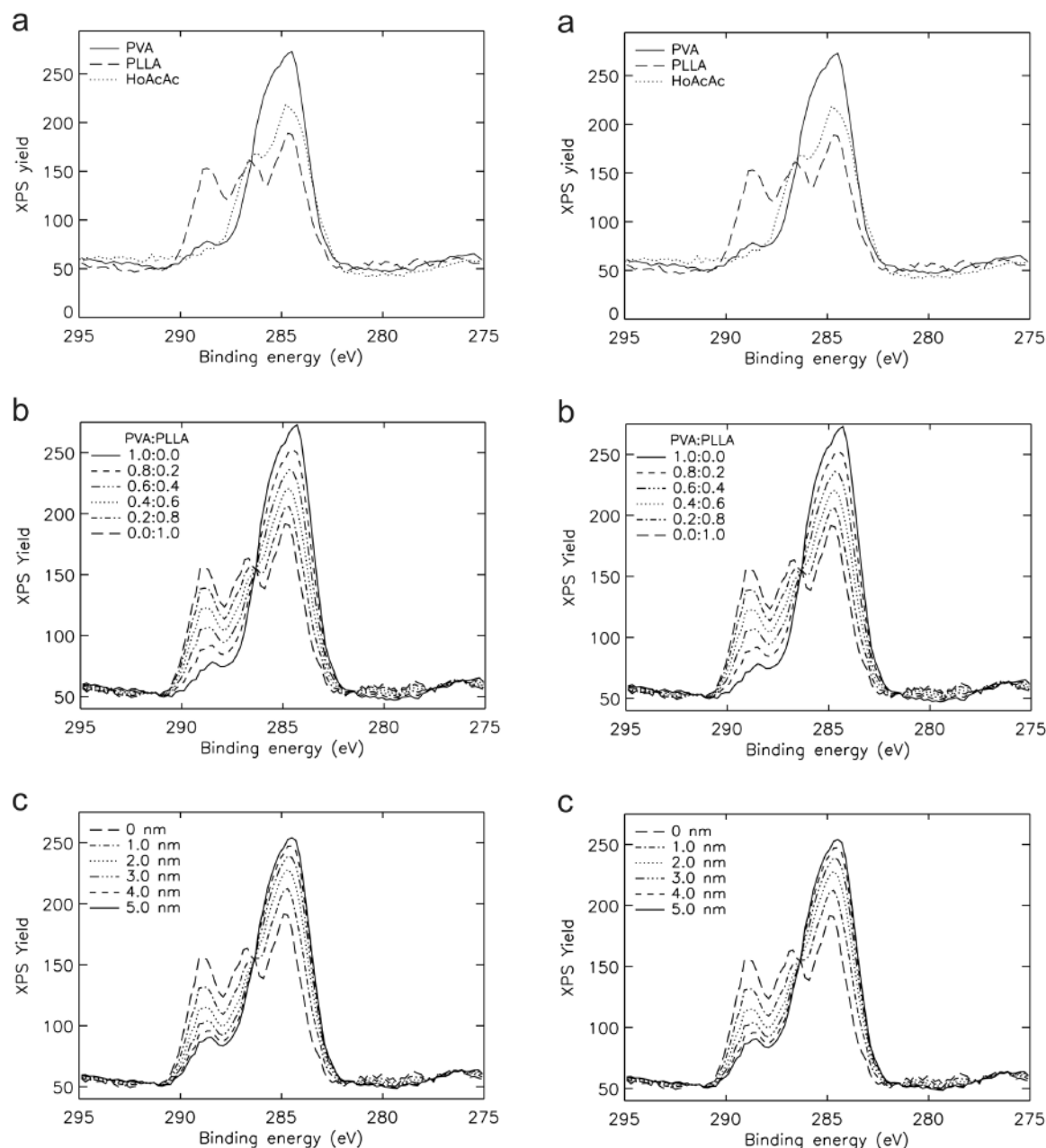


Fig. 2 C1s XPS signals for PLLA, PVA and HoAcAc samples (a) and simulated C1s XPS signals for different PVA/PLLA mixtures (b, model 1) and PVA layers with different thickness on PLLA (c, model 2)

Fig. 3 C1s XPS signals for PLLA-MS (a), and C1s (b) and Ho4d (c) XPS signals for Ho-PLLA-MS after several washing steps (1-3x: washed 1 to 3 times with water; 9x: washed 3 times with water, 3 times with 0.1 M HCl, and 3 times with water; sieved: sieving step using 8 l of water)

4. Discussion

The surface composition of PLLA microspheres loaded with and without HoAcAc before and after neutron irradiation can be established by combining the results of contact angle measurements, the PVA assay, SEM-images and XPS-analyses. The PLLA-MS used in this study were prepared using a solvent evaporation process. During this process, PVA acts as a surfactant and is adsorbed at the water/organic solvent interface. The hydrophilic hydroxyl groups of the PVA chains are located in the water phase, whereas the hydrophobic non-hydrolysed vinyl acetate regions are in the organic phase. After evaporation of the solvent and hardening of the microspheres this can result in residual amounts of PVA on the surface [20]. Such a PVA layer would result in a good wettability of PLLA-based microspheres. Indeed, contact angle measurements showed that PLLA films with and without holmium have a much lower contact angle after coating with PVA. Lee et al. [11] used a PVA assay to determine the thickness of a PVA layer on the surface of microspheres. Using a colorimetric PVA assay on destructed microspheres, we showed that the different microspheres, even the extensively washed, contained 0.2-0.3% PVA (w/w). If it is assumed that the PVA would be present on the outer layer of the microspheres, this layer should be in a range of 25 to 35 nm. The poor suspending behaviour of the extensively washed (Ho)-PLLA-MS indicates that it is unlikely that they were completely surrounded by surface adsorbed PVA. XPS analysis showed that the surface of Ho-PLLA-MS mainly consisted of PLLA and that the amount of PVA that covered the surface was limited to less than 10% (model 1, section 2.10) or the PVA layer was thinner than 1 nm (model 2, section 2.10). The last option is not very likely because Boury et al. [22] demonstrated that a monolayer of PVA is at least thicker than 1 nm. Consequently, the PVA detected in the microspheres is not preferentially present on the surface but it is dissolved in the core of the microspheres. It has indeed been reported that PVA and PLLA are (partly) miscible [23].

In contrast, several articles have reported that PLLA nano- and microspheres are covered with a layer of PVA [14,24,25]. However, these particles were not as extensively washed as ours. Likely, a sieving process using a large volume of water (in our case 8 l per 5 g of microspheres) removed essentially all PVA from the surface of the microspheres.

There was no difference in suspending behaviour of PLLA-MS before and after neutron irradiation, which indicates that the chemical composition of the surface had not changed. This was indeed confirmed by XPS (Fig. 4a). On the other hand, PLLA-MS showed a better suspending behaviour overall than Ho-PLLA-MS (Table 1). XPS spectra of Ho-PLLA-MS after neutron irradiation show that there was Ho present on the surface. Moreover, contact angle measurements demonstrate that a Ho-PLLA film was more hydrophobic than a PLLA film. Therefore, the reason that the HoAcAc-loaded microspheres show an inferior suspending behaviour after neutron irradiation is probably caused by surface exposed HoAcAc. Before neutron irradiation, extensively washed Ho-PLLA-MS have a surface which mainly consists of PLLA, whereas HoAcAc is present in the inner core of the microspheres. After neutron irradiation, small scales are released from the microspheres (Fig. 1) resulting in the exposure of HoAcAc on the surface. Gamma irradiation had no effect on the suspending behaviour of microspheres and no surface changes were seen with XPS and SEM. These results are in agreement with the work of Montanari et al. [26].

Contact angle measurements of PLLA films with and without HoAcAc show that their wetting can be substantially improved by coating their surfaces with Pluronic F68 or F127. No differences in contact angles of films were seen between these two types of Pluronic. As predicted by contact angle measurements on Pluronic coated PLLA films, suspending experiments show that even neutron irradiated Ho-PLLA-MS can be homogeneously suspended with minimal effort in 1% Pluronic F68 or F127 in 10% ethanol.

5. Conclusion

The present study demonstrates that using a pharmaceutically acceptable vehicle consisting of 1% Pluronic F68 or F127 in 10% ethanol, a homogeneous suspension of radioactive Ho-PLLA-MS can be obtained, making these systems feasible for further clinical evaluation.

Acknowledgements

The authors wish to thank P. Snip and J. Woittiez of the nuclear reactor, NRG, Petten, The Netherlands for sample irradiations. This research was supported by the Technology Foundation STW (UGT.6069), applied science division of NWO and the technology programme of the Ministry of Economic Affairs.

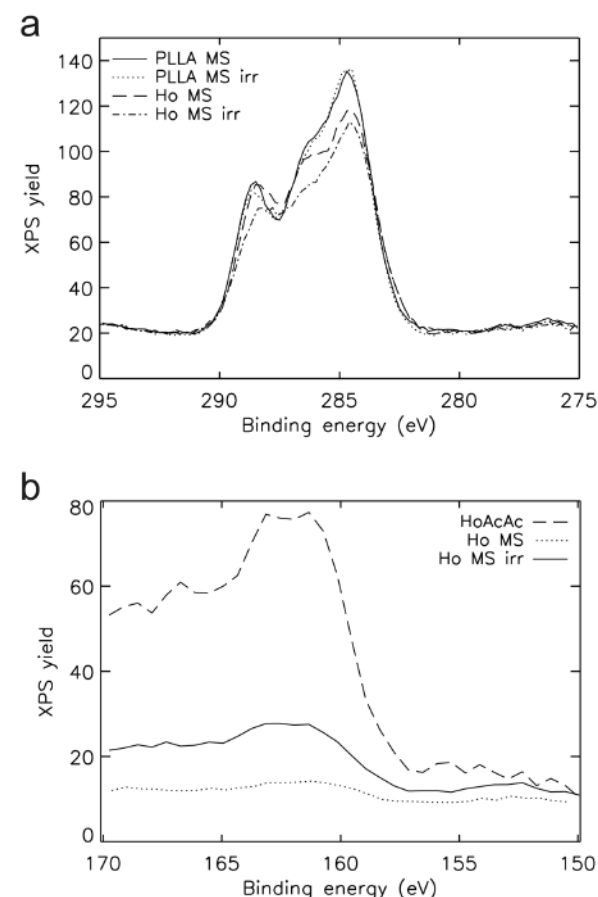
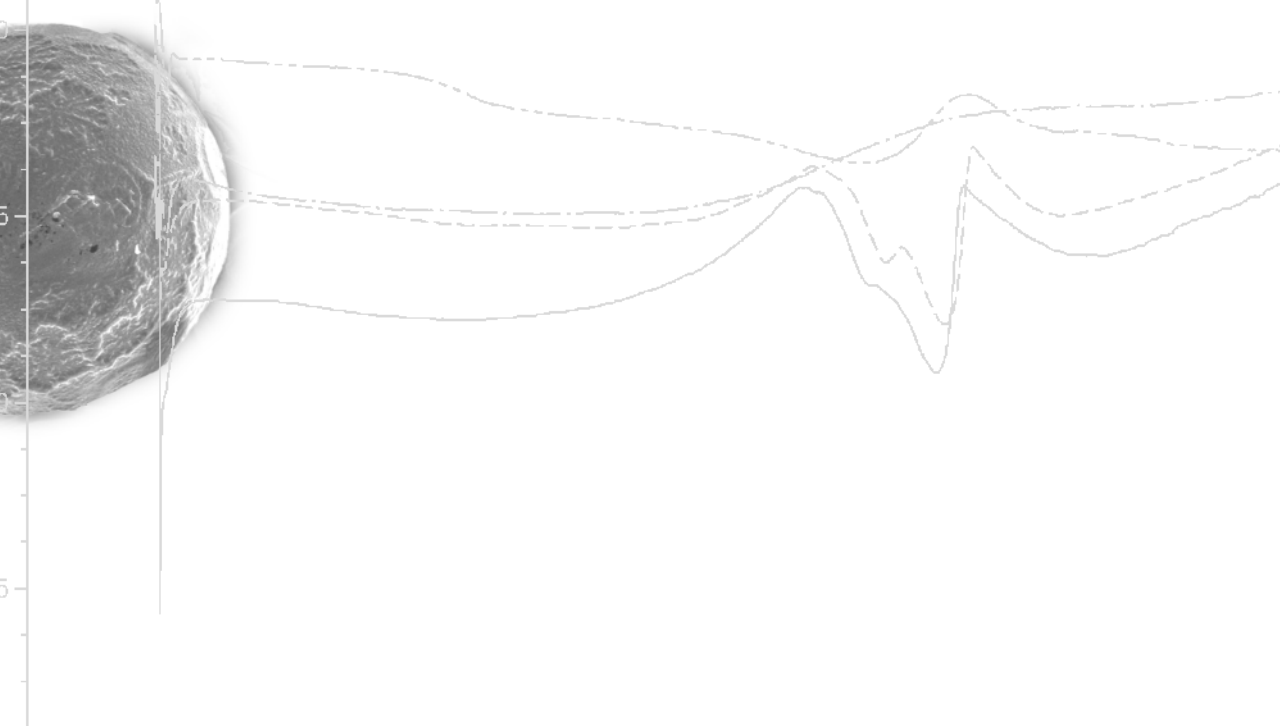


Fig. 4 C1s (a) and Ho4d (b) XPS signals for neutron irradiated and non-irradiated PLLA-MS and Ho-PLLA-MS

References

- [1] Nijsen JFW, van het Schip AD, Hennink WE, Rook DW, van Rijk PP, De Klerk JMH. Advances in nuclear oncology: Microspheres for internal radionuclide therapy of liver metastases. *Current Medicinal Chemistry* 2002;9:73-82.
- [2] Carr BI. Hepatic arterial 90Yttrium glass microspheres (Therasphere) for unresectable hepatocellular carcinoma: Interim safety and survival data on 65 patients. *Liver Transpl* 2004; 10 Suppl 2: S107-S110.
- [3] Salem R, Thurston KG, Carr BI, Goin JE, Geschwind JF. Yttrium-90 microspheres: radiation therapy for unresectable liver cancer. *J Vasc Interv Radiol* 2002;13:S223-S229.
- [4] Nijsen JF, Zonnenberg BA, Woittiez JR, Rook DW, Swildens-van Woudenberg IA, van Rijk PP, van het Schip AD. Holmium-166 poly lactic acid microspheres applicable for intra-arterial radionuclide therapy of hepatic malignancies: effects of preparation and neutron activation techniques. *Eur J Nucl Med* 1999;26:699-704.

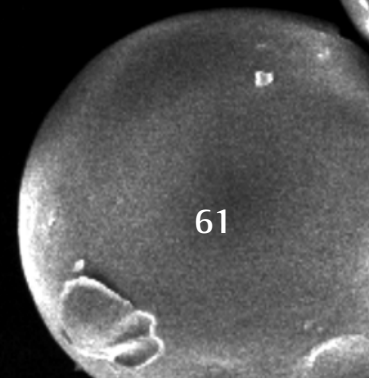
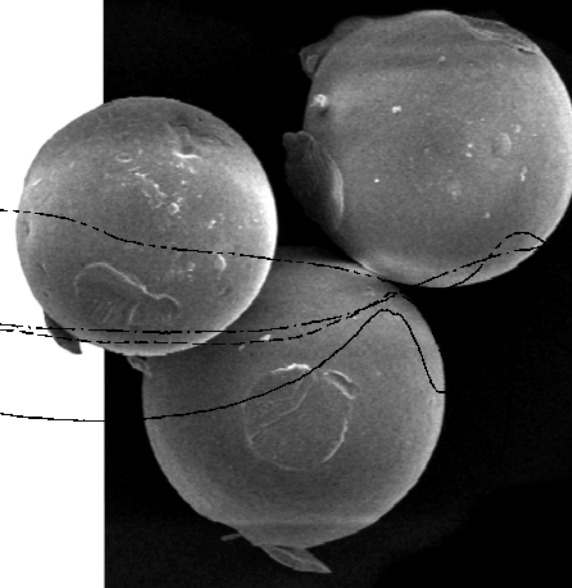
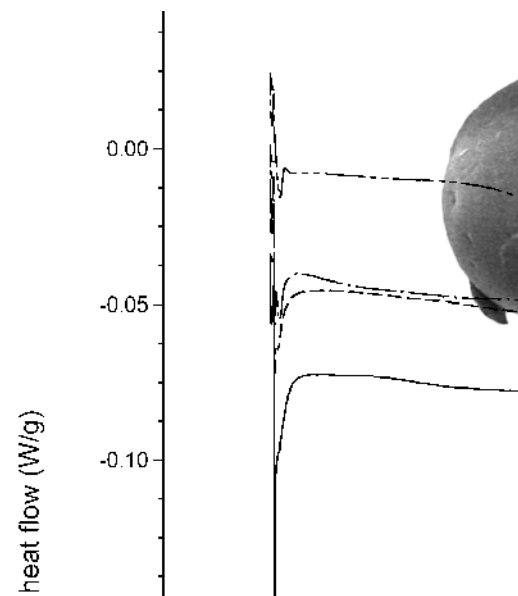
- [5] Nijssen JF, van het Schip AD, van Steenberghe MJ, Zielhuis SW, Kroon-Batenburg LM, van de Weert M, van Rijk PP, Hennink WE. Influence of neutron irradiation on holmium acetylacetonate loaded poly(L-lactic acid) microspheres. *Biomaterials* 2002;23:1831-9.
- [6] Sarfaraz M, Kennedy AS, Cao ZJ, Sackett GD, Yu CX, Lodge MA, Murthy R, Line BR, Van Echo DA. Physical aspects of yttrium-90 microsphere therapy for nonresectable hepatic tumors. *Med Phys* 2003;30:199-203.
- [7] Athanasiou KA, Niederauer GG, Agrawal CM. Sterilization, toxicity, biocompatibility and clinical applications of polylactic acid/polyglycolic acid copolymers. *Biomaterials* 1996;17:93-102.
- [8] Montanari L, Costantini M, Signoretti EC, Valvo L, Santucci M, Bartolomei M, Fattibene P, Onori S, Faucitano A, Conti B, Genta I. Gamma irradiation effects on poly(DL-lactide-co-glycolide) microspheres. *J Contr Rel* 1998;56:219-29.
- [9] Sintzel MB, Merkli A, Tabatabay C, Gurny R. Influence of irradiation sterilization on polymers used as drug carriers-A review. *Drug Develop Ind Pharm* 1997;23:857-78.
- [10] Kiss E, Bertoti I, Vargha-Butler EI. XPS and wettability characterization of modified poly(lactic acid) and poly(lactic/glycolic acid) films. *J Colloid Interface Sci* 2002;245:91-8.
- [11] Lee SC, Oh JT, Jang MH, Chung SI. Quantitative analysis of polyvinyl alcohol on the surface of poly(D, L-lactide-co-glycolide) microparticles prepared by solvent evaporation method: effect of particle size and PVA concentration. *J Contr Rel* 1999;59:123-32.
- [12] Torche AM, Le Corre P, Albina E, Jestin A, Le Verge R. PLGA microspheres phagocytosis by pig alveolar macrophages: influence of poly(vinyl alcohol) concentration, nature of loaded-protein and copolymer nature. *J Drug Target* 2000;7:343-54.
- [13] Zambaux MF, Bonneaux F, Gref R, Maincent P, Dellacherie E, Alonso MJ, Labrude P, Vigneron C. Influence of experimental parameters on the characteristics of poly(lactic acid) nanoparticles prepared by a double emulsion method. *J Contr Rel* 1998;50:31-40.
- [14] Sahoo SK, Panyam J, Prabha S, Labhasetwar V. Residual polyvinyl alcohol associated with poly (D,L-lactide-co-glycolide) nanoparticles affects their physical properties and cellular uptake. *J Contr Rel* 2002; 82: 105-14.
- [15] Jewell RC, Khor SP, Kisor DF, Lacroix KAK, Wargin WA. Pharmacokinetics of RheothRx injection in healthy male volunteers. *J Pharm Sci* 1997;86:808-12.
- [16] Babanalbandi A, Hill DJT, Whittaker AK. Volatile products and new polymer structures formed on ⁶⁰Co γ-radiolysis of poly(lactic acid) and poly(glycolic acid). *Polymer Degr Stab* 1997;58:203-14.
- [17] Tanuma S, Powell CJ, Penn DR. Calculations of electron inelastic mean free paths (IMFPS).4. Evaluation of calculated IMFPS and of the predictive IMFP formula TPP-2 for electron energies between 50 and 2000 eV. *Surf Interface Anal* 1993;21:165.
- [18] Powell CJ, Jablonski A. NIST Electron Inelastic-Mean-Free-Path Database, Version 1.1, National Institute of Standards and Technology, Gaithersburg, MD, 2000.
- [19] Seah MP, Dench WA. Quantitative electron spectroscopy of surfaces: A standard data base for electron inelastic mean free paths in solids. *Surf Interface Anal* 1979;1:2.
- [20] Boury F, Marchais H, Benoit JP, Proust JE. Surface characterization of poly(alpha-hydroxy acid) microspheres prepared by a solvent evaporation/extraction process. *Biomaterials* 1997;18:125-36.
- [21] Shakesheff KM, Evora C, Soriano I, I, Langer R. The Adsorption of Poly(vinyl alcohol) to Biodegradable Microparticles Studied by X-Ray Photoelectron Spectroscopy (XPS). *J Colloid Interface Sci* 1997; 185: 538-47.
- [22] Boury F, Ivanova T, Panaiotov I, Proust JE, Bois A, Richou J. Dynamic Properties of Poly(DL-Lactide) and Polyvinyl-Alcohol Monolayers at the Air-Water and Dichloromethane Water Interfaces. *J Colloid Interface Sci* 1995;169:380-92.
- [23] Park JW, Im SS. Miscibility and morphology in blends of poly(L-lactic acid) and poly(vinyl acetate-co-vinyl alcohol). *Polymer* 2003;44:4341-54.
- [24] Mu L, Feng SS. Vitamin E TPGS used as emulsifier in the solvent evaporation/extraction technique for fabrication of polymeric nanospheres for controlled release of paclitaxel (Taxol). *J Contr Rel* 2002;80:129-44.
- [25] Scholes PD, Coombes AG, Illum L, Davis SS, Watts JF, Ustariz C, Vert M, Davies MC. Detection and determination of surface levels of poloxamer and PVA surfactant on biodegradable nanospheres using SSIMS and XPS. *J Contr Rel* 1999;59:261-78.
- [26] Montanari L, Cilurzo F, Conti B, Genta I, Groppo A, Valvo L, Faucitano A, Buttafava A. Gamma irradiation effects and EPR investigation on poly(lactide-co-glycolide) microspheres containing bupivacaine. *Farmaco* 2002;57:427-33.



Chapter 4

Removal of chloroform from biodegradable therapeutic microspheres by radiolysis

SW Zielhuis, JFW Nijssen, L Dorland,
GC Krijger, AD van het Schip and WE Hennink



Abstract

Radioactive holmium-166 loaded poly(L-lactic acid) microspheres are promising systems for the treatment of liver malignancies. These microspheres are loaded with holmium acetylacetonate (HoAcAc) and prepared by a solvent evaporation method using chloroform. After preparation the microspheres (Ho-PLLA-MS) are activated by neutron irradiation in a nuclear reactor. It was observed that relatively large amounts of residual chloroform (1000-6000 ppm) remained in the microspheres before neutron irradiation. Since it is known that chloroform is susceptible for high-energy radiation, we investigated whether neutron and gamma irradiation could result in the removal of residual chloroform in HoAcAc-loaded and placebo PLLA-MS by radiolysis. To investigate this, microspheres with relatively high and low amounts of residual chloroform were subjected to irradiation. The effect of irradiation on the residual chloroform levels as well as other microsphere characteristics (morphology, size, crystallinity, molecular weight of PLLA and degradation products) were evaluated.

No chloroform in the microspheres could be detected after neutron irradiation. This was also seen for gamma irradiation at a dose of 200 kGy. Phosgene, which can be formed as the result of radiolysis of chloroform, was not detected with gas chromatography mass spectrometry (GC-MS). A precipitation titration showed that radiolysis of chloroform resulted in the formation of chloride. Gel permeation chromatography and differential scanning calorimetry showed a decrease in molecular weight of PLLA and crystallinity, respectively. However, no differences were observed between irradiated microsphere samples with high and low initial amounts of chloroform.

In conclusion, this study demonstrates that neutron and gamma irradiation results in the removal of residual chloroform in PLLA microspheres.

1. Introduction

Radionuclide loaded microspheres are attractive and promising systems for the treatment of liver malignancies. When microspheres with a size between 20–50 μm are administered into the hepatic artery of patients suffering from liver malignancies, they will preferentially lodge in and around the tumour and subsequently irradiate the surrounding tissue [1]. Regarding its physical properties, holmium-166 is the ideal radionuclide for such therapies because it is the only element which can be neutron-activated to a beta- and gamma-emitter with a logistically favourable half-life, and which can also be visualized by MRI [1,2]. Using a solvent evaporation technique, non-radioactive holmium-165 can be incorporated into poly (L-lactic acid) (PLLA) microspheres as its acetylacetonate complex (HoAcAc). In a subsequent step the microspheres (Ho-PLLA-MS) can be rendered radioactive by neutron irradiation [3].

Organic solvents such as chloroform are widely used for the preparation of PLLA microspheres [4,5], and it is also the solvent of choice for the preparation of Ho-PLLA-MS [3]. However, these solvents are difficult to remove quantitatively and consequently traces hereof remain in the microspheres [6-8]. The ICH-guidelines (The International Conference on Harmonisation of Technical Requirements for Registration of Pharmaceuticals for Human Use) prescribe a very low limit of 60 ppm for chloroform in pharmaceuticals [9]. Methods currently applied to reduce the organic solvent levels in polymeric microparticles are drying at elevated temperatures and reduced pressure [10] or extraction using super critical carbon dioxide [6,11].

It is known that chloroform is highly susceptible for decomposition with high-energy radiation [12]. Microspheres receive a very high radiation dose in a nuclear reactor [13], and thus it is possible that residual chloroform decomposes during neutron activation resulting in the reduction or complete removal of the solvent. However, it should be realized that previous studies concerning the effect of radiation on residual solvents were done in a different setting. In particular, the removal of chlorinated hydrocarbons from wastewater using UV- and gamma irradiation has been demonstrated. However, radiolysis of chlorinated solvents in polymer matrices has not been investigated before.

Provided that removal of residual solvent in microspheres can be achieved by irradiation, it is furthermore extremely important that the reaction products,

which are the result of radiolysis, are not harmful for patients. The papers which have been published about the effect of UV- and gamma-irradiation on chlorinated hydrocarbons report on the formation of chloride as an end product of radiolysis [12,14-16]. However, another reaction radiolysis product that could be formed is the very toxic phosgene [16-18]. It is thus important to get a clear insight into the radiolytic pathway(s) of residual chlorinated solvents in polymeric microparticles.

In this study we investigated whether neutron and gamma irradiation will result in the reduction/removal of residual chloroform in HoAcAc-loaded and placebo PLLA-microspheres. Microspheres prepared with a solvent evaporation process were dried at 50 °C or 70 °C under vacuum in order to obtain samples with high and low levels of residual chloroform and subsequently neutron irradiated or gamma irradiated with various dosages. The microspheres were studied for their morphology, residual solvent levels, degradation products, and for the molecular weight and crystallinity of PLLA.

2. Materials and methods

2.1 Materials

All chemicals were commercially available and used as obtained. Acetylacetone, 2,4-pentanedione (AcAc; > 99%), chloroform (CHCl_3 ; HPLC-grade), poly(vinyl alcohol) (PVA; average MW 30 000 – 70 000, 88% hydrolyzed), ammonium hydroxide (NH_4OH ; 29.3% in water) were supplied by Sigma Aldrich (Steinheim, Germany). Sodium hydroxide (NaOH ; 99.9%) was purchased from Riedel-de Haën (Seelze, Germany). Holmium (III) chloride hexahydrate ($\text{HoCl}_3 \cdot 6\text{H}_2\text{O}$; 99.9%) and dichloromethane (CH_2Cl_2 ; HPLC-grade) were obtained from Phase Separations BV (Waddinxveen, The Netherlands). Poly(L-lactic acid) (PLLA; intrinsic viscosity 0.09 dl/g in chloroform at 25°C) was purchased from Purac Biochem (Gorinchem, The Netherlands). Hydrochloric acid (HCl ; 37%), nitric acid (HNO_3 ; 65.0%), silver nitrate (AgNO_3 ; 99.9%) and ethyl acetate (99.9%) were purchased from Merck (Darmstadt, Germany).

2.2 Preparation of HoAcAc and microspheres

HoAcAc was prepared as described previously [3]. In brief: acetylacetone (180 g) was dissolved in water (1080 g). The pH of this solution was brought to 8.50

with an aqueous solution of ammonium hydroxide. Holmium chloride (10 g dissolved in 30 ml water) was added to this solution. After 15 hours incubation at room temperature, the formed HoAcAc crystals were collected by centrifugation and washed with water.

HoAcAc (10 g) and PLLA (6 g) were dissolved in 186 g chloroform. The resulting homogeneous solution was added to one litre of an aqueous solution of PVA (2%). The mixture was stirred (500 rpm) for 40 hours at room temperature and the formed microspheres were collected by centrifugation. The microspheres were washed three times with water, three times with 0.1 M HCl and finally three times with water. The washed microspheres were fractionated according to size using stainless steel sieves with a pore size of 20 and 50 μm , with a wet sieving system consisting of an Electromagnetic Sieve Vibrator (EMS 755) combined with an Ultrasonic Processor (UDS 751) (both from Topas GmbH, Dresden, Germany). The collected microsphere fraction (about 4 grams, size between 20 and 50 μm) was divided into two equal portions of 2 grams and dried at 50 °C for 48 h at normal pressure or at 70 °C under vacuum for 5 h using a rotating Glass Oven (B-580 GKR, Buchi).

Placebo PLLA-microspheres without HoAcAc loading were prepared in the same way. All microsphere batches were prepared in duplicate; ~ 500 mg per batch was packed in polyethylene vials.

2.3 Neutron and gamma irradiation

Routinely, microspheres were neutron activated in a reactor facility in Delft or gamma-irradiated with various dosages. Since the reactor facility of Petten was used in previous studies of our group [3,13], some microsphere batches were also neutron irradiated at this facility. Neutron irradiations were performed in the pneumatic rabbit system (PRS) in the reactor facilities in Delft and Petten. The thermal neutron flux in the Delft facility was $5 \times 10^{12} \text{ cm}^{-2} \cdot \text{s}^{-1}$, while the thermal neutron flux in Petten was $30 \times 10^{12} \text{ cm}^{-2} \cdot \text{s}^{-1}$. The irradiation times were 6 and 1 h, respectively, to ensure equal doses of microsphere-associated radioactivity (~14 GBq, immediately after irradiation).

Gamma sterilization of the samples with a dose of 25.0 kGy was performed using a cobalt-60 source (Isotron, Ede, The Netherlands). A Gammacell 200 cobalt-60 high dose rate research irradiator (Nordion, Canada) was used for irra-

diation of the samples with higher dosages from 100 kGy up to 1000 kGy. Also, this irradiator was used to study the effect of temperature during irradiation because differences in temperature in the Petten and Delft reactor facilities were expected due to differences in their thermal neutron fluxes [19]. To ensure low levels of microsphere-associated radioactivity, analyses of the neutron-irradiated samples were performed after one month storage at room temperature in closed vials.

2.4 Determination of holmium and water content in microspheres

The holmium content in microspheres was determined by a complexometric titration as described before [20]. The water content in the microspheres was determined with the Karl-Fisher method. Therefore, 50 mg microspheres were dissolved in 1 ml of Hydranal Coulomat A (Riedel de Haen, Seelze, Germany) and the water concentration was determined using a Mitsubishi moisture meter model CA-05 (Tokyo, Japan) from which the residual water content of the microspheres was calculated.

2.5 Determination of particle size distribution and evaluation of the surface morphology of the microspheres

The particle size distribution of radiated and non-radiated microspheres was determined using a Coulter counter (Multisizer 3, Beckman Coulter, The Netherlands) equipped with a 100- μ m orifice.

The surface morphology of the Ho-PLLA-microspheres was investigated by scanning electron microscopy (SEM) using a Philips XL30 FEGSEM. A voltage of 5 or 10 kV was applied. Samples of the different microsphere batches were mounted on aluminium stubs and sputter-coated with a Pt/Pd layer of about 10 nm.

2.6 Determination of chloride and chlorine content

Gas chromatographic analyses were performed on a Shimadzu type 14 B GC equipped with a flame ionization detector, employing an OV-17 on Chromosorb W at 175 °C. The injection port and the detector temperature were 200 °C. Microsphere samples (50 mg) were dissolved in 2 ml of dichloromethane for the analysis of chloroform. Standards were prepared by adding varying amounts of

chloroform to dichloromethane solutions containing PLLA (25 mg/ml) or both PLLA (12.5 mg/ml) and HoAcAc (12.5 mg/ml). The detection limit is defined as a signal-to-noise ratio of three [21]. The concentration of chloroform in the microspheres (ppm) was converted to concentrations of chlorine (ppm) (1000 ppm chloroform corresponds with 892 ppm chlorine). To verify the results of the GC-analyses, the total chlorine content of microspheres was also determined by neutron activation (NRG, Petten, The Netherlands) [22]. Some selected samples with a residual solvent level below the detection limit of conventional GC were also subjected to headspace GC. These analyses were performed using European Pharmacopoeia method 2.4.24, 'identification and control of residual solvents for water insoluble substances', and were carried out by Farmalyse B.V., Zaandam, the Netherlands [23].

The concentration of chloride in the different microspheres was determined using a precipitation titration. Therefore, microspheres (100 mg) were heated for one hour at 100 °C to evaporate residual chloroform. GC analyses showed that the chloroform levels were indeed below detection limit. Thereafter, the microspheres were dissolved in 2 ml of 2 M NaOH at 100 °C and the resulting solutions were neutralized with 2 M HNO₃. The solutions were subsequently titrated with 0.005 M AgNO₃ and the endpoint was detected potentiometrically.

2.7 Gas Chromatography-Mass Spectrometry (GC-MS)

GC-MS for the detection of phosgene after derivatisation with N,N-dibutylamine (DBA), according to the method of Schoene et al. [24], was performed at the Netherlands Organisation for Applied Scientific Research (TNO, Prins Maurits Laboratory, Delft, The Netherlands) (in the results named as method-1). Neutron irradiated microspheres samples (~50 mg), which were dried at 50 °C, were extracted with 1 ml hexane. Next, 20 μ l of DBA was added and this solution was subsequently analysed. The detection limit of phosgene was determined by analysing solutions of phosgene in hexane, after the addition of 20 μ l of DBA.

Identification of organic acids, including lactate, lactyl lactate and longer oligomers of lactic acid, was carried out by GC-MS on a Hewlett Packard 5890 series II gas chromatograph linked to a HP 5989B MS-Engine mass spectrometer (in the results named as method-2). Prior to this GC-MS analysis, the organic

acids were trimethylsilylated with N,N-bis (trimethylsilyl)tri-fluoroacetamide/pyridine/trimethylchlorosilane (5:1:0.05 v/v/v) at 60 °C for 30 min. The gas chromatographic separation was performed on a 25m x 0.25mm capillary CP Sil 19CB column (film thickness 0.19 mm) from Varian/Chrompack, Middelburg, The Netherlands.

2.8 Gel Permeation Chromatography (GPC)

The weight-average molecular weight (M_w) and number-average molecular weight (M_n) of PLLA were determined by GPC with two thermostated (35 °C) columns in series (PL gel Mixed-B, Polymer Laboratories) equipped with a refractive index detector (type 410, Waters, Milford, USA). Samples of approximately 5 mg were dissolved in 5 ml chloroform and filtered through 0.45 μ m HPLC-filters (Waters). Elution was performed with chloroform and the flow-rate was 1 ml/min. The columns were calibrated using poly(styrene) standards of known molecular weights (Polymer Laboratories, Shodex and Tosoh, Amherst, USA). Analyses were performed in duplicate.

2.9 Differential Scanning Calorimetry (DSC)

Modulated DSC (MDSC) analysis was performed with a DSC Q1000 (TA Instruments, USA). Samples of approximately 5 mg were transferred into aluminium pans. Scans were recorded under 'heating only' conditions, with a heating rate of 1 °C/min and cooling rate of 2 °C/min. The settings were periods of 30 s and a temperature modulation amplitude of 0.5 °C was applied. Samples were heated from 20 °C to 200 °C. The Universal Analysis 2000 software (version 3.9A) was used for evaluation. Analyses were performed in duplicate.

3. Results and Discussion

3.1 Preparation of microspheres

Ho-PLLA-MS with 17.0 ± 0.5 % (w/w) of holmium, corresponding with a loading of the HoAcAc complex of ~ 50 % (w/w), were prepared using a solvent evaporation method with chloroform as organic solvent [3].

The water content of Ho-PLLA-MS and PLLA-MS batches dried at 50 °C for 48 h at normal pressure or at 70 °C under vacuum for 5 h was 2 ± 0.5 % (w/w). Previous work from our group demonstrated that the amount of water in Ho-

PLLA-MS had an influence on the microsphere characteristics after neutron irradiation in terms of the morphology and size distribution [3]. Since the used drying method resulted in equal water contents, possible differences in the microsphere characteristics after irradiation are not caused by different amounts of water in the microspheres.

3.2 Particle size distribution and SEM analysis of microspheres

After sieving, more than 97 % (volume-based) of the microspheres had a size between 20 and 50 μ m. No differences in size distributions were observed after gamma irradiation (25 kGy), whereas after neutron irradiation more than 94 % of the microspheres had a size between 20 and 50 μ m.

SEM analysis of microspheres showed drying-related differences in their morphology. Ho-PLLA-MS that were dried at 50 °C had a smooth surface (Fig. 1a), whereas small fragments were released from the surface and the surfaces showed more roughness after neutron irradiation (Fig 1b). Importantly, the

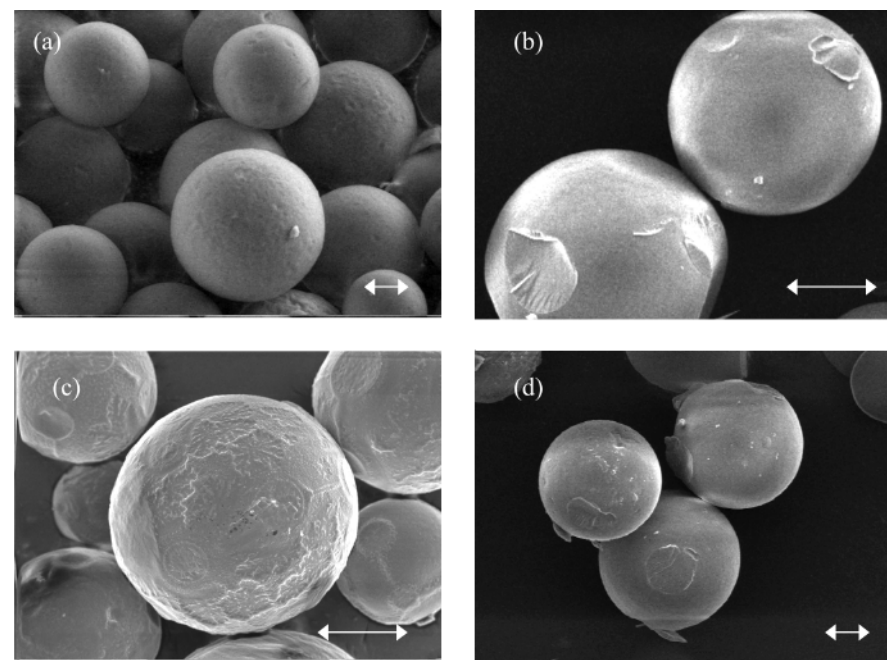


Fig. 1 SEM pictures of Ho-PLLA-MS dried at 50 °C before (a) and after (b) neutron irradiation and Ho-PLLA-MS dried at 70 °C before (c) and after (d) neutron irradiation. Bars represent 10 μ m.

microspheres retained their spherical character. Ho-PLLA-MS that were dried at 70 °C showed a surface that was slightly wrinkled (Fig. 1c). After neutron irradiation, their surfaces showed more roughness and also small fragments were formed (Fig. 1d). The formation of these fragments is very probably the cause of the small changes in the particle size distribution (97 vs. 94 %). After γ -irradiation no surface changes were observed using SEM-analysis (not shown). Placebo PLLA-MS (before and after neutron irradiation) had the same morphology as Ho-PLLA-MS (SEM pictures not shown).

3.3 Determination of chlorine and chloride levels

The chloride and chlorine levels in the different microspheres dried at 50 °C before and after neutron irradiation and gamma irradiation are shown in table 1. The (Ho)-PLLA-MS had a chloroform content, as determined by GC, varying from 1100 to 6700 ppm, which corresponds with 1000 to 6000 ppm chlorine. Table 1 also shows that the chlorine contents in non-irradiated microspheres as

Table 1 chlorine (Cl) and chloride (Cl⁻) contents (in ppm \pm 10 %) in PLLA-MS and Ho-PLLA-MS. Samples were dried at 50 °C and subsequently irradiated in different ways.

irradiation*	batch**	Cl before irradiation (GC)	Cl before irradiation (neutron activation analysis)	Cl after neutron irradiation (GC)	Cl ⁻ after neutron irradiation (titration)
neutron Delft	A	1,000	1,000	nd***	1,000
neutron Delft	B	1,500	1,500	nd	1,500
γ 25 kGy	A	1,000	1,000	1,000	nd
γ 25 kGy	B	1,500	1,500	1,500	nd
neutron Delft	C	4,400	4,400	nd	1,000
neutron Delft	D	1,400	1,400	nd	1,500
γ 25 kGy	C	4,400	4,400	4,400	nd
γ 25 kGy	D	1,400	1,400	1,400	nd
neutron Petten	E	6,000	6,000	nd	2,000
neutron Petten	F	5,000	5,000	nd	1,700
neutron Petten	G	5,000	5,000	nd	1,700
neutron Petten	H	1,800	1,800	nd	600
γ 100 kGy	I	2,000	2,000	1,400	600
γ 200 kGy	I	2,000	2,000	nd	2,000
γ 400 kGy	I	2,000	2,000	nd	2,000
γ 500 kGy	I	2,000	2,000	nd	2,000
γ 1000 kGy	I	2,000	2,000	nd	2,000

* neutron irradiated in the Delft or Petten facility or gamma-irradiated with various dosages

** A, B, E and F are PLLA-MS batches. C, D, G, H and I are Ho-PLLA-MS batches.

*** nd: not detectable

determined with neutron activation analysis and GC were similar, indicating that no residual chloride (from hydrochloric acid, that was used during the washing procedure) remained in the microspheres.

After the standard gamma sterilization dose of 25 kGy, no significant changes were seen for the chlorine concentration, and no chloride could be detected in (Ho)-PLLA-MS (see Table 1). The initial chlorine content of the microsphere batch was 2000 ppm and after irradiation with a dose of 100 kGy, the chloride and chlorine levels were 600 and 1400 ppm. Chlorine was quantitatively converted into chloride after an irradiation dose of 200 kGy. This demonstrates that at higher doses of gamma irradiation radiolysis of CHCl₃ occurred.

Table 1 shows that after neutron irradiation, no chloroform could be detected with GC in both HoAcAc-loaded and placebo PLLA-MS dried at 50 °C with high initial levels of chloroform. As for gamma irradiated samples, chloride was detected in these microspheres implying that radiolysis also had occurred after neutron irradiation.

Radiolysis of chloroform results in the formation of chloride, as was previously described by Hatashita et al. [15] and Taghipour et al. [12]:

Step 1: $\text{H}_2\text{O} + \text{gamma ray} \rightarrow \text{H}_2\text{O}^+ + \text{e}^-$ (with a yield of 0.28 μmol per absorbed Joule). Taghipour et al. [12] furthermore reported the formation of $\cdot\text{H}$, $\cdot\text{OH}$, H_2O_2 , H_2 , OH^- and H^+ .

Step 2: $\text{CHCl}_3 + \text{e}^- \rightarrow \cdot\text{CHCl}_2 + \text{Cl}^-$

Step 3: decomposition of $\cdot\text{CHCl}_2$ by H_2O and O_2 to 2 Cl^- , CO , CO_2 and H_2O

It is important to note that the above given radiolysis of chloroform occurs in water. In contrast, the water content in our microspheres is rather low (2 %). It is, therefore, likely that other free radicals or ‘lost electrons’ are the initiators of the radiolysis of chloroform in PLLA microspheres. Indeed, Montanari et al. described the radiolysis of PLGA and the formation of radicals by electron loss [25]. Table 1 shows that chlorine was quantitatively converted into chloride for samples which were irradiated in the Delft facility (Table 1.). In contrast, samples which were neutron-irradiated in the Petten facility showed a chloride content which was about one third of the initial chlorine amount. The differences in chloride content between the two reactor facilities can be caused by a tempera-

ture difference during irradiation. However, varying the temperature in the facilities of either Delft or Petten to study the effect of temperature differences is impossible. Therefore, the effect of temperature during irradiation was studied at a fixed gamma dose of 200 kGy, since at this dose chlorine was also converted into chloride (Table 1.). The temperature was varied between 30 to 70 °C and the results are given in Fig. 2. This graph shows after irradiation that the Cl^-

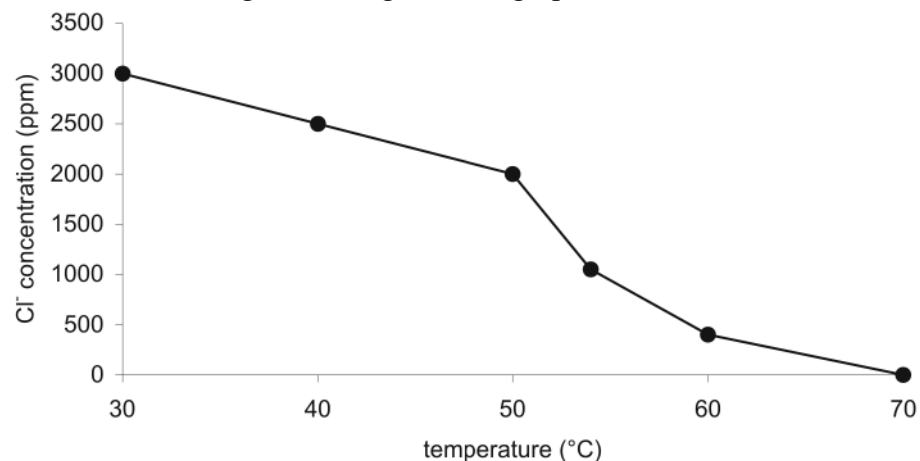


Fig. 2 Cl^- concentrations (ppm) in Ho-PLLA-MS dried at 50 °C after gamma irradiation with 200 kGy at varying temperatures

concentration in the microspheres slightly decreased from 30 to 50 °C. Above 50 °C a strong decrease in Cl^- concentration was observed. DSC-analysis (shown in Fig. 3) showed that the onset of the glass transition temperature of the microspheres started at 50 °C. Therefore, it is likely, that with increasing temperature chloroform evaporated particularly above the T_g of the PLLA matrices during irradiation, which resulted in lower Cl^- levels.

Ho-PLLA-MS and PLLA-MS dried at 70 °C for 5 h had a chlorine content below the GC detection limit (~300 ppm chloroform). However, neutron activation analysis of these samples showed that their chlorine content varied from 50-100 ppm, corresponding with 60-110 ppm chloroform. These levels are just above the earlier mentioned chloroform limit (from the ICH-guidelines) of 60 ppm. If these samples were subsequently neutron irradiated no chloroform could be detected using headspace GC, making Ho-PLLA-MS suitable for clinical application considering their residual solvent levels.

3.4 Gas Chromatography-Mass Spectrometry (GC-MS)

No phosgene could be detected in neutron-irradiated microspheres using GC-MS (method-1), which means that the level was below detection limit (20 ppb). However, it cannot be excluded that phosgene was formed in microspheres during radiation. However, phosgene might have reacted with the water present in the microspheres (2 %, section 3.2).

GC-MS (method-2) of PLLA-MS and Ho-PLLA-MS dried at 50 °C and 70 °C before irradiation showed that trace amounts of lactic acid were present. After neutron irradiation the amount of lactic acid increased substantially. Moreover, lactic acid oligomers like the lactyl-lactate dimer, trimer and tetramer were also detected. We previously showed that chain scission of PLLA occurred during neutron irradiation of (Ho-)PLLA-MS [1,13]. The detection of lactic acid oligomers confirms these findings.

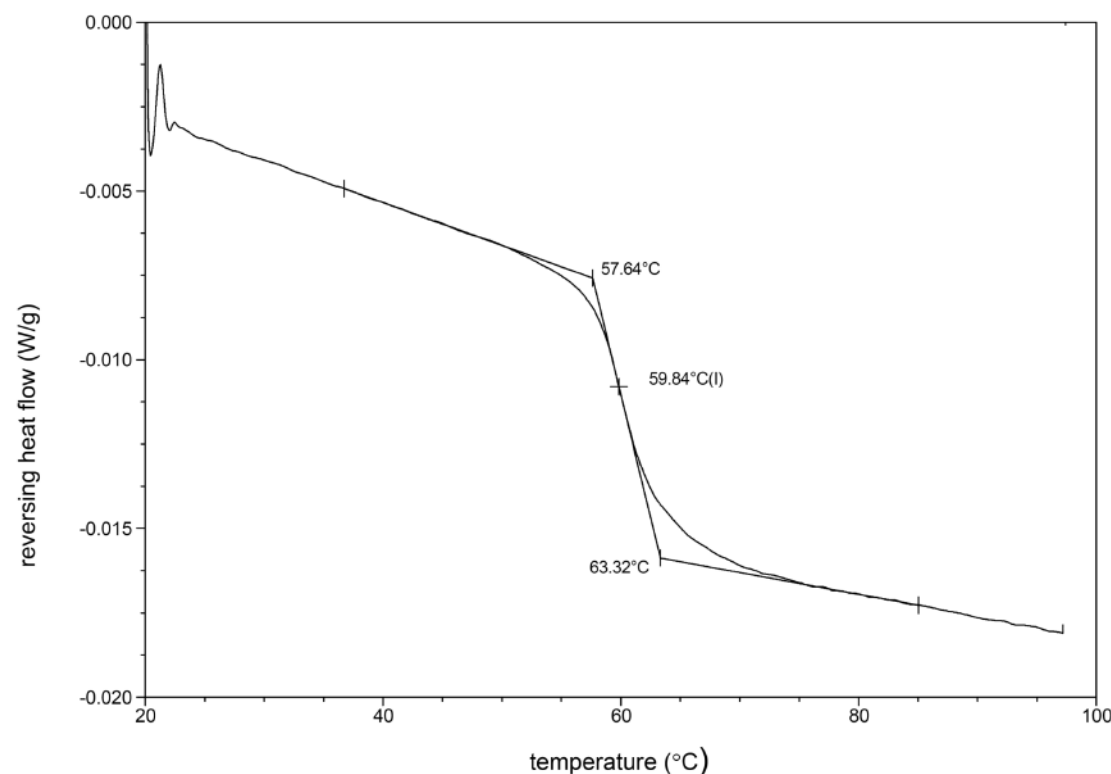


Fig. 3 Enlargement of the MDSC thermogram (reversing heat flow) of Ho-PLLA-MS irradiated with 200 kGy. The glass transition starts at 50 °C and the T_g was determined at 60 °C.

3.5 Molecular weight determinations

The molecular weights of PLLA in (Ho)-PLLA-MS before and after irradiation (gamma, neutron) are given in Table 2. GPC analysis of Ho-PLLA-MS showed that the M_w and M_n of PLLA were lower than the molecular weights in PLLA-MS. As reported before, this decrease in molecular weight is not caused by Ho-induced degradation of PLLA [13,26], but is due to interactions between PLLA and Ho-AcAc which results in a decrease in the hydrodynamic volume of PLLA and thus in an apparent lower molecular weight. After gamma irradiation (25 kGy) the M_w and M_n of PLLA in PLLA-MS and Ho-PLLA-MS decreased with ~45 % and ~20 %, respectively. This decrease in molecular weights is caused by chain scission induced by gamma irradiation [25], and was independent of the applied drying procedure of the samples. Higher dosages of gamma-irradiation

(from 100 up to 1000 kGy) resulted in a further decrease of the molecular weight (M_w from 9,000 to 1,600 and M_n from 6,000 to 1,400 g/mol; Table 2). In agreement with previous findings [13] neutron irradiation of (Ho)-PLLA-MS caused a substantial decrease (~95%) in the M_w and M_n of PLLA. Again, the changes in molecular weight due to neutron irradiation were independent of the residual chloroform levels of the microspheres.

3.6 Differential Scanning Calorimetry (DSC)

Table 3 summarizes the results of the DSC-analysis of the different microspheres and some representative thermograms are given in Figures 4 and 5. No differences in the DSC-pattern were observed between PLLA-MS which were

Table 2. Weight average and number average molecular weights of PLLA in Ho-PLLA-MS, PLLA-MS and PLLA references which were dried and subsequently irradiated in different ways

sample	drying procedure	irradiation	Mw	Mn
PLLA-MS	50 °C	non	85,000	40,000
PLLA-MS	50 °C	γ 25 kGy	45,000	18,000
PLLA-MS	50 °C	neutron*	2200	1900
PLLA-MS	70 °C vacuum	non	84,000	40,000
PLLA-MS	70 °C vacuum	γ 25 kGy	43,000	17,000
PLLA-MS	70 °C vacuum	neutron*	2200	2000
Ho-PLLA-MS	50 °C	non	66,000	48,000
Ho-PLLA-MS	50 °C	γ 25 kGy	55,000	31,000
Ho-PLLA-MS	50 °C	neutron*	1,500	1,200
Ho-PLLA-MS	70 °C vacuum	non	64,000	48,000
Ho-PLLA-MS	70 °C vacuum	γ 25 kGy	53,000	30,000
Ho-PLLA-MS	70 °C vacuum	neutron*	1,700	1,200
Ho-PLLA-MS	50 °C	γ 100 kGy	9,000	6,000
Ho-PLLA-MS	50 °C	γ 200 kGy	6,100	4,700
Ho-PLLA-MS	50 °C	γ 400 kGy	4,600	3,300
Ho-PLLA-MS	50 °C	γ 500 kGy	3,200	2,500
Ho-PLLA-MS	50 °C	γ 1000 kGy	1,600	1,400
PLLA(control)	-	non	88,000	41,000
PLLA (control)	-	γ 25 kGy	49,000	21,000
PLLA (control)	-	neutron*	2400	2100

* neutron irradiated in the Delft facility

Table 3. DSC data of Ho-PLLA-MS, PLLA-MS and PLLA references which were dried and subsequently irradiated in different ways

sample	drying procedure	irradiation	Tg (°C)	Tm max melting (°C)	enthalpy (J/g) **
PLLA-MS	50 °C	non	70	176	55
PLLA-MS	50 °C	γ 25 kGy	68	174	49
PLLA-MS	50 °C	neutron*	nd	116	12
PLLA-MS	70 °C vacuum	non	69	177	57
PLLA-MS	70 °C vacuum	γ 25 kGy	60	173	52
PLLA-MS	70 °C vacuum	neutron*	nd	114	13
Ho-PLLA-MS	50 °C	non	60	141	35
Ho-PLLA-MS	50 °C	γ 25 kGy	60	139	32
Ho-PLLA-MS	50 °C	neutron*	50	nd	nd
Ho-PLLA-MS	70 °C vacuum	non	62	135	40
Ho-PLLA-MS	70 °C vacuum	γ 25 kGy	66	141	8
Ho-PLLA-MS	70 °C vacuum	neutron*	50	nd	nd
Ho-PLLA-MS	50 °C	γ 100 kGy	63	143	23
Ho-PLLA-MS	50 °C	γ 200 kGy	60	129	15
Ho-PLLA-MS	50 °C	γ 400 kGy	59	nd	nd
Ho-PLLA-MS	50 °C	γ 500 kGy	58	nd	nd
Ho-PLLA-MS	50 °C	γ 1000 kGy	49	nd	nd
PLLA (control)	-	non	66	176	54
PLLA (control)	-	γ 25 kGy	nd	176	49
PLLA (control)	-	neutron*	nd	119	15

* neutron irradiated in the Delft facility

** corrected for HoAcAc loading

dried at 50 °C for 48 h or at 70 °C under vacuum, for 5 h. Gamma irradiation (25 kGy) of PLLA-MS did not result in major changes in the DSC-pattern (Fig. 4). However, after neutron irradiation both the melting temperature (T_m) and melting enthalpy decreased tremendously whereas no glass transition temperature (T_g) was detected (Fig. 4). Comparable DSC data were previously obtained with samples neutron irradiated in the Petten reactor facility [13].

Before irradiation, Ho-PLLA-MS had a lower T_g , T_m and melting enthalpy than non-loaded PLLA-MS (Table 3). Gamma irradiation (25 kGy) of Ho-PLLA-MS did not result in major changes in the DSC-pattern (Fig. 5). However, with increased dose the T_g as well as the T_m and melting enthalpy decreased significantly. These results are in agreement with the GPC-data of Table 2, which show that polymer degradation had occurred. With doses of 400 kGy or higher and also after neutron irradiation of Ho-PLLA-MS lowering of the T_g was observed, whereas no T_m was detected (Fig. 5). This means that neutron and high dose

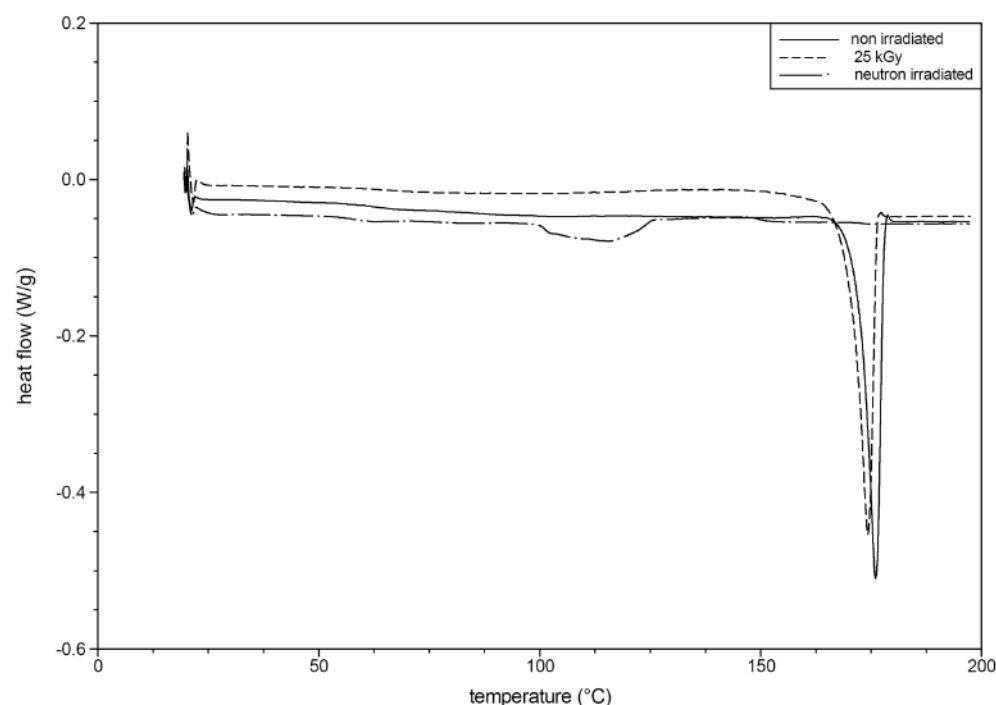


Fig. 4 MDSC thermograms (heat flow) of PLLA-MS before and after gamma irradiation (25 kGy and neutron irradiation).

gamma irradiation result in a substantial decrease in PLLA molecular weight by which crystallization was prevented. It is however important to note that the structural integrity of the Ho-PLLA-MS was preserved.

4. Conclusion

This study shows that residual chloroform in Ho-PLLA-MS can be effectively removed by neutron irradiation or a gamma-irradiation at a dose of 200 kGy. As a result of radiolysis chloroform was converted into chloride and no harmful phosgene could be detected in Ho-PLLA-MS. Although the microspheres were affected by these high-energy radiations in terms of their molecular weight and crystallinity, the particles retained their integrity and desired size between 20-50 μ m, which is the main requirement for their clinical application.

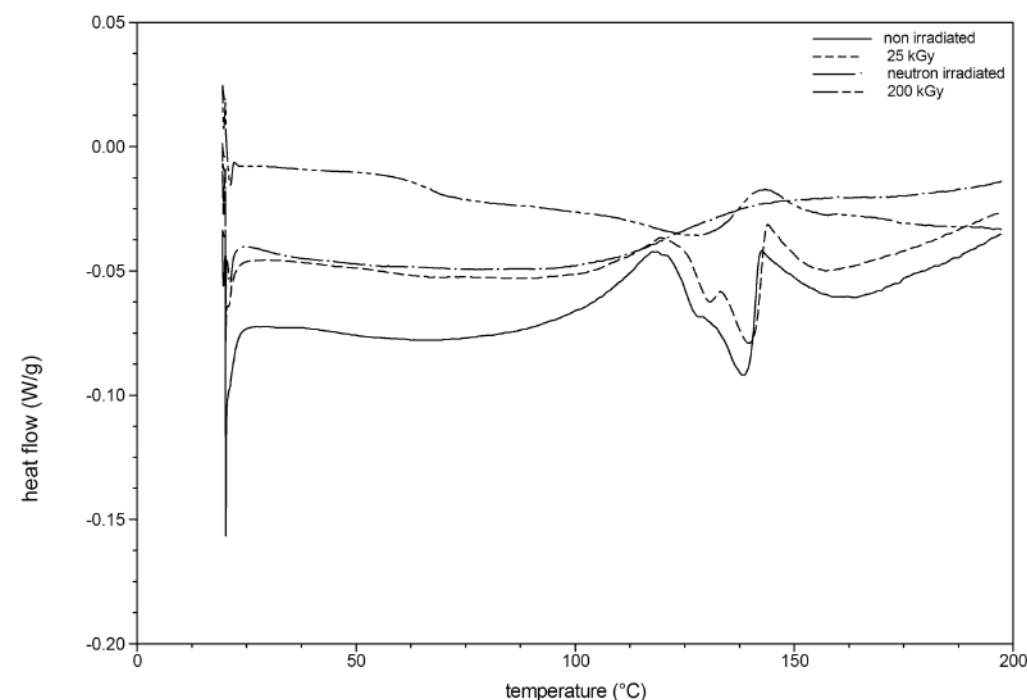


Fig. 5 MDSC thermograms (heat flow) of Ho-PLLA-MS before and after gamma irradiation (25 kGy and 200 kGy) and neutron irradiation.

Acknowledgements

The authors wish to thank P. Snip and Dr. J.R. Woittiez of the NRG, (Petten, The Netherlands) for sample neutron irradiations, W.A.M. van Maurik from EMSA, Faculty of Biology, Utrecht University, Utrecht, The Netherlands for SEM acquisition and W. van de Bogaard, Dr. J.C. Hoogvliet and Dr. O.A.G.J. van der Houwen from the faculty of Pharmaceutical Sciences, Utrecht University, The Netherlands, for their support in the GC-analysis and chloride titrations. Moreover, we are grateful to L. Luthjens, M. Hom and R. Abellon from the Department of Optoelectronic Materials and J. Kroon of Department of Radiation, Radionuclides and Reactor (Delft University of Technology, The Netherlands) for their assistance with neutron and gamma irradiations.

This research was supported by the Technology Foundation STW (UGT.6069), applied science division of NWO and the technology programme of the Ministry of Economic Affairs, and by the Nijbakker-Morra foundation.

References

- [1] Nijsen JFW, van het Schip AD, Hennink WE, Rook DW, van Rijk PP, de Klerk JMH. Advances in nuclear oncology: Microspheres for internal radionuclide therapy of liver metastases. *Curr Med Chem* 2002;9:73-82.
- [2] Nijsen JFW, Seppenwoolde JH, Havenith T, Bos C, Bakker CJG, van het Schip AD. Liver Tumors: MR Imaging of Radioactive Holmium Microspheres—Phantom and Rabbit Study. *Radiology* 2004;231:491-9.
- [3] Nijsen JFW, Zonnenberg BA, Woittiez JR, Rook DW, Swildens-van Woudenberg IA, van Rijk PP, van het Schip AD. Holmium-166 poly lactic acid microspheres applicable for intra-arterial radionuclide therapy of hepatic malignancies: effects of preparation and neutron activation techniques. *Eur J Nucl Med* 1999;26:699-704.
- [4] O'Donnel PB, McGinity JW. Preparation of microspheres by solvent evaporation technique. *Adv Drug Del Rev* 1997;28:25-42.
- [5] Chung TW, Huang YY, Liu YZ. Effects of the rate of solvent evaporation on the characteristics of drug loaded PLLA and PDLLA microspheres. *Int J Pharm* 2001;212:161-9.
- [6] Koegler WS, Patrick C, Cima MJ, Griffith LG. Carbon dioxide extraction of residual chloroform from biodegradable polymers. *J of Biomed Mater Res* 2002;63:567-76.
- [7] Mumper RJ, Jay M. Poly(L-lactic acid) microspheres containing neutron-activatable holmium-165: a study of the physical characteristics of microspheres before and after irradiation in a nuclear reactor. *Pharm Res* 1992;9:149-54.
- [8] Benoit J, Courteille F, Thies C. A physicochemical study of the morphology of progesterone-loaded poly (-lactide) microspheres. *Int J Pharm* 1986;29:95-102.
- [9] B'Hymer C. Residual solvent testing: A review of gas-chromatographic and alternative techniques. *Pharm Res* 2003;20:337-44.
- [10] Freitas S, Merkle HP, Gander B. Microencapsulation by solvent extraction/evaporation: reviewing the state of the art of microsphere preparation process technology. *J Control Release* 2005;102:313-32.
- [11] Herberger J, Murphy K, Munyakazi L, Cordia J, Westhaus E. Carbon dioxide extraction of residual solvents in poly(lactide-co-glycolide) microparticles. *J Control Release* 2003;90:181-95.
- [12] Taghipour F, Evans GJ. Radiolytic dechlorination of chlorinated organics. *Radiat Phys Chem* 1997;49:257-64.
- [13] Nijsen JF, van het Schip AD, van Steenbergen MJ, Zielhuis SW, Kroon-Batenburg LM, van de Weert M, van Rijk PP, Hennink WE. Influence of neutron irradiation on holmium acetylacetonate loaded poly(L-lactic acid) microspheres. *Biomaterials* 2002;23:1831-9.
- [14] Mucka V, Polakova D, Pospisil M, Silber R. Dechlorination of chloroform in aqueous solutions influenced by nitrate ions and hydrocarbonate ions. *Radiat Phys Chem* 2003;68:787-91.
- [15] Hatashita M, Yamamoto T, Wu XZ. Chromatographic study of Gamma-ray irradiated degradation of chlorinated hydrocarbon in water. *Anal Sci* 2001;17 supplement:623-5.
- [16] Dowideit P, Mertens R, vonSonntag C. Non-hydrolytic decay of formyl chloride into CO and HCl in aqueous solution. *J Am Chem Soc* 1996;118:11288-92.
- [17] Chen FY, Pehkonen SO, Ray MB. Kinetics and mechanisms of UV-photodegradation of chlorinated organics in the gas phase. *Water Res* 2002;36:4203-14.
- [18] Keeler JR, Hurt HH, Nold JB, Lennox WJ. Estimation of the LCt50 of Phosgene in Sheep. *Drug Chem Toxicol* 1990;13:229-39.
- [19] Mumper RJ, Ryo UY, Jay M. Neutron-activated holmium-166-poly (L-lactic acid) microspheres: a potential agent for the internal radiation therapy of hepatic tumors. *J Nucl Med* 1991;32:2139-43.
- [20] Zielhuis SW, Nijsen JFW, Figueiredo R, Feddes B, Vredenberg AM, van het Schip AD, Hennink WE. Surface characteristics of holmium-loaded poly(l-lactic acid) microspheres. *Biomaterials* 2005;26:925-32.
- [21] Miller JC, Miller JN. *Statistics for Analytical Chemistry*. Chichester: Ellis Horwood Limited, 2005.
- [22] Franca YV, Leitao F, Shihomatsu HM, Scapin WS, de Moraes NMP, Salvador VL, Figueiredo AMG, Muccillo ENS, Muccillo R. Determination of yttrium and lanthanum in zirconium dioxide by HPLC, X-ray fluorescence and neutron activation analyses. *Chromatographia* 1999;49:91-4.
- [23] European Pharmacopoeia. 4th edition Strasbourg: Council of Europe, 2002.
- [24] Schoene K, Bruckert HJ, Steinhanses J. Derivatization of Acylating Gases and Vapors on the Sorbent Tube and Gas-Chromatographic Analysis of the Products by Atomic Emission and Mass-Spectrometric Detection. *Fresenius J of Anal Chem* 1993;345:688-94.
- [25] Montanari L, Costantini M, Signoretti EC, Valvo L, Santucci M, Bartolomei M, Fattibene P, Onori S,

Chapter 4

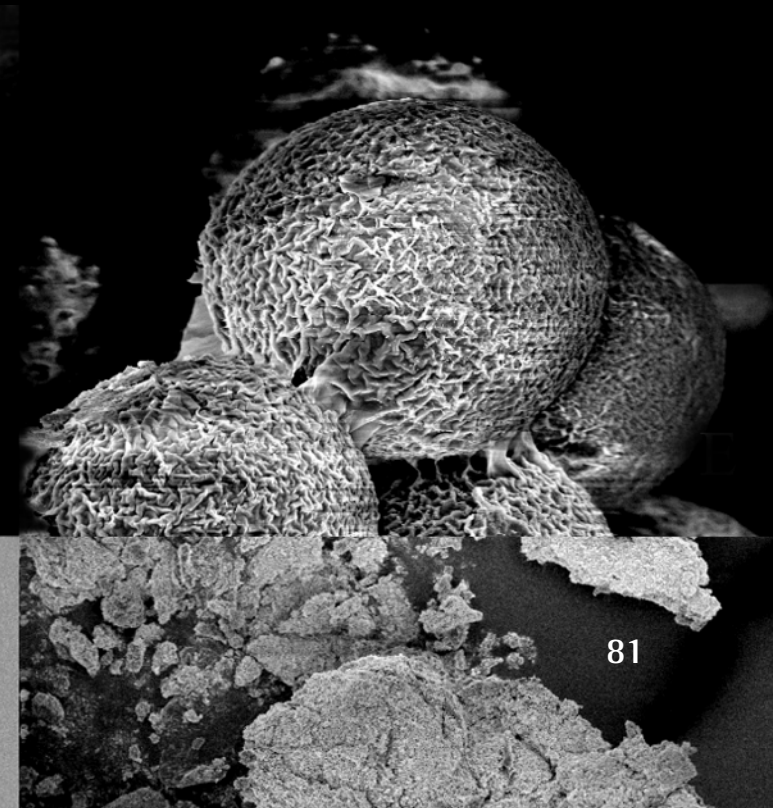
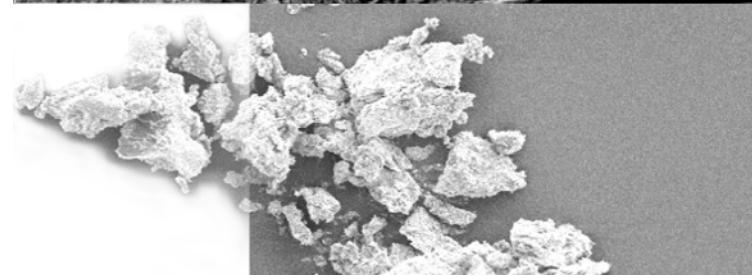
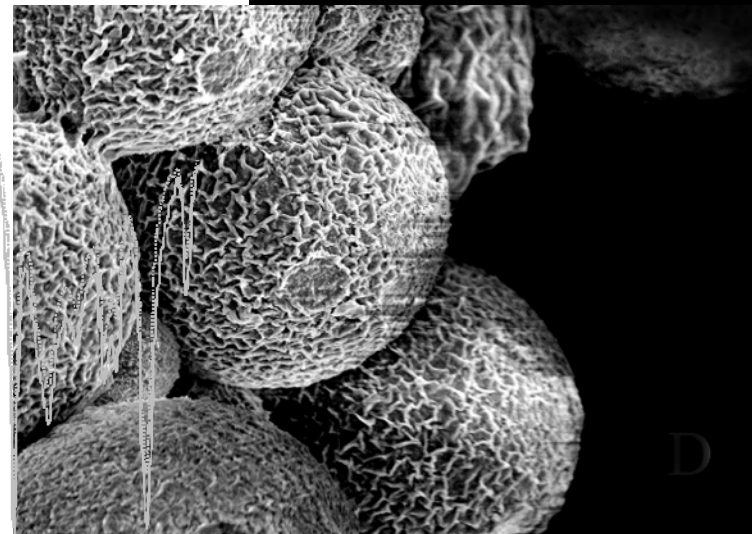
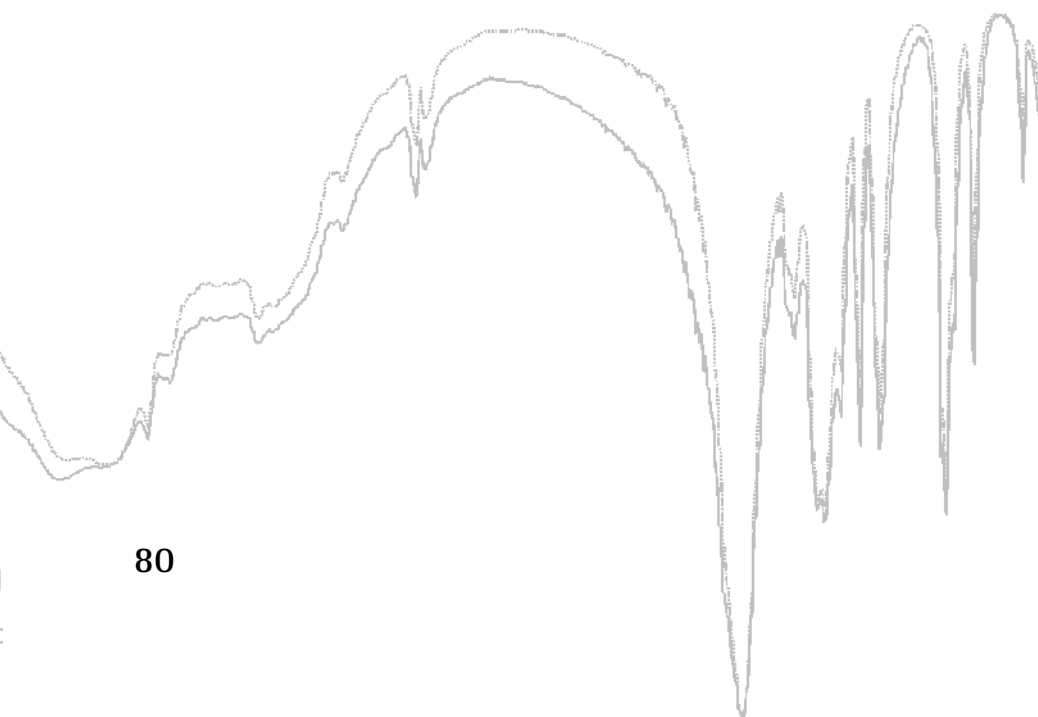
Faucitano A, Conti B, Genta I. Gamma irradiation effects on poly(DL-lactide-co-glycolide) microspheres. *J Control Release* 1998;56:219-229.

[26] Nijsen JFW, van Steenberghe MJ, Kooijman H, Talsma H, Kroon-Batenburg LM, van de Weert M, van Rijk PP, de Witte A, van het Schip AD, Hennink WE. Characterization of poly(L-lactic acid) microspheres loaded with holmium acetylacetonate. *Biomaterials* 2001;22:3073-81.

Chapter 5

Holmium loaded poly(L-lactic acid) microspheres: an in vitro degradation study

SW Zielhuis, JFW Nijsen, GC Krijger, AD van het Schip and WE Hennink



Abstract

The clinical application of holmium loaded poly (L-lactic acid) (PLLA) microspheres for the radionuclide treatment of liver malignancies requires in depth understanding of the degradation characteristics of the microspheres and the nature of the formed degradation products. To this end, an in-vitro degradation study of these microspheres was conducted.

PLLA- microspheres with and without HoAcAc loading, and before and after neutron or gamma irradiation, were incubated in a phosphate buffer at 37 °C for 12 months. At different time points the microspheres were analyzed with differential scanning calorimetry (DSC), scanning electron microscopy, particle size analysis and infrared spectroscopy; the molecular weight of PLLA was determined with gel permeation chromatography. The release of holmium into the buffer was determined by measurement of metastable radioactive holmium (Ho-166m).

In contrast with the other microsphere formulations that retained their spherical shape after 52 weeks of incubation in buffer, only the neutron-irradiated Ho-PLLA-MS disintegrated after a period of 24 weeks. At the end of the experiment (52 weeks) highly crystalline fragments, as evidenced from DSC analysis, were present. Infrared spectroscopy showed that these fragments consisted of holmium lactate. However, despite the fact that the microspheres disintegrated at week 24, holmium was not detected in the buffer solution and was consequently retained in the formed holmium lactate crystals.

In conclusion, this study demonstrates that the degradation of neutron-irradiated Ho-PLLA-MS was substantially accelerated by the HoAcAc incorporation and subsequent neutron irradiation. The degradation of these microspheres in aqueous solution resulted in the formation of insoluble holmium lactate microcrystals without release of Ho^{3+} .

1. Introduction

Radioembolization is a minimally invasive treatment for liver malignancies that can be used when curative surgery is not possible [1-3]. This treatment makes use of radionuclide-loaded microparticles with a size of 20–50 μm that are delivered into the blood vessels in and around the tumour after administration via a catheter. When these microspheres are administered into the hepatic artery of patients suffering from liver malignancies, they will lodge in and around the tumour and directly irradiate the tumour [1,2]. Radioactive microspheres can be obtained by neutron irradiation in a nuclear reactor. Therefore, the microspheres should be loaded with an element that can be easily neutron activated.

Holmium-165 is a non-radioactive element with a high cross-section of 64 barn and a natural abundance of 100% [1,4], allowing a fast and simple neutron activation procedure. Neutron irradiation of holmium-165 results in the formation of radioactive holmium-166 (physical half-life of 26.8 h), a β -emitter ($E_{\text{max}} = 1.84 \text{ MeV}$) suitable for radionuclide therapy that also emits photons (80.6 keV, 6.2 %) usable for imaging with a gamma camera. Holmium-165 can be incorporated into poly (L-lactic acid) (PLLA) microspheres as its acetylacetonate complex (HoAcAc) using a solvent evaporation technique [5].

It is important that therapeutic radiopharmaceuticals have a high radiochemical stability. The release of radioactive holmium from the microspheres will result in distribution over other organs than the liver, which can lead to serious adverse events. Previous papers report that, although the molecular weight of the PLLA decreased due to the neutron irradiation, the microspheres retained their integrity [5]. Moreover, two days after administration, the amount of holmium-166 in urine and faeces of treated rabbits was less than 0.1 % of the administered dose [6] indicating that holmium remained stably incorporated in the microspheres. However, the long-term effects concerning the chemical toxicity and biocompatibility of Ho-PLLA-MS are unknown and need further examination. Consequently, a clear insight into the degradation characteristics of the microspheres and the nature of the formed degradation products is essential. It is well known that gamma irradiation also changes the properties of polymeric microspheres [7] and therefore besides the effect of neutron irradiation, the effect of gamma irradiation on the degradation characteristics of the microspheres was also studied. Gamma irradiation is a well-established sterilization

method for PLLA and might therefore be a useful option for the sterilization of Ho-PLLA-MS [8].

Hydrolysis of ester bonds in poly(lactic acid) results in the formation of soluble lactic acid oligomers which are ultimately converted into lactic acid [9-11]. By this hydrolytic process, PLLA microspheres disintegrate and finally 'dissolve' in time. The degradation of (drug-loaded) PLLA microspheres is dependent on many factors, such as the size, morphology, molecular weight of PLLA and the type of drug and drug loading [12,13]. In view of this, there are two factors that can have a large influence on the degradation of Ho-PLLA-MS. The first factor is the neutron irradiation [5], which results in substantial decrease in molecular weight of PLLA and a loss of its crystallinity [14]. The second factor is the high drug loading, because 50 % of the microsphere matrix consists of HoAcAc. It was demonstrated that the Ho-ion interacts with the carbonyl groups of PLLA [15] which in turn might affect the hydrolytic degradation of PLLA.

In order to understand the consequences of these factors, an in-vitro degradation study was conducted. Knowledge of the degradation pattern of Ho-PLLA-MS is of great importance for evaluation of the biocompatibility of these microspheres in animals and their application in patients.

2. Materials and Methods

2.1 Materials

All chemicals were commercially available and used as obtained. Acetylacetone, 2,4-pentanedione (AcAc; > 99 %), chloroform (CHCl_3 ; HPLC-grade), poly(vinyl alcohol) (PVA; average MW 30 000 – 70 000, 88 % hydrolyzed) and ammonium hydroxide (NH_4OH ; 29.3% in water) were supplied by Sigma Aldrich (Steinheim, Germany). Sodium hydroxide (NaOH ; 99.9 %) was purchased from Riedel-de Haën (Seelze, Germany). Holmium (III) chloride hexahydrate ($\text{HoCl}_3 \cdot 6\text{H}_2\text{O}$; 99.9 %) was obtained from Phase Separations BV (Waddinxveen, The Netherlands). L-lactic acid (90 % solution; USP-grade) and poly(L-lactic acid) (PLLA; inherent viscosity 1.14 dl/g in chloroform at 25 °C) were purchased from Purac Biochem (Gorinchem, The Netherlands). Hydrochloric acid (HCl ; 37 %), sodium azide (NaN_3 ; 99 %), di-sodium hydrogen phosphate dihydrate ($\text{Na}_2\text{HPO}_4 \cdot 2\text{H}_2\text{O}$; 99 %), sodium dihydrogen phosphate dihydrate ($\text{NaH}_2\text{PO}_4 \cdot 2\text{H}_2\text{O}$; 99 %) and lithium chloride (LiCl ; > 99 %) were purchased from Merck (Darmstadt, Germany).

Dichloromethane (DCM, HPLC-grade), dimethylformamide (DMF, HPLC-grade) and tetrahydrofuran (THF, HPLC-grade) were obtained from Biosolve (Valkenswaard, The Netherlands).

2.2 Preparation of HoAcAc and microspheres

HoAcAc was prepared as described previously [5]. In brief: acetylacetone (180 g) was dissolved in water (1080 g). The pH of this solution was brought to 8.50 with an aqueous solution of ammonium hydroxide. Holmium chloride (10 g dissolved in 30 ml water) was added to this solution. After 15 hours incubation at room temperature, the formed HoAcAc crystals were collected by centrifugation and washed with water.

HoAcAc (10 g) and PLLA (6 g) were dissolved in 186 g chloroform. The resulting homogeneous solution was added to one litre of an aqueous solution of PVA (2 %). The mixture was stirred (500 rpm) for 40 hours at room temperature and the formed microspheres were collected by centrifugation. The microspheres were washed three times with water, three times with 0.1 M HCl and finally three times with water. The washed microspheres were size fractionated with a wet sieving system consisting of an Electromagnetic Sieve Vibrator (EMS 755) combined with an Ultrasonic Processor (UDS 751) (both from Topas GmbH, Dresden, Germany). The collected microspheres (about 4 grams, size between 20 and 50 μm) were dried at 70 °C under vacuum for 5 h using a rotating Glass Oven (B-580 GKR, Buchi). The holmium content in microspheres was determined by a complexometric titration as described previously [16]. Placebo PLLA-microspheres without HoAcAc loading were prepared in the same way. After drying, microspheres (~250 mg) were packed in polyethylene vials.

2.3 Neutron and gamma irradiation

Neutron irradiations were performed in the pneumatic rabbit system (PRS) in the reactor facility in Delft (Department of Radiation, Radionuclides and Reactor, Delft University of Technology, The Netherlands). The polyethylene vials with Ho-PLLA-MS (~250 mg) were neutron-irradiated with a thermal neutron flux of $5 \times 10^{12} \text{ cm}^{-2} \cdot \text{s}^{-1}$ during 6 h. The neutron-irradiated microspheres were stored in closed vials at room temperature and analyzed after one month. Gamma sterilization of the samples with a dose of 25.0 kGy was performed using a cobalt-60 source (Isotron, Ede, The Netherlands).

2.4 Degradation of microspheres

Microsphere samples (100 mg) were incubated in test tubes containing 5 ml of an isotonic phosphate buffer (174 mM, pH 7.4) and continuously shaken at 37 °C. Sodium azide (0.05 %) was added to the buffer to prevent bacterial growth. At predetermined time points (1, 4, 8, 12, 16, 24, 32, 40 and 52 weeks), samples were centrifuged for 5 min at 2000 rpm and the supernatant was collected. The microspheres were washed two times with water, dried for three days at room temperature (without further treatment) and weighed. The microspheres and supernatant were used for further analysis.

2.5 Release of holmium

The release of holmium from neutron-irradiated microspheres was determined by measurement of metastable radioactive holmium (Ho-166m) in the supernatant and in the degraded microspheres using a low-background γ -counter (Tobor, Nuclear Chicago, USA). Ho-166m is a metastable isotope formed in a small fraction (7 ppm of the total amount of newly formed isotopes) during activation of Ho-165. The concentration of Ho-166m in the samples was low but detectable. After the decay of Ho-166 (half-life of 26.8 h) during one month of storage, Ho-166m (half-life ~1200 year) is the only persisting radioactive isotope in the microspheres and can therefore be reliably and accurately detected as demonstrated previously [17].

2.6 Holmium lactate

Holmium lactate was prepared as follows. (L)-lactic acid (1.0 g) was dissolved in 10 ml of distilled water and the pH was adjusted to 6.0 with a sodium hydroxide solution (1 M). Holmium chloride (4.2 g) was dissolved in 20 ml of water and subsequently added to the sodium lactate solution, and a precipitate was formed. The reaction was performed at pH 6.0 since it is known that at higher pH-values holmium hydroxide can be formed [18]. The precipitated holmium lactate was washed three times with water and dried for 48 h at 50 °C.

2.7 Determination of particle size distribution and evaluation of the surface morphology of the microspheres

The particle size distribution of microspheres was determined using a Coulter

counter (Multisizer 3, Beckman Coulter, The Netherlands) equipped with a 100- μ m orifice.

The surface morphology of the Ho-PLLA-microspheres was investigated by scanning electron microscopy (SEM) using a Philips XL30 FEGSEM. A voltage of 5 or 10 kV was applied. Samples of the different microsphere batches were mounted on aluminium stubs and sputter-coated with a Pt/Pd layer of about 10 nm.

2.8 Gel Permeation Chromatography (GPC)

The weight-average molecular weight (M_w) and number-average molecular weight (M_n) of PLLA of non-irradiated and gamma-irradiated PLLA- and Ho-PLLA-MS were determined by GPC with two thermostated (35 °C) columns in series (PL gel Mixed-D, Polymer Laboratories, Amherst, USA). A refractive index detector (type 410, Waters, Milford, USA) was used. Samples of approximately 10 mg were dissolved in 5 ml chloroform and filtered through 0.45 μ m HPLC-filters (Waters). Elution was performed with chloroform and the flow-rate was 1 ml/min.

The M_w and M_n of PLLA of the neutron-irradiated PLLA-MS and Ho-PLLA-MS were determined by another GPC-method using two thermostated (40 °C) columns in series (Mesopore, Polymer Laboratories). Samples of approximately 10 mg were dissolved in 5 ml THF and filtered through 0.45 μ m HPLC-filters (Waters). Elution was performed with THF and the flow-rate was 1 ml/min. The Mesopore column was used since low molecular weights of PLLA were expected due to the neutron irradiation [14,19] and THF is a suitable solvent for (neutron-irradiated) PLLA [19].

The columns were calibrated using poly(styrene) standards of known molecular weights (Shodex and Tosoh, Polymer Laboratories). Analyses were performed in duplicate.

2.9 Differential Scanning Calorimetry (DSC)

Modulated DSC (MDSC) analyses were performed with a DSC Q1000 (TA Instruments, USA). Samples of approximately 5 mg were transferred into aluminium pans. Scans were recorded under 'heating only' conditions, with a heating rate of 1 °C/min and cooling rate of 2 °C/min. The settings were periods of 30 s and a temperature modulation amplitude of 0.5 °C was applied. Samples

were heated from 20 °C to 230 °C. The Universal Analysis 2000 software (version 3.9A) was used for evaluation. Analyses were performed in duplicate.

2.10 Infrared spectroscopy

Infrared spectra were recorded on a Bio-Rad FTS 6000 spectrometer (Cambridge, USA), in the range of 400-4000 cm⁻¹ (scan number 64, resolution 2 cm⁻¹). Samples of microspheres and of holmium lactate were mixed with spectroscopy grade KBr (Merck, Darmstadt, Germany) and pressed into a tablet using a pressure of 8·10³ kg/cm².

3. Results and discussion

3.1 Release of holmium and weight loss

The characteristics of the prepared Ho-PLLA-MS were in compliance with previous results [5,14,16]. In brief: the holmium loading was 17.0 ± 0.5 %, corresponding with a loading of HoAcAc of ~50 % (w/w). More than 97 % of the microspheres (with and without HoAcAc-loading) had a size between 20-50 µm after sieving. No differences in size distributions were observed after gamma irradiation (25 kGy), whereas after neutron irradiation still more than 95 % of the microspheres had a size between 20 and 50 µm.

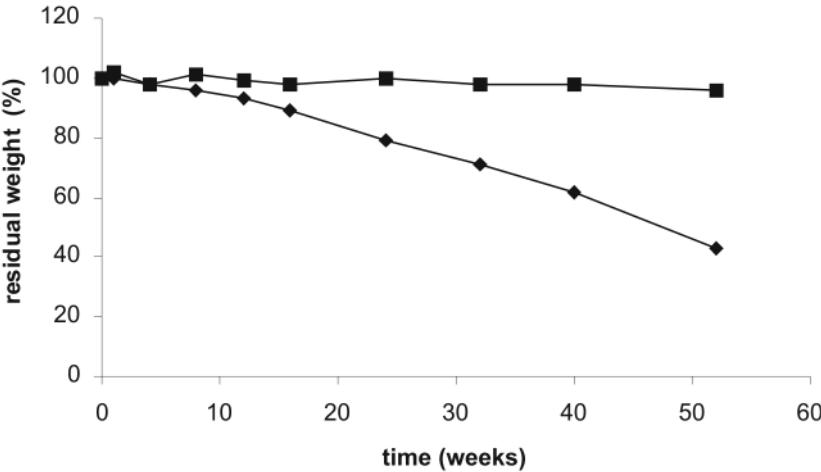


Fig. 1 Weight loss of neutron-irradiated PLLA-MS and neutron-irradiated Ho-PLLA-MS during degradation time. The weight loss of neutron-irradiated PLLA-MS is comparative to the weight loss of the other microsphere formulation and is shown here as a typical example.

In chapter 7 of this thesis we showed that hardly any release of holmium occurred during 270 h incubation of Ho-PLLA-MS in a phosphate buffer (0.5 % ± 0.2 %) [20]. In the present study the release was followed for longer times and it was shown that during a time span of 52 weeks only 0.7 % ± 0.2 % had released. The weight loss of neutron-irradiated Ho-PLLA-MS incubated in buffer in time is given in Figure 1. This figure shows that the weight of these microspheres decreased in time; the total weight loss was ~ 60 % at the end of the degradation experiment (52 weeks). In contradistinction, the other microsphere formulations showed no significant weight loss during 52 weeks, which is in line with data reported on the in vitro degradation of PLLA fibers [21].

3.2 SEM and particle size distribution

Particle size analysis showed that the size of neutron-irradiated Ho-PLLA-MS remained more or less constant during the first 16 weeks of incubation (Fig. 2). Thereafter, the particle size changed considerably and remained almost constant again from week 24 till week 52. No significant particle size changes were observed for the other microsphere formulations.

SEM analysis showed that PLLA-MS without HoAcAc-loading, including the neutron-irradiated ones, retained their spherical shape and smooth surface until

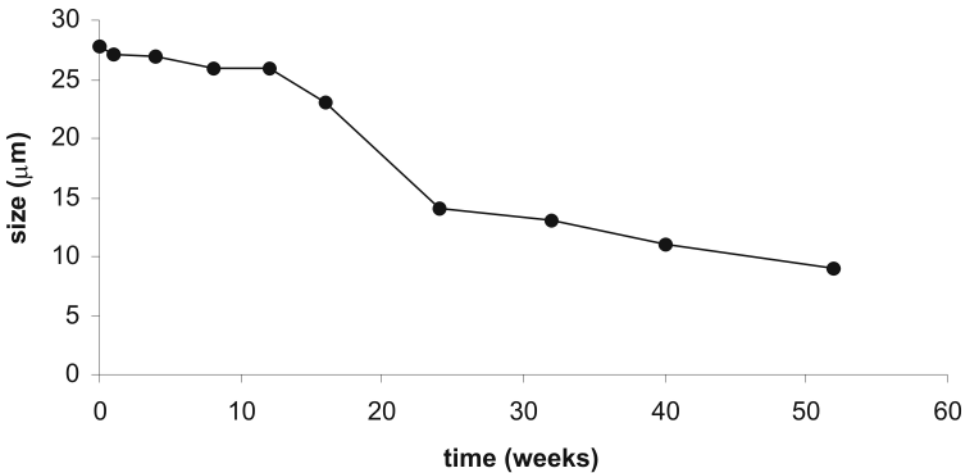


Fig. 2 Mean particle size of neutron irradiated Ho-PLLA-MS during the degradation experiment.

the end of the degradation experiment (52 weeks) (Fig. 3A-C). In contradistinction, SEM showed that Ho-PLLA-MS (Fig. 3D) and gamma-irradiated Ho-PLLA-MS (Fig. 3E) had a wrinkled surface, but retained their spherical shape. SEM analysis of neutron-irradiated Ho-PLLA-MS showed that these microspheres disintegrated after 24 weeks of incubation in buffer (Fig. 3G) and that fragments were present (Fig. 3H) consisting of small needle-shaped crystals (Fig. 3I).

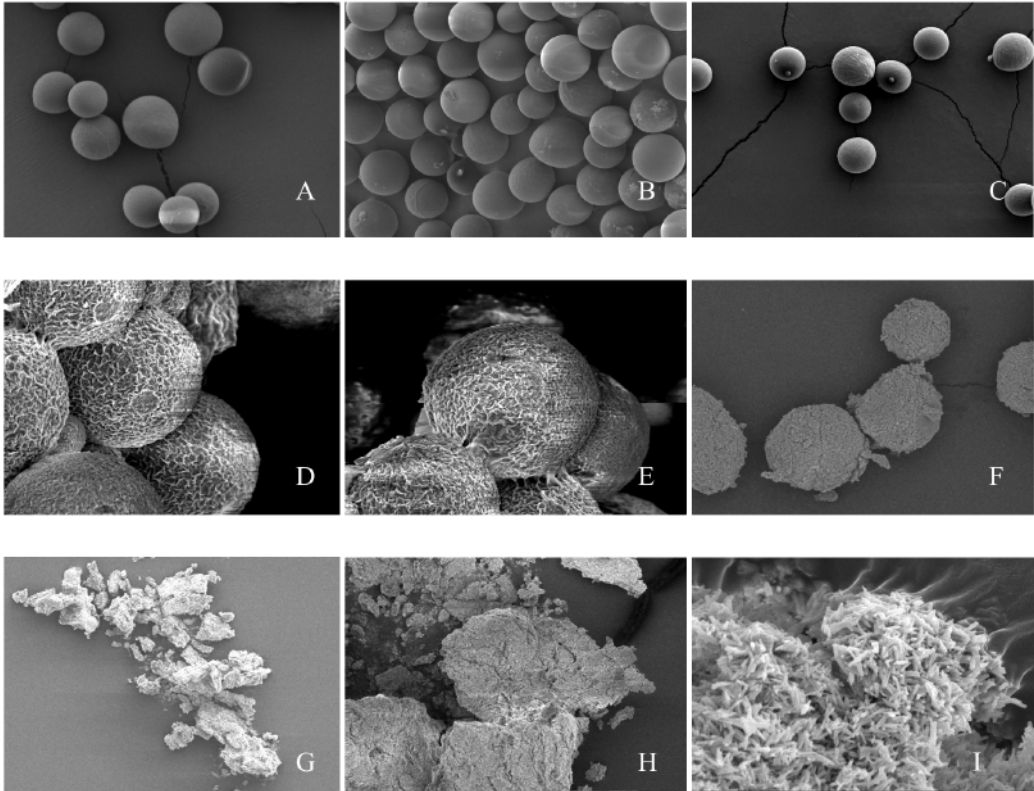


Fig. 3 SEM-pictures of PLLA-MS (A), gamma irradiated PLLA-MS (B), neutron irradiated PLLA-MS (C), Ho-PLLA-MS (D) and gamma irradiated Ho-PLLA-MS (E) after 52 weeks of incubation in buffer. (F), (G) and (H) are neutron irradiated Ho-PLLA-MS after 12, 24 and 52 weeks of incubation in buffer respectively. (I) is a detailed picture of (H) and shows the presence of needle shaped crystals.

3.3 GPC

The initial molecular weights of PLLA in the different microsphere formulations before incubation in buffer are given in Table 1 and were in compliance with previous studies [14,15]. In summary, the M_w and M_n of PLLA in Ho-PLLA-MS were lower than the molecular weights in PLLA-MS. This decrease in molecular weight is not caused by holmium-induced degradation of PLLA [14,15], but is due to interactions between PLLA and Ho-AcAc which results in a decrease in the hydrodynamic volume of PLLA and thus in an apparently lower molecular weight. After gamma irradiation (25 kGy) the M_w and M_n of PLLA in PLLA-MS decreased with ~45 % and ~25 %, respectively, and the M_w and M_n of PLLA in Ho-PLLA-MS decreased with ~20 % and ~35 %, respectively. Neutron irradiation of (Ho)-PLLA-MS caused a substantial decrease (~95%) of the M_w and M_n of PLLA, likely due to chain scission [14]. The M_w and M_n of PLLA in PLLA-MS as a function of degradation time are shown in Fig. 4. A slight decrease in both M_w and M_n was observed for non-irradiated PLLA-MS in time. The M_w and M_n of PLLA in gamma-irradiated PLLA-MS decreased faster in time ending up with a M_w and M_n of ~27,000 and ~20,000 g/mole, respectively. It has indeed been reported that gamma irradiation accelerates the hydrolytic degradation of PLA [22] which is ascribed to the higher number of hydrophilic end groups (COOH and OH) which accelerates PLLA decomposition autocatalytically [22].

Table 1. M_w and M_n of PLLA in non-irradiated (non), gamma-irradiated (gamma) and neutron-irradiated (neutron) PLLA-MS.

sample	irradiation	M_w	M_n
PLLA-MS	non	114,000	65,000
PLLA-MS	gamma	66,000	48,000
PLLA-MS	neutron	2,200	1,900
Ho-PLLA-MS	non	63,000	46,000
Ho-PLLA-MS	gamma	52,000	30,000
Ho-PLLA-MS	neutron	1,900	1,500

The M_w of PLLA in neutron-irradiated PLLA-MS decreased from ~2000 to ~1100 g/mol in 12 weeks of incubation in buffer and remained more or less constant hereafter, which explains that these microspheres stayed intact during the degradation experiment (Fig. 3C, SEM analysis). These GPC-results are in

agreement with the paper of Suuronen et al [23], who followed the degradation of PLLA plates for a period of 5 years and showed that the molecular weight of PLLA decreased from ~50,000 to ~3,000 g/mol after 2 years of incubation in buffer and remained at ~3,000 g/mol during the following 3 years.

Remarkably, PLLA in degraded non-irradiated as well as gamma- and neutron-irradiated Ho-PLLA-MS could not be analyzed with GPC since it was not possible to dissolve Ho-PLLA-MS in suitable solvents like chloroform, DCM, THF, DMF with and without 10 mM of LiCl, even after heating of the solvents to 50 °C. As shown before, Ho^{3+} interacts with the carbonyl groups of PLLA [15], and obviously these interactions increase in time yielding an insoluble matrix.

3.4 DSC

Table 2 summarizes the results of the DSC-analysis of the different microspheres before incubation in buffer. The results were in compliance with previous studies [14,15]. In summary, compared to non-irradiated PLLA-MS, gamma irradiation of PLLA-MS did not result in major changes in the T_g , T_m and melting enthalpy. However, after neutron irradiation both the melting temperature (T_m) and melting enthalpy of PLLA decreased tremendously, whereas no glass transition temperature (T_g) was detected. Non-irradiated Ho-PLLA-MS had a lower T_g , T_m and melting enthalpy than non-loaded PLLA-MS (Table 2) indicating that the PLLA-phase in Ho-PLLA-MS had a low degree of crystallinity [15]. Gamma irradiation of Ho-PLLA-MS did not result in changes of the T_g , T_m and melting enthalpy. In contrast, after neutron irradiation of Ho-PLLA-MS lowering of the T_g was observed, whereas no T_m was detected due to the loss of crystallinity [14].

Table 2. T_g , T_m and melting enthalpy of PLLA-MS and Ho-PLLA-MS

sample	irradiation	T_g (°C)	T_m max (°C)	melting enthalpy (J/g) *
PLLA-MS	non	70	177	55
PLLA-MS	gamma	68	174	48
PLLA-MS	neutron	nd	116	15
Ho-PLLA-MS	non	60	152	30*
Ho-PLLA-MS	gamma	60	150	30*
Ho-PLLA-MS	neutron	50	nd	nd

*melting enthalpy was corrected for the HoAcAc loading, nd: non detectable

The T_g , T_m and melting enthalpy of PLLA-MS and Ho-PLLA-MS after incubation in buffer are shown in Figure 5. In time, a slight decrease in T_g and T_m was observed for non-irradiated PLLA-MS and gamma-irradiated PLLA-MS, whereas the melting enthalpy first slightly decreased and later increased. A decrease in T_m and an increase in the melting enthalpy was also observed for neutron-irradiated PLLA-MS. The increase in crystalline fraction in time can be explained by the observation that degradation of PLLA mainly occurred in its amorphous phase [21,24]. Moreover, it has been reported that crystallisation of the amorphous phase can occur during the degradation process [21,25], which is likely also the case in this study.

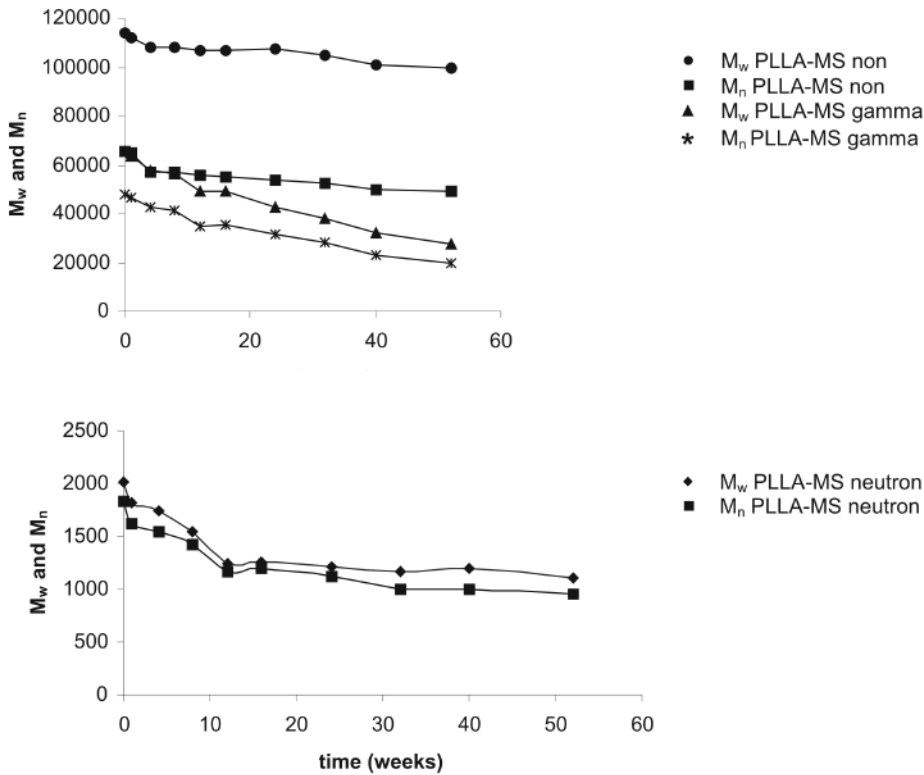


Fig. 4 M_w and M_n of PLLA in non-irradiated (non), gamma-irradiated (gamma) and neutron irradiated (neutron) PLLA-MS as a function of degradation time.

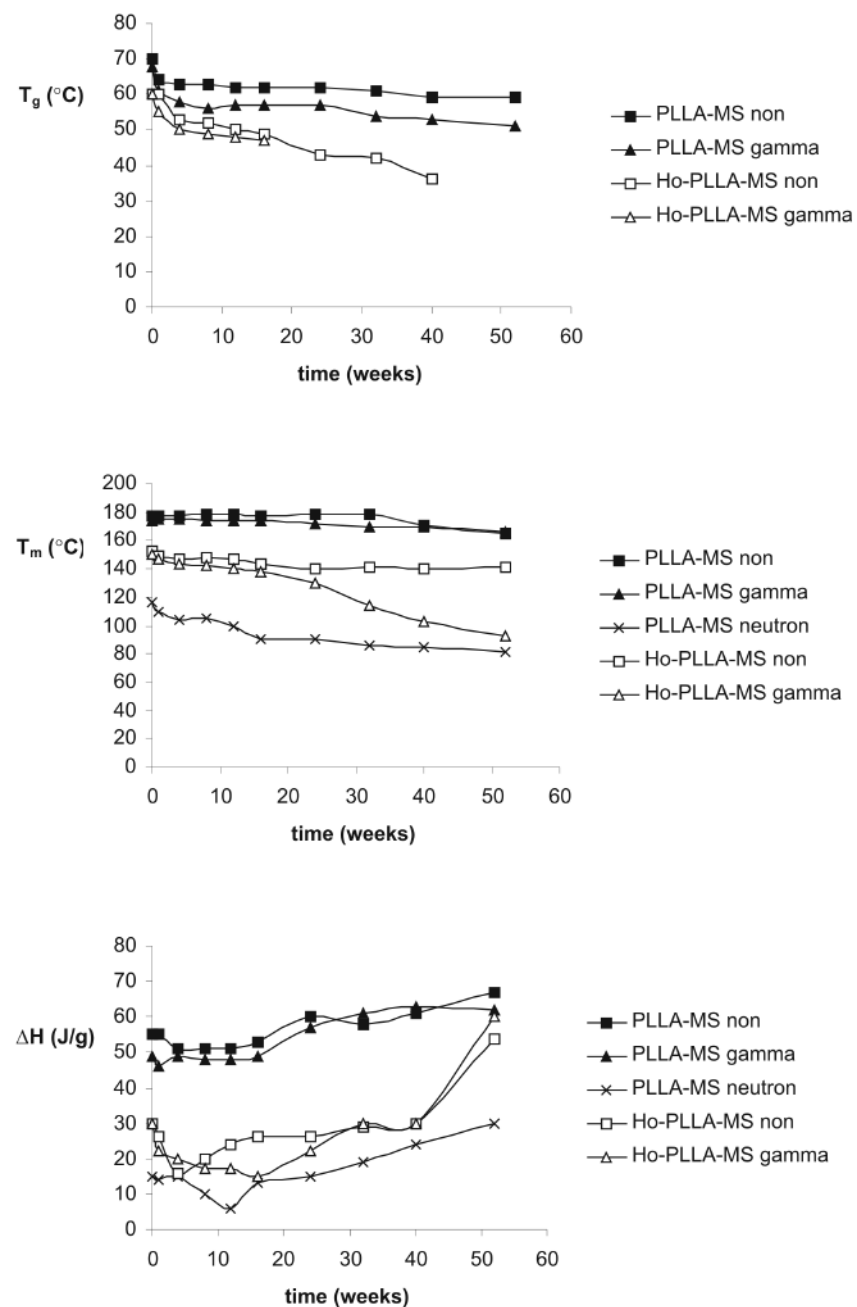


Fig. 5 T_g , T_m and melting enthalpy of non-irradiated (non), gamma-irradiated (gamma) and neutron irradiated (neutron) microspheres as a function of degradation time.

The T_g and T_m of both non- and gamma-irradiated Ho-PLLA-MS decreased somewhat faster than the T_g and T_m of PLLA-MS formulations as a function of the degradation time. No T_g of non-irradiated and gamma-irradiated Ho-PLLA-MS could be observed after 40 and 16 weeks of incubation in buffer respectively probably due to crystallisation of the amorphous phase during the degradation process [21,25].

For neutron-irradiated Ho-PLLA-MS neither a T_g nor a T_m could be detected in the degraded microspheres. The absence of a T_g might be caused by the interaction of Ho^{3+} with the carbonyl groups of PLLA [15], which results in a rigid structure. The absence of crystallinity in neutron-irradiated Ho-PLLA-MS likely caused their relatively fast degradation. Generally, with decreasing crystallinity in microspheres the degradation rate increases [13]. An explanation for the observation that neutron-irradiated Ho-PLLA-MS did degrade while neutron-irradiated PLLA-MS did not degrade in the timeframe studied, might be caused by the HoAcAc-loading. Previous research has shown that HoAcAc is responsible for a low degree of crystallinity of the PLLA phase [15]. Remarkably, neutron-irradiated Ho-PLLA-MS which were incubated in buffer for 52 weeks showed a sharp T_m at 201 °C (Fig. 6) which corresponds with that of holmium lactate (Figure 6).

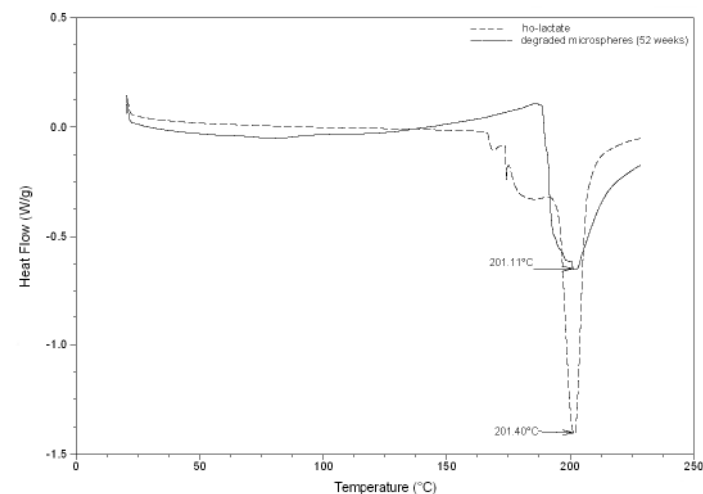


Fig. 6 DSC-thermogram of the insoluble residue after 52 weeks of degradation of neutron irradiated Ho-PLLA-MS and a holmium lactate reference

3.5 Infrared spectroscopy

The IR-spectra of neutron-irradiated Ho-PLLA-MS, which were degraded for 52 weeks, and holmium lactate are given in Fig. 7. The IR-spectra were in compliance with each other, which demonstrates, and supported by the DSC results (Fig. 6), that the degradation of neutron-irradiated Ho-PLLA-MS results in the formation of insoluble holmium lactate microcrystals.

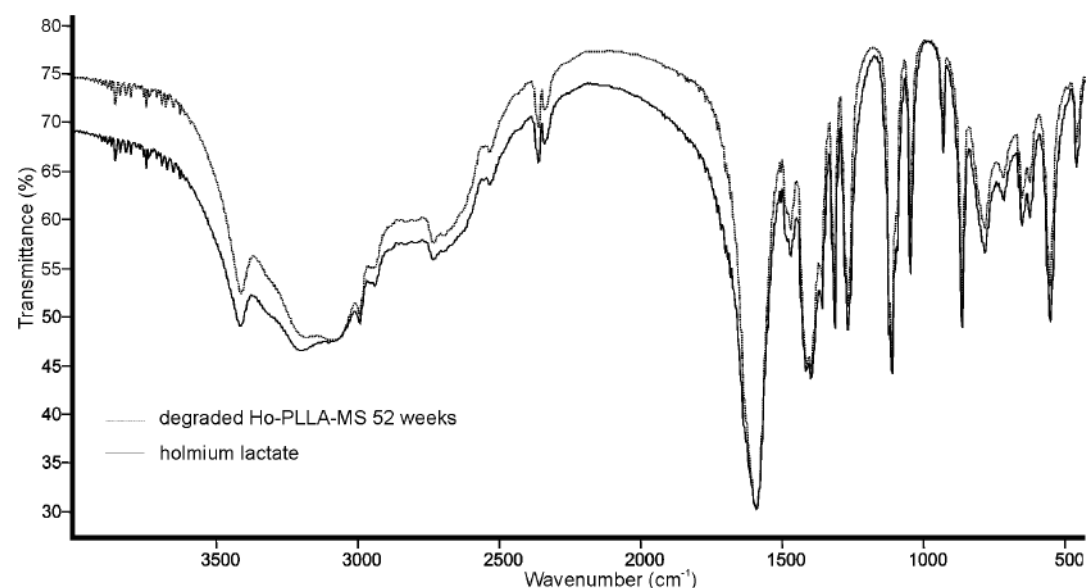


Fig. 7 IR-spectra of the insoluble residue after 52 weeks of degradation of neutron irradiated Ho-PLLA-MS and a holmium lactate reference.

4. Conclusions

The degradation of Ho-PLLA-MS is strongly influenced by its HoAcAc-loading and neutron irradiation. In contradistinction to neutron-irradiated PLLA-MS and non-irradiated Ho-PLLA-MS, neutron-irradiated Ho-PLLA-MS disintegrated after a period of 24 weeks of incubation in buffer, with as a result the formation of insoluble holmium lactate microcrystals. Hardly any holmium was released into the buffer (< 1 %), and the total weight after degradation, namely 40% of the initial weight of the microspheres, corresponds with the calculated weight of

holmium lactate, assuming that Ho^{3+} is complexed by three lactate groups. In conclusion, this study demonstrates that in contradistinction to neutron-irradiated PLLA-MS and non-irradiated Ho-PLLA-MS, neutron-irradiated Ho-PLLA-MS undergo hydrolytic degradation and as a result disintegrate. This process resulted in the formation of insoluble holmium lactate. An in-vivo study (Chapter 6 of this Thesis) will give a decisive answer about the consequences of the degradation characteristics and formation of holmium lactate for the biocompatibility of neutron-irradiated Ho-PLLA-MS.

Acknowledgements

The authors wish to thank W.A.M. van Maurik from EMSA, Faculty of Biology, Utrecht University, Utrecht, The Netherlands for SEM acquisition, J. Kroon of Department of Radiation, Radionuclides and Reactor (Delft University of Technology, The Netherlands) for his assistance with neutron irradiations and M.J. van Steenbergen (Faculty of Pharmaceutical Sciences, Utrecht University, Utrecht, The Netherlands) for his assistance in the GPC-analyses. This research was supported by the Technology Foundation STW (UGT.6069), applied science division of NWO and the technology programme of the Ministry of Economic Affairs, the Nijbakker-Morra foundation and foundation De Drie Lichten.

References

- [1] Nijssen JFW, van het Schip AD, Hennink WE, Rook DW, van Rijk PP, De Klerk JMH. Advances in nuclear oncology: Microspheres for internal radionuclide therapy of liver metastases. *Curr Med Chem* 2002; 9: 73-82.
- [2] Lambert B, Van de WC. Treatment of hepatocellular carcinoma by means of radiopharmaceuticals. *Eur J Nucl Med Mol Imaging* 2005; 32: 980-9.
- [3] van Hazel G, Blackwell A, Anderson J, Price D, Moroz P, Bower G, Cardaci G, Gray B. Randomised phase 2 trial of SIR-Spheres plus fluorouracil/leucovorin chemotherapy versus fluorouracil/leucovorin chemotherapy alone in advanced colorectal cancer. *J Surg Oncol* 2004; 88: 78-85.
- [4] Handbook of Chemistry and Physics, 84th edition. CRC Press, Boca Raton (FL) 2003.
- [5] Nijssen JFW, Zonnenberg BA, Woittiez JR, Rook DW, Swildens-van Woudenberg IA, van Rijk PP, van het Schip AD. Holmium-166 poly lactic acid microspheres applicable for intra-arterial radionuclide therapy of hepatic malignancies: effects of preparation and neutron activation techniques. *Eur J Nucl Med* 1999; 26: 699-704.

- [6] van Es RJ, Nijsen JFW, van het Schip AD, Dullens HF, Slootweg PJ, Koole R. Intra-arterial embolization of head-and-neck cancer with radioactive holmium-166 poly(L-lactic acid) microspheres: an experimental study in rabbits. *Int J Oral Maxillofac Surg* 2001; 30: 407-13.
- [7] Sintzel MB, Merkli A, Tabatabay C, Gurny R. Influence of irradiation sterilization on polymers used as drug carriers-A review. *Drug Develop Ind Pharm*. 23, 857-878. 1997.
- [8] Athanasiou KA, Niederauer GG, Agrawal CM. Sterilization, toxicity, biocompatibility and clinical applications of polylactic acid/polyglycolic acid copolymers. *Biomaterials* 1996; 17: 93-102.
- [9] Lu L, Peter SJ, Lyman MD, Lai HL, Leite SM, Tamada JA, Vacanti JP, Langer R, Mikos AG. In vitro degradation of porous poly(L-lactic acid) foams. *Biomaterials* 2000; 21: 1595-605.
- [10] Vert M, Li S, Garreau H. More About the Degradation of La/Ga-Derived Matrices in Aqueous-Media. *J Control Release* 1991; 16: 15-26.
- [11] Grizzi I, Garreau H, Li S, Vert M. Hydrolytic Degradation of Devices Based on Poly(DL-Lactic Acid) Size-Dependence. *Biomaterials* 1995; 16: 305-11.
- [12] McGinity JW, O'Donnell PB. Preparation of microspheres by the solvent evaporation technique. *Adv Drug Deliv Rev* 1997; 28: 25-42.
- [13] Anderson JM, Shive MS. Biodegradation and biocompatibility of PLA and PLGA microspheres. *Adv. Drug Del. Rev.* 28, 5-24. 1997.
- [14] Nijsen JFW, van het Schip AD, van Steenberg MJ, Zielhuis SW, Kroon-Batenburg LM, van de Weert M, van Rijk PP, Hennink WE. Influence of neutron irradiation on holmium acetylacetonate loaded poly(L-lactic acid) microspheres. *Biomaterials* 2002; 23: 1831-9.
- [15] Nijsen JFW, van Steenberg MJ, Kooijman H, Talsma H, Kroon-Batenburg LM, van De WM, van Rijk PP, De Witte A, van het Schip AD, Hennink WE. Characterization of poly(L-lactic acid) microspheres loaded with holmium acetylacetonate. *Biomaterials* 2001; 22: 3073-81.
- [16] Zielhuis SW, Nijsen JFW, Figueiredo R, Feddes B, Vredenberg AM, van het Schip AD, Hennink WE. Surface characteristics of holmium-loaded poly(l-lactic acid) microspheres. *Biomaterials* 2005; 26: 925-32.
- [17] Seppenwoolde JH, Nijsen JF, Bartels LW, Zielhuis SW, van het Schip AD, Bakker CJ. Internal radiation therapy of liver tumors: Qualitative and quantitative magnetic resonance imaging of the biodistribution of holmium-loaded microspheres in animal models. *Magn Reson Med* 2004; 53: 76-84.
- [18] Hardonk MJ, Dijkhuis FWJ, Hulstaert CE, Koudstaal J. Heterogeneity of Rat-Liver and Spleen Macrophages in Gadolinium Chloride-Induced Elimination and Repopulation. *Journal of Leukocyte Biology* 1992; 52: 296-302.
- [19] Hafeli UO, Roberts WK, Pauer GJ, Kraeft SK, Macklis RM. Stability of biodegradable radioactive rhenium (Re-186 and Re-188) microspheres after neutron-activation. *Appl Radiat Isot* 2001; 54: 869-79.
- [20] Zielhuis SW, Nijsen JFW, de Roos RR, Krijger GC, van Rijk PP, Hennink WE, van het Schip AD.

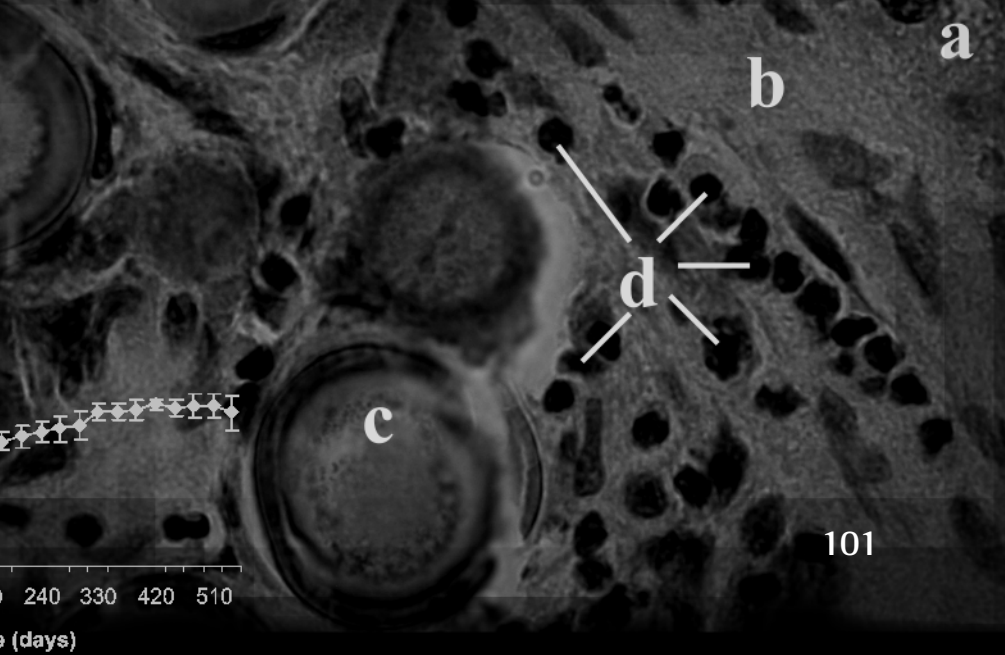
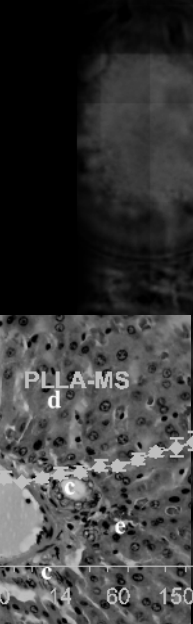
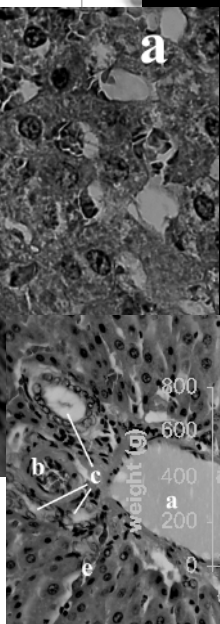
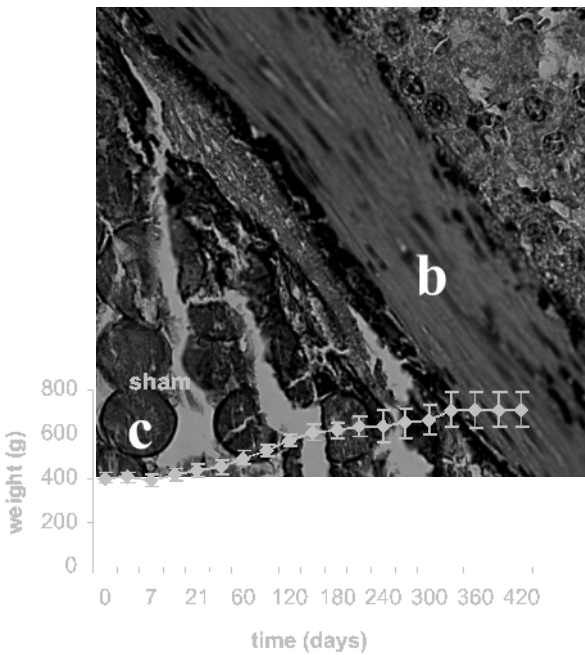
Production of GMP-grade radioactive holmium loaded poly(l-lactic acid) microspheres for clinical application. *Int J Pharm* 2006.

- [21] Yuan XY, Mak AFT, Yao KD. In vitro degradation of poly(L-lactic acid) fibers in phosphate buffered saline. *Journal of Applied Polymer Science* 2002; 85: 936-43.
- [22] Bittner B, Mader K, Kroll C, Borchert HH, Kissel T. Tetracycline-HCl-loaded poly(DL-lactide-co-glycolide) microspheres prepared by a spray drying technique: influence of gamma-irradiation on radical formation and polymer degradation. *J Control Release* 1999; 59: 23-32.
- [23] Suuronen R, Pohjonen T, Hietanen J, Lindqvist C. A 5-year in vitro and in vivo study of the biodegradation of polylactide plates. *J Oral Maxillofac Surg* 1998; 56: 604-14.
- [24] Freiberg S, Zhu XX. Polymer microspheres for controlled drug release. *Int J Pharm* 2004; 282: 1-18.
- [25] Bergsma JE, Rozema FR, Bos RRM, Boering G, Debruijn WC, Pennings AJ. In-Vivo Degradation and Biocompatibility Study of In-Vitro Pre-Degraded As-Polymerized Polylactide Particles. *Biomaterials* 1995; 16: 267-74.

Chapter 6

Biocompatibility
study of holmium
loaded poly
(L-lactic acid)
microspheres in rats

SW Zielhuis, JFW Nijssen, JH Seppenwoolde, CJG Bakker, GC Krijger, HFJ Dullens,
BA Zonnenberg, PP van Rijk, WE Hennink and AD van het Schip



Abstract

The aim of this study was to get insight into the biocompatibility of holmium-166 loaded poly(L-lactic acid) microspheres (Ho-PLLA-MS). These microspheres have very interesting features for diagnosis and treatment of both primary and metastatic liver tumours. The biocompatibility of Ho-PLLA-MS was studied in healthy male Wistar rats. The rats were divided into four treatment groups: sham, decayed neutron-irradiated Ho-PLLA-MS, Ho-PLLA-MS and placebo microspheres without HoAcAc-loading. After implantation of the microspheres into the liver of the rats, the animals were monitored (body weight, temperature, liver enzymes) for a period of 14 to 18 months. Some of the rats that received previously neutron-irradiated Ho-PLLA-MS were periodically scanned with magnetic resonance imaging (MRI) to see if holmium was released from the microspheres. After sacrifice, the liver tissue was histologically evaluated. Bone tissue was subjected to neutron activation analysis in order to examine whether accumulation of released holmium in the bone had occurred, since it is known that holmium is a ‘bone-seeker’.

No measurable clinical and biochemical toxic effects were observed in any of the treatment groups. Furthermore, histological analyses of liver tissue samples only showed signs of a slight chronic inflammation and no significant differences in the tissue reaction between rats of the four different treatment groups could be observed. The non-irradiated PLLA-MS and Ho-PLLA-MS stayed intact during the observed period of eighteen months. In contrast, fourteen months after administration, the neutron-irradiated Ho-PLLA-MS were not completely spherical anymore, indicating that degradation had started. However, the holmium loading had not been released as was illustrated with MRI and affirmed by neutron activation analysis of bone tissue.

In conclusion, neutron-irradiated Ho-PLLA-MS have a good biocompatibility and can be applied safely in-vivo.

1. Introduction

More than half of the one million patients diagnosed with colorectal cancer each year world wide, will develop liver metastases at some point in the course of their disease [1,2]. When these patients are not treated, their median survival is 6–12 months [2]. It is estimated that only 20–30 % of patients with colorectal metastases are candidates for curative liver resection [3]. Patients with primary liver cancer (with a yearly incidence of 600,000) have the same poor prognosis as well.

Local radionuclide therapy using radioactive microspheres is a promising therapy for the non-operable group of patients suffering from liver malignancies [4]. In contrast to normal liver tissue, which receives most of its blood flow from the portal vein, liver malignancies are almost exclusively dependent on arterial blood supply [5]. Based on this difference in blood supply, it has been demonstrated that radioactive microspheres with a diameter between 20 and 50 μm that are injected into the hepatic artery, selectively lodge in and around the tumours and thereby irradiate the surrounding tissue [4,5].

The treatment of cancer with holmium-166 loaded microspheres has obvious advantages over the use of other radionuclides, because holmium is the only element which can be easily neutron-activated (it has a cross-section of 64 barn [4]) to a beta- and gamma-emitter with a logistically favourable half-life (Table 1), and it can also be visualized by magnetic resonance imaging (MRI) [6,7]. Using a solvent evaporation technique, non-radioactive holmium-165 can be incorporated into poly(L-lactic acid) (PLLA) microspheres as its acetylacetonate complex (HoAcAc). In a subsequent step, the microspheres (Ho-PLLA-MS) can be neutron activated [8].

Table 1. Physical characteristics of holmium-165/holmium-166

natural abundancy	100% holmium-165	
production	holmium-165 (n, γ), holmium-166	
half-life	26.8 h	
γ -rays	energy (keV)	percentage (%)
	80.6	6.71
	1379.4	0.93
β -rays	1773.1	48.7
	1854.7	50.0
tissue range (β -rays)	8.6 mm	

In contradistinction to most radiopharmaceuticals where the amount of the administered drug is in the nanogram-scale, effective treatment of patients with radioactive Ho-PLLA-MS requires the administration of 500-800 mg of microspheres. Therefore, besides the radiotoxicity, also the biocompatibility of this new radiopharmaceutical has to be studied in order to evaluate its clinical applicability. The two main components of Ho-PLLA-MS are HoAcAc and PLLA (both around ~50% w/w). PLLA is a biodegradable and biocompatible polymer, which degrades, depending on factors such as its molecular weight and crystallinity, in a timeframe of months to years [9]. The effects of neutron irradiation on PLLA has been studied and reported in previous papers [8,10,11]. Although the molecular weight of the PLLA decreased due to the irradiation, the chemical entity of the polymer was retained [10]. However, it needs to be studied what the consequences of this decrease in molecular weight are in terms of the degradation characteristics of Ho-PLLA-MS and the subsequent possible release of HoAcAc. HoAcAc is a water-insoluble complex consisting of Ho^{3+} coordinated with three acetylacetonate ligands and with one or two water molecules [12]. Although the toxicity of HoAcAc is not known yet, the toxicity of Ho^{3+} and acetylacetonate has been studied. Compared with heavy metals, the toxicity of the rare-earth metal holmium is relatively low; LD₅₀ values of intravenously or intraperitoneally holmium salts are in the range of 50-500 mg/kg bodyweight [13]. It has been shown that non-complexed holmium can accumulate in the skeleton and the liver [14]. The LD₅₀ of acetylacetonate after oral administration, inhalation or skin and eye contact in rodents is about 1000 mg/kg [15].

The purpose of this study was to investigate the short and long term chemical toxicity of Ho-PLLA-MS in healthy rats as well as their biodegradation and release of the holmium loading. Microspheres were implanted into the liver of the rats, and the animals were intensively monitored (body weight, temperature, liver enzymes). Furthermore, the paramagnetic behaviour of holmium allowed the visualisation of the microspheres *in vivo* with MRI. After the rats were sacrificed, the liver tissue was histologically evaluated. Bone tissue was subjected to neutron activation analysis in order to examine if holmium had released and if accumulation in the bone had occurred.

2. Materials and Methods

2.1 Animals

The experiments were performed in agreement with The Netherlands Experiments on Animals Act (1977) and the European Convention for the Protection of Vertebrate Animals used for Experimental Purposes (1986). Approval was obtained from the University Animal Experiments Committee (DEC-UMC nr. 0303032). The experiments were performed using 48 male pathogen-free, inbred Wistar rats (HsdCpb:WU; Harlan, Horst, The Netherlands) with an age of 12-14 weeks including a quarantine period of 2 weeks. The rats were housed in Macrolon cages (groups of 2 or 3 animals per cage) with sawdust provided as bedding. A standard pelleted rat maintenance diet (RMH-TM, Hope Farms, Woerden, The Netherlands) and acidified water were provided *ad libitum*.

2.2 Preparation of microspheres

Microspheres with and without HoAcAc loading were prepared as previously described [8,11]. After preparation, the microspheres (~250 mg) were packed in polyethylene vials and gamma- or neutron-irradiated, both resulting in a sterile product. Gamma sterilization of microspheres with a dose of 25.0 kGy was performed using a cobalt-60 source (Isotron, Ede, The Netherlands). Neutron irradiations were performed in the pneumatic rabbit system in the reactor facility in Delft. Ho-PLLA-MS were neutron-irradiated with a thermal neutron flux of $5 \times 10^{12} \text{ cm}^{-2} \cdot \text{s}^{-1}$ and the irradiation time was 6 h. To ensure low levels of microsphere-associated radioactivity, the animal experiments were performed after decaying the microspheres for one month storage at room temperature in closed vials.

After neutron irradiation or gamma sterilization, microspheres (~250 mg) were mixed with 0.1 ml Gelofusine® (Vifor Medical SA, Switzerland). The resulting paste was divided into six portions and pressed into the cone of a 1 ml syringe (BD Plastipak, Madrid, Spain). After drying for 48 h at room temperature, a solid cylindrically shaped cluster of 32 ± 3 mg microspheres was formed in the cone of the syringe (dimensions 1.5 x 8 mm). The cylindrically shaped plugs were removed from the syringe and subsequently implanted into rats (see section 2.3).

2.3 Implantation of the microsphere plugs into rats

Rats were divided in four treatment groups (12 animals per group) which received neutron-irradiated Ho-PLLA-MS, gamma-sterilized Ho-PLLA-MS, gamma-sterilized PLLA-MS or Gelofusine®. Prior to and 4 and 12 h after the operation 0.1 ml of buprenorfin hydrochloride (Temgesic®, 0.3 mg/ml injection; Reckitt and Coleman, Hull, England) was injected subcutaneously for pain relief. The rats were anaesthetized using N₂O and halothane (Albic BV, Maassluis, The Netherlands) as inhalation anaestheticum. During the operation, dryness of the rat's eyes was prevented using vitamin A ointment (Ophthosan®, AST Farma B.V., Oudewater, The Netherlands). When the animals were fully sedated, a laparotomy was performed by ventral mid-line incision in order to expose the lobes of the liver. The microsphere plug was placed in a trocar needle (outer diameter 2 mm, Instruvet, Cuijk, The Netherlands) and the intact plug was injected into the *lobus hepatis dexter lateralis*. A sham operation was performed by injecting 0.1 ml Gelofusine® instead of microspheres. After the implantation procedure, 5 ml of saline was given intraperitoneally and the incision wound was closed with Vicryl® 4.0 suture material (Eticon, Sommerville, USA).

2.4 Biocompatibility evaluation

Blood samples (~ 500 µl) were taken using a saphenous vein puncture and collected into gel barrier capillary blood collection tubes (Capiject® T-Mg, Terumo, Elkton, USA) at the start of the operation, 3 days after operation, weekly during the first month and monthly during the rest of the study. Blood was centrifuged at 3000 rpm for 10 min and the serum was frozen at -20°C. The serum samples were analyzed at the Department of Clinical Chemistry (University Medical Center Utrecht, The Netherlands) for alkaline phosphatase (ALP) as an indicator of biliary toxicity and for alanine aminotransferase (ALAT), aspartate amino transferase (ASAT) and gamma glutamyltransferase (γ-GT) as indicators of hepatocellular toxicity. After blood sampling, the rats were weighed and their body temperature was measured rectally.

At six predetermined time points (3, 30, 90, 180, 300 and 420 days for sham operated and neutron-irradiated Ho-PLLA-MS and 3, 30, 180, 300, 420 and 540 days for gamma-sterilized PLLA-MS and Ho-PLLA-MS) two rats from each

group were sacrificed using CO₂. At autopsy the thoracic (heart and lungs) and abdominal organs (liver, stomach, intestines, kidneys and spleen) were inspected for macroscopical aberrations and fixed in phosphate-buffered 4% formaldehyde (Klinipath, Duiven, The Netherlands). Tissue samples from the liver near the implantation site were taken in order to evaluate the tissue reaction on the microspheres. The liver tissue was embedded in paraffin wax and 6 µm thick sections were prepared after every 60 µm. The sections were stained with haematoxylin-eosin and histologically evaluated with light microscopy. The tissue response was rated according to the following scoring system: - = no presence till ++++ = extensive presence of lymphocytes, granulocytes, macrophages and foreign body giant cells. The tissue samples were also examined (and scored) for the proliferation of bile ducts and the formation of a layer of connective tissue around the microspheres (rate of encapsulation) as well as changes in the morphology of the microspheres.

2.5 Neutron activation analysis

The concentration of holmium in bone tissue was measured by instrumental neutron activation analysis at the Reactor Institute of the Delft University of Technology in Delft, The Netherlands, as described earlier [16,17]. About 300 mg of bone material was weighed into a polyethylene capsule. Together with standard holmium material (CertiPUR Holmium ICP Standard (traceable to SRM from NIST), Merck, Darmstadt, Germany) the samples were irradiated for 1.0 h in a thermal neutron flux of $5 \times 10^{12} \text{ cm}^{-2} \cdot \text{s}^{-1}$. Neutron irradiations were performed in the pneumatic rabbit system (PRS) in the reactor facility in Delft (Department of Radiation, Radionuclides and Reactor, Delft University of Technology, The Netherlands). After a decay time of 6 days the gamma radiation of these samples was measured for 1 hour in a planar Ge(Li) detector (Princeton gamma-tech, Germany). The addition of standard holmium material to the bone tissue samples was used to determine the detection limit [18].

2.6 Magnetic Resonance Imaging (MRI) and Computed Tomography (CT)

To study the release of holmium from the site of implantation, two rats (neutron-irradiated Ho-PLLA-MS, 14 months surviving) were periodically scanned with MRI. Ho-PLLA-MS packed together in a cylindrical element results in a

macroscopic magnetic susceptibility effect. On gradient echo MRI, this susceptibility effect causes signal loss with a characteristic pattern: in the transverse plane (perpendicular to the cylindrical elements, which were oriented parallel to the main magnetic field) this pattern is a black circular region, encircled by a wider black ring (generally much larger than the actual size of the cylindrical elements). The volume is approximately proportional to the amount of paramagnetic material [19] and can be used to study the actual amount of Ho-PLLA-MS. A 1.5 T clinical MR scanner (Gyrosan Intera NT, Philips Medical Systems, Best, The Netherlands) was used. For calibration purposes, a series of Ho-PLLA-MS plugs (5-50 mg Ho-PLLA-MS) was investigated in a phantom experiment. The plugs were aligned with the main magnetic field and investigated in the middle of a large cylindrical cup, filled with a solution of 19.2 mg/L $\text{MnCl}_2 \cdot 4 \text{H}_2\text{O}$ (Merck, Darmstadt, Germany) to mimic the MR signal from tissue protons. Transverse images were made using spoiled gradient echo imaging with a field of view (FOV) 256 mm, in-plane resolution 1 mm, slice thickness 20 mm, echo time (TE) 5.0 msec, repetition time (TR) 60 ms, flip angle 15 degrees, 8 signal averages, duration 1:25. The animals were anaesthetized using 0.3 ml of Hypnorm® (Janssen Pharmaceutica, Beerse, Belgium). The rats underwent MR imaging just after implantation and after 2, 6, 9, and 14 months. The imaging protocol included a transverse gradient echo acquisition with the same parameters as for the calibration experiment. Just before termination, the shape of the plugs was investigated by helical scanning with a clinical CT scanner (Brilliance CT, Philips Medical Systems, Best, The Netherlands) with a collimation of 64x0.625 mm, FOV 250 mm, in-plane resolution 0.48 mm, section thickness 1 mm, 120 kV tube voltage with 200 mA per slice tube current, rotation time 1 second, pitch 0.678, reconstruction filter B (soft tissue filter). After acquisition and reconstruction of the MR images, the size of artifacts was determined by measuring the diameter of the outer ring of signal loss. A calibration curve was made by plotting the observed artifact size against given amounts of Ho-PLLA-MS [19].

3. Results and discussion

3.1 Clinical and biochemical evaluation

Plugs composed of microspheres were implanted in the liver of rats in order to study the tissue response and biodegradation. The trauma that was caused because of the implantation by use of the trocar needle did not result in major bleedings in the liver tissue.

Changes in body weight are an indicative parameter for toxic effects in laboratory animals [20]. The average body weight of the different rat groups in time is given in Fig. 1. The initial body weight of rats (~ 400 g) in all treated groups were in compliance with normal values for Wistar rats as well as their growth in the period after the operation [20]. After a period of around 300 days, a body weight of 600-700 g was reached and thereafter no further growth was observed. No significant differences in body weight between the four groups were observed. The body temperature of the rats was intensively monitored during the study and no signs of hypothermia (temperatures below 38 °C) or fever (temperature above 39.5 °C) were observed in any of the four groups.

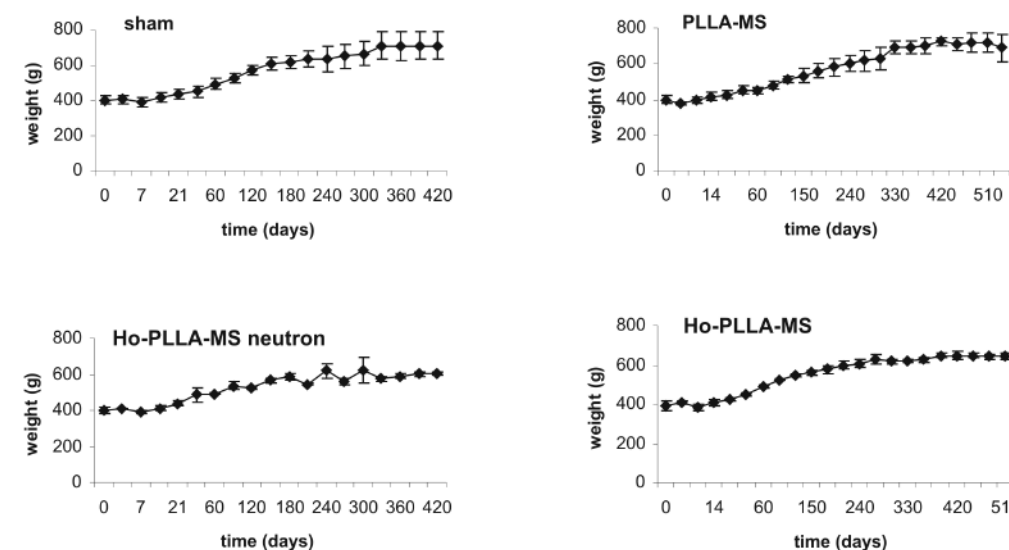


Fig. 1 Body weight values (g) of rats of the different groups in time. Bars represent the SD. sham (sham operated), PLLA-MS (gamma-sterilized PLLA-MS), Ho-PLLA-MS neutron (neutron-irradiated Ho-PLLA-MS) and Ho-PLLA-MS (gamma-sterilized Ho-PLLA-MS).

Serum enzyme levels of ALP, ASAT, ALAT and γ -GT of rats in the microsphere treated groups were compared to that of rats in the sham-operated group (Figure 2). This figure shows that the serum enzyme levels remained more or less stable during the study and no significant differences in serum enzyme levels were observed between the different groups.

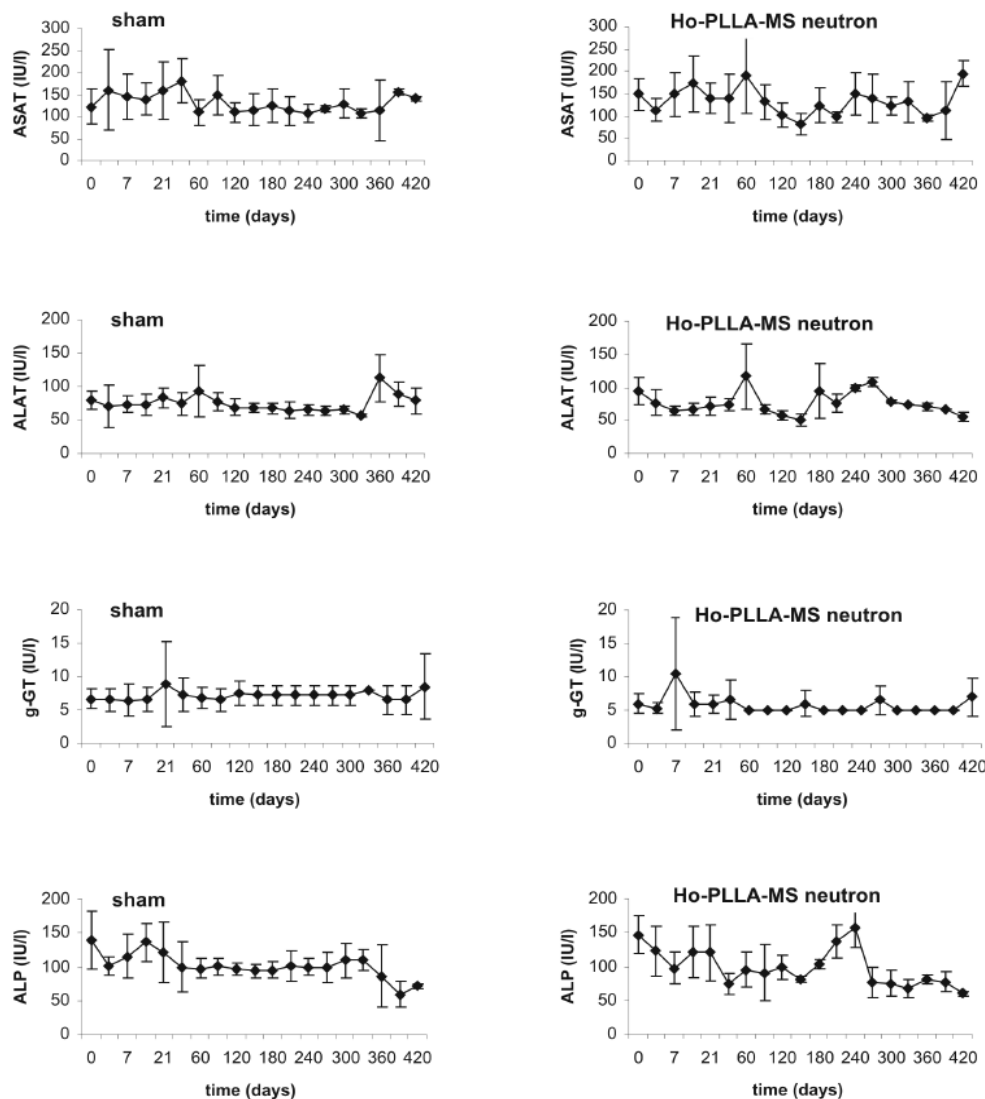


Fig. 2 Serum enzyme levels (ASAT, ALAT, γ -GT and ALP) of rats of sham and neutron-irradiated Ho-PLLA-MS treated groups in time. Bars represent the SD. Because of the negligible differences in serum enzyme levels between the four groups only the data of the most relevant group (neutron-irradiated Ho-PLLA-MS) and the sham-operated group are shown.

3.2 Histology

At autopsy no major deviations were found in the inspected thoracic and abdominal organs of the rats of the different groups. Irrespective of the treatment that the rats received, only slight thickening of the liver edges was observed.

An overview of the nature and extent of the observed major liver tissue reactions as observed by light microscopic examination after implantation of microsphere plugs is given in Table 2. No infiltration of granulocytes, macrophages or foreign body giant cells was observed in any of the samples, so these parameters are not included in Table 2. To illustrate the observed effects, some representative light micrographs of liver tissue samples are shown in Fig. 3A-D.

The sham operation (0.1 ml of Gelofusine® was injected into the liver of rats) resulted in a slight inflammatory reaction in the liver tissue after 3 days up to 1 month. This slight inflammation was characterised by the presence of a few lymphocytes (Table 2). Also some proliferation of bile ducts was observed and at the site of injection some connective tissue was present. After 14 months the histology of the liver tissue was completely normal: no histological aberrations could be observed (Table 2). At day 3 after implantation of gamma-sterilized PLLA-MS a slight inflammatory reaction was seen in the liver tissue, which was characterised by the infiltration of lymphocytes at the area around the microspheres. Also proliferation of bile ducts was observed and the implanted microsphere plug was surrounded by a layer of connective tissue. At 1 month after implantation, the number of infiltrating lymphocytes and bile ducts was

Table 2. Histological changes in the liver after the implantation of the microspheres

treatment	time	lymphocytes*	bile ducts	connective tissue
sham	3 days	±**	±	+
	1 month	±	±	±
	14 months	-	-	-
PLLA-MS gamma-sterilized	3 days	±	±	±
	1 month	++	+	±
	18 months	±	±	±
Ho-PLLA-MS gamma-sterilized	3 days	±	+	+
	1 month	+	+	+
	18 months	+	+	+
Ho-PLLA-MS, neutron irradiated	3 days	+	±	±
	1 month	±	±	+
	14 months	±	±	±

* No infiltration of granulocytes, macrophages or foreign body giant cells were observed in any of the samples and are therefore not mentioned here.

** = till ++ = slightly present till extensively present, - = not present

somewhat increased (Table 2). After 18 months only a slight number of infiltrating lymphocytes was observed and no further proliferation of bile ducts could be observed. The implanted microspheres retained their size and shape and were present as a cluster that remained surrounded by a small layer of a fibrous capsule. At one month post implantation, gamma-sterilized Ho-PLLA-MS evoked a mild tissue reaction comparable to gamma-sterilized PLLA-MS in terms of the infiltration of lymphocytes, the proliferation of bile ducts and the presence of a layer of connective tissue around the implanted microspheres (Fig. 3A and Fig. 3C). After a period of 18 months, the number of infiltrated lymphocytes and proliferation of bile ducts was comparable to the observed tissue reaction after the implantation of gamma-sterilized PLLA-MS (Table 2). The implanted gamma-sterilized Ho-PLLA-MS retained their size and shape and were present as a cluster that was surrounded by a small layer of connective tissue.

Implantation of decayed neutron-irradiated Ho-PLLA-MS also induced a mild tissue response (Fig 3B), which was comparable to that of gamma-sterilized PLLA-MS and gamma-sterilized Ho-PLLA-MS (see also Table 2). After a period of 14 months only a very small number of infiltrating lymphocytes could be observed and there was hardly any proliferation of bile ducts. However, in contradistinction to gamma-sterilized PLLA-MS and gamma-sterilized Ho-PLLA-MS, the neutron-irradiated Ho-PLLA-MS were not completely spherical anymore and showed disintegration indicating that degradation had started (Fig. 3D). This result is in agreement with the results of the in-vitro degradation study described in Chapter 5 of this thesis. In this study, non-irradiated and neutron-irradiated microspheres with and without HoAcAc-loading were incubated in phosphate buffer at 37 °C for a period of one year. In analogy with the present in-vivo study, only the neutron-irradiated Ho-PLLA-MS showed degradation. This is probably caused by the low molecular weight of the PLLA due to the neutron irradiation and the low crystallinity caused by the Ho-AcAc loading [10]. The in-vitro study also showed that as a result of degradation holmium lactate was formed. In this in-vivo study no adverse reactions towards this degradation product could be observed.

The biocompatibility of PLA based microspheres in term of tissue response has been extensively described in the literature [21-24]. In general, the implantation of biodegradable microspheres results in various chronological effects [9]. The

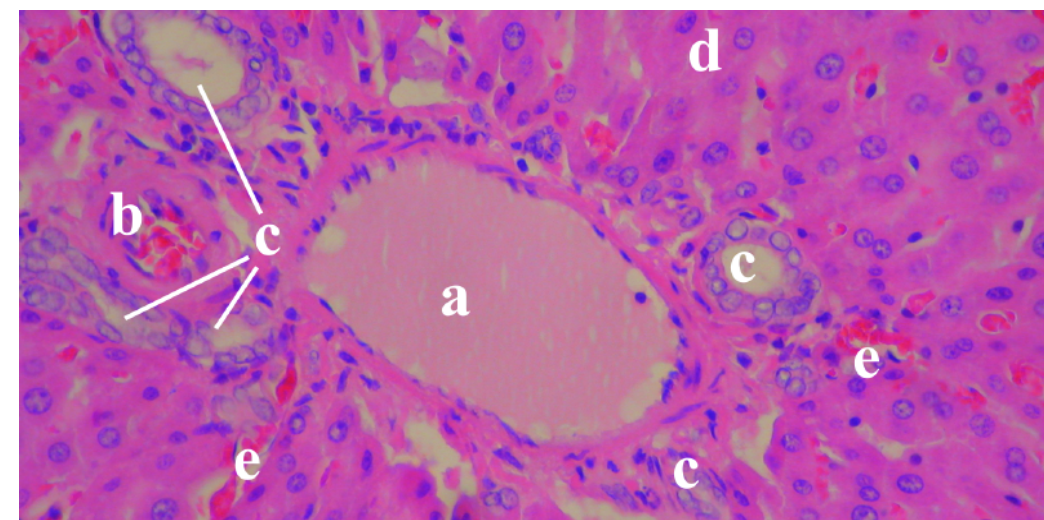


Fig. 3A Microphotograph (400x) of liver tissue section (stained with haematoxylin-eosin (HE)) taken from a rat in which a plug of gamma-sterilized Ho-PLLA-MS was implanted and which was terminated after one month: a) branch portal vein, b) branch of liver artery, c) bile ducts, d) normal hepatocytes e) sinusoids overfilled with erythrocytes (congestion due to the method of euthanasia).

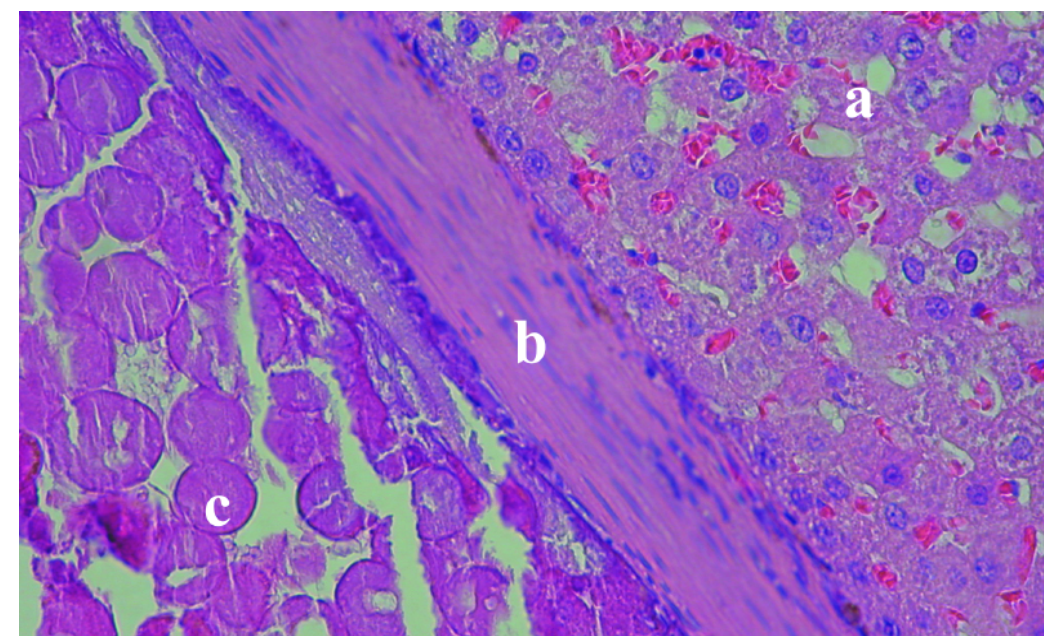


Fig. 3B Microphotograph (400x) of liver tissue section (stained with HE) taken from a rat in which a plug of neutron-irradiated Ho-PLLA-MS was implanted and which was terminated after one month: a) liver parenchyma, b) connective tissue, c) microspheres. Note that the microspheres show some damage due to the preparation of the histological slide.

first few days post implantation, an acute inflammatory reaction accompanied by the infiltration of granulocytes is observed which is likely due to trauma caused by the injection of the microspheres. The acute inflammation is followed by a chronic inflammation accompanied by the infiltration of monocytes and lymphocytes. Hereafter granulation tissue is formed. If degradation of the implanted microspheres occurs and the degraded microsphere fragments have become smaller than 10 μm , macrophages/foreign body giant cells can phagocytise these fragments. When particles are not completely resorbed, a fibrous capsule around the particles will be formed. It must be mentioned that almost all biocompatibility studies are conducted after subcutaneously or intramuscularly injection [9] and that no biocompatibility studies after implantation in liver tissue have been performed. Nevertheless, the results of this study are in good agreement with the studies performed after subcutaneously or intramuscularly injection of PLA-based microspheres that were described in the literature [9]. In the present study, infiltration of lymphocytes (Fig. 3C) was observed in all liver tissue samples. This is a typical sign of a slight chronic inflammation caused by the presence of slowly degrading microspheres [9]. Due to the fact that the microspheres were implanted in the liver, also some bile duct proliferation was observed in the liver tissue [25].

In all liver tissue samples from sham operated and microsphere treated rats congestion of red blood cells was seen (Fig. 3A). This congestion has no relation with microsphere toxicity; it is a typical reaction due to the euthanatic procedure using CO_2 [26].

3.3 Release of holmium

The in-vitro release of holmium was studied in Chapter 5 and it was shown that during a period of 52 weeks less than 1% of the holmium loading was released. As mentioned in the introduction, the toxicity of the element holmium (Ho^{3+}) is relatively low (50-500 mg/kg bodyweight), but non-complexed Ho^{3+} can accumulate in the skeleton [14]. Therefore, the possible release of holmium from the microspheres was followed in vivo by MRI and bone tissue samples were subjected to neutron activation analyses.

This possible release of holmium from the implantation site was monitored during the study by MRI. The calibration plot (Fig. 4) of microsphere plugs

shows increasing artifact sizes with increasing amounts of Ho-PLLA-MS. As expected, the diameter of the artifact increased proportional to the cube root of the amount of Ho-PLLA-MS [19]. Given the implanted amount of ~ 32 mg, the size of the observed artifacts for the in vivo experiments corresponded well with the predicted value from the calibration plot and over time, no significant decrease in artifact size was observed (Fig. 4). CT imaging showed that the implanted microsphere plug still had a cylindrical shape 14 months post implantation (Fig. 4). The calibration plot (Fig. 4) showed that MR measurement is more sensitive to a change in the amount of Ho-PLLA-MS at lower amounts, but that for higher amounts the relative error of the diameter measurement decreased. The in vivo imaging (Fig. 4) showed that no holmium had released: no significant change in artifact size was observed.

Neutron activation analyses of bone tissue samples from rats treated with gamma-sterilized Ho-PLLA-MS (from rats sacrificed 18 months post implantation) and neutron-irradiated Ho-PLLA-MS (from rats sacrificed 14 months post implantation) were performed. The detection limit of the used method was 0.5

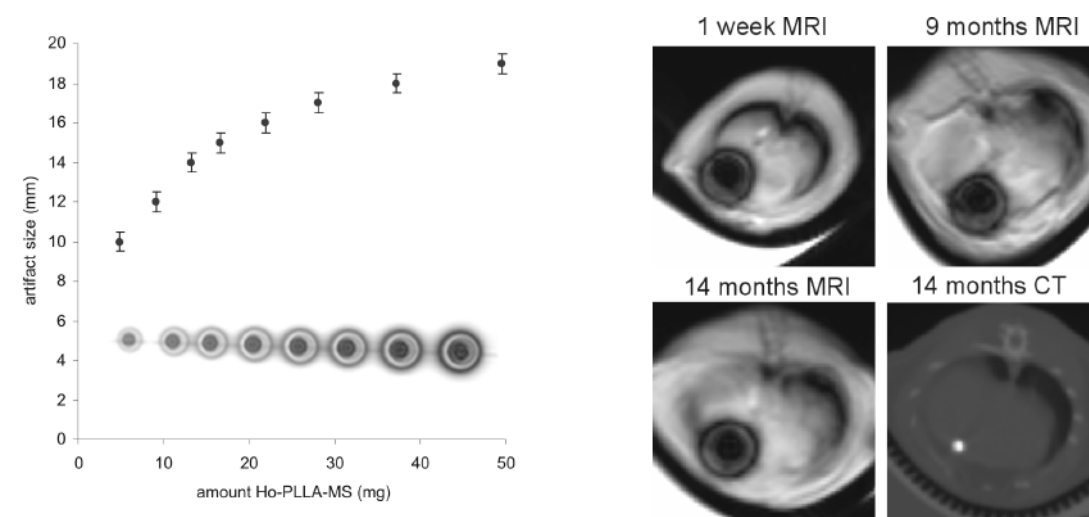


Fig. 4 (left) Calibration plot of artifact sizes versus amount of Ho-PLLA-MS. The inset in the graph is a chunked and rotated MR image of the artifacts in transverse orientation at 1.5 Tesla (not to scale) showing increasing artifact sizes for increasing amounts of Ho-PLLA-MS. (right) In vivo transverse images of a rat with an implanted cylinder of neutron-irradiated Ho-PLLA-MS at three stages after implantation, including an axial CT image at 14 months. The MR images show a transverse section through the center of the cylinders. The observed artifacts show no significant decrease in size over time.

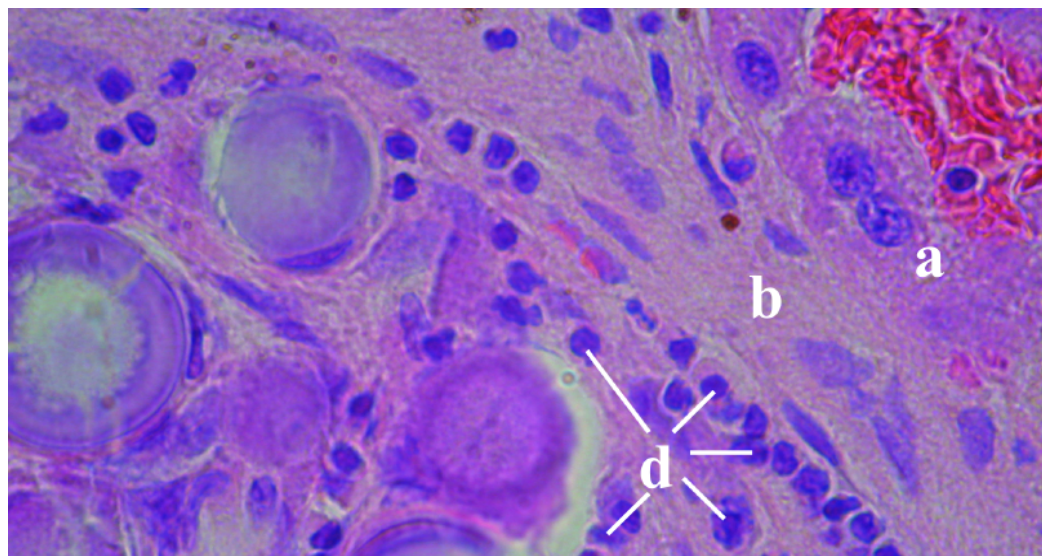


Fig. 3C Microphotograph (1000x) of liver tissue section (stained with HE) taken from a rat in which a plug of gamma-sterilized Ho-PLLA-MS was implanted and which was terminated after one month: a) liverparenchyma, b) connective tissue, c) microsphere. The microspheres are surrounded by connective tissue, which is infiltrated by lymphocytes (d).

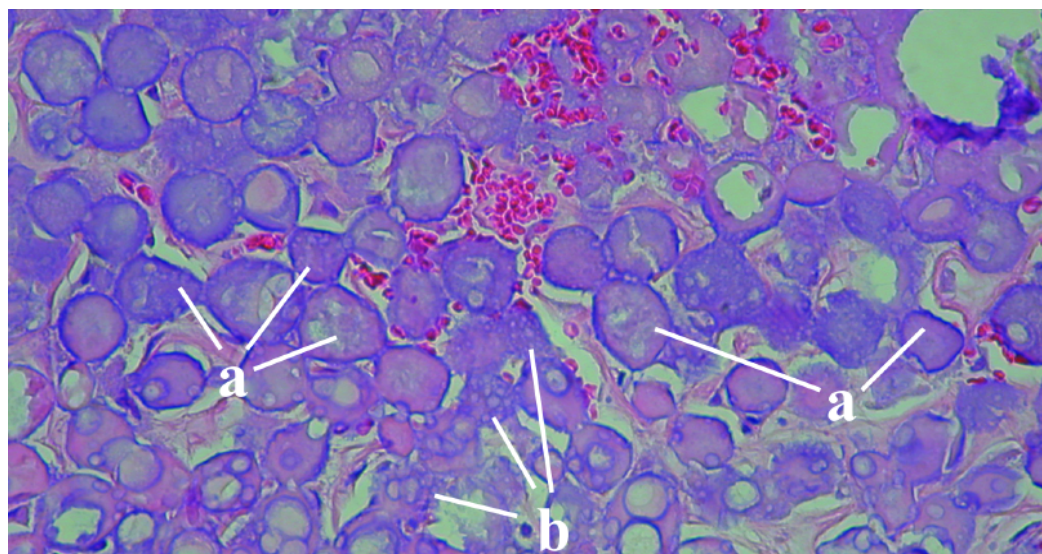


Fig. 3D Microphotograph (400x) of liver tissue section (stained with HE) taken from a rat in which a plug of neutron-irradiated Ho-PLLA-MS was implanted and which was terminated after fourteen months: The particles are not completely spherical anymore (a) indicating that degradation has started. Some of the microspheres show disintegration (b).

ppm of holmium. Importantly, the holmium concentration in the bone samples was below the detection limit (0.5 ppm), and proofs that hardly any holmium had been released from the microspheres, which is in agreement with the MRI-results.

4. Final discussion and conclusion

This study demonstrates that the implantation of neutron-irradiated Ho-PLLA-MS in the liver of rats did not result in toxic effects. No changes in body weight, temperature or liver enzymes have been observed. Histological analyses of liver tissue samples only showed signs of a slight/moderate infiltration of lymphocytes accompanied by minor local fibrosis and bile duct proliferation and no significant differences in the tissue reaction between rats from the control treatment groups could be observed. Fourteen months post implantation the neutron-irradiated Ho-PLLA-MS were not completely spherical anymore and showed disintegration indicating that degradation had started. However, the holmium loading had not been released. The fact that in vivo no measurable amount of holmium was released from the microspheres is in agreement with the results of the in-vitro degradation study described in Chapter 5 of this thesis. Previously, it was demonstrated that holmium and PLLA interact with each other [27]. These interactions most probably account for the low release of holmium from neutron-irradiated Ho-PLLA-MS. The in-vitro study also showed that as a result of degradation holmium lactate was formed. In this in-vivo study no adverse reactions towards this degradation product could be observed. In conclusion, neutron-irradiated Ho-PLLA-MS have a good biocompatibility and can be applied safely in vivo.

Acknowledgements

The authors wish to thank R. de Roos (Department of Nuclear Medicine, University Medical Center, Utrecht, The Netherlands) for the preparation of the microspheres and J. Kroon of Department of Radiation, Radionuclides and Reactor (Delft University of Technology, The Netherlands) for his assistance with neutron irradiations.

This research was supported by the Technology Foundation STW (UGT.6069), applied science division of NWO and the technology programme of the Ministry of Economic Affairs, the Nijbakker-Morra foundation and foundation De Drie Lichten.

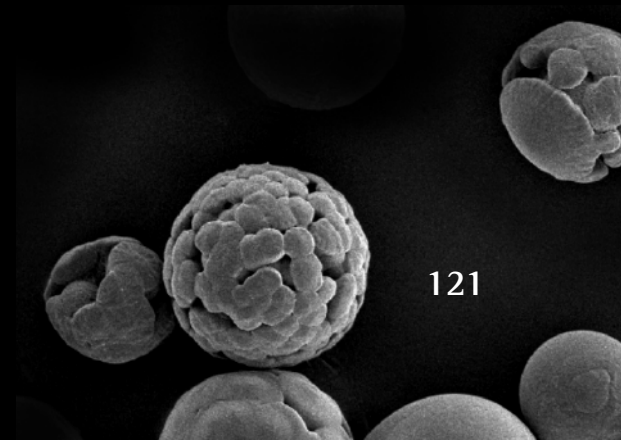
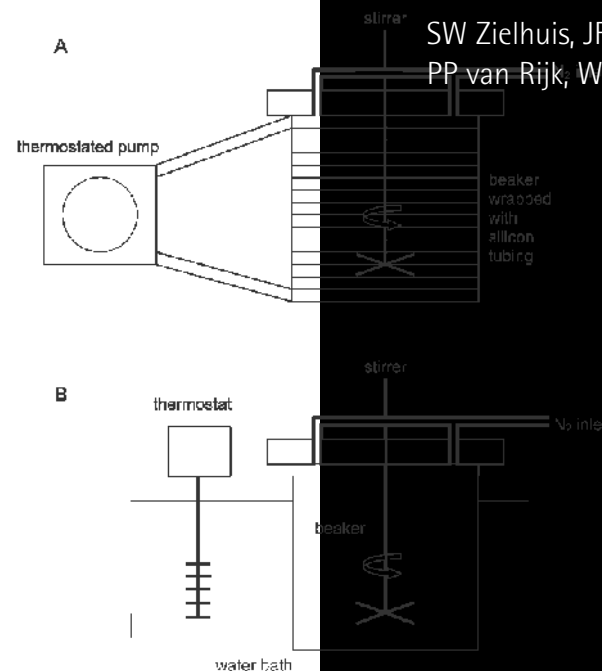
References

- [1] Parkin DM, Bray F, Ferlay J, Pisani P. Global cancer statistics, 2002. *Ca Cancer J Clin* 2005; 55: 74-108.
- [2] Bentrem DJ, Dematteo RP, Blumgart LH. Surgical therapy for metastatic disease to the liver. *Annu Rev Med* 2005; 56: 139-56.
- [3] Bennett JJ, Cao D, Posner MC. Determinants of unresectability and outcome of patients with occult colorectal hepatic metastases. *J Surg Oncol* 2005; 92: 64-9.
- [4] Nijsen JFW, van het Schip AD, Hennink WE, Rook DW, van Rijk PP, De Klerk JMH. Advances in nuclear oncology: Microspheres for internal radionuclide therapy of liver metastases. *Curr Med Chem* 2002; 9: 73-82.
- [5] Lambert B, Van de WC. Treatment of hepatocellular carcinoma by means of radiopharmaceuticals. *Eur J Nucl Med Mol Imaging* 2005; 32: 980-9.
- [6] Nijsen JFW, Seppenwoolde JH, Havenith T, Bos C, Bakker CJG, van het Schip AD. Liver Tumors: MR Imaging of Radioactive Holmium Microspheres—Phantom and Rabbit Study. *Radiology* 2004; 231: 491-9.
- [7] Seppenwoolde JH, Nijsen JFW, Bartels LW, Zielhuis SW, van het Schip AD, Bakker CJG. Internal radiation therapy of liver tumors: Qualitative and quantitative magnetic resonance imaging of the biodistribution of holmium-loaded microspheres in animal models. *Magn Reson Med* 2004; 53: 76-84.
- [8] Nijsen JFW, Zonnenberg BA, Woittiez JR, Rook DW, Swildens-van Woudenberg IA, van Rijk PP, van het Schip AD. Holmium-166 poly lactic acid microspheres applicable for intra-arterial radionuclide therapy of hepatic malignancies: effects of preparation and neutron activation techniques. *Eur J Nucl Med* 1999; 26: 699-704.
- [9] Anderson JM, Shive MS. Biodegradation and biocompatibility of PLA and PLGA microspheres. *Adv Drug Del Rev* 28, 5-24. 1997.
- [10] Nijsen JFW, van het Schip AD, van Steenberg MJ, Zielhuis SW, Kroon-Batenburg LM, van de Weert M, van Rijk PP, Hennink WE. Influence of neutron irradiation on holmium acetylacetonate loaded poly(L-lactic acid) microspheres. *Biomaterials* 2002; 23: 1831-9.
- [11] Zielhuis SW, Nijsen JFW, Figueiredo R, Feddes B, Vredenberg AM, van het Schip AD, Hennink WE. Surface characteristics of holmium-loaded poly(L-lactic acid) microspheres. *Biomaterials* 2005; 26: 925-32.
- [12] Kooijman H, Nijsen JFW, Spek AL, van het Schip AD. Diaquatris(pentane-2,4-dionato-O,O')holmium(III) monohydrate and diaquatris(pentane-2,4-dionato-O,O')holmium(III) 4-hydroxypentan-2-one solvate dihydrate. *Acta Crystallogr C* 2000; 56: 156-8.
- [13] Thunus L, Lejeune R. Overview of transition metal and lanthanide complexes as diagnostic tools. *Coord Chem Rev* 1999; 184: 125-55.
- [14] Zielhuis SW, Nijsen JFW, Seppenwoolde JH, Zonnenberg BA, Bakker CJG, Hennink WE, van Rijk PP, van het Schip AD. Lanthanide bearing microparticulate systems for multi-modality imaging and targeted therapy of cancer. *Curr Med Chem Anti-Canc Agents* 2005; 5: 303-13.
- [15] Ballantyne B, Cawley TJ. 2,4-Pentanedione. *J Appl Toxicol* 2001; 21: 165-71.
- [16] Bode P. Automation and quality assurance in the NAA facilities in Delft. *Journal of Radioanalytical and Nuclear Chemistry* 2000; 245: 127-32.
- [17] Afassi ZB. Determination of Trace Elements. New York: John Wiley and Sons, 1994.
- [18] Miller JC, Miller JN. Statistics for Analytical Chemistry. Chichester: Ellis Horwood Limited, 2005.
- [19] Bos C, Viergever MA, Bakker CJG. On the artifact of a subvoxel susceptibility deviation in spoiled gradient-echo imaging. *Magn Reson Med* 2003; 50: 400-4.
- [20] Handbook of Toxicology. Boca Raton: CRC Press, 2002.
- [21] Bergsma JE, Rozema FR, Bos RRM, Boering G, Debruijn WC, Pennings AJ. In-Vivo Degradation and Biocompatibility Study of In-Vitro Pre-Degraded As-Polymerized Polylactide Particles. *Biomaterials* 1995; 16: 267-74.
- [22] Athanasiou KA, Niederauer GG, Agrawal CM. Sterilization, toxicity, biocompatibility and clinical applications of polylactic acid/polyglycolic acid copolymers. *Biomaterials* 1996; 17: 93-102.
- [23] Daugherty AL, Cleland JL, Duenas EM, Mrsny RJ. Pharmacological modulation of the tissue response to implanted polylactic-co-glycolic acid microspheres. *Eur J Pharm Biopharm* 1997; 44: 89-102.
- [24] Cadee JA, Brouwer LA, Den Otter W, Hennink WE, Van Luyn MJ. A comparative biocompatibility study of microspheres based on crosslinked dextran or poly(lactic-co-glycolic)acid after subcutaneous injection in rats. *J Biomed Mater Res* 2001; 56: 600-9.
- [25] Nijsen JFW. Thesis: Radioactive holmium poly(L-lactic acid) microspheres for treatment of hepatic malignancies: efficacy in rabbits. 109-122. 2001. 26-4-2001.
- [26] Feldman DB, Gupta BN. Histopathologic changes in laboratory animals resulting from various methods of euthanasia. *Lab Anim Sci* 1976; 26: 218-21.
- [27] Nijsen JFW, van Steenberg MJ, Kooijman H, Talsma H, Kroon-Batenburg LM, van de Weert M, van Rijk PP, De Witte A, van het Schip AD, Hennink WE. Characterization of poly(L-lactic acid) microspheres loaded with holmium acetylacetonate. *Biomaterials* 2001; 22: 3073-81.

Chapter 7

Production of GMP-grade radioactive holmium loaded poly(L-lactic acid) microspheres for clinical application

SW Zielhuis, JFW Nijssen, R de Roos, GC Krijger, PP van Rijk, WE Hennink and AD van het Schip



Abstract

Radioactive holmium-166 loaded poly(L-lactic acid) microspheres have been found to be promising systems in the treatment of liver malignancies. The microspheres are loaded with holmium acetylacetonate (HoAcAc) and prepared by a solvent evaporation method. After preparation, the microspheres (Ho-PLLA-MS) are activated by neutron irradiation in a nuclear reactor. In this paper the aspects of the production of a (relatively) large-scale GMP batch (4 gram, suitable for treatment of 5-10 patients) of Ho-PLLA-MS are described.

The critical steps of the Ho-PLLA-MS production process (sieving procedure, temperature control during evaporation and raw materials) were considered, and the pharmaceutical quality of the microspheres was evaluated.

The pharmaceutical characteristics (residual solvents, possible bacterial contaminations and endotoxins) of the produced Ho-PLLA-MS batches were in compliance with the requirements of the European Pharmacopoeia. Moreover, neutron irradiated Ho-PLLA-MS retained their morphological integrity and the holmium remained stably associated with the microspheres; it was observed that after 270 h (10 times the half-life of Ho-166) only 0.3 ± 0.1 % of the loading was released from the microspheres in an aqueous solution.

In conclusion, Ho-PLLA-MS which are produced as described in this paper, can be clinically applied, with regard to their pharmaceutical quality.

1. Introduction

1.1 Holmium-166 loaded microspheres

Radionuclide loaded microspheres are promising systems for the treatment of liver malignancies. It has been shown that microspheres with a size of 20–50 μm when administered into the hepatic artery of patients suffering from liver malignancies, lodge in and around the tumour, and irradiate the surrounding tissue [1]. In view of its physical properties, holmium-166 is the ideal radionuclide for such therapies. Namely, holmium is the only element which can both be neutron-activated to a beta- and gamma-emitter with a logistically favourable half-life, and which can also be visualized by MRI [1-3]. Using a solvent evaporation technique, non-radioactive holmium-165 as its acetylacetonate complex (HoAcAc) can be incorporated into poly (L-lactic acid) (PLLA) microspheres. In a next step, the microspheres (Ho-PLLA-MS) can be made radioactive by neutron irradiation [4].

Before Ho-PLLA-MS can be clinically applied in a phase-1 trial, the entire production procedure must be in compliance with the Good Manufacturing Practice regulations (GMP) promulgated by the European Agency for the Evaluation of Medicinal Products (EMA) [5]. Although many papers have been published about the production of microspheres, none of the papers describe the setup of a GMP production process. Furthermore, for clinical application in human patients, production of microspheres at milligram-scale is far from enough; for the treatment of one patient with Ho-PLLA-MS, a quantity of 500-1000 mg is needed [4]. In this paper the GMP-production of a relatively large batch (4 gram) of Ho-loaded PLLA microspheres is described in detail. The critical steps of the Ho-PLLA-MS production process were identified and investigated, and the pharmaceutical quality of the microspheres before and after neutron irradiation was evaluated.

1.2 Requirements for clinical application

The effects of neutron irradiation on the characteristics of Ho-PLLA-MS have been extensively studied in previous papers [4,6,7]. Although the molecular weight of the PLLA decreases due to the irradiation, the chemical entity of the polymer is retained [6]. However, the consequences of this decrease in molecular weight in terms of safety for the patient need to be studied. It is also impor-

tant for therapeutic radiopharmaceuticals to have a high radiochemical stability. The release of radioactive holmium from the microspheres in the human body, which might lead to distribution of radioactivity to other organs than the liver, can lead to serious adverse events and must consequently be prevented. Finally, the microspheres must retain their size and shape after irradiation to ensure a selective biodistribution and to prevent excessive exposure of non-target organs to the irradiation.

For clinical application radioactive Ho-PLLA-MS must also fulfill the following requirements of the European Pharmacopoeia [8]:

- The absence of microbial contamination
- A limited amount of endotoxins. The limit for parenteral drugs is 5.0 EU/kg body weight.
- An acceptable amount of residual solvents (which are used during the solvent evaporation process). The ICH-guidelines (The International Conference on Harmonisation of Technical Requirements for Registration of Pharmaceuticals for Human Use) give limits of 60 and 600 ppm for chloroform and dichloromethane, respectively [9].

Once Ho-PLLA-MS are produced according to GMP and meet all above mentioned specifications, clinical application in cancer treatment can be initiated.

2. Materials and Methods

2.1 Materials

All chemicals were commercially available and used as obtained. Acetylacetone, 2,4-pentanedione (AcAc; > 99%), chloroform (CHCl_3 ; HPLC-grade), poly(vinyl alcohol) (PVA; molecular weight 30 000 – 70 000, 88% hydrolyzed), ammonium hydroxide (NH_4OH ; 29.3% in water) and holmium(III) acetylacetonate hydrate (HoAcAc; 99.9 %) were supplied by Sigma Aldrich (Steinheim, Germany). Sodium hydroxide (NaOH ; 99.9%) was purchased from Riedel-de Haën (Seelze, Germany). Holmium (III) chloride hexahydrate ($\text{HoCl}_3 \cdot 6\text{H}_2\text{O}$; 99.9%) and dichloromethane (CH_2Cl_2 ; HPLC-grade) were obtained from Phase Separations BV (Waddinxveen, The Netherlands). Poly(L-lactic acid) (PLLA; inherent viscosity 1.14 dl/g in chloroform 25°C) was purchased from Purac Biochem (Gorinchem, The Netherlands). Hydrochloric acid (HCl ; 37%), sodium azide (NaN_3 ; 99 %), di-sodium hydrogen phosphate dihydrate ($\text{Na}_2\text{HPO}_4 \cdot 2\text{H}_2\text{O}$; 99 %)

and sodium dihydrogen phosphate dihydrate ($\text{NaH}_2\text{PO}_4 \cdot 2\text{H}_2\text{O}$; 99%) were purchased from Merck (Darmstadt, Germany). Water for injections (according to the European Pharmacopoeia [8]) was obtained from Braun (Melsungen, Germany).

2.2 Preparation of HoAcAc and microspheres

The equipment used for preparation of Ho-PLLA-MS by solvent evaporation and subsequent sieving and drying steps was made of borosilicate glass, stainless steel, silicon rubber or polytetrafluoroethylene and was steam sterilised at 121 °C for 30 min at the Central Sterilisation Department of the University Medical Center Utrecht. Preparation of HoAcAc and Ho-PLLA-MS was carried out in a class-D clean room [8].

HoAcAc was prepared as described previously [4]. Acetylacetone (180 g) was dissolved in water (1080 g) and the pH of this solution was brought to 8.50 with an aqueous solution of ammonium hydroxide. Holmium chloride (10 g dissolved in 30 ml water) was added at once to this solution. After 15 hours incubation at room temperature, the formed HoAcAc crystals were collected by centrifugation and washed with water.

HoAcAc (10 g) and PLLA (6 g) were dissolved in chloroform (186 g) (solution A). 20 g of PVA was dissolved in 1000 g of boiling water, and the solution was allowed to cool down to room temperature (solution B). Solution A was added at once to solution B and the mixture was stirred (500 rpm) for 40 hours and the temperature during the solvent evaporation process was maintained at room temperature using a setup as shown in Fig. 1. In order to accelerate evaporation of the solvent, nitrogen gas (filtered through a 0.22 µm HEPA-filter) was flushed (15 l/min) over the stirring mixture (Fig.1). The formed microspheres were collected by centrifugation and washed three times with water, three times with 0.1 M HCl and finally three times with water. The washed microspheres were fractionated according to size using stainless steel sieves with a pore size of 20 and 50 µm and using 1 l of water (Fig. 2, method A). The sieving system consisted of an Electromagnetic Sieve Vibrator (EMS 755) combined with an Ultrasonic Processor (UDS 751) (both from Topas GmbH, Dresden, Germany). The collected microspheres (~ 4 g) were dried at 70 °C under vacuum for 5 h using a rotating glass oven (B-580 GKR, Buchi, Zurich, Switzerland). After drying, the microspheres (500 mg) were packed in high-density polyethylene vials (type A, Posthumus Products, Beverwijk, The Netherlands).

In addition to the standard preparation method as described above, microspheres were also prepared by varying the following four parameters:

1- the sieving procedure. The obtained microspheres were suspended in water (200 ml) and fractionated according to size using stainless steel sieves of 20 and 50 μm with a sprinkler system (Analysette 3 system, Fritsch GmbH, Idar Oberstein, Germany) using 8 l of water (Fig. 2 method B).

2- the organic solvent. Dichloromethane (DCM) instead of chloroform was used as a solvent for the preparation of Ho-PLLA-MS since higher residues of DCM are allowed by the ICH-guidelines: the ICH-guidelines give limits of 60 and 600 ppm for chloroform and dichloromethane, respectively [9].

3- the origin of HoAcAc. Commercially available HoAcAc obtained from Sigma Aldrich (Steinheim, Germany) instead of HoAcAc as synthesised by ourselves.

4- the temperature control during the solvent evaporation process (Fig. 1). For the preparation of Ho-PLLA-MS on a gram-scale with a solvent evaporation process, large amounts of chloroform (186 g) have to be evaporated. This will probably result in a (drastic) lowering of temperature of the water/ CHCl_3 mixture and requires, therefore, controlled maintenance of temperature to ensure evaporation of the organic solvent. The temperature of the PVA solution during solvent evaporation was, therefore, maintained at room temperature and meanwhile monitored.

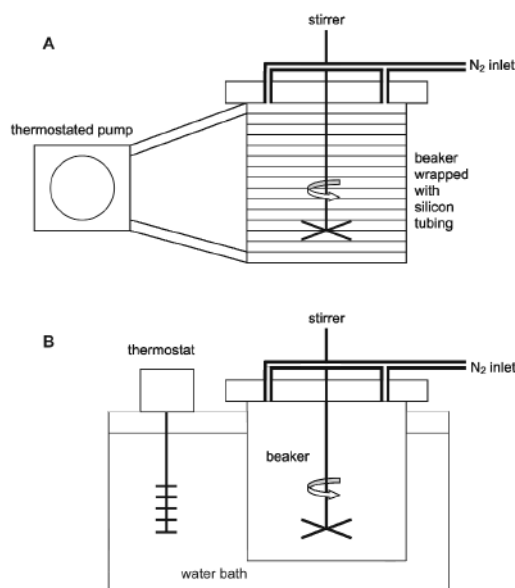


Fig. 1 Temperature control during the solvent evaporation process. Set up A: A glass beaker (inner diameter 13 cm, height 16 cm, volume 1.5 l) with four 1 cm (depth) baffles was wrapped with a silicon tube (external diameter 12 mm). The silicon tube was connected to a thermostated chamber equipped with a circulator (Thermo Haake DC 10, Karlsruhe, Germany). The temperature of the chamber was maintained at 37 °C during stirring with a 4-bladed propeller stirrer (type R 1345, IKA® Werke GmbH & Co. KG, Staufen, Germany). Set up B: The same beaker was placed in a water bath of which the temperature was maintained at 25 °C.

2.3 Neutron irradiation

Ho-PLLA-MS (~250 mg) packed in polyethylene vials were neutron-irradiated at the Reactor Institute in Delft, The Netherlands with a thermal neutron flux of $5 \times 10^{12} \text{ cm}^{-2} \cdot \text{s}^{-1}$ for 6 h. Analyses of the neutron-irradiated microspheres were performed after decay for one month storage at room temperature in closed vials.

2.4 Determination of holmium content in microspheres

The holmium content in microspheres was determined by a complexometric titration as described previously [7].

2.5 Particle size distribution and Scanning Electron Microscopy (SEM)

The particle size distribution of radiated and non-radiated microspheres was determined using a Coulter Counter (Multisizer 3, Beckman Coulter, The Netherlands) equipped with a 100- μm orifice.

The surface morphology of the Ho-PLLA-MS was investigated by SEM using a Philips XL30 FEGSEM. A voltage of 5 or 10 kV was applied. Samples of microspheres were mounted on aluminium stubs and sputter-coated with a Pt/Pd layer of about 10 nm.

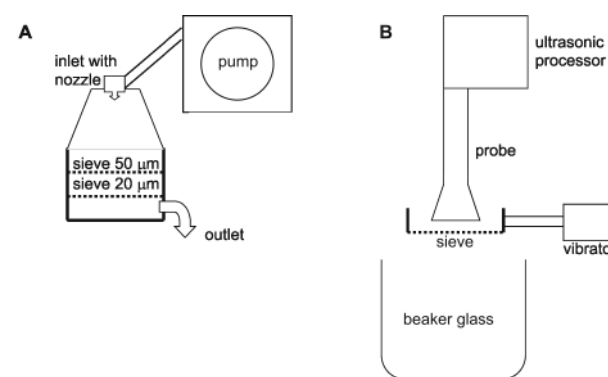


Fig. 2 Sieving procedure of microspheres. A: standard sieving procedure B: sieving procedure using an ultrasonic probe and vibrator.

2.6 Microbiological examination

Microbiological examination of three batches of Ho-PLLA-MS before neutron irradiation was performed using the European Pharmacopoeia method 2.6.12, 2.6.13 and 2.6.14 [8] and were carried out by Bactimm B.V., Nijmegen, The Netherlands. The batches were prepared according to the standard preparation method as described in section 2.2. The temperature of the water/chloroform mixture during the solvent evaporation process of these batches was maintained at room temperature with method A as represented in Fig. 1.

2.7 Residual solvents

The residual solvents levels of three batches of Ho-PLLA-MS after neutron irradiation were determined using European Pharmacopoeia method 2.4.24, 'identification and control of residual solvents for water insoluble substances' [8], and were carried out by Farmalyse B.V., Zaandam, The Netherlands.

2.8 Release of holmium

The release of holmium from neutron irradiated Ho-PLLA-MS (after decaying for one month, see section 2.3) was tested in triplicate with a method in analogy with the method as described by Hafeli et al. [10] which is comparable to the rotating basket method described in the European Pharmacopoeia (method 2.6.12) [8]. Microsphere samples (250 mg) were dispersed in 50 ml of an isotonic phosphate buffer (174 mmol, pH 7.4) in a 50 ml test tube (Greiner- Bio One, Frickenhausen, Germany). The tubes (in triplicate) were closed with a cap containing a nylon filter with a pore size of 3 mm (Millipore, Billerica, USA). The tubes were placed upside down in a beaker glass containing 200 ml of the same isotonic phosphate buffer. Sodium azide (0.05%) was added to prevent bacterial growth during the release experiment. The temperature of the buffer was 37 °C and the tubes were rotated with a speed of 50 rpm. After 270 h (10 times the half-life of Ho-166) the release system was dismantled. The release of holmium was determined by comparing the measured activity of Ho-166m in the beaker glass versus the activity of the microspheres in the tubes using a low-background γ -counter (Tobor, Nuclear Chicago, USA). Ho-166m is a metastable isotope formed in a small fraction (7 ppm of the total amount of newly formed isotopes) during activation of Ho-165. Due to the low concentration of Ho-166m in

the samples and its long half life (~ 1200 y), the actual activity of Ho-166m is very low. However, after the decay of Ho-166 (with a half life of 26.8 h), Ho-166m is the only persisting isotope and can therefore still be detected reliably as demonstrated previously [11].

3. Results and Discussion

3.1 Preparation of microspheres

Ho-PLLA-MS with 17.0 ± 0.5 % (w/w) of holmium, corresponding with a loading of the HoAcAc complex of ~ 50 % (w/w), were prepared according to the standard preparation method [4]. The microspheres have a rather broad size distribution (10-60 μm) (Fig. 3). Sieving with either method A or method B was very effective in narrowing down the particle size distribution: more than 97% (v/v) of the microspheres had a size between 20-50 μm after sieving, which is the desired size for an optimal targeting [1]. Sieving method A is preferred since this method is less time consuming than method B (10 min versus 45 min) and less water is needed for the total sieving procedure (1 l versus 8 l). The total mass of microspheres was about 4 g after sieving.

Since higher residues of dichloromethane are allowed by the ICH-guidelines [9], this solvent was also tested. The particle size distribution and yield were equal to Ho-PLLA-MS prepared with chloroform. However, the holmium content of the microspheres prepared using dichloromethane was 9 %, which is much

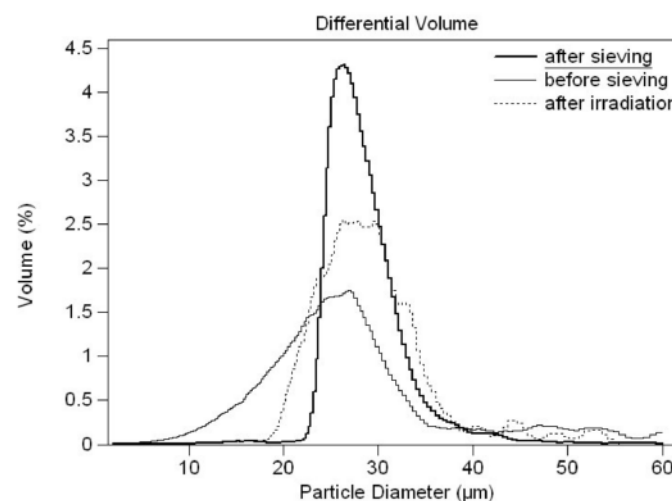


Fig. 3 Typical population distribution of microspheres before and after sieving, and after irradiation in a nuclear reactor.

lower than in the microspheres that were prepared with chloroform (17 %). Previous studies showed that the solubility of the holmium-complex in PLLA is influenced by the way of solvent removal. HoAcAc is less soluble in films (up to 8%, prepared by the quick evaporation of chloroform) than in microspheres (17 %, prepared by the solvent evaporation method as described in section 2.2). The difference in HoAcAc loading between microspheres prepared by either chloroform or dichloromethane might be caused by the higher water solubility (leading to a fast solvent extraction) and the lower boiling point (leading to a fast solvent evaporation) of dichloromethane as compared to chloroform. A high holmium content of the microspheres is required in order to achieve therapeutic amounts of radioactivity in a relatively small amount of microspheres (500-800 mg). The low holmium content of the microspheres prepared using dichloromethane does not meet this requirement and makes them unsuitable for clinical application. A small amount of microspheres will result in lodging of the microspheres in and around the tumour while sparing healthy liver tissue [12], and will prevent filling of the supplying vessels of the liver [11] which will cause unnecessary damage to healthy liver tissue. Furthermore, in contrast to microspheres prepared with chloroform, Ho-PLLA-MS which were prepared with dichloromethane had a very irregular shape (Fig. 4). It has been reported previously that the use of dichloromethane can lead to the formation of microspheres with an irregular shape [13,14]. The consequences of this irregular microsphere morphology in terms of aggregation of the microspheres during administration in the catheter or blood vessels are not known. HoAcAc obtained from a commercial source (Sigma Aldrich) is unsuitable for

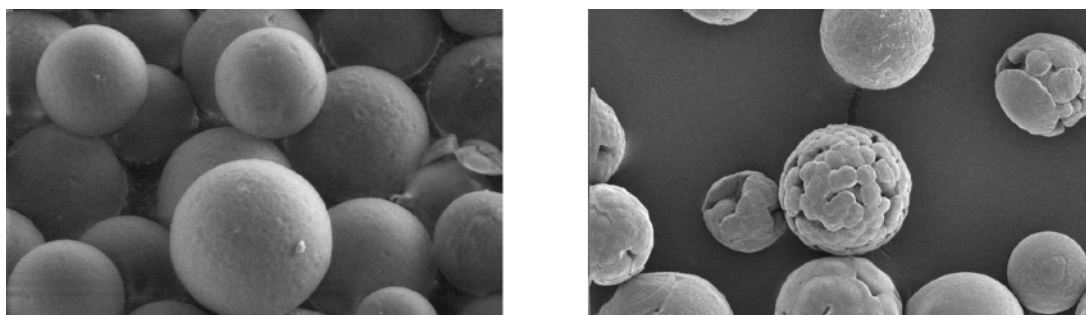


Fig. 4 SEM pictures of Ho-PLLA-MS produced with chloroform (left) and with dichloromethane (right).

the preparation of microspheres (5 attempts were made). Visual differences were clearly observed between the HoAcAc obtained from Sigma Aldrich (small orange coloured rhombic crystals) and HoAcAc as synthesised by ourselves (pink needle-shaped crystals). During the washing step with 0.1 M HCl severe flocculation of the particles occurred and no microspheres could be obtained. Previous studies have demonstrated that the synthesis of HoAcAc is a delicate procedure [4,15], which can in some cases lead to the formation of impure material. These impurities are probably the cause of the unsuccessful preparation of Ho-PLLA-MS with HoAcAc obtained from Sigma Aldrich.

Fig. 5 demonstrates that without temperature control, the temperature of the water/chloroform mixture decreased tremendously (from ~20 °C to ~8 °C) and remained at this temperature. As a result the chloroform could not be quantitatively evaporated within 40 h. The two types of temperature control (see Fig. 1) were both sufficient to maintain the temperature at room temperature and both resulted in the quantitative evaporation of chloroform from the water phase after 40 h. However, a set-up with an open water bath (situation B, Fig.1) is very susceptible for bacterial contamination and, therefore, undesirable in a GMP-production process.

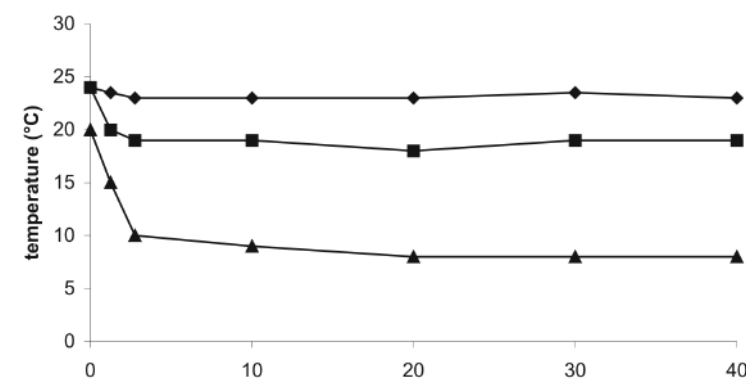


Fig. 5 Temperature monitoring during the solvent evaporation process (40 h). (▲): No temperature control, (■): Set up A, (◆): Set up B

3.2 Pharmaceutical quality of microspheres

No colony forming units (CFU) (aerobe bacteria, anaerobe bacteria and fungi) could be found in the examined microsphere batches. The production of Ho-PLLA-MS is a very time consuming process (the total time is around 4 days) and in several production steps water is used. This makes the process very vulnerable to bacterial contamination and growth. However, we introduced several germ-reducing steps in the production process (see section 2.2), which are:

- boiling of the PVA solution
- flushing with filtered (0.22 μm HEPA-filter) nitrogen gas over the stirring water / chloroform mixture
- washing the microspheres with 0.1 M HCl
- drying of the microspheres for 5h at 70 °C under vacuum.

These germ-reducing steps are apparently sufficient to obtain CFU-free microspheres. Considering the fact that microspheres are subsequently neutron irradiated with a very high dose of radiation, the sterility of the microspheres that are administered to a patient can consequently be guaranteed.

The endotoxin level detected ranged from $3.7 \cdot 10^{-4}$ to $6.1 \cdot 10^{-4}$ EU/mg microspheres. The limit for parenteral drugs is 5.0 EU/kg body weight [8]. The maximum amount of endotoxins that is allowed to be administered to a patient of 70 kg is 350 EU. If, in our case, 800 mg of Ho-PLLA-MS will be administered to patients, the total amount of endotoxins (~ 0.5 EU) is far below the given limits. With respect to their residual solvent levels, Ho-PLLA-MS were in compliance with the ICH-guidelines [9]. No residual solvents were detected in the three batches of neutron irradiated Ho-PLLA-MS. The absence of chloroform in microspheres, which is used during the production process, is caused by an intensive drying process (70 °C under vacuum) and the subsequent neutron irradiation of Ho-PLLA-MS.

3.3 Radiochemical stability

Although neutron irradiation resulted in a very high radiation dose to the Ho-PLLA-MS [6], only minor changes in the particle size distribution were observed. After irradiation, still more than 94 % (v/v) of the microspheres had the desired particle size between 20 and 50 μm (Fig. 3).

Moreover, neutron irradiated Ho-PLLA-MS were very stable. After 270 h (10

times the half-life of Ho-166) only 0.3 ± 0.1 % of Ho had released from the microspheres in the buffer. Previously, it was demonstrated that holmium and PLLA interact with each other [16]. These interactions are probably the cause of the high stability of neutron irradiated Ho-PLLA-MS.

4. Conclusion

In this paper the GMP-production of Ho-PLLA-MS is described. It is demonstrated that it is possible to prepare microspheres by a solvent evaporation process on a gram-scale. The pharmaceutical characteristics (residual solvents, CFU and endotoxins) of the microspheres are in compliance with the requirements of the European Pharmacopoeia. Furthermore, neutron irradiated microspheres have a high radiochemical stability and retain their size and shape. In conclusion, radioactive Ho-PLLA-MS which are produced as described in this paper, can be clinically applied, considering their pharmaceutical quality.

Acknowledgements

The authors wish to thank W.A.M. van Maurik from EMSA, Faculty of Biology, Utrecht University, Utrecht, The Netherlands for SEM acquisition. Moreover, we are grateful to J. Kroon of Department of Radiation, Radionuclides and Reactor (Delft University of Technology, The Netherlands) for his assistance with neutron irradiations. We thank Dr. H. Talsma for valuable discussions. This research was supported by the Technology Foundation STW (UGT.6069), applied science division of NWO and the technology programme of the Ministry of Economic Affairs, the Nijbakker-Morra foundation, foundation De Drie Lichten and by the Maurits and Anna de Kock foundation.

References

- [1] Nijssen JFW, van het Schip AD, Hennink WE, Rook DW, van Rijk PP, De Klerk JMH. Advances in nuclear oncology: Microspheres for internal radionuclide therapy of liver metastases. *Current Medicinal Chemistry* 2002; 9: 73-82.
- [2] Nijssen JF, Seppenwoolde JH, Havenith T, Bos C, Bakker CJ, het Schip AD. Liver Tumors: MR Imaging of Radioactive Holmium Microspheres—Phantom and Rabbit Study. *Radiology* 2004.
- [3] Zielhuis SW, Nijssen JF, Seppenwoolde JH, Zonnenberg BA, Bakker CJ, Hennink WE, van Rijk PP, het

Schip AD. Lanthanide bearing microparticulate systems for multi-modality imaging and targeted therapy of cancer. *Curr Med Chem Anti -Canc Agents* 2005; 5: 303-13.

[4] Nijsen JF, Zonnenberg BA, Woittiez JR, Rook DW, Swildens-van Woudenberg IA, van Rijk PP, het Schip AD. Holmium-166 poly lactic acid microspheres applicable for intra-arterial radionuclide therapy of hepatic malignancies: effects of preparation and neutron activation techniques. *Eur J Nucl Med* 1999; 26: 699-704.

[5] De Vos FJ, De Decker M, Dierckx RA. The good laboratory practice and good clinical practice requirements for the production of radiopharmaceuticals in clinical research. *Nucl Med Commun* 2005; 26: 575-9.

[6] Nijsen JF, van het Schip AD, van Steenberg MJ, Zielhuis SW, Kroon-Batenburg LM, van de Weert M, van Rijk PP, Hennink WE. Influence of neutron irradiation on holmium acetylacetonate loaded poly(L-lactic acid) microspheres. *Biomaterials* 2002; 23: 1831-9.

[7] Zielhuis SW, Nijsen JF, Figueiredo R, Feddes B, Vredenberg AM, het Schip AD, Hennink WE. Surface characteristics of holmium-loaded poly(l-lactic acid) microspheres. *Biomaterials* 2005; 26: 925-32.

[8] European Pharmacopoeia. 2002.

[9] B'Hymer C. Residual solvent testing: A review of gas-chromatographic and alternative techniques. *Pharmaceutical Research* 2003; 20: 337-44.

[10] Hafeli UO, Roberts WK, Pauer GJ, Kraeft SK, Macklis RM. Stability of biodegradable radioactive rhenium (Re-186 and Re-188) microspheres after neutron-activation. *Appl Radiat Isot* 2001; 54: 869-79.

[11] Seppenwoolde JH, Nijsen JF, Bartels LW, Zielhuis SW, het Schip AD, Bakker CJ. Internal radiation therapy of liver tumors: Qualitative and quantitative magnetic resonance imaging of the biodistribution of holmium-loaded microspheres in animal models. *Magn Reson Med* 2004; 53: 76-84.

[12] Nijsen F, Rook D, Brandt C, Meijer R, Dullens H, Zonnenberg B, de Klerk J, van Rijk P, Hennink W, van het Schip AD. Targeting of liver tumour in rats by selective delivery of holmium-166 loaded microspheres: a biodistribution study. *Eur J Nucl Med* 2001; 28: 743-9.

[13] Chung TW, Huang YY, Liu YZ. Effects of the rate of solvent evaporation on the characteristics of drug loaded PLLA and PDLLA microspheres. *Int J Pharm* 2001; 212: 161-9.

[14] Wang YM, Sato H, Horikoshi I. In vitro and in vivo evaluation of taxol release from poly(lactic-co-glycolic acid) microspheres containing isopropyl myristate and degradation of the microspheres. *Journal of Controlled Release* 1997; 49: 157-66.

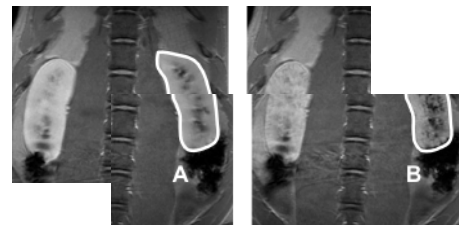
[15] Kooijman H, Nijsen F, Spek AL, van het SF. Diaquatrakis(pentane-2,4-dionato-O,O')holmium(III) monohydrate and diaquatrakis(pentane-2,4-dionato-O,O')holmium(III) 4-hydroxypentan-2-one solvate dihydrate. *Acta Crystallogr C* 2000; 56: 156-8.

[16] Nijsen JF, van Steenberg MJ, Kooijman H, Talsma H, Kroon-Batenburg LM, van De WM, van Rijk PP, De Witte A, Van Schip AD, Hennink WE. Characterization of poly(L-lactic acid) microspheres loaded with holmium acetylacetonate. *Biomaterials* 2001; 22: 3073-81.

Chapter 8

Holmium loaded alginate microspheres for multimodality imaging and therapeutic applications

SW Zielhuis, JH Seppenwoolde, CJG Bakker, U Jahnz,
BA Zonnenberg, AD van het Schip, WE Hennink and JFW Nijssen



Abstract

In this paper the preparation and characterization of holmium-loaded alginate microspheres is described. The rapid development of medical imaging techniques offers new opportunities for the visualisation of (drug-loaded) microparticles. Therefore, suitable imaging agents have to be incorporated into these particles. For this reason, the element holmium was used in this study in order to utilize its unique imaging characteristics. The paramagnetic behaviour of this element allows visualisation with MRI and holmium can also be neutron-activated resulting in the emission of gamma-radiation, allowing visualisation with gamma cameras, and beta-radiation, suitable for therapeutic applications.

Almost monodisperse alginate microspheres were obtained by JetCutter technology where alginate droplets of a uniform size were hardened in an aqueous holmium chloride solution. Ho^{3+} binds via electrostatic interactions to the carboxylate groups of the alginate polymer and as a result alginate microspheres loaded with holmium were obtained. The microspheres had a mean size of $159\text{ }\mu\text{m}$ and a holmium loading of $1.3 \pm 0.1\%$ (w/w) (corresponding with a holmium content based on dry alginate of $18.3 \pm 0.3\%$ (w/w)). The binding capacity of the alginate polymer for Ho^{3+} (expressed in molar amounts) is equal to that for Ca^{2+} , which is commonly used for the hardening of alginate. This indicates that Ho^{3+} has the same binding affinity as Ca^{2+} . In line herewith, dynamic mechanical analyses demonstrated that alginate gels hardened with Ca^{2+} or Ho^{3+} had similar viscoelastic properties. The MRI relaxation properties of the microspheres were determined by a MRI phantom experiment, demonstrating a strong R_2^* effect of the particles.

Alginate microspheres could also be labelled with radioactive holmium by adding holmium-166 to alginate microspheres, previously hardened with calcium (labelling efficiency 96 %). The labelled microspheres had a high radiochemical stability (94 % after 48 h incubation in human serum), allowing therapeutic applications for treatment of cancer.

The potential in-vivo application of the microspheres for a MR-guided renal embolization procedure was illustrated by selective administration of microspheres to the left kidney of a pig. Anatomic MR-imaging showed the presence of holmium-loaded microspheres in the kidney.

In conclusion, this study demonstrates that the incorporation of holmium into alginate microspheres allows their visualisation with a gamma camera and MRI. Holmium-loaded alginate microspheres can be used therapeutically for embolization and, when radioactive, for local radiotherapy of tumours.

1. Introduction

Image-guided local delivery of drug-loaded microparticles administered by direct injection or via a catheter will result in a more effective treatment of patients with therapeutic agents like radionuclides [1,2], pharmaceutically active proteins or chemotherapeutics. The rapid development of medical imaging techniques offers new opportunities for visualisation and directing of the biodistribution of these particles in-vivo [3,4].

In order to achieve visualisation of particulate systems with modalities like MRI and a gamma camera, appropriate imaging agents have to be incorporated into the particles. Previous studies have demonstrated that the element holmium offers excellent opportunities for medical imaging [1,2]. It is well known that paramagnetic ions, among which Ho^{3+} , alter the responses of the MRI signal by shortening its relaxation times. Since different relaxation times generally result in an enhanced contrast in certain types of MR sequences, paramagnetic elements are used as MRI contrast agents [1,5,6].

Moreover, holmium can also be neutron-activated to yield holmium-166 (a gamma and beta-emitter) with a logistically favourable half-life (26.8 h) for therapeutic applications [7,8]. The photons (80.6 keV, 6.2 %) allow visualisation with a gamma camera whereas the beta-radiation ($E_{\text{max}} = 1.84\text{ MeV}$) can be used for therapeutic applications such as the local radiotherapy of tumours.

In this study, alginate was chosen as a hydrophilic polymer for the preparation of holmium-loaded microparticles, which can potentially be visualised in-vivo. Alginate is a polysaccharide that can be found in seaweed and in some bacteria. It is a copolymer of β -D-mannuronic acid and α -L-guluronic acid with a degree of polymerization ranging from 50 to 200,000 [9]. Microspheres based on alginate are under investigation for delivery of proteins [10], encapsulation of living cells [11] and chemo-embolization [12]. Alginate microspheres can be prepared by dropping an aqueous alginate solution into an aqueous solution of CaCl_2 [9]. The carboxylic acid groups of the guluronic residues of alginate bind strongly to Ca^{2+} ions by which the polymer chains are crosslinked and a hydrogel is formed [9,13,14]. Besides divalent ions also trivalent ions from the group of lanthanides have the capability to bind to alginate [13]. Surprisingly, no diagnostic and therapeutic applications have been described with lanthanide alginate microspheres so far.

In this paper we describe the use of the JetCutter technology [15] to produce almost monodisperse alginate microspheres which were hardened with holmium or calcium. The holmium loaded alginate microspheres (Ho-alginate-ms) were characterized for their size and size distribution, holmium content and in vitro MR relaxation properties. The calcium-loaded microspheres were investigated for radiolabeling properties.

As mentioned, image-guided arterial administration of drug loaded microspheres to their aimed site of action via a catheter will result in a more effective treatment. Consequently, it is very important to get a good insight into the elastic properties of these alginate microspheres, since catheter occlusion or clumping in vessels can occur when the particles are not deformable [16,17]. Therefore, the viscoelastic properties of both holmium-alginate and calcium-alginate gels were investigated. Finally, the feasibility of the use of the Ho-alginate-ms in vivo was shown in an embolization procedure in a pig in which these microspheres were administered to the left kidney under MR-guidance.

2. Materials and Methods

2.1 Materials

All chemicals were commercially available and used as obtained. Sodium alginate (Protanal, LF20/40) was supplied by FMC (Drammen, Norway). Sodium hydroxide (NaOH; 99.9%) was purchased from Riedel-de Haën (Seelze, Germany). Holmium (III) chloride hexahydrate ($\text{HoCl}_3 \cdot 6\text{H}_2\text{O}$; 99.9%) was obtained from Phase Separations BV (Waddinxveen, The Netherlands). Manganese(II) chloride tetrahydrate ($\text{MnCl}_2 \cdot 4\text{H}_2\text{O}$; 99.9%), calcium chloride dihydrate ($\text{CaCl}_2 \cdot 2\text{H}_2\text{O}$; 99.9%), nitric acid (HNO_3 ; 65%), and hydrochloric acid (HCl; 37%) were purchased from Merck (Darmstadt, Germany). Agar powder (USP Grade) was purchased from Life Technologies GIBCO BRL (Paisley, Scotland). Magnevist® (gadolinium diethylenetriamine pentaacetic acid; Gd-DTPA) was obtained from Schering (Berlin, Germany).

2.2 Preparation of microspheres

Ho-alginate-ms were prepared using the JetCutting technology as recently described by Prusse et al. [15] (Fig. 1). This technology is based on the following principle. A continuous jet of fluid is pressed through a nozzle and then

passes a rotating cutting tool. This cuts the jet into identical cylindrical segments, which subsequently take a spherical shape due to the surface tension of the fluid. In this study, alginate droplets were hardened in a holmium chloride solution. Since droplet generation is achieved by a mechanical cutting step, the viscosity of the fluid is less important as compared to other methods [15]. Fluids with a viscosity of several Pa·s were successfully processed and beads ranging from 120 μm to 4 mm and with a narrow size distribution were produced [15]. The technology was previously successfully applied for bio-encapsulation processes [11].

An aqueous solution of sodium alginate (2 % w/v) was processed (flow rate 0.15 ml/s) and the resulting droplets were hardened in either a 5.0 mM calcium chloride or 5.0 mM holmium chloride solution (300 ml). After preparation, the microspheres were washed three times with water, resuspended in deionised water and stored in closed vials.

2.3 Characterization of Ho-alginate-ms: holmium loading and size

200 mg of hydrated Ho-alginate-ms were destructed in 40 ml of 'aqua regia' (three parts of hydrochloric acid and one part of nitric acid). After 15 min of incubation the solution was neutralized with 5.0 M sodium hydroxide and the holmium concentration was determined by a complexometric titration as previously described [18]. The same analytical procedure was also followed to determine the holmium content of the dry microspheres. Therefore, Ho-alginate-ms

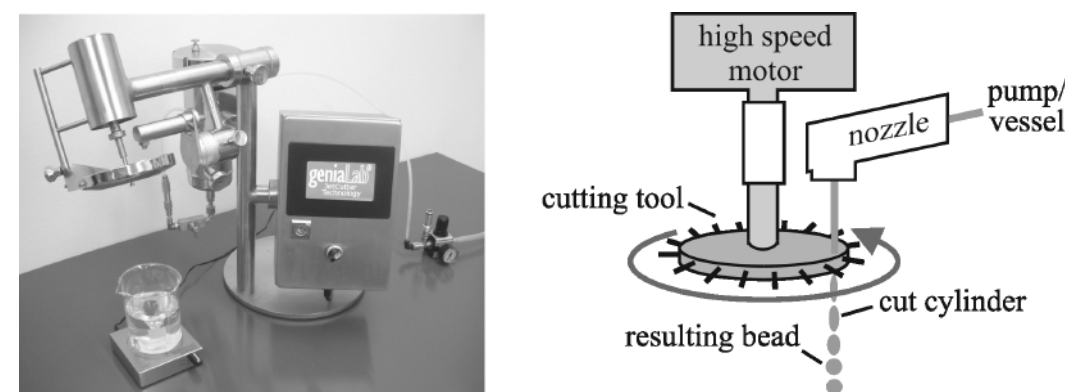


Fig. 1 Picture (left) and a schematic drawing (right) of the JetCutter apparatus.

were dried at 50°C for 24 h and 200 mg of the dried microspheres were destructed in 'aqua regia' and titrated after neutralization. Analyses were performed in triplicate. The particle size distribution was determined using a light microscope. Microspheres were placed on a glass plate with a 200 µm grid and a microscopic picture was taken. From this picture, 100 microspheres were randomly selected and their size was established. This procedure was performed in triplicate.

2.4 Dynamic mechanical analysis (DMA)

DMA measurements on alginate gels were performed on a DMA 2980 Dynamic Mechanical Analyser (TA Instruments, Inc., New Castle, USA) in the "controlled force" mode. Holmium and calcium loaded alginate gels with a cylindrical shape were prepared (n=3) by slowly adding 5 ml of a 5 mM electrolyte solution to 2 ml of a 2 % sodium alginate solution. After incubating for 48 h, alginate gels with a cylindrical shape (length and diameter ~ 1 cm) were obtained. The edges of the cylinders were cut off with a lancet knife and the alginate hydrogel cylinders (length and diameter ~ 8 mm) were clamped between a parallel-plate compression clamp with a diameter of 0.6 cm. A force ramp from 0.001 to 5 N (depending on the gel strength) at a rate of 0.5 N/min was applied. The modulus was calculated from the linear part of the plot of the stress against the fractional deformation according to the method of Meyvis et al [19].

2.5 MRI phantoms

The relevant MR relaxation parameters are R_1 ($=1/T_1$), R_2 ($=1/T_2$) and R_2^* ($=1/T_2^*$) which describe the longitudinal, the intrinsic transverse, and the effective transverse relaxation of the MRI-signal, respectively. The MR relaxation properties of the Ho-alginate microspheres in agar gels were determined as follows. An agar gel matrix was prepared by dissolving 20 g of agar powder in 1 l of boiling deionized water in which 30 mg of manganese(II) chloride tetrahydrate was dissolved. Manganese chloride was used to adjust the relaxation properties of the gel to that of human tissue (T_1 approximately 500 msec, T_2 approximately 45 msec). Subsequently, the hot agar solution was poured into test tubes (25 ml) containing Ho-alginate-ms and the resulting suspension (containing 0.25 to 4 mg/g of microspheres) was stirred. Next, a gel was formed upon cooling to

room temperature. To prevent trapping of air bubbles in the gels, the heated microsphere/agar suspensions were sonicated during cooling. The Ho-alginate-ms were homogeneously (visual observation) distributed in the formed agar gels. Measurement of the R_1 and R_2 relaxation rates of the MR signal was performed on 1.5 Telsa (Gyrosan Intera NT, Philips Medical Systems, Best, The Netherlands) using an acquisition that combines a multi-spin echo (SE) with an inversion recovery sequence [20], at a field of view (FOV) of 256 mm, 10 mm slice thickness, matrix of 128*256, one signal acquired. The R_2^* relaxation rates were measured as described previously [2] with a multi-echo gradient echo sampling of a spin-echo with an echo spacing of 1.55 msec centred around an echo time (TE) of 30 msec. Relaxation rates were calculated assuming exponential signal curves, resulting in an average relaxation time for each gel. Relaxation rates of the gels were averaged and plotted against concentration.

2.6 Radiolabeling of microspheres

Radiolabeling of microspheres with holmium-166 was performed with microspheres that were previously hardened with Ca^{2+} (see section 2.2). Holmium-166 was obtained by neutron irradiation of 8.0 mg holmium chloride (corresponding with 3.0 mg of Ho-165) (packed in polyethylene vials) with a thermal neutron flux of $5 \times 10^{12} \text{ cm}^{-2} \cdot \text{s}^{-1}$ at the Reactor Institute Delft (Department of Radiation, Radionuclides and Reactor, Delft University of Technology, The Netherlands). After neutron activation, the holmium-166 chloride (with an activity of 100 MBq) was dissolved in 3 ml of distilled water and subsequently added to 2.5 g of Ca-alginate microspheres. After incubation for 3 h at room temperature, the microspheres were centrifuged at 2000 rpm for 3 min and the supernatant was removed. The microspheres were washed 2 times with 5 ml of distilled water. The labelling efficiency was determined by measuring the activity of the supernatant plus the washing fractions and the microspheres using a VDC-404 dose calibrator (Veenstra Instruments, Joure, the Netherlands). The radiochemical stability of the holmium-166 labelled microspheres was tested by incubation of the microspheres (2.5 g) for 48 h in 10 ml human serum at 37 °C. Release of holmium-166 from the microspheres was determined by measuring the radioactivity of the pellet and supernatant in the same way as described for determination of the labelling efficiency.

2.7 In-vivo embolization

To show the feasibility of a MRI-guided embolization procedure using Ho-alginate-ms, the particles were introduced into the left kidney of a healthy domestic pig (75 kg). The pig was sedated with ketamine (10 mg/kg, intramuscular) and anesthetized with thiopental (4 mg/kg, intravenous [IV]) before it was intubated and connected to a respirator for intermittent positive pressure ventilation with a mixture of oxygen and air (1:1 v/v). During the MR-experiment, anaesthesia was maintained by continuous infusion of midazolam (0.3 mg/kg/h, IV), while analgesia was obtained by continuous infusion of sufentanyl citrate (1 µg/kg/h, IV) and muscle relaxation by infusion of pancuronium bromide (0.1 mg/kg/h, IV). For positioning of the catheter, a passive tracking technique [21] was used that allowed real-time depiction of paramagnetic markers (dysprosium oxide) that were mounted on 4-F headhunter catheters (Cordis, Rhoden, The Netherlands). Before tracking, the major abdominal arterial vasculature was visualised with three-dimensional contrast-enhanced MR angiography (3D-CE-MRA) by injection of 20 ml of Gd-DTPA. Acquisition was done with FOV 350*350, 70 coronal slices of 1.0 mm, matrix 512*296, TR/TE = 5.1/1.6 msec, flip 40, one signal average during breath hold of 30 sec at maximum. Then, the catheter and guide wire were inserted and navigated during the passive tracking. The tip of the injection catheter was placed 2 cm in the left renal artery. The frame rate of the tracking sequence was 5 frames per second. Before administration of the microspheres, anatomic T₂*-weighted gradient-echo (T₂*-w GE) images were made (FOV 350*245, 15 coronal slices of 4.0 mm, matrix 256*204, TR/TE = 500/4.6, 9.2 msec, flip 90, two signal averages). Then, an injection of 10 ml saline containing 50 mg of Ho-alginate-ms was monitored with a dynamic T₂*-w GE sequence (TR/TE/flip = 22/4.6/15°, 2.2 sec per dynamic). The volume of 10 ml was injected in 60 seconds. After injection the anatomic T₂*-weighted acquisition was repeated.

The experiment was performed in agreement with The Netherlands Experiments on Animals Act (1977) and the European Convention for the Protection of Vertebrate Animals used for Experimental Purposes (1986). Approval was obtained from the University Animal Experiments Committee.

3. Results and discussion

3.1 Preparation and characterisation of Ho-alginate-ms

Using the JetCutting technology with holmium chloride as a hardening agent, alginate microspheres were successfully produced. The following parameters which gave optimal calcium alginate beads with a diameter of ~160 µm, were also used for the successful production of Ho-alginate-ms: nozzle diameter 100 µm, mass throughput of the alginate solution 0.15 g/sec, cutting tool with 48 wires of 90 µm diameter each, rotating at 14,100 rpm. The microspheres had an almost round shape (Fig. 2) and monodisperse size with the mean diameter of a typical batch being 159 ± 19 µm.

The holmium content of the wet and dry alginate microspheres was 1.3 ± 0.1 % (w/w) and 18.3 ± 0.3 % (w/w), respectively. Guluronic residues of alginate bind to di- and trivalent cations such as Ca²⁺ and Ho³⁺ resulting in a three-dimensional network of alginate polymer chains held together by these ions. The model that describes this network is the “egg-box” model [9]. According to this model, one divalent cation is surrounded by four guluronate or mannuronate groups. Regarding the molecular weight of this surrounding structure (M = 700 g/mol) and the amount of holmium per dry weight of alginate (18.3 % w/w) it can be concluded that these surrounding units are almost quantitatively filled

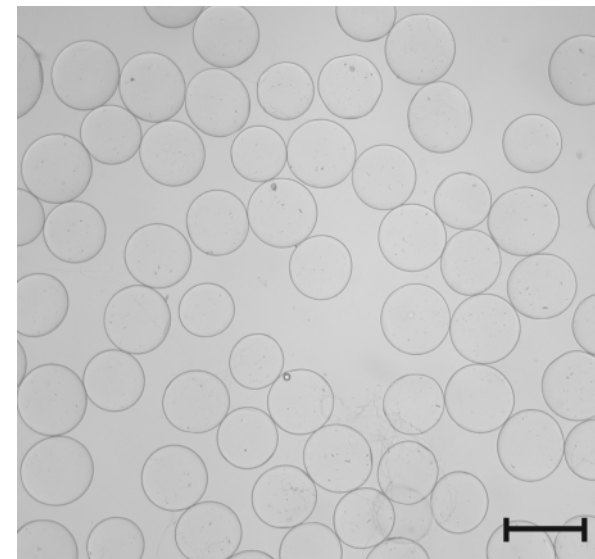


Fig. 2 Microscopic image of Ho-alginate-ms. The bar represents 200 µm.

with a Ho^{3+} ion. DeRamos et al. studied the binding of alginate with divalent alkaline earths and trivalent lanthanide ions [13]. They demonstrated that both divalent alkaline earths and trivalent lanthanide ions interact with the guluronate residues of alginate, although lanthanide ions with a relatively small radius (which is the case for holmium [3]) also showed some interaction with mannuronate residues. The calculated molar ratio confirms the finding that the small trivalent lanthanide ion Ho^{3+} has the same binding characteristics as Ca^{2+} .

3.2 Dynamic mechanical analysis

DMA showed that gels which were hardened with Ca^{2+} or Ho^{3+} had a modulus of 0.15 ± 0.02 MPa and 0.14 ± 0.02 MPa, respectively. The similar elastic behaviour of the gels again indicates that Ho^{3+} and Ca^{2+} have analogous binding characteristics to alginate.

3.3 MRI phantoms

Measurements of the relaxation rates showed that there was no significant R1 and R2 effect from the Ho-alginate-ms on the MR signal (Fig. 3). However, a considerable R2* effect was observed, allowing for good visualization with T2*-weighted imaging. Such a R2* effect can be expected for a highly paramagnetic

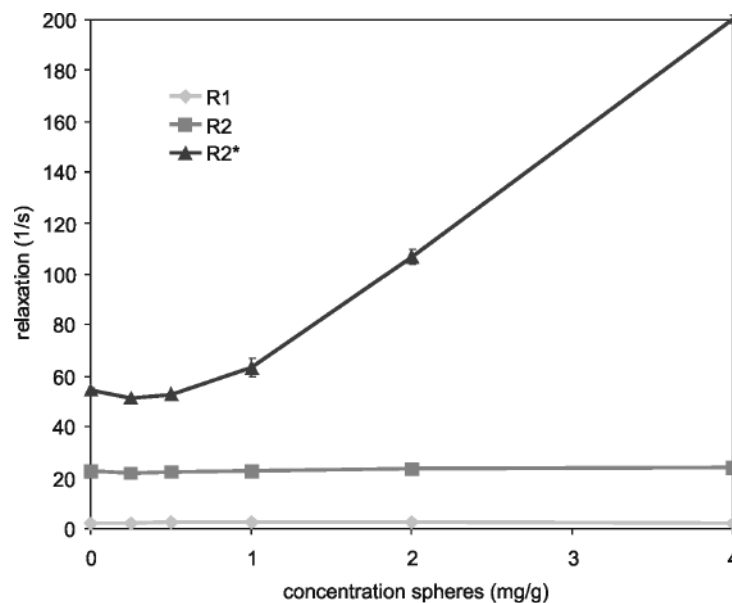


Fig. 3 Relaxation rates R1, R2, and R2* versus concentration of Ho-alginate-ms in agar gel.

element like holmium. The R2* effect showed a linear concentration dependence for concentrations of Ho-alginate-ms above 1 mg of the microspheres/g agar gel, which enables the estimation of the local amount of these microspheres in human tissue [2].

3.4 Radiolabeling of microspheres

Incubation of 2.5 g of Ca-alginate-ms in 3 ml distilled water for 3 h at room temperature with 100 MBq holmium-166 chloride solution in water to exchange Ca^{2+} for Ho^{3+} , resulted in a labelling efficiency of $96 \pm 2\%$. The radiochemical stability after incubation in human serum for 48 h was found to be $94 \pm 2\%$. These results demonstrate that alginate-ms can also be efficiently labelled with holmium-166 afterwards, and that the radiolabel remains stably associated to the microsphere matrix even in the presence of serum proteins. In this study low amounts of radioactivity were used, in order to proof the principle of radiolabeling. For diagnostic or even therapeutic application, a higher specific activity is required. Assuming that a quantity of 50 mg of alginate-ms is used for an embolization procedure, an amount of $\sim 55 \mu\text{g}$ of holmium can be labelled to the microspheres. Irradiation of this amount of holmium in a nuclear reactor with a thermal neutron flux of $5 \times 10^{14} \text{ cm}^{-2} \cdot \text{s}^{-1}$ for 72 h, results in an activity of 5.40 GBq. This amount of radioactivity is suitable for nuclear imaging and for therapeutic applications [8].

3.5 In-vivo embolization

The embolization potential of the Ho-alginate-ms was evaluated in an in-vivo experiment, in which the kidney of a pig was arterially catheterized via the renal artery and subsequently embolized. During injection the deposition of the microspheres was depicted with dynamic T2*-weighted MR imaging. This acquisition showed a distinct increase in regions with signal loss (changes in T2* visible as black 'dots') in the left kidney, indicating that lodging of the Ho-alginate-ms in the vasculature of the kidney indeed occurred. The large size of the microspheres ($\sim 160 \mu\text{m}$) resulted in the successful embolization of the renal arterioles. Spherical shaped and deformable microspheres with a size between 150 and 250 μm have shown to be attractive agents for embolization procedures [17]. The anatomical images (Fig. 4) showed a clear soft-tissue contrast and

regions of signal loss due to the presence of the microspheres, which are detectable by the increased signal voids. The signal voids that are observed before administration are caused by the collection of the injected contrast agent (for the angiography) in the medulla and the base of the kidney. The use of MRI allows acquiring functional information (like blood flow and tissue perfusion), which can be of great importance during evaluation of an embolization procedure. The fact that the deposition of the Ho-alginate-ms can be followed with dynamic MR imaging also allows real-time monitoring of the microsphere administration. Another advantage is the inherent soft-tissue contrast of MRI, which can also be exploited during planning and evaluation of the embolization procedure.

4. Conclusion

This study shows that by use of the JetCutter technology almost monodisperse Ho-alginate-ms were successfully produced. The holmium loading allows visualisation with MRI and moreover, microspheres could also be labelled with radioactive holmium allowing local radiotherapy of tumours and imaging with a gamma camera. An exemplary in vivo pig experiment showed the use of the alginate microspheres in a MR-guided renal embolization procedure.

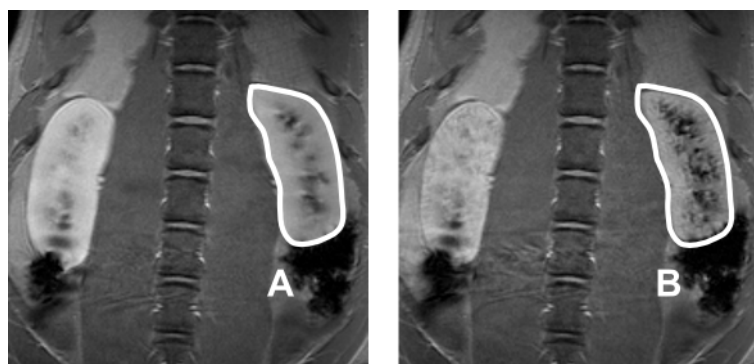


Fig. 4 Anatomical T2*-weighted images of the left kidneys (boundary indicated by the white solid lines) before (A) and after (B) administration of Ho-alginate-ms.

Acknowledgements

This research was supported by the Technology Foundation STW (UGT.6069), applied science division of NWO and the technology programme of the Ministry of Economic Affairs. The authors wish to thank M.J. van Steenberg for his assistance in the DMA measurements.

References

- [1] Nijssen JFW, Seppenwoolde JH, Havenith T, Bos C, Bakker CJG, van het Schip AD. Liver Tumors: MR Imaging of Radioactive Holmium Microspheres—Phantom and Rabbit Study. *Radiology* 2004;231:491-9.
- [2] Seppenwoolde JH, Nijssen JFW, Bartels LW, Zielhuis SW, van het Schip AD, Bakker CJG. Internal radiation therapy of liver tumors: Qualitative and quantitative magnetic resonance imaging of the biodistribution of holmium-loaded microspheres in animal models. *Magn Reson Med* 2004;53:76-84.
- [3] Zielhuis SW, Nijssen JFW, Seppenwoolde JH, Zonnenberg BA, Bakker CJG, Hennink WE, van Rijk PP, het Schip AD. Lanthanide bearing microparticulate systems for multi-modality imaging and targeted therapy of cancer. *Curr Med Chem Anti -Canc Agents* 2005;5: 303-13.
- [4] Jain TK, Morales MA, Sahoo SK, Leslie-Pelecky DL, Labhasetwar V. Iron oxide nanoparticles for sustained delivery of anticancer agents. *Mol Pharm* 2005;2:194-205.
- [5] Thunus L, Lejeune R. Overview of transition metal and lanthanide complexes as diagnostic tools. *Coord Chem Rev* 1999;184:125-55.
- [6] Fossheim S, Johansson C, Fahlvik AK, Grace D, Klaveness J. Lanthanide-based susceptibility contrast agents: assessment of the magnetic properties. *Magn Reson Med* 1996; 35:201-6.
- [7] Nijssen JFW, van het Schip AD, Hennink WE, Rook DW, van Rijk PP, de Klerk JMH. Advances in nuclear oncology: Microspheres for internal radionuclide therapy of liver metastases. *Curr Med Chem* 2002;9:73-82.
- [8] Nijssen JFW, Zonnenberg BA, Woittiez JR, Rook DW, Swildens-van Woudenberg IA, van Rijk PP, van het Schip AD. Holmium-166 poly lactic acid microspheres applicable for intra-arterial radionuclide therapy of hepatic malignancies: effects of preparation and neutron activation techniques. *Eur J Nucl Med* 1999;26:699-704.
- [9] Simpson NE, Stabler CL, Simpson CP, Sambanis A, Constantinidis I. The role of the CaCl₂-guluronic acid interaction on alginate encapsulated betaTC3 cells. *Biomaterials* 2004;25:2603-10.
- [10] Barrias CC, Lamghari M, Granja PL, Sa Miranda MC, Barbosa MA. Biological evaluation of calcium alginate microspheres as a vehicle for the localized delivery of a therapeutic enzyme. *J Biomed Mater Res A* 2005;74:545-52.
- [11] Schwinger C, Koch S, Jahnz U, Wittlich P, Rainov NG, Kressler J. High throughput encapsulation of murine fibroblasts in alginate using the JetCutter technology. *J Microencaps* 2002;19:273-80.

- [12] Misirli Y, Ozturk E, Kursaklioglu H, Denkbaz EB. Preparation and characterization of Mitomycin-C loaded chitosan-coated alginate microspheres for chemoembolization. *J Microencapsul* 2005; 22: 167-78.
- [13] DeRamos CM, Irwin AE, Nauss JL, Stout BE. C-13 NMR and molecular modeling studies of alginic acid binding with alkaline earth and lanthanide metal ions. *Inorg Chim Acta* 1997;256:69-75.
- [14] Min JH, Hering JG. Arsenate sorption by Fe(III)-doped alginate gels. *Water Res* 1998;32:1544-52.
- [15] Prusse U, Dalluhn J, Breford J, Vorlop KD. Production of spherical beads by JetCutting. *Chem Eng Technol* 2000; 23:1105-10.
- [16] Spies JB, Allison S, Flick P, McCullough M, Sterbis K, Cramp M, Bruno J, Jha R. Polyvinyl alcohol particles and tris-acryl gelatin microspheres for uterine artery embolization for leiomyomas: results of a randomized comparative study. *J Vasc Interv Radiol* 2004;15: 793-800.
- [17] Kwak BK, Shim HJ, Han SM, Park ES. Chitin-based embolic materials in the renal artery of rabbits: Pathologic evaluation of an absorbable particulate agent. *Radiology* 2005;236:151-8.
- [18] Zielhuis SW, Nijssen JFW, Figueiredo R, Feddes B, Vredenberg AM, van het Schip AD, Hennink WE. Surface characteristics of holmium-loaded poly(l-lactic acid) microspheres. *Biomaterials* 2005;26:925-32.
- [19] Meyvis TKL, Stubbe BG, van Steenberg MJ, Hennink WE, De Smedt SC, Demeester J. A comparison between the use of dynamic mechanical analysis and oscillatory shear rheometry for the characterisation of hydrogels. *Int J Pharm* 2002;244:163-8.
- [20] In den Kleef JJ, Cuppen JJ. RLSQ: T1, T2, and rho calculations, combining ratios and least squares. *Magn Reson Med* 1987;5:513-24.
- [21] Bakker CJG, Hoogeveen RM, Hurtak WF, van Vaals JJ, Viergever MA, Mali WP. MR-guided endovascular interventions: susceptibility-based catheter and near-real-time imaging technique. *Radiology* 1997;202:273-6.

Chapter 9

Lanthanide loaded liposomes for multimodality imaging and therapy

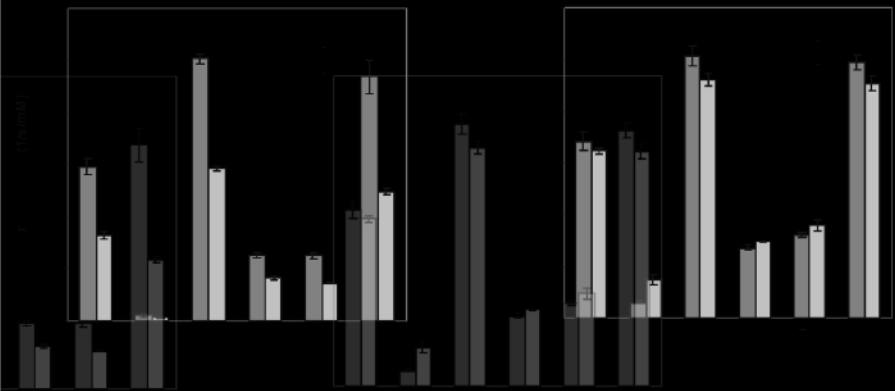
SW Zielhuis, JH Seppenwoolde, VAP Mateus, CJG Bakker, GC Krijger, G Storm, BA Zonnenberg, AD van het Schip, GA Koning, and JFW Nijsen



Table 2. Efficiency and stability of radiolabeled liposomes

liposome type	loading (mol %)		radionuclide
	GdAcAc	DTPA-lipid	
A	0	20	¹⁶⁶ Ho
C	10	10	¹⁶⁶ Ho
D	20	3	^{99m} Tc

Table 1. Liposome characteristics



Abstract

Although many advanced molecular imaging agents are being investigated pre-clinically, none of them are especially designed for the purpose of multimodality imaging. Liposomes have proven to be very promising carrier systems for diagnostic agents for use in e.g. SPECT and MRI as well as for therapeutic agents to treat diseases like cancer. Nanosized liposomes were designed and labelled with the radionuclides holmium-166 (both a beta- and gamma emitter and also highly paramagnetic) or technetium-99m, and co-loaded with paramagnetic gadolinium allowing multimodality SPECT and MR-imaging and radionuclide therapy with one single agent. Diethylenetriaminepentaacetic acid bisoctadecylamide (an amphiphilic molecule with a chelating group suitable for labelling with radionuclides) and gadoliniumacetylacetonate (GdAcAc) (a small lipophilic paramagnetic molecule) were incorporated in liposomes. The liposomes were characterized by measuring their mean size and size distribution, gadolinium content and radiochemical stability after incubation in human serum for 48 h. The MRI-properties (in-vitro) were determined by use of relaxivity measurements at 1.5 and 3.0 Tesla in order to evaluate their potency as imaging agents.

The liposomes were successfully labelled with holmium-166, resulting in a high labelling efficiency ($95 \pm 1\%$) and radiochemical stability ($>98\%$), and co-loaded with GdAcAc. Labelling of liposomes with technetium-99m was somewhat less efficient ($85 \pm 2\%$) although their radiochemical stability was sufficient ($95 \pm 1\%$). MRI-measurements showed that the incorporation of GdAcAc had a strong effect on the relaxivity of the liposomes.

The developed and characterized liposomes allow multimodality imaging and therapy, which makes these new agents highly attractive for future applications.

1. Introduction

It is the ultimate goal of molecular imaging to achieve highly specific visualisation of fundamental biological processes based on morphologic, physiologic, molecular, and genetic markers of diseases like cancer [1]. This goal is believed to be realised through the development of multimodality imaging facilities and highly specific diagnostic agents. For an optimal diagnostic procedure and subsequent treatment it is important to accurately pinpoint anatomically the position of the imaging agent [2]. This can be accomplished through multimodality imaging by use of both single photon emission tomography (SPECT) and magnetic resonance imaging (MRI) [3]. Merging images of SPECT and MRI combines the high sensitivity of SPECT with the anatomical information of MRI [2]. However, at this moment no imaging agents have been designed that can be visualised with both SPECT and MRI. In order to achieve multimodality imaging with a single agent, both radionuclides and MRI-contrast agents have to be combined in one targeted vehicle. Furthermore, if multimodality imaging agents are also loaded with therapeutic agents, targeted therapy of for example cancer, can be subsequently visualised [4]. Specific imaging and targeted therapy can be achieved by using liposomes, which can be targeted to tumour sites [5-8]. These vesicles (~ 50 -500 nm) consist of an aqueous space surrounded by a lipid bilayer. Liposomes can be labelled with radionuclides like indium-111 [9] and technetium-99m [10] by linking the radiolabel to the lipid bilayer, either directly or via the use of a chelator. These liposomes have been applied for the scintigraphic detection of lymph nodes [10] or inflammation [11]. For radiotherapeutic purposes alpha- [12] and beta-emitters [13] have been incorporated in liposomes. Liposomes have also been used to enhance (tumour) diagnosis with MRI by loading them with highly paramagnetic elements, with gadolinium as most pronounced example [4]. These liposomes were successful in the detection of lymph nodes [14] and the visualisation of prostate adenocarcinoma in animal models [15]. Loading of liposomes with gadolinium can be achieved by required incorporating amphiphilic gadolinium derivatives into the liposomal bilayers [4], to obtain an enhanced MR-contrast. This contrast generally results from shortening of the longitudinal relaxation time (T_1) of the MRI signal by the local magnetic field inhomogeneities created by the loaded liposomes. It would be a great advantage if liposomes can be labelled with both paramagnetic

elements and radionuclides. This combined loading would allow imaging and therapy by use of one single agent, which can be visualised by two imaging modalities. It is furthermore a challenge to improve the relaxation properties of the liposomes allowing a more sensitive detection with MRI.

This paper describes the preparation and characterisation of liposomes loaded with both radionuclide and paramagnetic compound. Liposomes were labelled with holmium-166, a therapeutic radionuclide that has been thoroughly investigated by our research group because of its unique therapeutic and diagnostic characteristics [16-18]. Holmium can be easily neutron-activated to a beta- and gamma-emitter with a logistically favourable half-life (26.8 h), and can also be visualized by MRI [4]. It should be realised that because of the different size (as compared to holmium-loaded microspheres that can be used for treatment of liver malignancies [16,17]), the liposomes are expected to act as a T_1 shortening agent, whereas the large microspheres act as a T_2^* agent [17]. To enable scintigraphic detection, technetium labelled liposomes were prepared. The liposomes were made paramagnetic by co-incorporation of gadolinium utilizing a novel procedure based on a small lipophilic gadolinium complex.

Liposomes were characterised by measuring their radiochemical stability and MRI-properties in order to evaluate their potential usefulness as new multimodal diagnostic and therapeutic agents.

2. Materials and methods

2.1 Materials

All chemicals were commercially available and used as obtained. Acetylacetone, 2,4-pentanedione (AcAc; > 99%), chloroform (CHCl_3 ; HPLC-grade), cholesterol (Chol; >99%) and ammonium hydroxide (NH_4OH ; 29.3% in water) were supplied by Sigma Aldrich (Steinheim, Germany). Holmium (III) chloride hexahydrate ($\text{HoCl}_3 \cdot 6\text{H}_2\text{O}$; 99.9%) and gadolinium (III) chloride hexahydrate ($\text{GdCl}_3 \cdot 6\text{H}_2\text{O}$; 99.9%) were obtained from Phase Separations BV (Waddinxveen, The Netherlands). 1,2-Dipalmitoyl-sn-Glycero-3-Phosphocholine (DPPC) and 1,2-dipalmitoyl-sn-glycero-3-phosphoethanolamine-*N*-[methoxy(polyethylene glycol)-2000] (PEG-DSPE) were obtained from Lipoid (Ludwigshafen, Germany). Diethylenetriaminepentaacetic acid bisoctadecylamide (DTPA-lipid) was obtained from Gateway Chemical Technology Inc (St. Louis,

USA). Manganese (II) chloride tetrahydrate ($\text{MnCl}_2 \cdot 4\text{H}_2\text{O}$; 99.9%), hydrochloric acid (HCl ; 37%) and methanol (CH_3OH ; HPLC-grade) were obtained from Merck (Darmstadt, Germany). Stannous chloride dihydrate ($\text{SnCl}_2 \cdot 2\text{H}_2\text{O}$; 99.9%) was purchased from Riedel-de Haën, (Seelze, Germany).

2.2. Preparation of liposomes

Liposomes were prepared by the conventional thin film hydration technique as described previously [19] and consisted of DPPC, Chol, PEG-DSPE in a molar ratio of 1.85: 1: 0.15. Labelling of liposomes with the radionuclides holmium-166 and technetium-99m was achieved by use of the amphiphilic molecule diethylenetriaminepentaacetic acid bisoctadecylamide (DTPA-lipid), which was incorporated into the liposomal bilayer. This molecule consists of a chelating group to which two fatty acids (C18) are attached. The paramagnetic element gadolinium was incorporated into the bilayer of the liposomes in a new way using its acetylacetonate complex (GdAcAc), a small lipophilic molecule (see Fig. 1). GdAcAc was prepared as described previously for HoAcAc [16]. Acetylacetone (180 g) was dissolved in water (1080 g). The pH of this solution was brought to 8.50 with an aqueous solution of ammonium hydroxide. Gadolinium chloride (10 g dissolved in 30 ml water) was added to this solution. After 15 hours incubation at room temperature, the formed GdAcAc crystals were collected by centrifugation and washed with water.

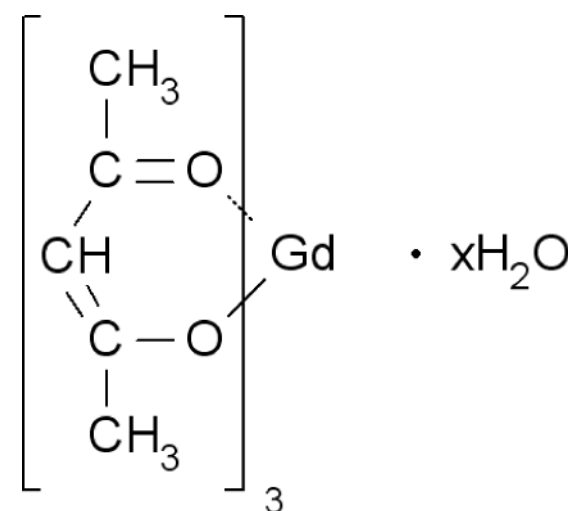


Fig. 1 Structural formula of gadolinium acetylacetonate (GdAcAc)

Four types of liposomes were prepared: liposomes loaded with 20 mol % DTPA-lipid (type A), 20 mol % GdAcAc (type B), a combination of 10 mol % of GdAcAc and 10 mol % DTPA-lipid (type C) or a combination of 20 mol % of GdAcAc and 3 mol % DTPA-lipid (type D). A schematic representation of the various liposome types is given in Fig. 2.

DTPA-lipid and GdAcAc were included in the liposomes by replacing equal molar amounts of DPPC. The lipid mixture (a total amount of 300 μ mol) was dissolved in a mixture of 5 ml chloroform and 2.5 ml of methanol and evaporated to dryness by rotary evaporation under vacuum. The resulting lipid film was further dried under a stream of nitrogen and subsequently hydrated in 6 ml of an ammonium acetate buffer (100 mM) with a pH of 5.0. The resulting lipid dispersion was extruded, using polycarbonate membrane filters (Poretics Corp., Livermore, USA) with a pore diameter of 600, 400, 200 and 100 nm for 2, 2, 6 and 8 times respectively. After preparation the type A and type C liposomes were labelled with holmium-166 and the type D liposomes were labelled with technetium-99m.

All liposomes were coated with polyethylene glycol (by use of PEG-DSPE), since it has been reported that this polymer has a positive influence on the in-vivo circulation time and the MRI-characteristics of the liposomes [4].

Liposome batches were prepared in duplicate.

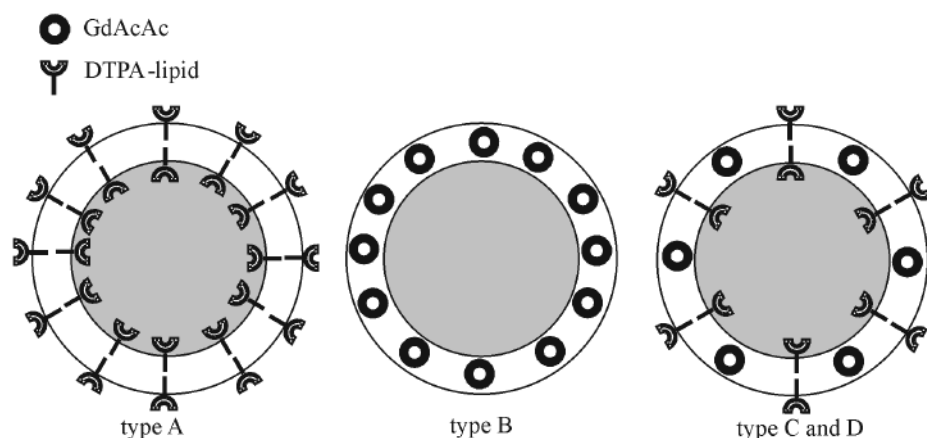


Fig. 2 Prepared liposome formulations. Type A liposomes contain 20 mol% DTPA-lipid, type B liposomes contain 20 mol% GdAcAc, type C liposomes contain 10 mol% GdAcAc and 10 mol% DTPA-lipid and type D liposomes contain 20 mol% GdAcAc and 3 mol% DTPA-lipid.

2.3 Liposome characterization

The phospholipid content was determined with a phosphate assay according to Rouser et al., in order to determine the total lipid concentration after extrusion [20]. The average size and size distribution (polydispersity index) of the liposomes were determined by dynamic light scattering using a Malvern ALV CGS-3 (Malvern Instruments Ltd., Worcestershire, United Kingdom). The polydispersity index is a measure for variation in particle size within a liposome population, and varies from 0 (complete monodispersity) to 1 (large variations in particle size). The amount of GdAcAc in the liposomes was measured by inductively coupled plasma optical emission spectrometry (ICP-OES). Liposome samples were lysed in a 1% Triton (w/v) solution. Samples were next introduced in an Optima 4300 CV (Perkin Elmer, Norwalk, USA) ICP-OES spectrometer. Total gadolinium content was determined by detecting emission at 336.223 nm and related to a standard calibration curve measured between 0 and 20 mg/L. The stability of GdAcAc loaded liposomes was determined by dialysation of 0.5 ml liposomes (25 μ mol) using Slide-A-Lyzer dialysis cassettes with a molecular weight cut-off of 10,000 (Pierce, Rockford, IL, USA) at 37 °C against 25 ml of 10 mM phosphate-buffered saline pH 7.4. After 48 h of dialysation the release of gadolinium in the buffer was measured with ICP-OES.

2.4 Radiolabeling of liposomes

Holmium-166 was obtained by neutron irradiation of 50 μ mol holmiumchloride (packed in polyethylene vials) for 4 h with thermal neutron flux of $5 \times 10^{12} \text{ cm}^{-2} \cdot \text{s}^{-1}$ at the Reactor Institute in Delft (Department of Radiation, Radionuclides and Reactor, Delft University of Technology, The Netherlands). After neutron activation holmiumchloride was dissolved in 0.5 ml of an ammonium acetate buffer with a pH of 5.0 (100 mM). Type A and type C liposomes were labelled with holmium-166. Therefore, the calculated amount of holmium which is 50% of the total molar amount of DTPA-lipid (since only half of the DTPA-lipid is available for labeling on the outer leaflet, see Fig. 2) was subsequently added to 0.5 ml of liposomes. The solution was incubated for 15 min at room temperature. Type D liposomes were labelled with technetium-99m. Therefore, 50 mg $\text{SnCl}_2 \cdot 2\text{H}_2\text{O}$ was dissolved in 50 ml 0.1 M HCl and this solution was subsequently flushed with a stream of nitrogen for 15 min. From this solution, 15 μ l

was added to 0.5 ml of liposomes followed by the addition of 50 MBq technetium-99m-pertechnetate (obtained from a molybdenum-99/technetium-99m generator (Mallinckrodt, Petten, The Netherlands)) in 0.1 ml saline. The solution was incubated for 15 min at room temperature.

The labelling efficiency of both holmium-166 and technetium-99m (fraction radionuclide bound to liposomes vs. free fraction) was determined in the liposome fraction after separation on a PD-10 desalting column (Amersham Biosciences, Uppsala, Sweden) and the radioactivity of both the liposomes and the desalting column was measured with a VDC-404 dose calibrator (Veenstra Instruments, Joure, The Netherlands).

The radiochemical stability of radionuclide labelled liposomes was determined after incubation of 0.5 ml of liposomes for respectively 48 h (for holmium-166) and 6 h (for technetium-99m) in 5 ml human serum at 37 °C. The stability was determined in the same way as described above for the labelling efficiency.

2.5 MRI phantoms

The relaxation properties that describe the influence of the liposomes on the MRI signal are the longitudinal and transverse relaxivity, r_1 and r_2 , respectively. The relation between the resultant relaxation $R_{i,eff}$ [s^{-1}], the concentration of the liposomes c [mM], and the relaxivity r_i [$s^{-1}mM^{-1}$] is given by $R_{i,eff} = R_{i,0} + r_i [c]$, with $i=1,2$ and $R_i = 1/T_i$ using 1, 2 for the longitudinal and transverse relaxation, respectively. The effects of the liposomes on the MR relaxation rates, i.e. the relaxivities r_1 and r_2 , were investigated in phantoms. Polystyrene test tubes with a volume of 5 ml were prepared by diluting 50-250 μ l liposomes with an ammonium acetate buffer (100 mM) with a pH of 5.0 containing 19.2 mg $MnCl_2$ / l. The end-volume was adjusted to 5.0 ml. The spiking of the buffer with manganese chloride was done to adjust the relaxation properties of background fluid in the phantoms to make them comparable to human tissue ($T_1/T_2 \approx 1000/100$ msec at 1.5 T). Consequently, the resulting concentration of the liposomes (expressed as the total amount of lipid) ranged between 0.5 and 2.5 mM. In order to compare the relaxation properties of GdAcAc-loaded liposomes with liposomes which were loaded with gadolinium by use of amphiphilic gadolinium derivatives [4] (the conventional way to prepare paramagnetic liposomes) type A liposomes were also labelled with gadolinium by using the DTPA-lipid.

Labelling of liposomes with gadolinium was done in the same way as described in section 2.4 for holmium-166 using the same molar amounts of gadolinium-chloride.

2.6 Relaxation measurements

Experiments were done on 1.5 and 3.0 Tesla clinical MRI scanners (Achieva, Philips Medical Systems, Best, The Netherlands), using a birdcage receive coil operating in quadrature mode. The tubes were put in a rectangular grid in foam and positioned in the iso-center of the magnet with their long axis oriented parallel to the main magnetic field. A single transverse slice of 10 mm (perpendicular to the long axis of the tubes) was measured in the middle of the tubes. To measure the T_1 and T_2 relaxation for each of the tubes, a multi-spin echo, combined with an inversion recovery experiment [22] was performed with the following parameters: field of view (FOV) 230x172 mm, matrix (MTX) 192x135, echo-time (TE) 8x20 msec, flip 90, 1 signal average, duration 332 s. With a routine implemented in the scanners' software [21], T_1 and T_2 maps were reconstructed. Then a circular region of interest was placed on each tube to calculate the average T_1 and T_2 values for each concentration. To calculate the r_1 and r_2 relaxivities (linear concentration dependence of the relaxation rates) for each type of the liposomes, relaxation rates $R_1 (=1/T_1)$ and $R_2 (=1/T_2)$ were plotted against concentration and followed by linear least square fitting.

3. Results and discussion

3.1 Preparation of liposomes and characterisation

Table 1 summarises the characteristics of the prepared liposomes. PEG was included in the liposome composition to obtain so-called long-circulating liposomes which have the ability to extravasate at solid tumour sites after intravenous administration [22]. The liposomes had a mean size around 130 nm and a low polydispersity index (< 0.07), indicating that size variation of the liposomes is very small. The produced liposomes have an average size, favorable for extravasation through 'leaky' tumor vasculature in tumors. [23]. ICP-OES showed that the initial amount of GdAcAc used for preparation of liposomes was comparable to the amount of GdAcAc loaded into the extruded liposomes (difference $< 10\%$), indicating an incorporation efficiency of about 100%.

Dialysis of GdAcAc loaded liposomes (type B, C and D) for 48 h against PBS showed that maximal 4 % of the total amount of gadolinium in the liposomes had been released. This low release demonstrated that the GdAcAc-loading remains stably associated with the liposomes.

Table 1. Liposome characteristics

liposome type	loading (mol %)		size (nm)
	GdAcAc	DTPA-lipid	
A	0	20	123 ± 10
B	20	0	138 ± 4
C	10	10	133 ± 6
D	20	3	125 ± 4

3.2 Labelling efficiency and radiochemical stability of the liposomes

Table 2 shows the labelling efficiency and radiochemical stability of the liposomes. The results from the phosphate assay were used to calculate the amount of DTPA-lipid in the liposomes. It was assumed that 50 % of these DTPA-groups were available for labelling with holmium-166 in view of the fact that approximately 50 % of the DTPA-lipid is located at the inner leaflet of the liposomal bilayer and is, therefore, not accessible for labelling (see Fig. 2).

Liposomes (type A) that were labelled with holmium-166 demonstrated a high labelling efficiency ($95 \pm 1\%$) and high radiochemical stability in human serum ($>98\%$). GdAcAc had no influence on the labelling of type C liposomes with holmium-166; labelling efficiency ($95 \pm 1\%$) and radiochemical stability ($>98\%$) did not differ from liposomes without GdAcAc (type A). This implicates that during the production of liposomes no Gd^{3+} ions (originating from GdAcAc) are captured by the DTPA-lipid, leaving these chelating groups available for labelling with Ho^{3+} .

Labelling of type D liposomes with technetium-99m resulted in a somewhat lower efficiency of $85 \pm 2\%$, although their radiochemical stability in human serum was high, namely $95 \pm 1\%$. This implicates that before administration of

Table 2. Efficiency and stability of radiolabeled liposomes

liposome type	loading (mol %)		radionuclide	labeling efficiency (%)	stability (%)
	GdAcAc	DTPA-lipid			
A	0	20	^{166}Ho	$95 - 1$	>98
C	10	10	^{166}Ho	$95 - 1$	>98
D	20	3	^{99m}Tc	$85 - 2$	$95 - 1$

liposomes to a patient free technetium-99m-pertechnetate has to be removed (for example with a PD-10 desalting column). In this study low amounts of radioactivity were used, in order to evaluate the feasibility of the radiolabeling approach. For diagnostic or even therapeutic application, a higher specific activity of the liposomes is required. Assuming that, for example, 1 ml of type C liposomes (corresponding with an attainable amount of $2.5 \mu\text{mol}$ DTPA-lipid) is used for administration to patients, an amount of $\sim 400 \mu\text{g}$ of holmium can be bound to the liposomes. Irradiation of this amount of holmium in a nuclear reactor with a thermal neutron flux of $5 \times 10^{14} \text{ cm}^{-2} \cdot \text{s}^{-1}$ for 10 h, results in an activity of 10.6 GBq (end of bombardment). This amount of radioactivity is suitable for therapeutic applications and for nuclear imaging [16].

3.3 MR relaxation properties of the liposomes

It is generally known that the presence of paramagnetic material affects the relaxation behaviour of the surrounding protons. In this study, we used an experimental method to investigate the relaxation effect of paramagnetic liposomes. The results of the relaxation measurements are shown in Fig. 3. In general, the

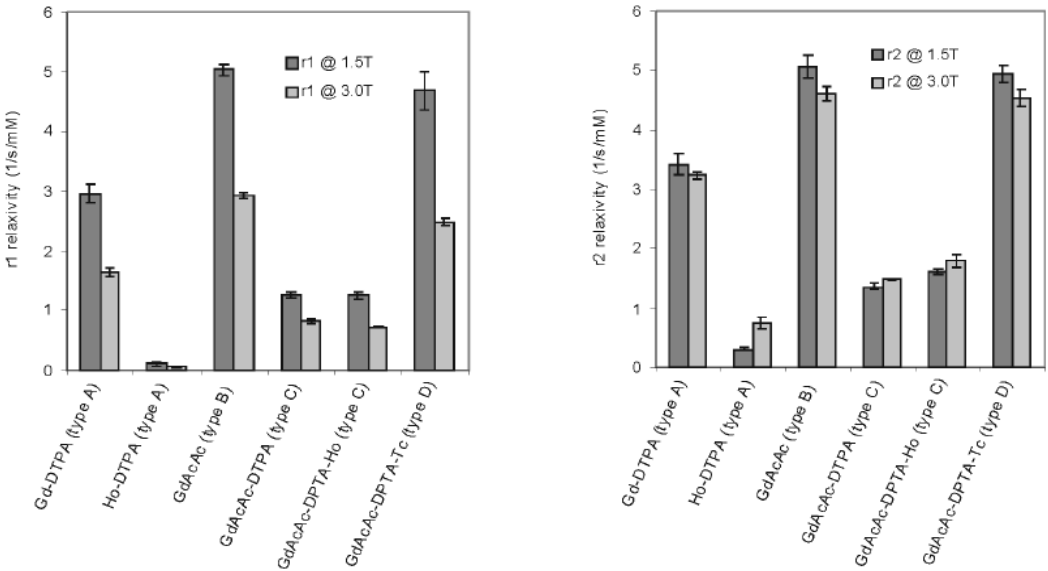


Fig. 3 Graphs of the longitudinal (left) and transverse (right) relaxivity for various designs of loaded liposomes, measured at 1.5 and 3.0 Tesla. The graphs generally show a decreased relaxivity for 3.0 Tesla in comparison to 1.5 Tesla. Type C liposomes are measured with holmium (GdAcAc-DTPA-Ho) and without holmium (GdAcAc-DTPA).

relative relaxivities measured at 1.5 T display a similar dependence of the various designs of the liposomes as those measured at 3.0 T. In most cases, the relaxivities at 1.5 T are significantly higher in comparison to 3.0 T, given the exceptions for the cases with the presence of holmium, in which the r_2 -relaxivities are significantly higher at 3.0 T, most probably due to an increased susceptibility effect. Taking the gadolinium-labelled DTPA-lipid liposomes (type A) as a reference point (the 'conventional way' to design paramagnetic liposomes), this figure shows that the relaxivity of the holmium-labelled DTPA-lipid liposomes (type A) is considerably less, as might be expected from the lower magnetic susceptibility of holmium versus gadolinium [24]. The relaxivity of GdAcAc loaded liposomes (type B) is substantially higher than the gadolinium-labelled DTPA-lipid liposomes (type A). This is due to the higher amount of paramagnetic material (gadolinium) per liposome, whereas normally, half of the DTPA-lipid is located at the inside of the liposome and can, therefore, not be labelled with gadolinium (see Fig. 2). The introduction of a small amount of DTPA-lipid (3 mol %) into the GdAcAc loaded liposomes (type D) slightly decreased the relaxivities. Trading half the GdAcAc for the incorporation of more DTPA-lipid (10 mol % GdAcAc and 10 mol % DTPA-lipid, type C) resulted in relaxivities about half of that of the Gd labelled DTPA-lipid liposomes. The presence of holmium bound to the DTPA-groups on the surface of the type C liposomes slightly changed the relaxivities, in particular the ratio r_2/r_1 , which indicates an increased susceptibility effect, originating from increased magnetic field gradients around the liposomes [25].

In general terms, the results indicate that the relaxivity of liposomes can be significantly enhanced by the increased incorporation of gadolinium as a small (AcAc) complex inside the liposomal bilayer in comparison to the conventional loading of liposomes with amphiphilic gadolinium derivatives. The incorporation of DTPA-lipid reduced this relaxivity somewhat, but enables the use of multiple modalities (labelling with technetium-99m) for diagnosis and therapy (labelling with holmium-166).

4. Conclusion

In conclusion, this study demonstrates that it is possible to prepare liposomes with a high GdAcAc-loading which can be labelled afterwards with radionuclides such as holmium-166 and technetium-99m. These novel liposomes have a high radiochemical stability and are highly paramagnetic, allowing for multimodality imaging and therapy with one single agent. These results represent a significant step forward in the direction of future multimodality imaging and therapy applications.

Acknowledgements

This research was supported by the Technology Foundation STW (UGP.6533), applied science division of NWO and the technology programme of the Ministry of Economic Affairs.

References

- [1] Sullivan DC, Kelloff G. Seeing into cells. The promise of in vivo molecular imaging in oncology. *EMBO Rep* 2005; 6: 292-6.
- [2] Maza S, Taupitz M, Wegner T, Muehler M, Zander A, Munz DL. Precise localisation of a sentinel lymph node in a rare drainage region with SPECT/MRI using interstitial injection of ^{99m}Tc -nanocolloid and superparamagnetic iron oxide. *Eur J Nucl Med Mol Imaging* 2005; 32: 250.
- [3] Yang D, Han L, Kundra V. Exogenous gene expression in tumors: Noninvasive quantification with functional and anatomic imaging in a mouse model. *Radiology* 2005; 235: 950-8.
- [4] Zielhuis SW, Nijsen JFW, Seppenwoolde JH, Zonnenberg BA, Bakker CJ, Hennink WE, van Rijk PP, van het Schip AD. Lanthanide bearing microparticulate systems for multi-modality imaging and targeted therapy of cancer. *Curr Med Chem Anti -Canc Agents* 2005; 5: 303-13.
- [5] Eliaz RE, Nir S, Marty C, Szoka FC. Determination and modeling of kinetics of cancer cell killing by doxorubicin and doxorubicin encapsulated in targeted liposomes. *Cancer Research* 2004; 64: 711-8.
- [6] Peer D, Margalit R. Loading mitomycin C inside long circulating hyaluronan targeted nano-liposomes increases its antitumor activity in three mice tumor models. *International Journal of Cancer* 2004; 108: 780-9.
- [7] Gabizon A, Horowitz AT, Goren D, Tzemach D, Shmeeda H, Zalipsky S. In vivo fate of folate-targeted polyethylene-glycol liposomes in tumor-bearing mice. *Clinical Cancer Research* 2003; 9: 6551-9.
- [8] Mulder WJ, Strijkers GJ, Habets JW, Bleeker EJ, van der Schaft DW, Storm G, Koning GA, Griffioen AW, Nicolay K. MR molecular imaging and fluorescence microscopy for identification of activated tumor endothelium using a bimodal lipidic nanoparticle. *FASEB J* 2005; 19: 2008-10.

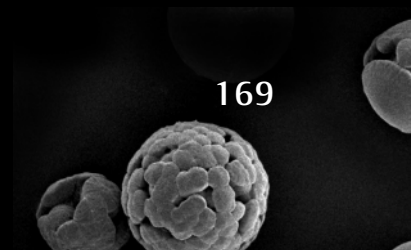
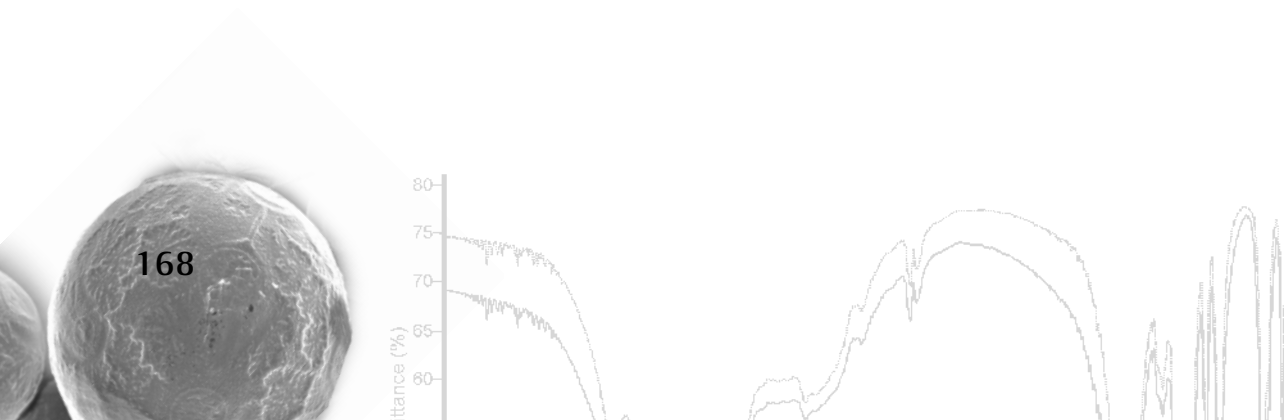
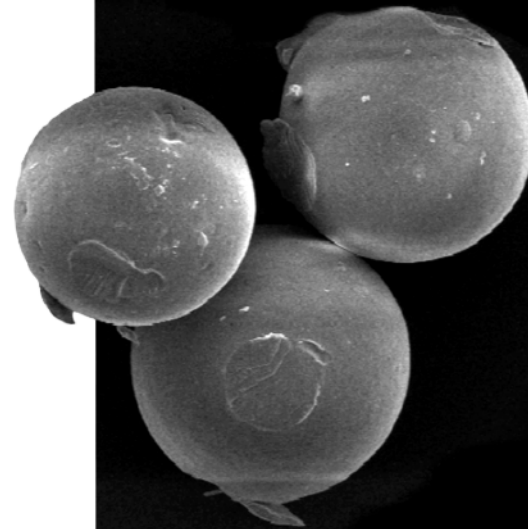
- [9] Harrington KJ, Mohammadtaghi S, Uster PS, Glass D, Peters AM, Vile RG, Stewart JS. Effective targeting of solid tumors in patients with locally advanced cancers by radiolabeled pegylated liposomes. *Clin Cancer Res* 2001; 7: 243-54.
- [10] Phillips WT, Andrews T, Liu H, Klipper R, Landry AJ, Blumhardt R, Goins B. Evaluation of [(99m)Tc] liposomes as lymphoscintigraphic agents: comparison with [(99m)Tc] sulfur colloid and [(99m)Tc] human serum albumin. *Nucl Med Biol* 2001; 28: 435-44.
- [11] Laverman P, Boerman OC, Oyen WJG, Dams ETM, Storm G, Corstens FHM. Liposomes for scintigraphic detection of infection and inflammation. *Adv Drug Del Rev* 1999; 37: 225-35.
- [12] Sofou S, Thomas JL, Lin HY, McDevitt MR, Scheinberg DA, Sgouros G. Engineered Liposomes for potential alpha-particle therapy of metastatic cancer. *J Nucl Med* 2004; 45: 253-60.
- [13] Hafeli U, Tiefenauer LX, Schbiger PA, Weder HG. A lipophilic complex with ¹⁸⁶Re/¹⁸⁸Re incorporated in liposomes suitable for radiotherapy. *Int J Rad Appl Instrum B* 1991; 18: 449-54.
- [14] Misselwitz B, Sachse A. Interstitial MR lymphography using Gd-carrying liposomes. *Acta Radiol Suppl* 1997; 412: 51-5.
- [15] Luciani A, Olivier JC, Clement O, Siauve N, Brillet PY, Bessoud B, Gazeau F, Uchegbu IF, Kahn E, Fria G, Cuenod CA. Glucose-receptor MR imaging of tumors: study in mice with PEGylated paramagnetic niosomes. *Radiology* 2004; 231: 135-42.
- [16] Nijsen JFW, Zonnenberg BA, Woittiez JR, Rook DW, Swildens-van Woudenberg IA, van Rijk PP, van het Schip AD. Holmium-166 poly lactic acid microspheres applicable for intra-arterial radionuclide therapy of hepatic malignancies: effects of preparation and neutron activation techniques. *Eur J Nucl Med* 1999; 26: 699-704.
- [17] Nijsen JFW, Seppenwoolde JH, Havenith T, Bos C, Bakker CJG, van het Schip AD. Liver Tumors: MR Imaging of Radioactive Holmium Microspheres—Phantom and Rabbit Study. *Radiology* 2004; 231: 491-9.
- [18] Seppenwoolde JH, Nijsen JFW, Bartels LW, Zielhuis SW, van het Schip AD, Bakker CJG. Internal radiation therapy of liver tumors: Qualitative and quantitative magnetic resonance imaging of the biodistribution of holmium-loaded microspheres in animal models. *Magn Reson Med* 2004; 53: 76-84.
- [19] Koning GA, Fretz MM, Woroniecka U, Storm G, Krijger GC. Targeting liposomes to tumor endothelial cells for neutron capture therapy. *Appl Radiat Isot* 2004; 61: 963-7.
- [20] Rouser G, Fkeischer S, Yamamoto A. Two dimensional thin layer chromatographic separation of polar lipids and determination of phospholipids by phosphorus analysis of spots. *Lipids* 1970; 5: 494-6.
- [21] In den Kleef JJ, Cuppen JJ. RLSQ: T1, T2, and rho calculations, combining ratios and least squares. *Magn Reson Med* 1987; 5: 513-24.
- [22] Storm G, Crommelin DJA. Liposomes: quo vadis? *Pharm Sci Technol To* 1998; 1: 19-31.
- [23] Charrois GJ, Allen TM. Rate of biodistribution of STEALTH liposomes to tumor and skin: influence of liposome diameter and implications for toxicity and therapeutic activity. *Biochim Biophys Acta* 2003; 1609: 102-8.

[24] Handbook of Chemistry and Physics, 84th edition. CRC Press, Boca Raton (FL) 2003.

[25] Fossheim SL, Fahlvik AK, Klaveness J, Muller RN. Paramagnetic liposomes as MRI contrast agents: influence of liposomal physicochemical properties on the in vitro relaxivity. *Magn Reson Imaging* 1999; 17: 83-9.

Chapter 10

Summary and concluding remarks



1. Summary

This thesis describes the research that was conducted necessary to start a clinical trial involving patients suffering from liver malignancies to be treated with radioactive holmium loaded microspheres. As discussed in the introduction of this thesis, only the minority of the patients can be treated by surgery or ablation methods. External beam irradiation would be a very effective way to treat liver tumours, but the required radiation dosages results in too much damage to the surrounding liver tissue [1,2]. In order to irradiate liver tumours in a selective way, internal radionuclide microsphere therapies have been developed [3]. These therapies make use of the delivery of radionuclide-loaded microspheres near the tumours by catheterisation of the hepatic artery. Yttrium-90 ($E_{\max} = 2.28$ MeV; half-life 64.1 h) loaded glass microspheres (TheraSphere®, MDS Nordion) and resin microspheres (SIR-Spheres®, Sirtex) are clinically applied [1]. In a recent study, 21 patients with unresectable colorectal liver metastases underwent standard chemotherapy (5-fluorouracil and leucovorin) or, in the experimental group, chemotherapy in combination with a single dose of SIR-Spheres®. The median survival was 29.4 months for patients who received both chemotherapy and SIR-Spheres® versus 12.8 months for patients who were treated with chemotherapy alone ($p = 0.025$) [4], which is a promising result. However, the use of yttrium-90 has some drawbacks. Yttrium-89, the element that forms yttrium-90 after neutron activation, has a very low cross-section of 1.3 barn [3], and as a consequence, the neutron activation of yttrium-89 in a nuclear reactor is very time-consuming, and thus very expensive. Furthermore, yttrium-90 is a pure β -emitter and can therefore not be visualised with gamma cameras. Consequently, no information can be gained on the biodistribution of yttrium-90 microspheres. Knowledge of the biodistribution of microspheres in combination with information about the radiation effects on the liver and surrounding organs is of great importance for application in patients.

Cancer treatment with holmium-166 has obvious advantages over yttrium-90. Holmium-165 has a natural abundance of 100 % and a high cross-section of 64 barn, and can therefore easily be neutron-activated to yield holmium-166 [3,5]. The photons (80.6 keV, yield 6.2 %) allow visualisation with a gamma camera whereas the beta-radiation ($E_{\max} = 1.84$ MeV) is suitable for the local radiotherapy of tumours. Holmium is furthermore highly paramagnetic, allowing visuali-

sation with magnetic resonance imaging (MRI) [6]. The possibility to visualise a therapeutic radionuclide with both a gamma camera and MRI is unique and makes holmium-166 a very attractive radionuclide for oncological diagnostic and treatment applications.

As demonstrated in a previous thesis from our department, holmium-loaded microspheres (Ho-PLLA-MS) have proven to be very suitable for treatment of liver malignancies [7]. However, after having shown the feasibility of this radionuclide therapy, further studies were necessary before Ho-PLLA-MS can be clinically applied in patients. Parallel to the pharmaceutical work also new diagnostic and therapeutic particles were developed in order to exploit the very attractive characteristics of holmium for multimodality imaging and cancer therapy.

Chapter 2 reviews the current literature on lanthanide-loaded particles that can be used for anticancer therapies and multimodality imaging. Elements from the group of lanthanides have very interesting physical characteristics for multimodal imaging applications and are the ideal candidates to be co-loaded either in their non-radioactive or radioactive form into particles such as liposomes and polymeric nanoparticles or microparticles for diagnostic and therapeutic purposes. The use of advanced drug delivery technology and the introduction of paramagnetic gadolinium have resulted in nanoparticulate and microparticulate systems with very promising MRI contrast properties for the detection of cancer. Other paramagnetic lanthanides such as erbium, dysprosium, terbium and holmium have also been used for advanced drug delivery based radionuclide therapies, whereas nuclear imaging and/or MRI and/or computed tomography can be used for monitoring the biodistribution of these systems.

In **Chapter 3** the surface characteristics of Ho-PLLA-MS before and after neutron irradiation were studied. This was done in order to get insight into the suspending behaviour of neutron-irradiated microspheres and to identify suitable surfactants for clinical application of these systems. X-ray photoelectron spectroscopy (XPS) and scanning electron microscopy (SEM) were used for surface characterization. XPS showed that the surface of non-irradiated Ho-PLLA-MS mainly consisted of PLLA, but that due to the neutron irradiation of Ho-PLLA-

MS holmium was present at the surface. The wettability of microspheres and PLLA films with and without holmium loading was investigated by means of suspending experiments and contact angle measurements. Holmium-loaded PLLA films had a much higher contact angle (85°) than non-loaded films (70°). Therefore, the appearance of holmium on the surface of Ho-PLLA-MS after neutron irradiation is probably the reason for their poor suspending behaviour in saline. Based on their surface characteristics, a pharmaceutically acceptable solvent (1% Pluronic F68 in 10% ethanol) was formulated with which a homogeneous suspension of radioactive Ho-PLLA-MS could be easily obtained.

Chapter 4 explains why the large amounts of residual chloroform (1000-6000 ppm) initially present in Ho-PLLA-MS, can be removed by neutron irradiation or gamma irradiation at a dose of 200 kGy. In order to study the effects of the high-energy radiation, microspheres with relatively high and low amounts of residual chloroform were subjected to irradiation and the residual chloroform levels as well as other microsphere characteristics (morphology, size, crystallinity, molecular weight of PLLA and degradation products) were subsequently evaluated. A precipitation titration showed that radiolysis of chloroform resulted in the formation of chloride, most likely as a result of the following mechanism: $\text{CHCl}_3 + e^-$ (caused by radiation of PLLA) $\rightarrow \cdot\text{CHCl}_2 + \text{Cl}^-$ followed by the decomposition of $\cdot\text{CHCl}_2$ by H_2O and O_2 to 2Cl^- , CO , CO_2 and H_2O . Gel permeation chromatography and differential scanning calorimetry showed a decrease in molecular weight of PLLA and crystallinity, respectively. However, no differences (morphology, crystallinity, M_w of PLLA and degradation products) were observed between irradiated microsphere samples with high and low initial amounts of chloroform. In view of these results, high-energy radiation proved to be a suitable method for the removal of residual chloroform from Ho-PLLA-MS.

The in vitro degradation characteristics of Ho-PLLA-MS and the nature of the formed degradation products have been investigated in **Chapter 5**. Microspheres with and without HoAcAc loading, and before and after neutron or gamma-irradiation were incubated in a phosphate buffer at 37 °C for 12 months and at different time points the microspheres and buffer were analyzed. The neutron-irradiated Ho-PLLA-MS disintegrated after a period of 24 weeks.

At the end of the experiment (12 months) there were still fragments present that were highly crystalline (as shown by DSC analysis) and infrared spectroscopy demonstrated that these fragments consisted of holmium lactate. However, despite the fact that the microspheres disintegrated, holmium was not detected in the buffer solution and was consequently retained in the formed holmium lactate crystals. In contrast, the other microsphere formulations retained their spherical shape after 12 months of incubation.

The biocompatibility of Ho-PLLA-MS was studied in 48 healthy male Wistar rats (**Chapter 6**). The rats were divided into four treatment groups: sham, neutron-irradiated Ho-PLLA-MS, Ho-PLLA-MS and placebo microspheres without HoAcAc-loading. The microspheres were implanted in the liver of the rats, and the animals were monitored (body weight, temperature, liver enzymes) for a period of 14 months. After sacrifice the liver tissue was histologically evaluated. Since holmium is a bone-seeker, bone tissue from rats of the neutron-irradiated Ho-PLLA-MS group was subjected to neutron activation analysis in order to examine whether accumulation of holmium in the bone had occurred. No effects on body weight, temperature and biochemical parameters were observed in any of the treatment groups. Histological analyses of liver tissue samples showed only signs of a slight chronic inflammation (observed at all time points) and no significant differences in tissue reaction between rats from the four different treatment groups could be observed. Fourteen months after administration only the neutron-irradiated Ho-PLLA-MS were somewhat affected, these microspheres were not completely spherical anymore, indicating that degradation had started. However, the holmium loading had not been released as was demonstrated using MRI and affirmed by neutron activation analysis of bone tissue. In view of these results, Ho-PLLA-MS can be considered biocompatible.

In **Chapter 7** the aspects of the production of a GMP batch of Ho-PLLA-MS are described. The critical steps of the Ho-PLLA-MS production process (sieving procedure, temperature control during evaporation of chloroform and the quality of raw materials) were considered and the pharmaceutical quality of the microspheres was evaluated. The pharmaceutical characteristics (residual solvents, possible bacterial contaminations and endotoxins) of the produced Ho-

PLLA-MS batches were in compliance with the requirements of the European Pharmacopoeia. Moreover, neutron-irradiated Ho-PLLA-MS retained their morphological integrity and the holmium remained stably associated with the microspheres; it was observed that after 270 h (10 times the half-life of Ho-166) only 0.3 ± 0.1 % of the loading was released from the microspheres in an aqueous solution. These results show that GMP-grade Ho-PLLA-MS can be clinically applied giving due consideration to their pharmaceutical quality.

Chapter 8 demonstrates that the incorporation of holmium into alginate microspheres allows their visualisation with both a gamma camera and MRI. The holmium-loaded alginate spheres can be used therapeutically for embolization and, when radioactive, for local radiotherapy of tumours. The alginate microspheres were produced by JetCutter technology and had a narrow size distribution. The microspheres had a mean size of $\sim 159 \pm 19$ μm and a holmium loading of 1.3 ± 0.1 % (w/w). Alginate microspheres could also be labelled with radioactive holmium by incubation of alginate microspheres with holmium-166 chloride (labelling efficiency 96 %). The labelled microspheres had a high radiochemical stability (after 48 h incubation in human serum, 94 % of holmium remained incorporated in the microspheres), allowing therapeutic applications for treatment of cancer. In a pig experiment, the potential in-vivo application of the holmium-loaded alginate microspheres for an MR-guided renal embolization procedure was shown. After selective administration of microspheres to the left kidney, anatomic MR-imaging revealed the presence of holmium-loaded microspheres in the embolized kidney.

In **Chapter 9** the preparation and characterisation of lanthanide loaded liposomes for multimodality imaging and cancer therapy was investigated. The liposomes were labelled with the radionuclides holmium-166 or technetium-99m by use of their complexation with diethylenetriaminepentaacetic acid bisoctadecylamide (an amphiphilic molecule with a chelating group suitable for labelling with radionuclides), and co-loaded with paramagnetic gadolinium by use of gadolinium acetylacetonate (GdAcAc), which was dissolved in the liposomal bilayer. This liposomal formulation allows multimodality SPECT- and MR-imaging and radionuclide therapy with a single agent. Labelling with holmium-166

resulted in a high labelling efficiency ($95 \pm 1\%$) and radiochemical stability (>98 %). Labelling of liposomes with technetium-99m was somewhat less efficient ($85 \pm 2\%$) although their radiochemical stability was sufficient ($95 \pm 1\%$). In-vitro MRI-measurements showed that the incorporation of GdAcAc had a strong effect on the relaxivity of the radionuclide labelled liposomes, which makes them highly attractive for future applications.

2. Concluding remarks

The field of nuclear medicine has a broad and multidisciplinary character. The expertise of physicians, physicists, chemists, biologists and pharmacists is of great importance for both daily practice and for the development of new therapeutic radiopharmaceuticals.

The department of Nuclear Medicine of the University Medical Center Utrecht started in the mid-nineties the development of holmium-166 loaded polymer-based microspheres (Ho-PLLA-MS) for treatment of liver malignancies [5]. Until now, the feasibility of the neutron activation was demonstrated [5] and the microspheres were physically and chemically characterised [5,8,9]. It was furthermore shown in rats [10] and rabbits [11] that the microspheres could be successfully targeted to liver tumours. In vivo imaging of the Ho-PLLA-MS can be performed with both gamma cameras [10,11] and MRI [6,11] and is of great importance for the evaluation of their biodistribution and dosimetry calculations. This thesis describes the pharmaceutical part of the preclinical research, which had to be conducted before clinical studies of Ho-PLLA-MS in cancer patients can be initiated.

Ho-PLLA-MS have to be produced according to the Good Manufacturing Practice Regulations (GMP) promulgated by the European Agency for the Evaluation of Medicinal Products (EMA) [12]. These regulations require that steps are taken to ensure that produced pharmaceuticals are safe, pure, and effective. GMP regulations require a quality approach to manufacturing, in order to eliminate mistakes and contamination. This in turn, protects the patients from receiving a product, which is not effective or even dangerous.

The details of a GMP production process are described in **chapter 7**.

All aspects of the production process are now well-defined, and this effort has led to the production of clinically applicable batches of Ho-PLLA-MS, with

respect to their pharmaceutical quality. The pharmaceutical characteristics (residual solvents, possible bacterial contaminations and endotoxins) of produced microspheres are in compliance with the requirements of the European Pharmacopoeia [13].

Neutron activation of Ho-PLLA-MS is a delicate procedure [5]. The neutron flux is continuously monitored, but besides neutrons also gamma-rays are generated in a nuclear reactor. An excessive dose of gamma-rays results in an unacceptable damage of the microspheres [5]. It is of great importance for the irradiation under GMP-conditions that the dose of gamma-rays is as low as possible, and well-defined. Therefore, the irradiation procedure of Ho-PLLA-MS has been fine-tuned in close collaboration with nuclear reactor physicists and resulted in the production of radioactive microspheres that can be clinically applied (**chapter 7**). In the near future the gamma-dose which the microspheres receive during neutron activation will also be monitored and will provide extra insurance that an optimal irradiation procedure has been performed.

Before administration of Ho-PLLA-MS via a catheter to a patient, the microspheres should be homogeneously suspended to prevent lodging of microsphere aggregates in the catheter during administration. Based on the hydrophobic character of neutron-irradiated Ho-PLLA-MS a pharmaceutically accepted suspending solvent consisting of 1% Pluronic F68 in 10% ethanol was formulated (**chapter 3**). This suspending solvent requires an appropriate sterilisation method like heat sterilisation. The consequences of sterilisation on the stability of the Pluronic F68 in this formulation have to be studied.

A biocompatibility study in rats has shown that the administration of neutron-irradiated Ho-PLLA-MS did not result in chemical toxic effects (**chapter 6**). This study was conducted with neutron-irradiated but decayed microspheres. The radiotoxic effects of Ho-PLLA-MS still have to be studied in order to determine the maximum tolerable radioactive dose for human patients. This study should be performed in large laboratory animals since the administration of radioactive microspheres by use of a catheter can only be performed in large animals like pigs.

Lanthanides, among which holmium, offer great opportunities for new anticancer therapies that can be visualized with different imaging modalities (**chapter 1**). Therefore, other lanthanide-loaded particles have been designed (**chapter 8 and 9**).

Holmium-loaded alginate microspheres with a mean size of 160 μm can be used therapeutically for embolization and, when radioactive, for local radiotherapy of tumours. The used production method, namely the JetCutter technology, is very suitable for GMP production. Due to their embolic and elastic properties these particles have favourable characteristics for treatment of for example head-and-neck cancer [14,15] and bone metastases [16].

Liposomes formulations were successfully labelled with radioactive holmium, allowing local radionuclide therapy and visualisation with a gamma camera. The incorporation of gadolinium acetylacetonate resulted in a strong effect on the relaxivity of the liposomes, allowing their detection with MRI. The produced liposomes have an average size (~ 130 nm), favorable for extravasation through ‘leaky’ tumor vasculature in tumors. [17]. Future in-vivo studies have to proof the potential of the lanthanide-loaded liposomes for diagnostic and therapeutic applications.

In conclusion, the preclinical research described in this thesis demonstrates that regarding the pharmaceutical quality and biocompatibility of Ho-PLLA-MS clinical research can be initiated. In our group complementary research on efficacy, dosimetry, quantitative SPECT and MRI of Ho-PLLA-MS is ongoing and will lead to clinical application of this new anticancer therapy in the near future. The term molecular imaging is used for the visualization of cellular processes at a molecular or genetic level of function by use of sophisticated diagnostic agents and different imaging modalities. Molecular imaging evolved rapidly over the past decade through the integration of cell biology, molecular biology and multimodality imaging and receives high interest from the field of medical technology and pharmacy. Loading molecular imaging probes with therapeutic agents like radionuclides would be a sophisticated new approach for treatment of cancer. Therefore, the possibility to image therapeutic radionuclides like holmium with different modalities such as gamma cameras, MRI and CT offers great opportunities for the development of new advanced radionuclide cancer therapies.

References

- [1] Murthy R, Nunez R, Szklaruk J, Erwin W, Madoff DC, Gupta S, Ahrar K, Wallace MJ, Cohen A, Coldwell DM, Kennedy AS, Hicks ME. Yttrium-90 microsphere therapy for hepatic malignancy: devices, indications, technical considerations, and potential complications. *Radiographics* 2005; 25 Suppl 1: S41-S55.
- [2] Ho S, Lau WY, Leung TW, Chan M, Johnson PJ, Li AK. Clinical evaluation of the partition model for estimating radiation doses from yttrium-90 microspheres in the treatment of hepatic cancer. *Eur J Nucl Med* 1997; 24: 293-8.
- [3] Nijsen JFW, van het Schip AD, Hennink WE, Rook DW, van Rijk PP, de Klerk JMH. Advances in nuclear oncology: Microspheres for internal radionuclide therapy of liver metastases. *Curr Med Chem* 2002; 9: 73-82.
- [4] van Hazel G, Blackwell A, Anderson J, Price D, Moroz P, Bower G, Cardaci G, Gray B. Randomised phase 2 trial of SIR-Spheres plus fluorouracil/leucovorin chemotherapy versus fluorouracil/leucovorin chemotherapy alone in advanced colorectal cancer. *J Surg Oncol* 2004; 88: 78-85.
- [5] Nijsen JFW, Zonnenberg BA, Woittiez JR, Rook DW, Swildens-van Woudenberg IA, van Rijk PP, van het Schip AD. Holmium-166 poly lactic acid microspheres applicable for intra-arterial radionuclide therapy of hepatic malignancies: effects of preparation and neutron activation techniques. *Eur J Nucl Med* 1999; 26: 699-704.
- [6] Nijsen JFW, Seppenwoolde JH, Havenith T, Bos C, Bakker CJG, van het Schip AD. Liver Tumors: MR Imaging of Radioactive Holmium Microspheres—Phantom and Rabbit Study. *Radiology* 2004; 231: 491-9.
- [7] Nijsen JFW. Thesis: Radioactive holmium poly(L-lactic acid) microspheres for treatment of hepatic malignancies: efficacy in rabbits. 109-122. 2001. 26-4-2001.
- [8] Nijsen JFW, van Steenbergen MJ, Kooijman H, Talsma H, Kroon-Batenburg LM, van de Weert M, van Rijk PP, De Witte A, van het Schip AD, Hennink WE. Characterization of poly(L-lactic acid) microspheres loaded with holmium acetylacetonate. *Biomaterials* 2001; 22: 3073-81.
- [9] Nijsen JF, van het Schip AD, van Steenbergen MJ, Zielhuis SW, Kroon-Batenburg LM, van de Weert M, van Rijk PP, Hennink WE. Influence of neutron irradiation on holmium acetylacetonate loaded poly(L-lactic acid) microspheres. *Biomaterials* 2002; 23: 1831-9.
- [10] Nijsen JFW, Rook DW, Brandt CJWM, Meijer R, Dullens HFJ, Zonnenberg BM, de Klerk JHM, van Rijk PP, Hennink WE, van het Schip AD. Targeting of liver tumour in rats by selective delivery of holmium-166 loaded microspheres: a biodistribution study. *Eur J Nucl Med* 2001; 28: 743-9.
- [11] Seppenwoolde JH, Nijsen JFW, Bartels LW, Zielhuis SW, van het Schip AD, Bakker CJG. Internal radiation therapy of liver tumors: Qualitative and quantitative magnetic resonance imaging of the biodistribution of holmium-loaded microspheres in animal models. *Magn Reson Med* 2004; 53: 76-84.
- [12] De Vos FJ, De Decker M, Dierckx RA. The good laboratory practice and good clinical practice requirements for the production of radiopharmaceuticals in clinical research. *Nucl Med Commun* 2005; 26: 575-9.
- [13] European Pharmacopoeia. 4th edition Strasbourg: Council of Europe, 2002.
- [14] van Es RJ, Nijsen JFW, van het Schip AD, Dullens HFJ, Slootweg PJ, Koole R. Intra-arterial embolization of head-and-neck cancer with radioactive holmium-166 poly(L-lactic acid) microspheres: an experimental study in rabbits. *Int J Oral Maxillofac Surg* 2001; 30: 407-13.
- [15] van Es RJ, Nijsen JFW, Dullens HFJ, Kicken M, van der Bilt A, Hennink WE, Koole R, Slootweg PJ. Tumour embolization of the Vx2 rabbit head and neck cancer model with Dextran hydrogel and Holmium-poly(L-lactic acid) microspheres: a radionuclide and histological pilot study. *J Craniomaxillofac Surg* 2001; 29: 289-97.
- [16] Simon N, Siffert R, Baron MG, Mitty HA, Rudavsky A. Preoperative irradiation of osteogenic sarcoma with intra-arterially injected yttrium-90 microspheres. Case report. *Cancer* 1968; 21: 453-5.
- [17] Charrois GJ, Allen TM. Rate of biodistribution of STEALTH liposomes to tumor and skin: influence of liposome diameter and implications for toxicity and therapeutic activity. *Biochim Biophys Acta* 2003; 1609: 102-8.

Samenvatting

Dit proefschrift beschrijft het onderzoek dat is uitgevoerd om klinisch onderzoek met radioactief holmium geladen microsferen te kunnen starten bij patiënten met levertumoren. Slechts een klein deel van deze patiëntengroep kan worden behandeld met chirurgie of ablatie technieken. Conventionele radiotherapie zou een erg effectieve behandelingsmethode voor levertumoren kunnen zijn, ware het niet dat de daarvoor benodigde stralingsdosis te veel schade veroorzaakt aan het omliggende leverweefsel. Om levertumoren op een heel selectieve manier te behandelen zijn interne radionuclide therapieën met microsferen ontwikkeld. Deze therapie maakt gebruik van het selectief bestralen van de levertumoren met behulp van radioactieve microsferen die door middel van catheterisatie via de leverslagader rondom de tumoren worden afgeleverd. Yttrium-90 ($E_{\max} = 2.28$ MeV; halfwaardetijd 64.1 h) geladen glas microsferen (TheraSphere®, MDS Nordion) en hars microsferen (SIR-Spheres®, Sirtex) worden op dit moment klinisch toegepast. In een recente studie, ondergingen 21 patiënten met chirurgisch onbehandelbare uitzaaingen van colontumoren in de lever standaard chemotherapie (5-fluorouracil en leucovorin) of, in de experimentele groep chemotherapie in combinatie met een enkele dosis SIR-Spheres®. De gemiddelde overleving was 29.4 maanden voor patiënten die behandeld werden met zowel chemotherapie als SIR-Spheres® tegenover 12.8 maanden voor patiënten die alleen chemotherapie ondergingen ($p = 0.025$), hetgeen een veelbelovend resultaat is. Echter, aan het gebruik van yttrium-90 kleven een aantal nadelen. Yttrium-89, het element dat yttrium-90 vormt na neutronenactivatie, heeft een erg lage cross-section van 1.3 barn, wat als gevolg heeft dat de neutronenactivatie van yttrium-89 in een kernreactor erg lang duurt en daardoor erg kostbaar is. Verder is yttrium-90 een pure β -straler die daardoor niet kan worden afgebeeld met gammacamera's. Hierdoor kan geen informatie worden verkregen over de biodistributie van de yttrium-90 microsferen. Gegevens over de biodistributie van deze microsferen in combinatie met informatie over de stralingseffecten op de lever en de omliggen-

de organen is van groot belang voor de klinische toepassing van deze therapie. De behandeling van kanker met het isotoop holmium-166 heeft grote voordelen boven het gebruik van yttrium-90. Holmium-165 heeft een natuurlijk voorkomen van 100 % en een hoge cross-section van 64 barn, waardoor op een eenvoudige manier holmium-166 kan worden geproduceerd. Holmium-166 zendt zowel fotonen als bètastraling uit. De fotonen (80.6 keV, 6.2 %) maken beeldvorming met een gammacamera mogelijk en de bètastraling ($E_{\max} = 1.84$ MeV) is geschikt voor de plaatselijke bestraling van tumoren. Holmium is daarnaast zeer paramagnetisch, waardoor beeldvorming met magnetic resonance imaging (MRI) mogelijk is. De mogelijkheid om een therapeutisch radionuclide af te beelden met zowel gammacamera's als MRI is uniek and maakt holmium-166 tot een zeer aantrekkelijk radionuclide voor diagnostische en therapeutische toepassingen bij kanker.

Zoals aangetoond in een eerder proefschrift van de afdeling Nucleaire Geneeskunde van het Universitair Medische Centrum Utrecht, zijn holmium geladen microsferen (Ho-PLLA-MS) zeer geschikt voor de behandeling van levertumoren. Voor de uiteindelijke klinische toepassing van Ho-PLLA-MS was (en is) aanvullend onderzoek nodig. Parallel aan dit (voornamelijk farmaceutisch) onderzoek zijn ook andere holmium bevattende therapeutische en diagnostische deeltjes ontwikkeld.

Hoofdstuk 2 geeft een overzicht van de huidige literatuur over lanthanide bevattende deeltjes die gebruik kunnen worden voor de behandeling van kanker en multimodale beeldvorming. Elementen uit de groep van de lanthaniden hebben erg interessante fysische eigenschappen en het laden van deeltjes, zoals liposomen en polymere micro- en nanodeeltjes, met (al dan niet radioactieve) lanthaniden biedt interessante mogelijkheden voor diagnostiek en therapie. Het inbouwen van paramagnetisch gadolinium in geavanceerde drug delivery syste-

men heeft veelbelovende MRI contrastmiddelen opgeleverd. Andere paramagnetische lanthaniden zoals erbium, dysprosium, terbium en holmium kunnen ook worden gebruikt voor radionuclide therapieën. De biodistributie van deze therapeutische radionucliden kan in beeld worden gebracht met gammacamera's, MRI en CT.

In **Hoofdstuk 3** werd het oppervlak van Ho-PLLA-MS bestudeerd, zowel voor als na het bestralen met neutronen. Dit werd gedaan om een inzicht te krijgen in het suspendeergedrag van met neutronen bestraalde microsferen. Met behulp van deze informatie kunnen geschikte oppervlakteactieve stoffen worden gezocht, waardoor de bestraalde microsferen gesuspendeerd kunnen worden voor toediening aan patiënten. Het oppervlak werd onderzocht door middel van X-ray photoelectron spectroscopy (XPS) en scanning electron microscopy (SEM). XPS liet zien dat het oppervlak van Ho-PLLA-MS voornamelijk bestond uit PLLA, maar dat na bestralen met neutronen ook holmium aanwezig was aan het oppervlak van de microsferen. Het bevochtigingsgedrag van microsferen en PLLA-films met en zonder holmium lading werd onderzocht door middel van suspendeerproeven en randhoekmetingen. Holmium geladen PLLA films hadden een veel hogere randhoek (85°) dan PLLA-films zonder lading (70°). Met inachtneming van deze randhoekmetingen is het hoogst waarschijnlijk dat het verschijnen van holmium aan het oppervlak van Ho-PLLA-MS na bestraling met neutronen verantwoordelijk is voor het slechte suspendeergedrag in fysiologisch zout. Met behulp van de randhoekmetingen werd een klinisch toepasbare formulering gekozen waarin bestraalde Ho-PLLA-MS snel en eenvoudig kunnen worden gesuspendeerd.

Hoofdstuk 4 legt uit hoe residuen chloroform (1000-6000 ppm) uit Ho-PLLA-MS kunnen worden verwijderd door middel van neutronbestraling of gammabestraling met een dosis groter dan 200 kGy. Om de effecten van bestra-

ling te onderzoeken werden microsferen met grote en kleine hoeveelheden residuaal chloroform bestraald en gekarakteriseerd. De hoeveelheid chloroform voor en na bestralen werd bepaald en de ook de morfologie, grootte, kristalliniteit, molecuulgewicht van het PLLA en de ontstane degradatieproducten werden onderzocht. Een neerslagtitratie liet zien dat de radiolyse van chloroform resulteerde in de vorming van chloride. Het volgende mechanisme is hier hoogstwaarschijnlijk voor verantwoordelijk:

$\text{CHCl}_3 + e^-$ (veroorzaakt door bestraling van PLLA) $\rightarrow \cdot\text{CHCl}_2 + \text{Cl}^-$ gevolgd door de ontleding van $\cdot\text{CHCl}_2$ door H_2O en O_2 tot 2Cl^- , CO , CO_2 en H_2O . Gel permeatie chromatografie (GPC) and differentiële scanning calorimetrie (DSC) lieten een afname zien in het molecuulgewicht van PLLA en de kristalliniteit. Er werden echter geen verschillen (morfologie, grootte, kristalliniteit, molecuulgewicht van het PLLA en de ontstane degradatieproducten) gevonden tussen bestraalde microsferen met grote en kleine hoeveelheden chloroform. Deze resultaten laten zien dat het bestralen van Ho-PLLA-MS een geschikte manier is om residuaal chloroform te verwijderen.

De in vitro degradatie van Ho-PLLA-MS werd onderzocht in **Hoofdstuk 5**. Microsferen met en zonder HoAcAc-lading, voor en na neutron- en gammabestraling werden geïncubeerd in een fosfaat buffer bij 37 °C voor een periode van 12 maanden. Op verschillende tijdstippen werden de microsferen en buffer geanalyseerd. De neutronen bestraalde Ho-PLLA-MS desintegreerden na een periode van 24 weken. Aan het eind van het experiment (12 maanden) waren hoog kristallijne fragmenten aanwezig. Infrarood spectroscopie liet zien dat deze fragmenten bestonden uit holmium lactaat. Ondanks het feit dat de microsferen desintegreerden werd er geen holmium gedetecteerd in de buffer. Hieruit kan worden afgeleid dat al het oorspronkelijk aanwezige holmium zich in de holmium lactaat kristallen bevond. In tegenstelling tot neutronen bestraalde Ho-PLLA-MS behielden alle andere microsferen hun ronden vorm gedurende het hele degradatie-experiment.

De biocompatibiliteit van Ho-PLLA-MS werd onderzocht in 48 mannelijke Wistar ratten (**Hoofdstuk 6**). De ratten werden onderverdeeld in vier behandelingsgroepen: sham, neutronen bestraalde Ho-PLLA-MS, Ho-PLLA-MS en placebo microsferen zonder HoAcAc-lading. De microsferen werden geïmplant in de levers van de ratten en de dieren werden intensief gevolgd (lichaamsgewicht, temperatuur en leverenzymen) voor een periode van 14 maanden. Na euthanasie van de dieren werd het leverweefsel histologisch onderzocht. Omdat holmium een zogenaamde botzoeker is werd ook botweefsel van ratten (behandeld met neutronenbestraalde Ho-PLLA-MS) onderzocht met neutronen activeringsanalyse om te zien of er accumulatie van holmium in het bot had plaatsgevonden.

Er werden in deze studie geen effecten op lichaamsgewicht, temperatuur en biochemische parameters gevonden. Histologische analyses van leverweefsel lieten alleen zeer lichte ontstekingsverschijnselen zien en er waren geen verschillen waarneembaar tussen ratten van de vier verschillende groepen. Veertien maanden na toediening vertoonden alleen de neutronen bestraalde Ho-PLLA-MS tekenen van degradatie: Deze microsferen waren niet volledig rond meer. MRI liet echter zien dat geen holmium was vrijgekomen. Ook kon geen holmium in het botweefsel worden aangetoond. In het licht van deze resultaten kan worden geconcludeerd dat Ho-PLLA-MS biocompatibel zijn.

In **Hoofdstuk 7** worden de aspecten van de GMP (good manufacturing practice) productie van Ho-PLLA-MS beschreven. De belangrijke stappen van het bereidingsproces (zeefprocedure, temperatuur controle tijdens het verdampen van chloroform en de kwaliteit van de grondstoffen) werden kritisch bekeken en de farmaceutische kwaliteit van het eindproduct werd geëvalueerd. De farmaceutische karakteristieken (oplosmiddel residuen, mogelijke bacteriële contaminatie en endotoxines) voldeden aan de eisen van de Europese Farmacopee. Verder behielden de Ho-PLLA-MS hun vorm na bestralen en was er geen lekkage van holmium uit de microsferen. Een in vitro release experiment in buffer liet zien dat na 270 uur (10 keer de halfwaardetijd van holmium-166) slechts 0.3 ± 0.1 % van de holmium lading was vrijgekomen uit de microsferen. Deze resultaten laten zien dat

Ho-PLLA-MS kunnen worden geproduceerd volgens GMP. Hierdoor is de farmaceutische kwaliteit van Ho-PLLA-MS geschikt voor klinische toepassing.

Hoofdstuk 8 laat zien dat door middel van het inbouwen van holmium in alginaat microsferen beeldvorming met gammacamera's en MRI mogelijk is. De holmium geladen alginaat microsferen kunnen worden gebruikt voor embolisatie, en wanneer radioactief, ook voor de lokale radiotherapie van tumoren. De alginaat microsferen werden geproduceerd door middel van de JetCutter technologie en hadden een nauwe deeltjesgrootte verdeling. De microsferen hadden een gemiddelde grootte van $\sim 159 \pm 19$ μm en een holmium lading van 1.3 ± 0.1 % (w/w). Alginaat microsferen konden ook worden gelabeld met radioactief holmium door de microsferen te incuberen met holmium-166 chloride (labelings-efficiëntie 96 %). De gelabelde microsferen hadden een hoge radiochemische stabiliteit (na 48 uur incubatie in humaan serum bleef 94 % van de holmium lading gebonden aan de microsferen), wat therapeutisch toepassing voor de behandeling van tumoren mogelijk maakt. De mogelijkheid tot klinische toepassing van holmium geladen alginaat microsferen werd geïllustreerd door middel van een varkensexperiment. Na selectieve toediening van microsferen aan de linker nier, kon de aanwezigheid van microsferen zichtbaar worden gemaakt met MRI.

In **Hoofdstuk 9** werd de bereiding en karakterisatie van lanthanide geladen liposomen voor multimodale beeldvorming en kankertherapie onderzocht. De liposomen werden gelabeld met zowel één van de radionucliden holmium-166 of technetium-99m door middel van complexatie met diethyleen-triamine-pentazijnzuur bisoctadecylamide (een amfifiel molecuul met een chelerende groep die geschikt is voor labeling met radionucliden) als met paramagnetisch gadolinium door middel van gadolinium acetylacetonaat (GdAcAc). GdAcAc werd geïncorporeerd in de liposomale bilaag. Deze liposoomformulering maakt multimodale beeldvorming met zowel SPECT als MRI en radionuclidetherapie mogelijk. Labeling met holmium-166 resulteerde in een hoge labelings-efficiëntie ($95 \pm 1\%$) en een hoge radiochemische stabiliteit ($> 98\%$). Labeling van liposomen met technetium-99m was iets minder efficiënt, hoewel de radiochemische stabiliteit voldoende was ($95 \pm 1\%$).

Hoe is het allemaal zo gekomen?

Na uitgeloot te zijn voor de studie Tandheelkunde (ik wilde dus eigenlijk tandarts worden) begin ik in augustus 1994 aan mijn studie Farmacie.

Het is inmiddels vier jaar later als ik me aan het oriënteren ben op een onderzoeksonderwerp. Ik vind in de hal van het Wentgebouw een briefje op het prikbord: GEZOCHT ENTHOUSIASTE STUDENT FARMACIE, HOLMIUM MICROSFEREN VOOR DE BEHANDELING VAN LEVERMETASTASEN, AFDELING NUCLEAIRE GENEESKUNDE. Van het onderzoeksonderwerp begrijp ik dan nog weinig. Holmium...nooit van gehoord. Microsferen...waren dat geen kleine bolletjes? Nucleaire geneeskunde....heeft dat niet iets met radioactiviteit te maken? Ik besluit maar eens te bellen voor meer informatie en een paar dagen later heb ik een afspraak in het AZU. Aangekomen bij receptie 12 word ik opgewacht door een AIO genaamd Frank. Ik loop met hem mee naar een kamertje waar twee mannen zitten, de een heeft een snor en heet Fred en de ander draagt een witte jas en heet Aalt. De man met de snor vertelt iets over radioactiviteit, levertumoren, holmium en GMP. De AIO knikt enthousiast en valt de man met de snor af en toe bij. De man met de witte jas zucht steeds diep als het woord GMP valt. Hij zucht nog dieper bij de woorden chloroform en pyrogenen, maar weet me te overtuigen dat er veel uitdagend werk ligt te wachten. Aangestoken door het enthousiasme, maar zonder nog te kunnen overzien waar ik aan begin, zeg ik ja en heb ik een onderzoeksplaats. Samen met mijn medestudent Rogier (die op dezelfde oproep was afgekomen) breng ik een half jaar door op de afdeling Nucleaire Geneeskunde en werken we aan de farmaceutische aspecten van een nieuwe kankertherapie.

Weer vier jaar later (het is dan 2002) ben ik klaar met mijn apothekersopleiding en moet ik gaan beslissen waar ik aan de slag zal gaan. Ik krijg een mooie kans: ik kan weer terug naar de Nucleaire en ik kan AIO worden op hetzelfde project waarmee ik me als student al had beziggehouden.

Nu, bijna 12 jaar na het begin van mijn studie, is het werk dan eindelijk gedaan en is het tijd om iedereen die mij heeft bijgestaan te bedanken.

-Prof. Dr. P.P. van Rijk, beste Peter, in 2003 was je congresvoorzitter van het EANM en koos je 'quality' als thema. Als hoofd van de afdeling Nucleaire Geneeskunde heb je kwaliteit hoog in het vaandel staan (ISO en GMP). Ik denk

dat we mede daardoor ook kwaliteit hebben kunnen leveren. Bedankt voor de mogelijkheden die ik heb gekregen.

-Prof. Dr. Ir. W.E. Hennink, beste Wim, zonder jouw enorme inzet was dit proefschrift nooit tot stand gekomen. Bijna iedere zin uit dit boekje is door jou binnenstebuiten gekeerd. Daarnaast kwam je steeds met nieuwe en zinvolle ideeën. Bedankt voor alles wat ik van je heb kunnen leren.

-Prof. Dr. Ir. M.A. Viergever, beste Max, ik moet toegeven dat ik me als apotheker eerst een vreemde eend in de bijt voelde in een onderzoeksschool waar beeldvorming en beeldverwerking 'core business' is. Ik had vooraf dan ook niet kunnen vermoeden dat imaging een belangrijke rol zou gaan spelen in mijn onderzoek. Bedankt voor alle mogelijkheden en het prettige wederzijdse contact.

-Dr. A.D. van het Schip, beste Fred, jouw bijdrage als co-promotor was onmisbaar. Je wist de rode draad van het onderzoek vast te houden door hoofd- en bijzaken te onderscheiden. Met onnavolgbare precisie heb je mijn artikelen gecorrigeerd. Dank voor je inzet en het vertrouwen dat ik kreeg.

-Dr. J.F.W. Nijsen, beste Frank, je was mijn dagelijkse begeleider, collega-onderzoeker en kamergenoot (tenminste, de eerste twee jaren). We hebben samen veel moois beleefd en ik wil je bedanken voor de geweldige samenwerking. Je hebt alles in het werk gesteld om dit onderzoek tot een succes te laten worden. Ik geef ook toe dat ik soms eigenwijs geweest ben, maar ik denk niet dat ik dat van een vreemde heb... Ik wens je alle succes toe in je verdere wetenschappelijke carrière. Wie weet wat er nog voor je in het verschiet ligt...

-Ik wil in dit dankwoord ook de naam van Aalt van Dijk noemen, die als ziekenhuisapotheker nauw betrokken was bij de afdeling Nucleaire Geneeskunde en zodoende een belangrijke bijdrage heeft geleverd aan het Holmiumproject. Hij overleed op 21 oktober 2004 op 58-jarige leeftijd.

-Een van de drijvende krachten achter het project is Bernard Zonnenberg die als oncoloog verbonden is aan de afdeling Nucleaire Geneeskunde. Bedankt voor je enorme bevlogenheid, je creatieve ideeën en motiverende woorden.

-Mijn collega-AIO Maarten Vente wil ik bedanken voor alle hulp die hij mij heeft geboden, maar bovenal voor de enorm leuke tijd die we als kamergenoten hebben gehad. Er liggen nog een aantal lastige klussen op jouw bordje, maar ik weet zeker dat het je gaat lukken.

-Alle MRI-data uit dit proefschrift zijn gegenereerd door Jan-Henry Seppenwoolde. Bedankt voor het scannen (meestal tot laat in de avond gewapend met drop en chocola) van al die ratten, konijnen en fantomen. Ik kan nu ook jou en Wilma bedanken voor de wederzijdse oppas en de contacten buiten het werk om. We zullen elkaar vast nog regelmatig blijven zien. Naast Jan-Henry wil ik ook Chris Bakker bedanken voor zijn bijdrage aan de artikelen.

-Als er iemand is die een pluim verdiend, is het Remmert de Roos wel. Bedankt voor al die bollen (inmiddels moet je bijna een kilo hebben geproduceerd!), analyses, het regelwerk en weet ik wat nog meer. Je bent een onmisbare factor in het Holmiumproject, maar bovenal was je een zeer prettige collega.

-Tim de Wit, ontzettend bedankt voor het oplossen van al mijn computerprobleempjes, zowel op het werk als bij mij thuis. Helaas zijn er geen SPECT-opnamen in dit proefschrift te vinden, maar dit lag niet aan jou, maar aan de onvindbare lymfklieren van K1 en K2. Ik wens je veel succes met je verdere werk en hoop dat je nog eens een portie zelfgevangen en zelfgerookte paling komt langsbrengen.

-Het Holmiumproject gaat in volle vaart verder. Ik wil Wouter Bult (nieuwe ontwikkelingen), Monique Hobbelink (klinische aspecten) en Peter Seevinck (MRI) veel succes wensen.

-Ik wil Wim van Beek hartelijk bedanken voor het meedenken en ontwerpen van het 'roterende-release-apparaat', de 'ratten-warmhoud-koker', de 'reageerbuis-schudbad-houder' en alle andere hulpmiddelen die ik nodig had voor mijn onderzoek. Ik heb je warme en oprechte persoonlijke belangstelling zeer gewaardeerd.

-Verder verdienen eigenlijk alle medewerkers van de afdeling Nucleaire Geneeskunde een pluim. Het waren mooie jaren. Bedankt voor al jullie hand- en spandiensten, steun en belangstelling. Tevens wil ik Hans van Asselt, mede namens Mirjam, bedanken voor de courgettes.

-Een andere afdeling waar ik veel tijd heb doorgebracht was de vakgroep Biofarmacie en Farmaceutische Technologie. Ik wil ook jullie ook bedanken voor de gezellige tijd en alle geboden hulp. In het bijzonder wil ik Mies van Steenbergen bedanken voor zijn enorme inzet en geduld (als ik weer eens vergeeten was hoe iets ook alweer werkte).

www.badgerbadgerbadger.com/Mieswathadikzonderjougemooten! Verder wil ik Mark Leemhuis bedanken voor het NMR-werk (helaas niet opgenomen in het proefschrift).

-Ik wil Gerben Koning bedanken voor zijn bijdrage aan het liposomenhoofdstuk, zowel in praktische zin als wat het schrijf- en denkwerk betreft. Het was een zeer prettige samenwerking.

-Een groot deel van de bestralingen zijn uitgevoerd in de kernreactor van de Technische Universiteit Delft. Ik wil Gerard Krijger bedanken voor al het werk dat hij gedaan heeft en in het bijzonder voor zijn enthousiasme voor het Holmiumproject.

-Piet Snip en Joost Wottiez (ECN) wil ik bedanken voor de bestralingen die zijn uitgevoerd in de kernreactor van Petten.

-Veel tijd heb ik besteed aan GC-bepalingen op chloroform en chloride-titraties. Ik wil Willy van den Bogaard bedanken voor al zijn hulp en de gezellige tijd. Verder wil ik ook de heer Van der Houwen danken voor zijn deskundige adviezen.

-I also want to thank the students from Portugal who stayed at our department to do their research project. Dear Raquel, you visited the Netherlands in 2003 and your work is presented in chapter 3 (surface characteristics). You did a very good job and it was a pleasure to know you! Dear Vanessa, you visited the Netherlands in 2004 and your work is presented in chapter 9 (liposomes). I was also very happy with your work and I enjoyed your enthusiasm.

-Kees Brandt en Anja van de Sar wil ik bedanken voor het vakkundig opereren van de ratten. Verder wil ik ook alle andere betrokken medewerkers van het GDL danken voor de goede zorgen voor mijn dieren.

-Zonder de hulp van een aantal experts was dit proefschrift niet wat het nu geworden is. Ik wil dan ook de volgende personen bedanken voor hun hulp en deskundigheid:

-Bert Dorland voor de GC-MS-analyses.

-Hub Dullens voor het maken van de histologische coupes en de interpretatie ervan.

-Pim van Maurik voor zijn assistentie bij de SEM-opnames.

-Arjen Vredenberg en Bas Feddes voor de XPS-bepalingen.

-Ulrich Jahnz and Peter Wittlich for the work we did together with the JetCutter.

-Gert Storm voor zijn commentaar op hoofdstuk 9.

- Hans Kemperman voor de klinisch chemische analyses.
- Carla Degenhardt van het Prins Maurits Laboratorium voor de fosgeen-bepalingen.
- De CSA voor al het sterilisatiewerk.

-Ik wil mijn paranimfen alvast bedanken voor het feit dat ze mij op 22 mei willen bijstaan. Beste Rogier, in 1998 begonnen we samen aan ons afstudeeronderzoek bij de Nucleaire, dus wat holmium microsferen betreft heb je ook nog de nodige kennis in huis. Verder denk ik met plezier terug aan onze mooie belevenissen in Australië.

Beste Matthijs, de Boomstraat was de basis voor onze vriendschap. Je bent een bijzonder mens en niet alleen omdat je zo geweldig snel 2-voor-12-vragen op kunt zoeken!

-Familie en vrienden, dank voor al jullie steun en belangstelling. Het boekje is nu eindelijk af, dus binnenkort kom ik weer eens langs als dat nog mag.

-Lieve Mir, een bijzonder moment was de ochtend van 19 oktober 2005. Tussen de weeën door hebben we samen de bloedwaarden van de ratten ingevoerd in Excel (samengevat in figuur 2 van hoofdstuk 6) en een paar uur later zette je ons tweede kind op de wereld! Maar ik wil je vooral bedanken voor wie je bent voor mij, Justus en Josefien. Wat hebben we het toch goed samen.

-Bovenal ben ik Hem dankbaar die de basis is van mijn bestaan.

De Heer zelf gaf de mensen de kennis,

zodat Hij om zijn wonderbaarlijke kruiden wordt geprezen.

Daarmee geneest Hij en neemt Hij de pijn weg,

de apotheker maakt er een balsem van.

Het werk van de Heer kent geen einde,

Hij brengt genezing op de aarde.

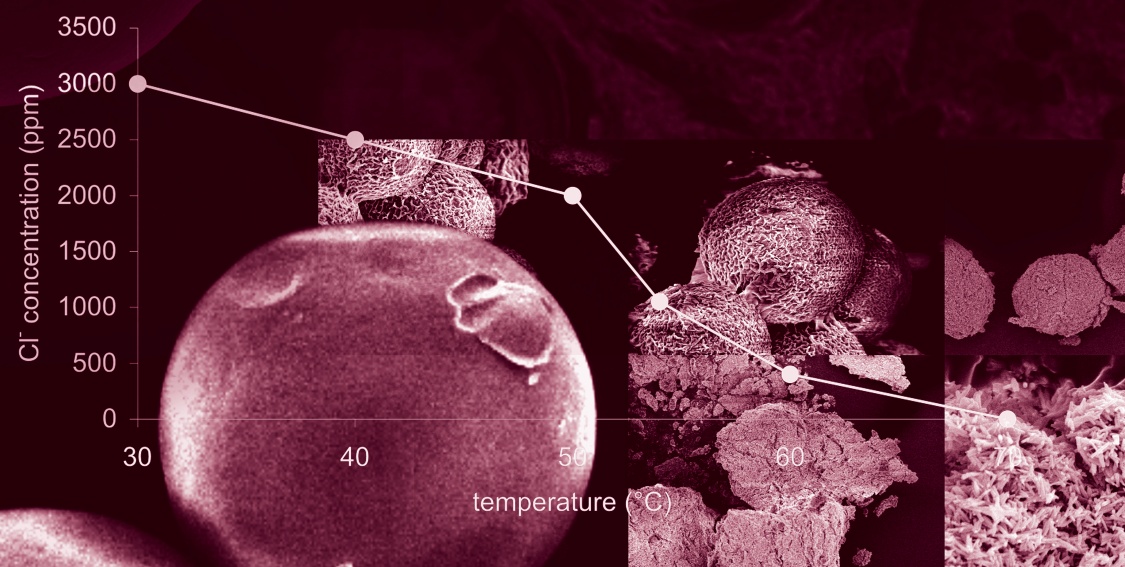
(Uit het apocriefe bijbelboek Wijsheid van Jezus Sirach 38: 6-8)

Publications

- SW Zielhuis, JFW Nijsen, JH Seppenwoolde, BA Zonnenberg, CJG Bakker, WE Hennink, PP van Rijk and AD van het Schip. Lanthanide bearing microparticulate systems for multi-modality imaging and targeted therapy of cancer. *Current Medicinal Chemistry Anticancer Agents* 2005, 5(3): 303-13
- SW Zielhuis, JFW Nijsen, R Figueiredo, B Feddes, AM Vredenberg, AD van het Schip and WE Hennink. Surface characteristics of holmium loaded Poly(L-lactic acid) microspheres. *Biomaterials* 2005, 26(8): 925-32
- SW Zielhuis, JFW Nijsen, R de Roos, GC Krijger, PP van Rijk, WE Hennink and AD van het Schip. Production of GMP-grade radioactive holmium loaded poly(L-lactic acid) microspheres for clinical application. *International Journal of Pharmaceutics* 2006, 311(1-2): 69-74
- SW Zielhuis, JFW Nijsen, L Dorland, GC Krijger, AD van het Schip and WE Hennink. Removal of chloroform from biodegradable therapeutic microspheres by radiolysis. *International Journal of Pharmaceutics* (accepted)
- SW Zielhuis, JFW Nijsen, GC Krijger, AD van het Schip and WE Hennink. Holmium loaded poly(L-lactic acid) microspheres: an in vitro degradation study. (submitted)
- SW Zielhuis, JFW Nijsen, JH Seppenwoolde, CJG Bakker, GC Krijger, HFJ Dullens, BA Zonnenberg, PP van Rijk, WE Hennink and AD van het Schip. Biocompatibility study of holmium loaded poly(L-lactic acid) microspheres in rats. (submitted)
- SW Zielhuis, JH Seppenwoolde, CJG Bakker, U Jahnz, BA Zonnenberg, AD van het Schip, WE Hennink and JFW Nijsen. Holmium loaded alginate microspheres for multimodality imaging and therapeutic applications. (submitted)
- SW Zielhuis, JH Seppenwoolde, VAP Mateus, CJG Bakker, GC Krijger, G Storm, BA Zonnenberg, AD van het Schip, GA Koning, and JFW Nijsen. Lanthanide loaded liposomes for multimodality imaging and therapy. (submitted)
- JFW Nijsen, AD van het Schip, MJ van Steenberg, SW Zielhuis, LM Kroon-Batenburg, M van de Weert, PP van Rijk and WE Hennink. Influence of neutron irradiation on holmium acetylacetonate loaded poly(L-lactic acid) microspheres. *Biomaterials* 2002, 23(8): 1831-9
- JH Seppenwoolde, JFW Nijsen, LW Bartels, SW Zielhuis, AD van het Schip and CJG Bakker. Internal radiation therapy of liver tumors: qualitative and quantitative magnetic resonance imaging of the biodistribution of holmium-loaded microspheres in animal models. *Magnetic Resonance in Medicine* 2005, 53(1): 76-84

Curriculum Vitae

Sander Zielhuis werd op 26 juni 1976 geboren in Zwolle en groeide op in de Veluwe plaats Wezep. In 1994 behaalde hij zijn VWO-diploma aan het Johannes Calvijn Lyceum te Kampen. Datzelfde jaar begon hij met zijn studie Farmacie aan de Universiteit Utrecht en startte in 1998 met zijn wetenschappelijke stage bij de afdeling Nucleaire Geneeskunde van het Universitair Medisch Centrum Utrecht. Op deze afdeling deed hij onderzoek naar de farmaceutische aspecten van radioactieve holmium microsferen voor de behandeling van levermetastasen. In 2000 behaalde hij het doctoraal diploma farmacie en in 2002 het apothekersdiploma. Na zijn studie kreeg hij de gelegenheid om als AIO verder te gaan met het Holmiumproject bij de afdeling Nucleaire Geneeskunde. De resultaten van het onderzoek zijn beschreven in dit proefschrift. Sinds februari 2006 is hij in dienst van Pharmachemie te Haarlem.



d

